

https://dspace.org/

The effect of liquids on the stress distribution in a glass fibre reinforced plastic road tanker

Armbruster, Michael Herman

2016
http://hdl.handle.net/10539/21352

Downloaded from a DSpace repository. https://dspace.org/

THE EFFECT OF LIQUIDS ON THE STRESS DISTRIBUTION IN A GLASS FIBRE REINFORCED PLASTIC ROAD TANKER

Michael Hermann Armbruster

A dissertation submitted to the Faculty of Engineering, University of the Witwatersrand, Johannesburg, in the fulfilment of the requirements for the degree of the Master of Science in Engineering

Johannesburg, 1992

DECLARATION

I declare that this dissertation is my own, unaided work. It is being submitted for the Degree of Master of Science in the University of the Witwatersrand, Johannesburg. It has not been submitted before for any degree or examination in any other University.



(Signature of candidate)

25 day of FEBRUARY 1992

ABSTRACT

The absence of reliable design data for Glass Reinforced Plastic (GRP) road tankers has been considered an obstacle for the local design and manufacture of such vehicles. This has prompted the analysis, using Finite Element Methods (FEM), of a filament wound cylindrical shell for a monocoque road tanker.

Results from the FEM analysis were compared to those from a theoretical analysis based on a combination of elasticity and beam theory. Two load cases were analysed: a pure internal pressure of 8.4 Bar; and the combined effect of 2g accelerations in the axial, sideways and vertical directions. The FEM method was validated by a model consisting of a small filament wound tube in steel supports which was tested with combined axial and bending load. The strain gauge results were compared to both FEM and beam theory solutions.

Correlations between the FEM and theoretical results were very good for the internal pressure load case. The combined accelerations loading resulted in larger differences between the results of the two methods. This was due to the stress concentrations at the supports, which were not allowed for by beam theory. The FEM inplane force resultan s correlated with the beam theory predictions for axial and vertical acceleration. There were significant differences for the sideways acceleration. Theoretical prediction of the moment and transverse shear resultants did not show good correlation with the FEM results. The strain gauge results from the validation model showed good correlation with the FEM and theoretical predictions.

DEDICATION

This work is dedicated to my parents, Helen and Hermann, for all the love and support they have given me.

ACKNOWLEDGEMENT :

My thanks go to the following companies and individuals for the assistance and generous financial support which they have provided during this project.

Sponsors of the Reinforced Plastics / Composites facility.
Mr. A. Mitchell : Acoustical Fibreglass Insulation (Pty) Ltd.
Mr. S. Herholdt : Acoustical Fibreglass Insulation (Pty) Ltd.
Mr Brengozs : The Paul Tingly Bursary scheme
- for their encouragement and financial assistance

Mr. C. Constancon : School of Mechanical Engineering.
Mr. M. Stone : School of Mechanical Engineering.
Mr. P. Lehman : Henred Freuhauf (Pty) Ltd.
Mr. J. Schoegelhoffer : TFM Manufacturing (Pty) Ltd.
Mr. D. Lawrence : Red Apple Plastics (Pty) Ltd.
Mr. M. Mulder : NCS Plastics (Pty) Ltd.
- for their guidance and technical advice.

Messrs. F. Bartens, Z.J. de Beer and A. Groenewald
: Aerodyne Technology (Pty) Ltd.
- for the donation of the filament wound tubes and financial support.

Many thanks to Dr. H.D. Chandler and my colleagues at the Reinforced Plastics / Composites facility for the guidence and help they have given me. A special thank you to Ms Hester Botes for the typing the bulk of the thesis and Andrew Craven for proof-reading.

TABLE OF CONTENTS

		Page
DECLARATION		i
ABSTRACT		ii
DEDICATION		iii
ACKNOWLEDGEMENTS		iv
TABLE OF CONTENTS		v
LIST OF FIGURES		x
LIST OF TABLES		xvi
LIST OF PLATES		xvii
LIST OF SYMBOLS		xviii
1	INTRODUCTION	1
1.1	Features of GRP Road Tankers	1
1.1.1	Capital cost	1
1.1.2	Corrosion resistance	1
1.1.3	Range of chemicals	2
1.1.4	Maintenance	2
1.1.5	Structural	3
1.1.6	Thermal	3
1.1.7	Fire resistance	4
1.1.8	Manufacture	4
1.1.9	Regulations	4
1.1.10	Special considerations	5
1.2	GRP Road Tankers for Southern Africa	5
1.3	Overall Aims of the study	6
2	LITERATURE SURVEY	8

3	ANALYTICAL WORK	15
3.1	Theory for Internal Pressure	15
3.2	Theory for Axial, Bending and Circumferential Stresses Arising from Acceleration A_x in the Axial Direction	17
3.2.1	Axial elongation and bending forces from hydrostatic pressure	20
3.2.2	Circumferential stresses from hydrostatic pressure	22
3.2.3	Elongation and bending from the acceleration of the shell	23
3.2.4	Summation of force resultants due to axial acceleration	25
3.3	Theory for Axial, Bending and Circumferential Stresses Arising from Acceleration in the Vertical (z) and Horizontal (y) Directions	25
3.3.1	Circumferential stresses due to the liquid hydrostatic pressure in the vertical and sideways directions	32
3.3.2	Summation of force resultants due to vertical or sideways acceleration	33
3.4	Shear Stresses in Beams due to Accelerations in the Axial, Vertical and Sideways Directions	34
3.5	Classical Lamination Theory	37
3.6	The Validation Model	40
4	FINITE ELEMENTS	43
4.1	The Road Tanker	43
4.1.1	General requirements	43

4.1.2 The finite element model of the road tanker 44
4.1.3 Computer programs 54

4.2 The Validation Model 61
4.2.1 The validation finite element model 61
4.2.2 Computer programs 67

5 EXPERIMENTAL

5.1 General Requirements 70

5.2 Description of Experimental Apparatus 70
5.2.1 Strain gauges 71
5.2.2 Wheatstone bridge and temperature compensation 76
5.2.3 Tensile testing machine 77
5.2.4 Instrumentation 78

5.3 Experimental procedure 78
5.3.1 Calibration of the tensile testing machine and plotter 78
5.3.2 Connection and cycling of the model 79
5.3.3 Experimental testing 80

6 RESULTS AND DISCUSSION 81

6.1 The Road Tanker 81
6.1.1 Internal pressure 81
6.1.2 Combined accelerations 96

6.2 The Validation model 114

6.2.1 Experimental observations 114

6.2.2 Finite element observations 118
6.2.3 Comparison of experimental, theoretical and FEM results 122

7 CONCLUSIONS 128

8 RECOMMENDATIONS 130

9 REFERENCES 131

LIST OF APPENDICES

APPENDIX A SPECIFICATION AND DRAWINGS OF THE PROPOSED ROAD TANKER
APPENDIX B SPECIFICATION AND DRAWINGS OF THE VALIDATION MODEL
APPENDIX C MATERIAL PROPERTIES FOR THE ROAD TANKER AND VALIDATION MODEL
APPENDIX D CLASSICAL LAMINATION THEORY
APPENDIX E THEORY FOR INTERNAL PRESSURE
APPENDIX F THEORY COMBINED ACCELERATIONS
APPENDIX G THEORY FOR STRAIN GAUGES
APPENDIX H LISTING OF MACLT CLASSICAL LAMINATION THEORY PROGRAM
APPENDIX I LISTING OF RTBEGIN AND RTEND PREPROCESSING PROGRAMS
APPENDIX J SUMMARISED LISTING OF ROAD TANKER FEM MODELS
APPENDIX K LISTINGS OF PREPROCESSING PROGRAMS FOR VALIDATION MODEL
APPENDIX L SUMMARISED LISTING OF VALIDATION FEM INPUT FILE
APPENDIX M LISTING OF MACONV GRAPHICS GENERATION PROGRAM
APPENDIX N LISTING OF THE MA3DCAD PREVIEW PROGRAM

APPENDIX O LISTINGS OF DATA TRANSFER PROGRAMS FOR FEM POST PROCESSING
APPENDIX P LISTING OF THE MATHFORY PROGRAM
APPENDIX Q SUMMARISED FEM AND THEORY OUTPUT FOR INTERNAL PRESSURE
APPENDIX R SUMMARISED FEM OUTPUT FOR 2g COMBINED ACCELERATION LOAD CASE
APPENDIX S FEM MAPS OF INTERNAL PRESSURE FORCE RESULTANTS
APPENDIX T FEM MAPS OF COMBINED ACCELERATION FORCE RESULTANTS
APPENDIX U FEM MAPS OF VALIDATION MODEL FORCE RESULTANTS
APPENDIX V SELECTED BIBLIOGRAPHY

LIST OF FIGURES

Figure		Page
3.1	Variation of hydrostatic pressure due to axial acceleration A_x	18
3.2	Beam theory idealisation of the A_x acceleration	20
3.3	Free body diagram	21
3.4	Axial force diagram	21
3.5	Shear force diagram	22
3.6	Bending moment diagram	22
3.7	Free body diagram	23
3.8	Axial force diagram	24
3.9	Shear force diagram	24
3.10	Bending moment diagram	24
3.11	Schematic for the road tanker under a vertical acceleration	26
3.12	Free body diagram	29
3.13	Axial force diagram	29
3.14	Shear force diagram	29
3.15	Bending moment diagram	30
3.16	Section 1 between back tan line and back support	30
3.17	Section 2 between back support and front support	31
3.18	Section 3 between front support and front tan line	32
3.19	Shear stresses in a beam of circular cross section	35
4.1	Schematic illustrating the loading and supports applied to the road tanker model	46
4.2	The FEM mesh of one half of the road tanker showing the original (dotted) and displaced (solid) shape	46
4.3	Node ordering for an S8R shell element	
4.4	Connection of the shell and ribs using multi-point constraint type 7	50

4.5 The applied loads result in force and moment resultants acting on the laminates 53
4.6 Example of the MA3DCAD screen display showing the tanker dome and the first ring 58

4.7 One half of the validation finite element model 63
4.8 A C3D20 three dimensional brick element 65

5.1 Schematic of the validation test model 71
5.2 Layout of the tube showing the positions of the rosettes 75
5.3 Schematic of a wheatstone bridge circuit 77

6.1 Original and displaced mesh of the road tanker FEM model with 8,4 Bar internal pressure 81
6.2 Non-dimensional axial force resultants (N_x') 84
6.3 Non-dimensional circumferential force resultants (N_ϕ') 85
6.4 Non-dimensional inplane shear force resultants ($N_{x\phi}'$) 88
6.5 Non-dimensional axial moment resultants (M_x') 89
6.6 Non-dimensional circumferential moment resultants (M_ϕ') 92
6.7 Non-dimensional twisting moment resultants ($M_{x\phi}'$) 93
6.8 Non-dimensional axial transverse shear force resultants (Q_x') 94
6.9 Non-dimensional circumferential transverse shear force resultants (Q_ϕ') 95
6.10 FEM plot of the tanker shape resulting from the 2g combined accelerations (side view) 96
6.11 FEM plot of the tanker shape resulting from the 2g combined accelerations (top view) 96
6.12 Detailed FEM plot of the tanker shape resulting from the 2g combined accelerations (side view) 97
6.13 Axial force resultant N_x in the top of the tanker (+z) 99

6.14 Axial force resultant N_x in the bottom of the tanker (-z) 101

6.15 Axial force resultant N_x in the left (+y) and right (-y) side of the tanker 103
6.16 Circumferential force resultant N_ϕ in the top (+z) of the tanker 105
6.17 Circumferential force resultant N_ϕ in the bottom (-z) of the tanker 106
6.18 Circumferential force resultant N_ϕ in the left (+y) and right side (-y) of the tanker 106
6.19 Inplane shear force resultant $N_{x\phi}$ in the top (+z) of the tanker 107
6.20 Inplane shear force resultant $N_{x\phi}$ in the bottom (-z) of the tanker 109
6.21 Inplane shear force resultant $N_{x\phi}$ in the left (+y) and right side (-y) of the tanker 110
6.22 Moment resultants in the top (+z) of the tanker 112
6.23 Moment resultants in the bottom (-z) of the tanker 112
6.24 Moment resultants in the left (+z) of the tanker 113
6.25 Moment resultants in the right (-y) of the tanker 113
6.26 Original and displaced mesh of the validation FEM model 119
6.27 Comparison of the experimental, theoretical and FEM axial and circumferential strains for band 1 at x = 96 mm 123
6.28 Comparison of the experimental, theoretical and FEM axial and circumferential strains for band 2 at x = 108 mm 124
6.29 Comparison of the experimental, theoretical and FEM axial and circumferential strains for band 3 at x = 120 mm 125
6.30 Comparison of the experimental, theoretical and FEM axial and circumferential strains for band 4 at x = 217,8 mm in the middle of the tube 125
6.31 Comparison of the experimental, theoretical and FEM inplane shear strains for all the bands 126

A1	Assembly of the composite road tanker	A 5
B1	Validation model with the position of the strain gauges at x = 96, 108, 120 and 217,8 mm	B 4
B2	Welded assembly of the ribs and rod	B 5
B3	Top bracket for ribs	B 6
B4	Bottom bracket for ribs	B 6
B5	Mounting shaft	B 7
D1	Coordinate systems: 1,2 are principal material coordinates x,ϕ are laminate or arbitrary coordinates	D 4
D2	Geometry of deformation in the $x\phi$ plane	D 8
D3	Inplane force and moment resultants on a flat plate	D 10
D4	Geometry of an N layered plate	D 11
E1	Segment of the tanker shell	E 2
E2	Section of a long circular pipe under the action of bending moments M_o and shearing forces Q_o	E 4
E3	Portion of the tanker between two adjacent rings	E 6
E4	Schematic of a 2:1 ellipsoidal dome showing the radii (a,b), local (x',y') and global (x,y,z) co-ordinates	E 8
E5	Schematic of the road tanker	E 10
F1.1	Variation of hydrostatic pressure from axial acceleration	F 2
F1.2	Beam theory idealisation of A_x acceleration	F 3
F1.3	Schematic showing the acceleration of the shell and ribs	F 5
F1.4	Free body diagram showing the effect of an offset between the reaction line of action and the tanker centre-line	F 6
G1	Orientation of the gauges on the validation model	G 4

G2	Schematic of the wheatstone bridge circuit	G 7
S1	FEM axial force resultants N_x superimposed on the "unrolled" tube	S 2
S2	FEM axial force resultants N_x superimposed on the "unrolled" tube	S 3
S3	FEM circumferential force resultants N_ϕ superimposed on the "unrolled" tube	S 4
S4	FEM circumferential force resultants N_ϕ superimposed on the "unrolled" tube	S 5
S5	FEM inplane shear force resultants $N_{x\phi}$ superimposed on the "unrolled" tube	S 6
S6	FEM inplane shear force resultants $N_{x\phi}$ superimposed on the "unrolled" tube	S 7
T1	FEM axial force resultants N_x superimposed on the "unrolled" tube	T 2
T2	FEM axial force resultants N_x superimposed on the "unrolled" tube	T 3
T3	FEM circumferential force resultants N_ϕ superimposed on the "unrolled" tube	T 4
T4	FEM circumferential force resultants N_ϕ superimposed on the "unrolled" tube	T 5
T5	FEM inplane shear force resultants $N_{x\phi}$ superimposed on the "unrolled" tube	T 6
T6	FEM inplane shear force resultants $N_{x\phi}$ superimposed on the "unrolled" tube	T 7
U1	FEM axial force resultants N_x superimposed on the "unrolled" tube	U 2
U2	FEM axial force resultants N_x superimposed on the "unrolled" tube	U 3

U3 FEM circumferential force resultants N_ϕ superimposed on the "unrolled" tube U 4

U4 FEM circumferential force resultants N_ϕ superimposed on the "unrolled" tube U 5

U5 FEM inplane shear force resultants $N_{x\phi}$ superimposed on the "unrolled" tube U 6

U6 FEM inplane shear force resultants $N_{x\phi}$ superimposed on the "unrolled" tube U 7

LIST OF TABLES

Table		Page
5.1	Band positions and rosette numbers	75
6.1	Voltage readings obtained from strain gauge circuit	115
6.2	Gauge voltage differences and apparent strains	116
6.3	Corrected gauge strains	117
6.4	Geometrical data and theoretical strains	118
6.5	Finite element force and moment resultants	120
6.6	Finite element strains calculated using classical lamination theory	121

LIST OF PLATES

Plate		Page
5.1	The tensile rig for the validation model showing the tensile test machine, validation model, power supply, temperature compensation, multi-meter and plotter	72
5.2	Detail of the validation model showing the positions of the ribs and strain gauges	72

LIST OF SYMBOLS

A - tube cross sectional area (m^2)
A_p - projected area (m^2)
A_r - cross sectional area of the circumferential ring (m^2)
A_x - acceleration in the axial directions (m/s^2)
A_y - acceleration in the sideways direction (m/s^2)
A_z - acceleration in the vertical direction (m/s^2)
b - shear width (m)
b - height of circumferential ring (m)
d_o - tube outside diameter (m)
d_i - tube inside diameter (m)
D - isotropic plate or shell flexural rigidity (Nm)
e_m - measured strain for insignificant transverse sensitivity (m/m)
e_{mx} - measured apparent strain in the axial direction (m/m)
e_{mt} - measured apparent strain perpendicular to the axial direction (m/m)
e_{m-45}, e_{mo}, e_{m45} - measured gauge strain from -45, 0, and 45° direction respectively (m/m)
e_{-45}, e_o, e_{45} - corrected gauge strains for -45, 0, and 45° directions respectively (m/m)
e_a - strain parallel to major axis of gauge (m/m)
e_t - strain perpendicular to major axis of gauge (m/m)
E - Young's modulus for an isotropic material (N/m^2)
E_1 - lamina longitudinal modulus (parallel to fibre direction) (N/m^2)
E_2 - lamina transverse modulus (perpendicular the fibre direction) (N/m^2)
E_3 - lamina normal modulus (normal to the fibre direction) (N/m^2)
E_x - laminate axial equivalent engineering modulus (N/m^2)
E_ϕ - laminate circumfential equivalent engineering modulus (N/m^2)
E_r - laminate radial equivalent engineering modulus (N/m^2)
E_1, E_l- longitudinal Young's modulus (N/m^2)
E_2, E_3, E_t - transverse Young's modulus (N/m^2)

e_x - axial normal strain (m/m)
e_ϕ, e_t - circumferential normal strain (m/m)
F - force (N)
F^p - hydrostatic force on domes (N)
F^d - force due to mass of ends and contents (N)
F_a - axial gauge factor
F_g - gauge factor supplied by the manufacturer
F_t - transverse gauge factor
F_x - axial force (N)
g - acceleration due to gravity (9,81 m/s²)
G_{12}, G_{13} - inplane shear modulus (N/m²)
G_{23} - transverse shear modulus (N/m²)
$G_{x\phi}$ - equivalent laminate elastic inplane shear modulus (N/m^2)
h_{ave} - average liquid head in the dome (m)
I - tube moment of inertia (m^4)
K - transverse sensitivity coefficient
l - distance between circumferential rings (m)
m - mass (kg)
m_f - fibre mass fraction of a laminate
m_t - total mass of tanker contents and shell (kg)
m_c^d - mass of the dome contents (kg)
m_c^c - mass of the cylinder contents (kg)
m_s^d - mass of the dome shell (kg)
m_s^c - mass of the cylinder shell (kg)
m_r - mass of rib (kg)
M - bending moment (Nm)
M_o - moment on the end of a cylinder (Nm)
M_x - axial moment resultant (Nm/m width)
M_x' - dimensionless axial moment resultant ($M_x/(pr_it)$)
M_ϕ - circumferential moment resultant (Nm/m width)
M_ϕ' - dimensionless circumferential moment resultant ($M_\phi/(pr_it)$)
$M_{x\phi}$ - inplane or twisting moment resultant (Nm/m width)
M_y^b - bending moment around the y axis at the back support (Nm) .

N_x - axial force resultant (N/m width)
N_x' - dimensionless axial force resultant = (N_x/pr_i)
$N_{x\phi}$ - inplane shear force resultant (N/m width)
N_ϕ - circumferential force resultant (N/m width)
N_ϕ' - dimensionless circumferential force resultant = (N_ϕ/pr_i)
N_θ - meridianal force resultant (N/m width)
N_r^l - number of large ribs
N_r^s - number of small ribs
p - uniform internal pressure (N/m²)
p(x) - internal pressure varying with x (N/m²)
p_{ave} - average pressure (N/m²)
P - reactive forces acting around the circumference of the ring (N)
Q - first moment of area (m^3)
Q_o - shearing force (N)
Q_x - axial transverse shear force resultant (N/m width)
Q_ϕ - circumferential transverse shear force resultant (N/m width)
r - axis in the radial direction
r - mean radius of the shell $(r_i+r_o)/2$ (m)
r_i - inside radius of cylinder (m)
r_o - outside radius of cylinder (m)
r_s - means a nominal radius of cylinder (m)
δR - change in gauge resistance as a result of strain (Ohm)
R_1, R_2, R_3, R_4 - wheatstone bridge arm resistances (Ohm)
R - original gauge resistance (Ohm)
R_b - reactions at the supports (N)
R_x - reaction force in the axial (x) direction (N)
R_y - reaction force in the sideways (y) direction (N)
R_z - reaction force in the vertical direction (N)
R_z^b - back reaction force in the vertical direction (N)
R_z^f - front reaction force in the vertical direction (N)
t - tube thickness (m)
t - cylinder and dome thickness (m)
T - torque, moment of a couple (Nm)

t_b - thickness of back dome (m)
t_f - thickness of front dome (m)
V - shear force (N)
V_z - shear force in the vertical direction (N)
V_f - fib e volume fraction of a lamina
V_{in} - wheatstone bridge excitation voltage (V)
V_{out} - wheatstone bridge output voltage (V)
w - load per unit length for baneding (N/m)
w - shell deflection in the radial direction (m)
x - axis in the axial or longitudinal direction (m)
x' - local axis in the radial direction for dome (m)
x_b - inside depth of back dome (m)
x_c - distance from tan line to back support (m)
x_d - distance from front support to tan line (m
x_f - inside depth of front dome (m)
x_l - unsupported span of cylinder between support (m)
x_{cyl}, L, x_t - length of cylinder tangent to tangent (m)
Xt - lamina longitudinal tension strength (N/m^2)
Xc - lamina longitudinal compression strength (N/m^2)
y - global co-ordinate direction in the sideways direction
y' - local axis in the axial direction for dome (m)
Y_e - Offset between force and neutral axis (m)
Yc - lamina transverse compression strength (N/m^2)
Yt - lamina transverse tension strength (N/m^2)
z - axis in the vertical direction

GREEK SYMBOLS

ρ - mass density (kg/m_3)
ρ_c - mass density of contents (kg/m_3)
ρ_s - mass density of shell (kg/m_3)
ρ_r - mass density of rib (kg/m_3)
ρ_d - mass density of dome (kg/m_3)

ν - isotropic Poisson's ratio
ν_{12}, ν_l - longitudinal Poisson's ratio
ν_{23}, ν_t - transverse Poisson's ratio
ν_o - Poisson's ratio of the standard calibration material
$\nu_{x\phi}$ - Equiv. laminate elastic in plane position ratio
τ_{12} - shear strength direction 12 (N/m^2)
τ_{13} - shear strength direction 13 (N/m^2)
τ_{23} - shear strength in direction 23 (N/m^2)
τ - shear stress (N/m^2)
τ_{max} - maximum shear stress (N/m^2)

SUPERSCRIPTS

^{b} - back
^{c} - contents
^{d} - dome
^{f} - front

SUBSCRIPTS

$_1$ - longitudinal in the fibre, axial (x) direction
$_2$ - transverse to the fibres in the plane of the lamina, circumferential(ϕ) or sideways (y) directions
$_3$ - transverse to the fibres normal to the plane of the lamina, radial (r) or vertical (z) directions
$_a$ - axial direction for strain gauges
$_c$ - contents
$_r$ - radial direction
$_s$ - shell
$_t$ - transverse direction for strain gauges
$_x$ - axial direction
$_y$ - sideways direction
$_z$ - vertical direction

ϕ - circumferential direction

COMPOSITES MATRIX DEFINITIONS

[A] - extensional stiffness matrix
[B] - coupling stiffness matrix
[D] - bending stiffness matrix
$\{e^o\}$ - laminate centreline strain vector (m/m)
{k} - laminate curvature vector
[Q] - reduced stiffness matrix
$[\bar{Q}]$ - transformed reduced stiffness matrix
[S] - compliance matrix
[T] - transformation matrix
$[T]^{-1}$ - inverse transformation matrix
$\{\sigma_1\}$ - stress vector in the lamina direction
$\{\sigma_x\}$ - stress vector in the global co-ordinate direction

1 INTRODUCTION

Glass reinforced plastic (GRP) road tankers have been in operation since 1963 when the first units were built in Europe. Since then thousands have been manufactured in Continental Europe, United Kingdom, Australia, Argentina, Canada and the USA and are used by some of the worlds largest petrochemical companies such as Chevron, Gulf Oil, BP, ESSO and Shell.

1.1 Features of GRP Road Tankers

The popularity of GRP tankers can largely be attributed to the special advantages they have over equivalent metal tankers. These have been mentioned in detail by various operators and manufacturers of these tankers (see Appendix V) and are summarised below.

1.1.1 Capital cost

Many of the GRP designs had a price advantage over metal tankers, especially when materials such as stainless steel and aluminium alloys were required. The manufacturing energy required for a GRP tanker was also less than for a metal tanker.

1.1.2 Corrosion resistance

The excellent corrosion resistant properties of GRP allowed for the transportation of a large variety of chemicals. This was determined by the selection of the resin system and could be further enhanced with the addition of a thermoplastic liner as part

of the corrosion barrier. This versatility enabled a single tanker to carry a variety of cargos.

1.1.3 Range of chemicals

Below is a list of some the chemicals which have been successfully transported in GRP tankers:
Food products such as milk, beer, wine, spirits, mineral water, vinegar, sugar and pharmaceuticals. Hydrocarbons such as petrol, diesel, jet fuels, hot fuel oils, hot lubricating oils, plasticisers, polymeric emulsions, alcohols, methanol, ethanol and styrene monomer. Chemicals such as sulphuric, hydrochloric, nitric, formic, muriatic and phosphoric acids, corrosive alkalies, caustic soda, bleaches, fertilisers, sodium hyperchlorate, spent pickle liquor and various chemical waste products. GRP has also been used to carry cold liquids and gases since the material did not exhibit the low temperatures ductile to brittle transition typical of most metals.

1.1.4 Maintenance

The smooth inner surface and seamless construction facilitated easy cleaning of the tanker and reduced the risk of contamination of the new cargo. Steam cleaning could be used as long as it did not exceed the allowable temperature of the corrosion barrier. The GRP did not suffer from chemical saturation problems associated with rubber liners, which were costly to maintain and replace. Rupture of these liners could result in severe corrosion damage in metal tankers. The GRP gave greater cargo versatility and extended service life and this has been further proven by the use of GRP lined metal tankers. A GRP tanker required little

maintenance and this resulted in less downtime and lower running costs. Repairs to the tanker did not require a totally gas free environment as no welding was required. Visual inspection of the laminate for corrosion or cracking would also be facilitated by the use of a clear unpainted laminate.

1.1.5 Structural

The high strength to weight ratio of GRP and the optimisation of material thickness and layer orientation offers considerable weight savings over metal designs. This resulted in an increase in payload for the same gross vehicle mass. GRP does not suffer from work or age hardening and has good fatigue properties. The impact properties of the GRP tankers are superior due to the seamless construction, larger shell thickness and the material's resilience and flexibility. In the event of a roll over accident GRP would not cause sparks and thus reduces the chance of ignition of any spilt flammable cargo. The use of a rectangular sandwich construction gave unsurpassed insulation, impact and fire survivability properties. This construction has improved structural efficiency which resulted in an increased payload. The lower centre of gravity improved the roll resistance and road holding.

1.1.6 Thermal

The lower coefficient of thermal conduction and thicker shell of a GRP tanker resulted in excellent thermal insulation properties. This was an advantage when transporting liquids at higher or lower temperatures as supplementary insulation could be avoided. Thermal properties also affected thermal stresses and reduced thermal fatigue during loading with hotter or colder cargoes.

1.1.7 Fire resistance

Perhaps the most surprising advantage of GRP tankers is the fire survivability in a fire engulfment accident. This could be attributed to the improved insulation and increased wall thickness of the GRP tanker shell which limited the heat from the fire from heating the contents. Tests carried out by the UK Ministry of Defence (1978) showed that the contents of both steel and aluminium tanks began to boil after a short time and actually fuelled the fire resulting in further damage or an increased explosion [illegible]e testing of the GRP tank resulted in the content's temperature being raised by only a few degrees during the entire duration of the fire test. Although the outer layer of the laminate had been charred, the glass fibres held it intact and insulated the inner layers from further burning and heat transfer.

1.1.8 Manufacture

Various processes have been used and these include hand layup, filament winding, sandwich construction and resin transfer. The reinforcement materials used were commonly E-glass and included woven roving (WR), unidirectional rovings (UD), chopped strand mat (CSM) and filament wound (FW) rovings which were laminated with either polyester, vinylester or epoxy resins. The variety of processes and materials enabled either series or one-off production to be economical.

1.1.9 Regulations

GRP tankers have been accepted by various regulatory bodies and these include:

- European Agreement concerning the transport of Dangerous products by road (ADR).
- U.K. Health and Safety Executive (HSE).
- U.S. Department of Transport (DOT).

1.1.10 Special considerations

There are however special considerations in the design and use of GRP tankers which warrant discussion. Due to the good electrical insulation properties of the material, special precautions must be taken to ensure that there is no buildup of electrostatic charge. The decreased stiffness of the tank warrants a more careful evaluation of the natural frequencies and buckling modes. Strict quality control of the design and manufacture of the tankers is essential as a GRP tanker would not have the large safety margins that are typical of the various GRP pressure vessel design codes. Special attention must also be given to the torsional stresses resulting from twisting of the shell. These could cause problems as a result of the relatively low inplane and interlaminar shear stresses of the filament wound materials.

1.2 GRP Road Tankers for Southern Africa

Considering the world-wide use of GRP tankers, it was surprising to discover that the South African experience was limited to a few GRP tanks which had been mounted on flat-bed trucks. A local GRP manufacturer had made enquiries overseas with respect to licensing agreements but was unsuccessful. Subsequent attempts to design these vehicles from existing GRP pressure vessel standards such as BS 4994 (1987) met with limited success due to the complexity of the load cases. Standards for metal road tankers were

of limited use as they gave wall thickness guidelines for metal tankers only. Although a number of local tanker manufacturers had considered GRP tankers, they felt that the design and manufacture of these vehicles was beyond their capabilities.

1.3 Overall Aims of the Study

A road tanker shell experiences varying loads in the course of its lifetime. These include static and dynamic loads during normal road use, pressure loads during test and product discharge conditions and impact loads during an accident. Clearly these are more complex than the pressure and bending loads experienced by a static horizontal tank. Approximately 14 different load conditions can apply but only two are covered by this research.

The effect that liquid surging has on the tanker's shell and supports has not been well documented. Belanger (1972) and Kenney (1966) have both mentioned the lack of understanding of road tanker stresses. The GRP tank design standard BS4994 (1987) states that tankers required special consideration and BS5500 (1988) states that road tankers are beyond the scope of that standard. The loading conditions are however more clearly defined by SABS 1398 (1983) and Kenney (1966). As there were no GRP tankers available locally for experimental testing, use was made of the ABAQUS Finite Element Method (FEM) program to model the effect of the liquid accelerating against the shell. A scale model of a filament wound tube mounted in metal supports, loaded in combined tension and bending was also evaluated. This allowed comparison of the FEM, theoretical and strain gauge results and served to validate the FEM method. The FEM road tanker model was also checked by comparing the analysis of a pure internal pressure case to a theory of elasticity analysis. The most severe

service condition (excluding accidents) were then modelled on FEM and compared to an analysis based on beam theory and elasticity.

2 LITERATURE SURVEY

Despite the large amount of service and marketing data available on GRP road tankers, technical information on the effects that the acceleration of liquids has on the tanker shell is limited. There is a draft standard for GRP tankers and various metal road tanker standards, but these are of limited use in this respect. Pressure vessel standards for metal and GRP tanks consider road tankers to be beyond their scope (BS 5500 -1988) or that they require special consideration (BS 4994-1987). The loading of a stationary horizontal tank covered by these standards does not include the twisting, acceleration of the liquid and vibration that the road tanker experiences.

One of the works most relevant to this study was by Kenney (1966) who described in detail the design, analysis and testing of a hand layup GRP tank which was mounted with five supports onto the sub-chassis of a truck. The load cases analysed were as follows:
- internal pressure of 1,4 Bar.
- vertical loading equivalent to five times normal gravity (5g).
- angular twist of 6°.
- a combination of all of the above applied simultaneously.

The tank material consisted of a hand-laid chopped strand mat (CSM) and woven roving (WR) laminated with polyester resin which was tested for strength and stiffness properties. Beam theory was used to analyse bending with the tank and the contents were modelled as a uniformly distributed load on a beam of equivalent length. All the calculations for bending, pressure and torsion assumed an isotropic strength of materials approach to calculate the principal stresses and directions. The effect of the material anisotropy, supports, ring stiffeners and end closures were ignored. After the manufacture of the tank, strain gauges were

located on the outside and tests were carried out in an attempt to simulate each of the loading conditions. Both the pressure and torsion tests were representative of the predicted loading. The bending simulation was however unrepresentative of the loading which results from the acceleration of the liquid and shell. The results of the combined tests did however produce some interesting results as follows:

- the torsional stresses were much higher than bending and pressure stresses.
- the principal directions were similar to theory.
- the principal stresses were approximately 20% higher than predicted.

In conclusion the author mentioned that the use of normal isotropic elastic theory was a large source of error and further work was necessary to predict more accurately the failure of GRP structures under complicated load conditions. He felt that filament winding was not ideal as interlaminar failure would occur under severe twisting, and mentioned that a tanker on fewer supports would tend to have its mountings pushed through the shell if it was not properly reinforced.

In contrast to the opinions of Kenney, Belanger (1972) discussed the development of a successful filament wound, self supporting road tanker. Although no design formulae were presented, he mentioned that the maximum and minimum stresses could be estimated by calculation but that their combination was almost unpredictable. This effect varies the direction of the principal stresses and he considered winding at a fixed helical angle ($\pm\theta$) to be too dangerous.

Experimental research was done by Zick (1951) on the stresses in horizontal steel vessels with saddle supports. The importance of

supporting the tank on only two saddles was emphasised as it is easier to determine the load share between them. He stated that horizontal vessels resting on saddle supports behave as beams. Much of his work dealt with the stresses at the saddles and several formulae were presented, most containing empirical constants determined from experimental tests on steel tanks. The road tanker load cases analysed cannot use Zick's analysis due to the complexity of the loadings, which act in the axial, vertical and lateral directions.

Some useful data was obtained from various South African road tanker manufacturers. A company called TFM (Pty) Ltd (1986) had commissioned an experimental strain gauge study on one of their 36000 litre welded aluminium road tankers after the discovery of cracks. The tanker was tested by loading with water (both half and full), tilting the full tank and then twisting the one end of the tanker relative to the other. A theoretical analysis based on beam theory considered the tanker and cargo weight as a uniformly distributed load acting on an equivalent beam, supported by the bogie and king pin respectively. Even with stress concentration factors of 2 to 3, the measured stress levels were not high enough to cause failure. Good correlation was achieved between theoretical and experimental results. Although no conclusions could be drawn from this study, the author mentioned that either metallurgical defects or harmonic resonance could have caused the cracking.

Design information was also obtained from another South African tanker manufacturer, Henred Freuhauf (1986). These were tender calculations for circular road tankers and were based on beam theory. The loadings consisted only of a vertical acceleration of 2g. A further calculation was made for a vertical acceleration of 1,5g as recommended by Freuhauf Omaha, the USA parent company. In

both cases the maximum stresses were limited to 20% of the ultimate tensile strength of the material as also specified by SABS 1398 (1983) and DOT MC-306. No mention was made of any other loadings.

Various standards covering road tankers and horizontal tanks are mentioned below. Although they do not present formulae to cover the load conditions experienced by a tanker, they give some indication of the superimposed loads and maximum stress values considered in the design of metal road tankers.

A United Kingdom draft specification (1985) covers a wide range of topics concerning the design, materials, construction, testing and repair of GRP tankers. According to this document, the vehicle must be designed to comply with relevant national requirements. Minimum test values for strength and stiffness are recommended for a variety of reinforcements when laminated with polyester resin. The acceptable range of glass content is specified. The laminated tank should consist of an outside surface layer, a chemical resistant inner layer and the structural laminate which must withstand all the design loads. A table is presented for minimum shell wall thicknesses which are given as a function of the volume, length, radius and stiffener spacing of the tanker. Requirements for stiffener spacing are also given. The tank mountings and means of attachment must be designed to withstand a static loading in any direction equal to twice the weight of the filled tank and attachments using a safety factor of four. When the tank constitutes the stress bearing member, it must be designed to withstand the stresses imposed. The use of directionally biased reinforcement must be carefully designed and controlled to align the high strength fibres in the correct direction. This standard does not however give any formulae on which a design can be based, nor are further

loading conditions mentioned for the tanker shell.

The combined acceleration loadcase covered by this thesis is a requirement from SABS 1398 (1983). It contains a section on design and relevant points are summarised: The capacity shall be such that when fully loaded the tank mass does not exceed the appropriate provincial road traffic ordinances. The maximum calculated stress values, which include stresses from design pressure, dynamic loading, fatigue loads and additional loads from auxiliary equipment, shall not exceed 20% of the tensile strength of the material used for its construction. Each tank and its structural attachments shall be designed to withstand a dynamic load equal to 19,6 m/s^2 (2g) in all directions under all load configurations. The loads from supports shall be borne by bulkheads, baffles or ring stiffeners and shall be distributed when practicable by using doubler pads or other means of avoiding stress concentrations. This standard also gives information regarding minimum wall thicknesses, circumferential reinforcement thickness and spacing, overturn protection, fittings, attachments and construction and inspection details for metal road tankers. No further information is given on the method of analysis to be used for the design of tankers.

An American standard which was used by Henred Freuhauf (1986) for the design of metal tankers was the DOT MC-306 (1981). The content is very similar SABS 1398 (1983) but does mention that the standard is not valid in conditions where the ASME pressure vessel design requirements apply. The values for the dynamic loadings are not mentioned except that the tanker must be able to sustain a rear impact equal to twice the load of the fully laden tanker. Another standard which also deals with metal road tankers is the Australian Standard AS 2809.1 (1985). This is very similar in content to SABS 1398 (1983) and DOT MC-306 (1981). Part 2 of

this standard, AS 2809.2 (1985) recommends that the design load for the tank and its attachments shall not be less than twice the mass of the tank, cargo and attachments. Hydrostatic pressure test, and stresses caused by the weight of equipment, reactions at the supports and thermal gradients must also be taken into account.

Another standard which appears to be derived from DOT MC-306 (1981) is the American ANSI/NFPA 385 (1985) which also recommends that the tank is required to be anchored with restraining devices which prevent relative movement between the tank and its supports. Mention is made of the 2g axial acceleration which the tanker must survive in the event of a rear collision. The overturn protection must be able to survive a 2g vertical load and a horizontal load in any direction equivalent to half the weight of the loaded tank.

A standard which provides information on the design of horizontal tanks is BS 5500 (1988). The formulas and correction factors are based on experimental work by Zick (1951) and beam theory is used with the assumption that the shell remained circular. The weight of the contents, tank and attachments are represented by a uniformly distributed load acting over an equivalent length. Force equilibrium, shear force and bending moment diagrams are evaluated. Equations for maximum bending moments, longitudinal stresses at mid-span and the supports; tangential, circumferential and shearing stresses at the saddles as well as approximations of stresses for internal ring stiffener supports are presented. The BS 5500 analysis does not cover the other loading conditions such as the axial and sideways acceleration and twisting of the tanker. The relationships and correction factors presented apply only at specified positions and for certain configurations.

The BS 4994 (1987) standard for the design and construction of vessels and tanks in reinforced plastics can be successfully applied for the design of filament wound GRP tanks. The requirements for the design, materials, construction, inspection, testing and erection of GRP vessels with or without a thermoplastic liner are specified. The standard recommends that vessels and tanks for transporting liquids require special consideration. The minimum factor of safety of eight ensures that environmental cracking is avoided This design factor is modified for deterioration of the materials, the effect of temperature and repeated loadings. For filament wound tanks there is also a further requirement that the behaviour of a vessel under combined loads be evaluated by a rigorous anisotropic stress/strain analysis. The response of the material must then be examined to ensure that the shear and normal strains present in each layer are less than the allowables. Alternately, the filament wound tank must be checked using a bi-axial design envelope. Design formulas for horizontal tanks are presented and based on beam theory. No mention was however made of any shear stresses although limits are specified on the compressive load to avoid buckling. Localised forces and moments at the supports are however not covered.

3 ANALYTICAL WORK

The two different loading conditions analysed in this research are combinations of the following:
- uniform internal pressure
- acceleration in the axial direction (A_x).
- acceleration in the sideways direction (A_y).
- acceleration in the vertical direction (A_z).

Use is made of the finite element method to analyse the effect of various combinations of these loads on the tanker. These results are compared to strength of materials and elasticity theory. The analysis of composite materials also requires special consideration. These topics are discussed in more detail in sections 3.1 to 3.5

3.1 Theory for Internal Pressure

The most common methods of discharging road tanker cargoes is either by pumping, gravity or pressure discharge. Corrosive chemicals are often unloaded by pressure discharge using compressed air at the off-loading site. This is popular with haulers of corrosive chemicals as the danger of accidental spills and the need for special corrosive resistant valves and pumps is avoided. Belanger (1972) stated that pressures of up to 2,4 Bar are used during emptying and that the GRP tankers were pressure tested yearly to 3,5 Bar. Minsker (1973) stated that GRP tankers were initially tested at 3,9 Bar and then yearly at 1,9 Bar. During testing the tanker was filled with water which is then pressurised. The incompressibility of the water makes this procedure less dangerous but tends to induce bending loads onto the shell as a result of the water's weight. In order to check

the accuracy of the FEM road tanker model, a pure pressure load of 8,4 Bar is modelled and then compared to an analysis based on the theory of elasticity. To facilitate accurate comparison, the tanker is assumed to contain gas pressure only, ie, the cargo has low density which does not contribute to bending in the shell. The self-weight of the tanker shell is also neglected for this analysis and this allows for accurate comparison without considering the associated bending effects. Global bending could complicate the analysis around the supports (Brownell, 1959). The value of 8,4 Bar is the pressure which gives the same maximum tensile stress as the 3,5 Bar pressure combined with the bending stresses induced by the water (see Appendix E). This pressure also corresponds to six times the operating pressure of 1,4 Bar recommended by Belanger (1972), and six times the operating pressure as recommended by the ASME 10 (1989) design standard for GRP vessels. The dynamic acceleration of the liquid cargo also results in pressure loads from within the tanker shell which are caused by the hydrostatic action of the liquid accelerating towards the ends of the tank. A full cargo of sulphuric acid accelerating at 19,61 m/s (2g) over a tanker length of 12,65 m could result in a maximum pressure of 4,6 Bar from the hydrostatic effects alone (neglecting surges and splashing).

For areas remote from any stress concentrations, the membrane stress analysis of Timoschenko (1959), Roark (1976) and Bruhn (1973) are valid. These membrane stresses can be written as stress resultants in the axial and tangential direction as follows

$N_x = p.r/2$ (Eqn 3.1)

$N_\phi = p.r$ (Eqn 3.2)

Due to the bending stiffness of the tanker shell, it may also carry transverse loadings by flexural stresses. Discontinuities

such as edges, holes, domes and stiffeners result in variations from membrane stress theory. The analysis of domes and the stresses at the dome-cylinder junction were discussed by Uddin (1986) and Szyszkowski (1987). For areas near the domes and ring stiffeners, the theory must be modified to accommodate the discontinuities that exist. The theory used here is based on an elasticity shell analysis by Timoschenko and Woinowsky-Krieger (1959). Although these equations are derived for isotropic shells, the orthotropic behaviour of the this tanker shell allows the use of the relationships for the theoretical prediction of the axial and circumferential force resultants. This requires the determination of the equivalent extensional and bending stiffnesses, these being obtained from classical lamination theory. The theoretical prediction of the transverse shear resultants Q_x and Q_ϕ and moment resultants M_x, M_ϕ, and $M_{x\phi}$ using the relationship from Timoschenko would be less accurate as these are highly dependent on the laminate construction and orientation. Timoschenko (1959) covered the general theory of cylindrical shells as well as the deformation of shells without bending. The theory accounted for the influence of the ring stiffeners and the discontinuity between the cylinder and dome of the road tanker and is summarised in Appendix E.

3.2 Theory for Axial, Bending and Circumferential Stresses Arising from Acceleration A_x in the Axial Direction.

When the tanker slows down at an axial acceleration A_x, the cargo and shell of the tanker are affected. Discussed below is a representation of what influence the axial acceleration would have on the stresses in the tanker shell. The magnitude of this acceleration (A_x) is specified by SABS 1398 (1983) to be 2g or 19.6m/s^2. This will occur during heavy braking and for this

analysis it is assumed that the rear bogie provides all of the braking force. Because the tanker is full and unbaffled, the cargo will exert a hydrostatic pressure under the influence of the acceleration. This will vary linearly with the length as shown in Figure 3.1. However, the following assumptions are made to allow the use of beam theory for the theoretical predictions.

- The centreline of the tanker is taken as the centreline of the beam. This assumption is justified by the geometry of the saddle support which has an included angle of 120° and is connected to a stiff circumferential ring. The effect of this assumption is checked by varying the theoretical offset between the beam centre-line and the bottom of the tanker.

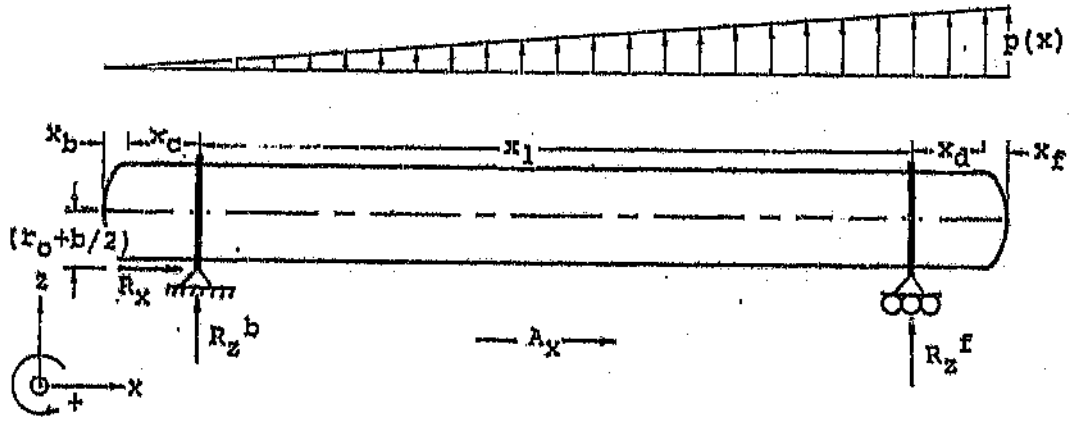

Figure 3.1 Variation of hydrostatic pressure due to axial acceleration A_x.

- The back support position is further simplified for this analysis. The axial reaction R_x will normally act at the road surface between the wheels and the road. Due to the difficulty of accurately representing the exact influence of the bogie on the shell with the spring and bogie flexibility, the above

idealisation is used to allow for comparison between FEM and beam theory.

- The back support is approximated by a pinned connection at the second rib from the rear. This is a worst case as the load will be shared between all the supports on a real tanker. A correct model of the exact load sharing between the supports will however require a model of the bogie and suspension geometry and is beyond the scope of this research. The assumption of all of the load passing into one support at the back is widely used in industry. Its validity is also checked by the evaluation of a validation model discussed in section 3.2.
- The entire axial braking reaction is absorbed by the rear support. This occurs when the bogie exerts the entire braking force and in reality, the bogie will provide the bulk of the braking in order to avoid jackknifing. This is an effect where the rear of the tanker slews sideways during heavy deceleration.
- The front is constrained in the vertical (z) direction but is free to move in the axial direction. This will impose the most severe axial loading as the entire shell between the supports will experience the axial force due to the pressure on the head.

The acceleration A_x results in three effects which are discussed separately. These are:

- the liquid's hydrostatic pressure results in an axial force which acts on the front dome and produces elongation and bending of the shell.
- the liquid's hydrostatic pressure results in circumferential stresses in the shell.
- the density of the cylinder, ribs and dome material result in stresses arising from the acceleration of the material.

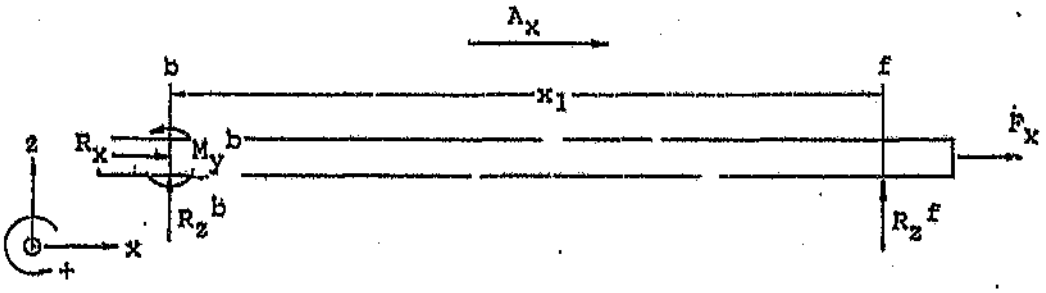

Figure 3.2 Beam theory idealisation of the A_x acceleration.

3.2.1 Axial elongation and bending forces from hydrostatic pressure

The analysis of the axial elongation and bending forces from hydrostatic pressure are summarised in Appendix F-1.1. All the symbols used here are defined in the derivation of the free body, axial force, shear force and bending moment diagrams and the results are as follows:

For axial force:

For $x_o \leq x \leq x_t$: $F_x = -R_x$

For $x < x_o$: $F_x = 0$ (Eqn 3.3)

For shear force:

For $x < x_o$: $V_z = 0$

For $x_o \leq x \leq (x_o+x_1)$: $V_z = R_z{}^b$

For $x \geq (x_o+x_1)$: $V_z = 0$ (Eqn 3.4)

For bending moment:

For $x < x_c$: $M_y = 0$.

For $x_c \leq x \leq (x_c+x_1)$: $M_y = R_z{}^b.(x - x_c) - M_y{}^b$

For $x > (x_c+x_1)$: $M_y = 0$ (Eqn 3.5)

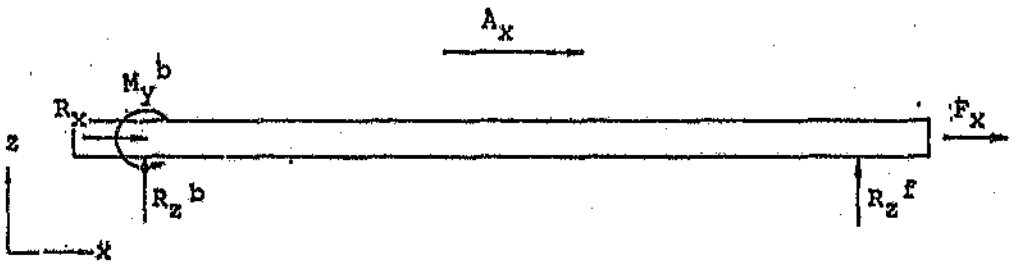

Figure 3.3 Free body diagram.

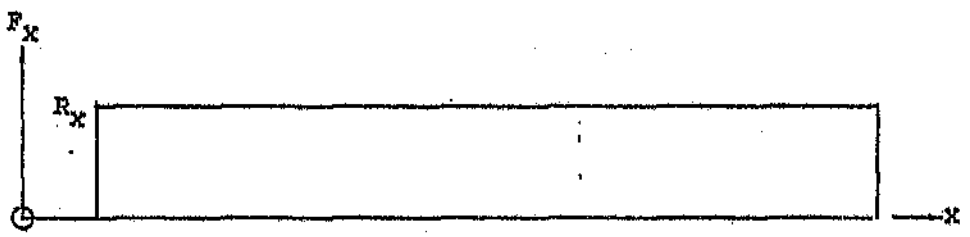

Figure 3.4 Axial force diagram.

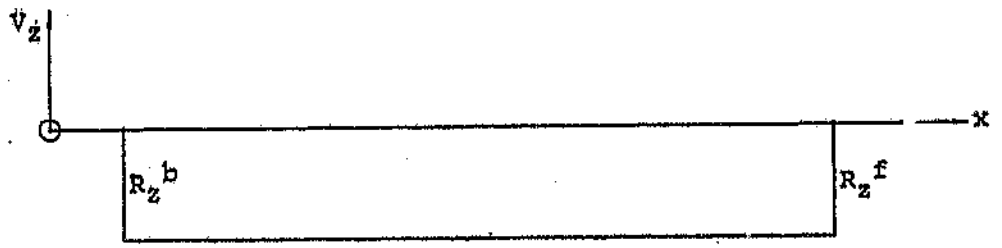

Figure 3.5 Shear force diagram.

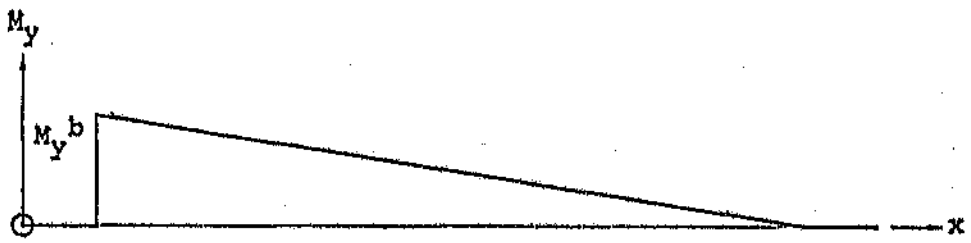

Figure 3.6 Bending moment diagram.

3.2.2 Circumferential stresses from hydrostatic pressure

The hydrostatic pressure resulting from the acceleration in the axial direction also causes circumferential or hoop stresses which are superimposed on the axial and bending stresses. For a cylindrical vessel with a dome in the shape of a 2:1 ellipsoid, this pressure p(x) varies as a function of x:

$p(x) = \rho_c . A_x . (x + r_i/2)$ for $0 \leq x \leq (x_t + x_f)$ (Eqn 3.6)

Hence the circumferential force resultant can be written as:

$N_\phi = p(x) . r_i$

$= \rho_c . A_x . (x + r_i/2) . r_i$ (Eqn 3.7)

3.2.3 Elongation and bending from the acceleration of the shell

The mass of the shell, ribs and domes also affect the stresses when the tanker decelerates due to the density and inertia of the tank. This acceleration acts as a body force on each of the components which constitute the tanker. These stresses can be calculated from Newton II i.e. $\Sigma F_x = \Sigma m.A_x$. This analysis is detailed in Appendix F-2.1 and results in the derivation of the free body, axial force, shear force and bending moment diagrams as follows:

For axial force:

For $0 \leq x < x_c$: $F_x = [m_s{}^d + \rho_s.A.x].A_x$

For $x_c \leq x \leq x_t$: $F_x = -[\rho_s.A.(x_t - x) + {}_x\Sigma^{xt} m_r + m_s{}^d].A_x$

(Eqn 3.8)

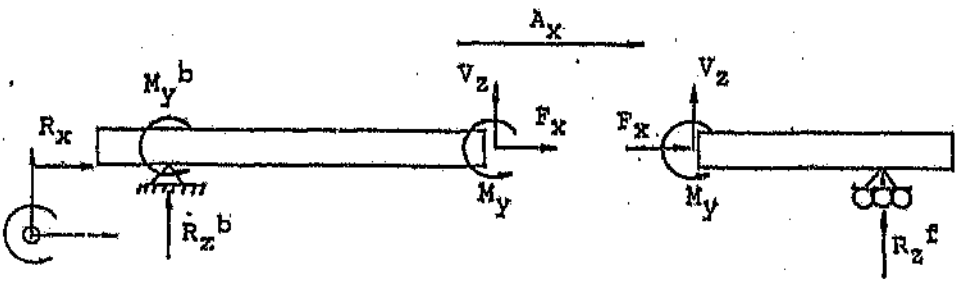

Figure 3.7 Free body diagram.

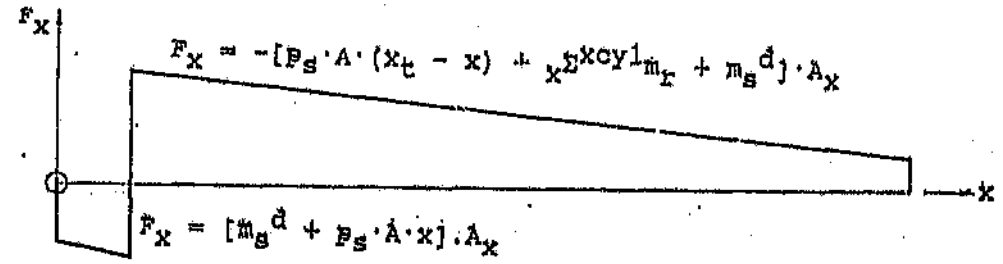

Figure 3.8 Axial force diagram.

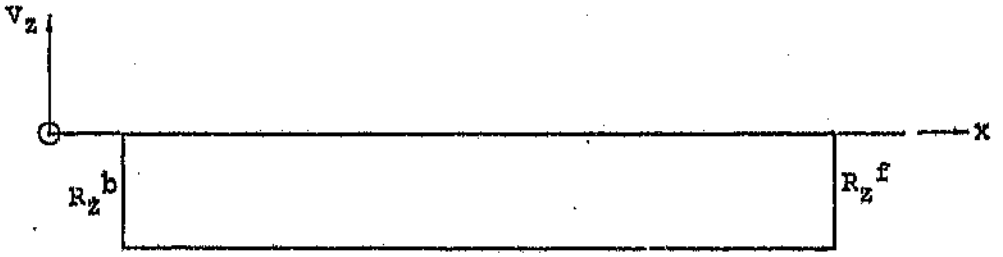

Figure 3.9 Shear force diagram.

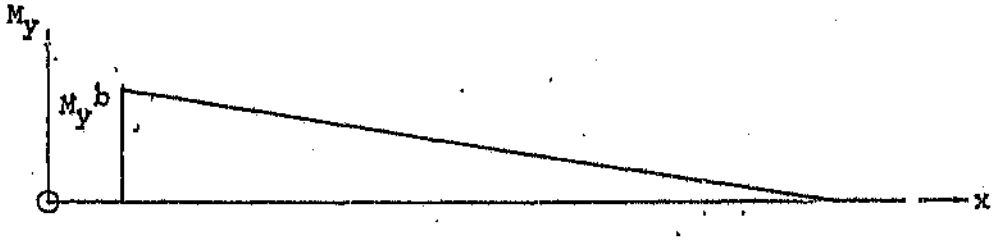

Figure 3.10 Bending moment diagram.

For shearing force:

For $x < x_c$ or $x > x_t$: $V_z = 0$

For $x_c \leq x \leq x_t$: $V_z = R_z{}^b$ (Eqn 3.9)

For bending moment:

For $x < x_c$ or $x > x_t$: $M_y = 0$

For $x_c \leq x_t \leq x_t$: $M_y = -M_y{}^b + R_z{}^b.(x - x_c)$ (Eqn 3.10)

3.2.4 Summation of force resultants due to axial acceleration

The force resultants due to the A_x loadings are as follows:

For axial force resultant N_x:

N_x = ΣBending + ΣAxial Force

$= - (\Sigma M_y.z/I.t) + \Sigma F_x/A.t$ (Eqn 3.11)

For circumferential force resultant N_ϕ:

$N_\phi = p_c.A_x.(x+r_i/2).r_i$ (Eqn 3.12)

For inplane shear force resultant $N_{x\phi}$:

$N_{x\phi} = \Sigma V_z.Q/(I.b).t$ (Eqn 3.13)

3.3 Theory for Axial, Bending and Circumferential Stresses Arising From Acceleration in the Vertical (z) and Horizontal (y) Directions

SABS 1398 (1983) requires the tank to withstand a vertical and sideways acceleration of 19.6 m/s^2. This will produce two effects namely:

- A uniformly distributed load across the tanker due to the mass

of the shell and its contents.
- A hydrostatic pressure which will vary linearly with the distance across the diameter of the tanker.

Roark and Young (1976) mentioned that a cylindrical tank supported at intervals on saddles and filled with liquid are difficult to analyse for stress. The results are often rendered uncertain by doubtful boundary conditions. However, from experimental studies it was concluded that for a circular tank supported at intervals and held circular at the supports by rings or bulkheads, the ordinary theory of flexure is applicable if the tank is completely filled.

Consider the bending loads induced by the weight of the tanker and its contents. The tanker is considered in the completely full condition. The lack of baffles does not allow for partial filling of the tanker as the surge effects will have a very severe effect on the tanker stress levels.

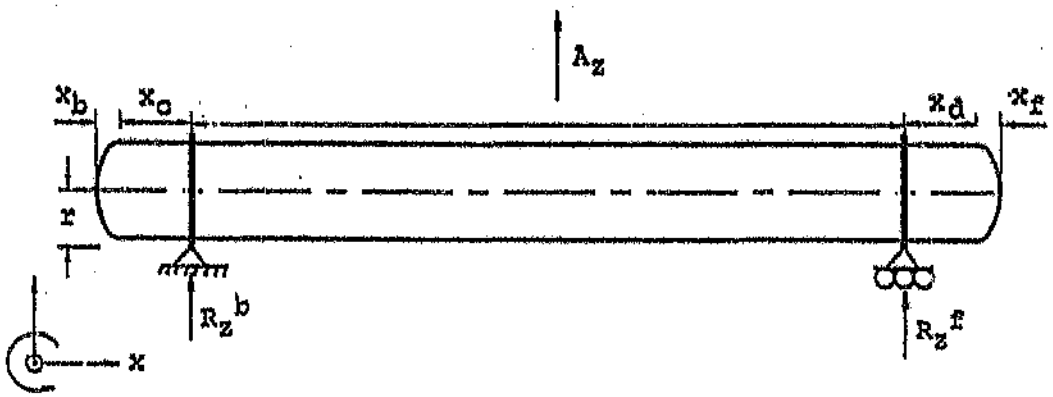

Figure 3.11 Schematic for the tanker under a vertical acceleration.

There is a difference in the support reaction for the vertical and horizontal direction. Because the acceleration A_y acts through the centre of the tanker and the supports are at the bottom, there is an additional toppling moment being exerted on the shell which occurs about the longitudinal axis. Brownell (1959), Roark (1976) and Timoschenko (1984) did not cover this loading geometry for beams as they are assumed to be symmetrically supported at their centre-line. The sideways reactions are not constant and will vary with sideways position along the support. The flexibility of the ring, support, shell chassis and springs will all have an effect in this variation. To allow the use of beam theory for the A_y acceleration, the assumption was made that the vertical and sideways support reactions are the same and that the reactions act at the neutral axis of the shell.

The alternative analysis of the effect of this overturning moment is difficult using beam theory as the effect is localised at the supports. Only an elasticity or experimental analysis could provide some comparison to the FEM model. This is however beyond the scope of this research and hence the sideways bending is modelled analytically using simple supports and the formulas 3.14 to 3.39 derived for the vertical (z) direction.

To allow the use of beam theory certain assumptions have been made in this research. The entire load of the tanker is assumed to act through two supports, one at either end. This problem is therefore reduced to statically determinate and can be solved. This assumption allows the evaluation of a worst case scenario where only one of the four back supports and one of the two front supports are bearing all the load. The assumption of a single support at each end is widely used by the tanker designers Henred Freuhauf (1985) and TFM (1978). This assumption also allows the use of design codes for horizontal tanks (BS4994 (1988), BS5500

Freuhauf (1985) and TFM (1978). This assumption also allows the use of design codes for horizontal tanks (BS4994 (1988), BS5500 (1988) and ASME 10 (1989)) for comparison.

From BS5500 (1988), the beam load per unit length, w is:

$$w = 2.m_t.A_z/(x_t + 4.x_b/3) \qquad \text{(Eqn 3.14)}$$

where

m_t = total mass of tanker shell and contents

A_z = the vertical acceleration of the tanker and (replaced by A_y for sideways acceleration)

x_t = cylindrical length of tank

x_b = x_f = mean depth of dished end

The hydrostatic force on the ends:

$$F^p = w.r \qquad \text{(Eqn 3.15)}$$

where r = mean shell radius.

The force due to mass of the ends and contents:

$$F^d = 2.x_b.w/3 \qquad \text{(Eqn 3.16)}$$

The reaction at supports (for $x_c = x_d$):

$$R^b = R^f = m_t.A_z/2 \qquad \text{(Eqn 3.17)}$$

The moment M^t consists of the moment due to mass of the dome M^d and the moment M^p due to offset of pressure force F^p:

$$M^t = M^d + M^p$$
$$= -2.x_b.w/3.(3.x_b/8) + w.r.(r/4)$$
$$= 1/4.w.(r^2 - x_b^2) \qquad \text{(Eqn 3.18)}$$

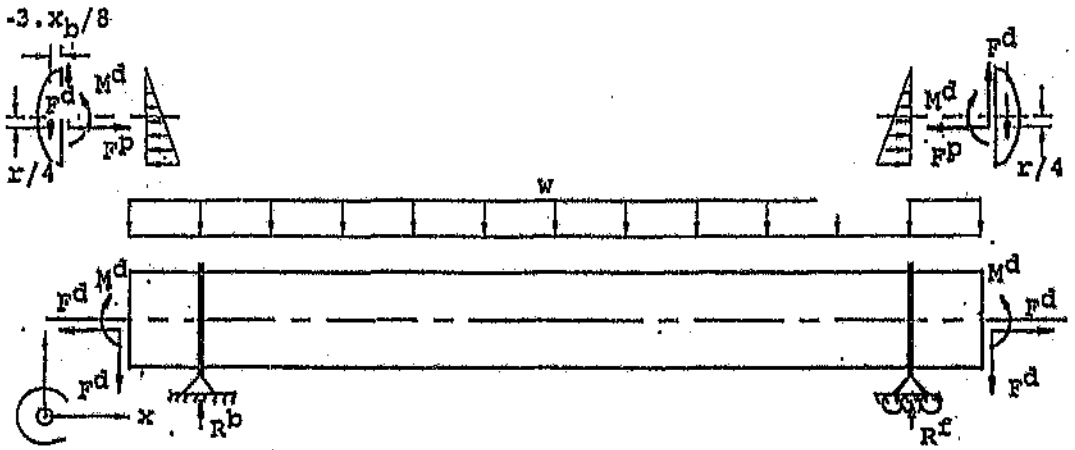

Figure 3.12 Free body diagram.

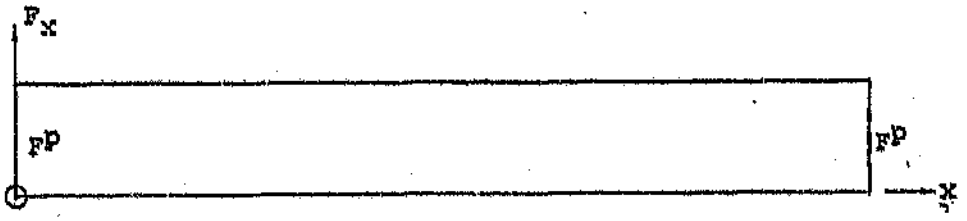

Figure 3.13 Axial force di a.

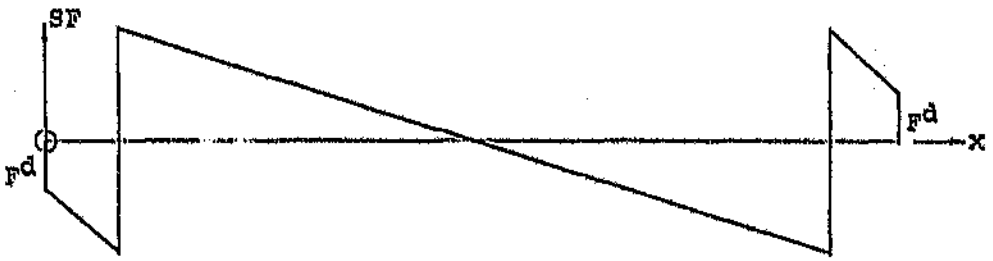

Figure 3.14 Shear force diagram.

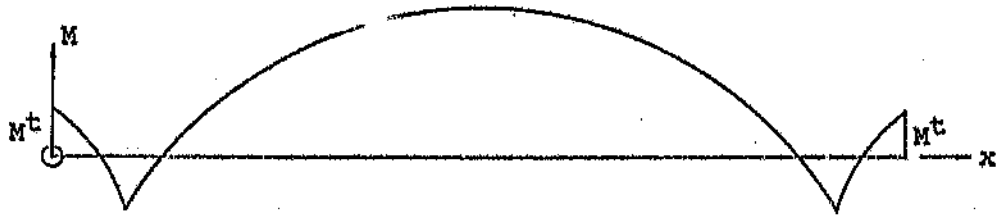

Figure 3.15 Bending moment diagram.

To calculate the equations for the shearing force and bending moment, we consider the tanker as three sections.

Section 1 : Between the back tan line and back support ($0 < x < x_c$)

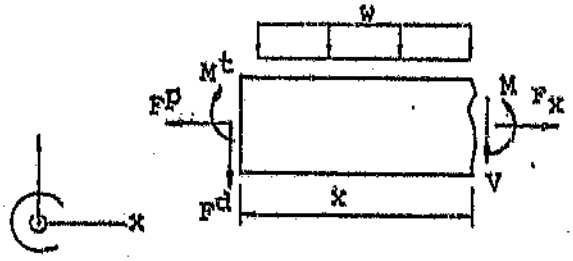

Figure 3.16 Section 1 between back tan line and back support.

$$[\Sigma F_x = 0] : F_x - F^p = 0$$
$$F_x = F^p$$

$$[\Sigma SF = 0] : V + F^d + w.x = 0$$
$$V = - F^d - w.x$$

$$[\Sigma M = 0] : M + w.x.(x/2) - M^t + F^d.x = 0$$
$$M = - w.x^2/2 + M^t - F^d.x$$

(Eqn 3.19)

Section 2 : Between back and front support ($x_a < x < x_t - x_d$)

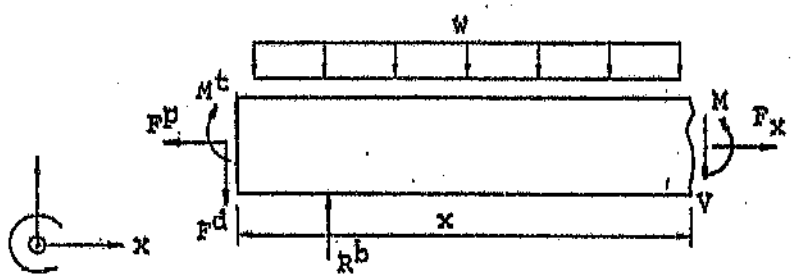

Figure 3.17 Section 2 between back support and front support.

$[\Sigma F_x = 0]$: $F_x - F^p = 0$

$F_x = F^p$

$[\Sigma SF = 0]$: $V + w.(x - x_a) + w.x_c - R^b + F^d = 0$

$V = R^b - F^d - w.x$

$[\Sigma M = 0]$: $M+w.(x-x_c).\ x-x_c)/2+w.x_c.(x-x_c/2)-R^b.(x-x_c)+F^d.x-M^t=0$

$M = -w/2.x^2 + R^b.(x - xc) - F^d.x + M^t$

(Eqn 3.20)

Section 3 : Between front support and front

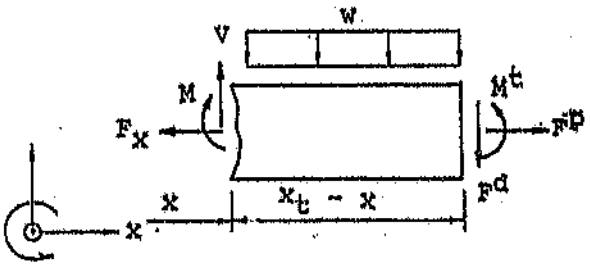

Figure 3.18 Section 3 between front support and front tan line.

$[\Sigma F_x = 0]$: $F_x = F^p$

$[\Sigma SF = 0]$: $V - w.(x_t - x) - F^d = 0$

$V = w.(x_t - x) + F^d$

$[\Sigma M = 0]$: $M + w.(x_t - x).(x_t - x)/2 + F^d.(x_t - x) - M^t = 0$

$M = - w/2.(x_{t2}^2 - 2.x_t.x + x^2) - F^d.(x_t - x) + M^t$

(Eqn 3.21)

3.3.1 Circumferential stresses due to the liquid hydrostatic pressure in the vertical and sideways directions

As well as contributing to the uniformly distributed load and axial loads on the shell, the liquid also exerts a pressure on the shell surface which will result in stresses in the circumferential directions. This pressure is hydrostatic and is a function of the head h which varied lineally from zero at the top of the tank (assumed full) to a maximum at the bottom. The pressure at any point in the tanker resulting from the vertical or

sideways acceleration:

$P = p_c \cdot |A_z| \cdot h$ (Eqn 3.22)

where

p_c = density of cargo

replace A_z with A_y for sideways acceleration

h = head in z or y direction

The head is the distance from the furthest side of the tank and is written in tanker co-ordination as

$h_z = |(z - r_i)|$ for A_z acceleration

$h_y = |(y - r_i)|$ for A_y acceleration (Eqn 3.23)

Note that $|A_z| = |A_y| = 19.6 m/s^2$. The effect of this pressure on the circumferential stress is presented in Roark (1979):

$\sigma_\phi = p.r_i/t$ (Eqn 3.24)

Hence the circumferential force resultants for acceleration in the vertical direction:

$N_\phi = p.r_i$

$= p_c \cdot |A_z| \cdot |(z - r_i)| \cdot r_i$ (Eqn 3.25)

and the circumferential force resultants for acceleration in the horizontal direction :

$N_\phi = p.r_i$

$= p_c \cdot A_y \cdot |(y - r_i)| \cdot r_i$ (Eqn 3.26)

3.3.2 Summation of force resultants due to vertical or sideways acceleration

For axial force resultant N_x for vertical acceleration:

$N_x = \Sigma$Bending + ΣAxial Force

$= - (\Sigma M_y . z/I.t) + \Sigma F_x/A.t$ (Eqn 3.27)

Note that z is replaced by y and M_y by M_z for sideways acceleration.

For circumferential force resultant N_ϕ

$$N_\phi = p_c.A_x.(x+r_i/2).r_i \qquad \text{(Eqn 3.28)}$$

For inplane shear force resultant $N_{x\phi}$

$$N_{x\phi} = \Sigma V_z/(I.b).t \qquad \text{(Eqn 3.29)}$$

Note that V_z by V_y for sideways acceleration.

3.4 Shear Stresses in Beams due to Accelerations in the Axial, Vertical and Sideways Directions

When a beam is subjected to non-uniform bending, both bending moments M and shear forces V act on the cross sections. The normal stress σ_x are obtained from the flexure formula and the shear stresses τ are associated with the shear force V. When a beam has a solid circular cross-section, it cannot be assumed that the shear stresses act parallel to the vertical axis. Timoschenko (1984) shows that the shear stresses at the boundary must act at a tangent to that boundary. Due to the symmetry condition, the shear stress at the centre of the beam will lie parallel to the vertical axis. Certain assumptions are made in the derivation of the formula below: The vertical components of the shear stresses are equal for all positions along line pq. The shear formula derived for rectangular beams are used to derive the equation for circular beams (vertical components). Since the direction of the shear stress is known, its magnitude can be calculated at any point of the cross-section.

Consider the shear stresses τ acting on line pq shown above in Figure 3.21. The first moment of area Q below the line pq with

respect to the y axis must be calculated. An element at a distance z from the y axis, has a thickness dz and length $2.\sqrt{(r^2 - z^2)}$ where r is the radius of the cross section.

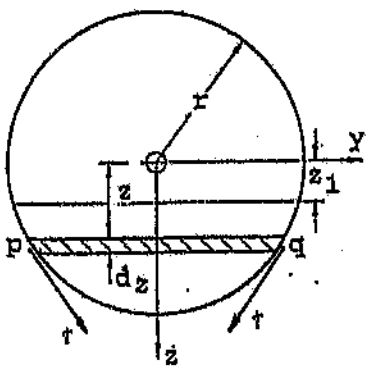

Figure 3.19 Shear stresses in a beam of circular cross section.

The first moment of area of this element is found by multiplying the area by z. Hence the entire Q is calculated as :

$$Q = \int_{z1}^{r} 2.z.\sqrt{(r^2 - z^2)}.dz$$

$$= 2/3.(r^2 - z_1^2)^{(2/3)} \qquad \text{(Eqn 3.30)}$$

The width b is :

$$b = 2\sqrt{(r^2 - z_1^2)} \qquad \text{(Eqn 3.31)}$$

The second moment of area I is :

$$I = \pi/4.r^4 \qquad \text{(Eqn 3.32)}$$

Hence the vertical component of the shear stresses is:

$$\tau = V.Q/(I.b)$$
$$= 4.V/(3.\pi.r^4).(r^2-z_1^2) \qquad \text{(Eqn 3.33)}$$

At a point p on the boundary of the cross section, the total shear stress τ is related by its vertical component, τ_z by the equation:

$$\tau = \tau_z/\cos\theta$$
$$= \tau_z.r/\sqrt{(r^2-z_1^2)} \qquad \text{(Eqn 3.34)}$$

Substitution of τ_z:

$$\tau = 4.V/(3.\pi.r^3).\sqrt{(r^2 - z_1^2)} \qquad \text{(Eqn 3.35)}$$

This is the equation for the shear stress at any point a distance z, from the y axis. When moving along the line pn this stress diminishes (assuming that the vertical components are constant) and reaches a minimum at point n where $\tau = \tau_z$. The maximum shear stress for a solid circle will occur at the neutral axis, thus substituting $z_1 = 0$ to get:

$$\tau_{max} = 4.V/(3.\pi.r^2)$$
$$= 4.V/(3.A) \qquad \text{(Eqn 3.36)}$$

where A is the cross sectional area of the beam. At the neutral axis the stresses lie parallel to the z axis and have constant magnitude (equal to τ_{max}) across the section. This approximate theory described gives reasonably accurate results for the shear stresses in a solid circular beams. Exact solutions obtained by the theory of elasticity show that the stresses are not constant along the neutral axis but that stresses are in error by only a few per cent.

If the beam has a hollow circular cross section, then it can be assumed with good accuracy that the shear stresses along the

neutral axis are vertical and uniformly distributed. The properties of the cross section are:

$Q = 2/3.(r_o^3 - r_i^3)$ = first moment of area
$I = \pi/4.(r_o^4 - ri^4)$ = moment of inertia
$b = 2.(r_o - r_i)$ = shear width
$A = \pi/4.(r_o^2 - r_i^2)$ = area of hollow section

(Eqn 3.37)

And hence the maximum stress is at the centre:

$$\tau_{max} = V.Q/(I.b)$$
$$= 4.V/(3.A).[(r_o^2 + r_o.r_i + r_i^2)/(r_o^2 - r_i^2)]$$

(Eqn 3.38)

For intermediate stresses away from the neutral axis:

$$b = b_{outside} - b_{inside} = 2\sqrt{(r_o^2 - z^2)} - 2\sqrt{(r_i^2 - z^2)}$$
$$Q = 2/3.(r_o^2 - z^2)^{3/2} - 2/3.(r_i^2 - z^2)^{3/2}$$

(Eqn 3.39)

Note that all the above relationships have been derived for the vertical shear stresses. The evaluation of shear stresses due to the axial acceleration is identical these also act vertically as a result of the geometry of the loading. The evaluation of the shear stresses resulting from the sideways direction would require the substitution of A_y for A_z, τ_y for τ_z, and y_1 for z_1 in equations 3.30 to 3.39.

3.5 Classical Lamination Theory

The analysis of a GRP road tanker is complicated by the properties of the composite material. These materials behave differently to conventional isotropic materials as a result of their anisotropy. Laminate design requires that one obtains maximum

advantage from the exceptional fibre directional properties while minimising the effects of the low transverse properties with careful orientation of the layers or lamina to match the loading environment. When designing in composites, it is desirable to work in terms of stress resultants or force per unit width. These can be described as the force or moment carried by a unit width of laminate in the axial, circumferential or radial directions, and has units of N/m width. The use of longitudinal and transverse fibre stresses to describe the shell loading will result in an excess of data as they vary with the orientation, material and positioning of the lamina in a laminate.

This research uses Classical Lamination Theory (CLT) which determines the effect that the stress resultants have on the lamina stresses. This analysis has been well documented by a number of references such as Jones (1975) and Rosen (1987). The use of CLT for the analysis of filament wound composites was documented by Swanson (1987). The analysis used by ABAQUS is also based on CLT (ABAQUS 1986).

CLT is divided into the following stages: Firstly the stress-strain relation for the thin plies or lamina are derived. The analysis is then developed for the assembly of plies called a laminate. This is developed into relations for thin, laminated shells which take into account the membrane force resultants and moment resultants. The resulting centreline strains and curvatures can then be translated back into lamina stresses and compared to the lamina strength allowables using an appropriate failure criteria. The use of existing plate and shell theory is facilitated by a set of representative extensional and bending stiffnesses for the laminate. The derivation of the relations is based on those from Jones (1975) and Rosen (1987) and is discussed in more detail in Appendix D. The analysis of isotropic

plates is well established and involves the separate analysis of the inplane loading and bending moments, the results then being superimposed. This occurs because the two loadings are uncoupled. For anisotropic plates such as composite laminates, coupling does occur and the inplane loading and bending are treated together. It is only for symmetrical laminate sequences that uncoupling occurs. This coupling is not desirable for the road tanker and all the laminates discussed in the rest of this analysis are both balanced and symmetrical.

When the loads on the laminate are known, they are evaluated to determine the lamina stresses in the longitudinal, transverse, normal and shear directions. These results are then checked by the Tsai-Wu failure criteria (Tsai 1986) to obtain the laminate strengths. Although this is used extensively during the design of the proposed tanker, it is not presented due to the excessively large volume of data generated. The use of CLT is therefore limited to the evaluation of the force and moment resultants. These can be derived from FEM, beam theory or elasticity and are used as inputs for further evaluation of the laminate strengths. Appendix C summarises the material properties used for the tanker analysis. Appendix D provides a summary of the laminated plate theory used for the MACLT.BAS program of Appendix H and the FEM analysis.

There are however details which apply specifically to the experimental validation model. For the theoretical prediction of the surface strains using strength of materials, reference is made to the laminate elastic constants. Their derivation is discussed in more detail in Appendix C and they are the equivalent moduli and Poisson's ratio for the complete laminate. For the tube shell these are determined from the MA-CLT.BAS program and are listed in Appendix C-5. Due to the $\pm 45^{\circ}$ laminate,

$E_x = E_t$ and the calculation of the inplane normal strains e_x and e_t is straightforward. The output from the analysis are the inplane force resultants N_x, N_t and N_{xt} and the inplane moment resultants M_x, M_t and M_{xt}. This data is converted into surface strains e_x, e_t and γ_{xt} to allow comparison to the theoretical and experimental results.

Jones (1975) showed that the centreline strains $\{e_0\}$ and curvatures $\{k\}$ could be related to the force $\{N\}$ and moment $\{M\}$ resultants by :

$$\begin{Bmatrix} \{e_0\} \\ \{k\} \end{Bmatrix} = \begin{bmatrix} A' & B' \\ B' & D' \end{bmatrix} \cdot \begin{Bmatrix} \{N\} \\ \{M\} \end{Bmatrix} \qquad \text{(Eqn 3.40)}$$

where A', B' and D' are the inverse of the A, B and D matrices as defined in Appendix D. The surface strains can then be determined from:

$$\begin{bmatrix} e_x \\ e_t \\ \gamma_{xt} \end{bmatrix} = \begin{bmatrix} e_{ox} \\ e_{ot} \\ \gamma_{oxt} \end{bmatrix} + \frac{t}{2} \cdot \begin{bmatrix} k_x \\ k_t \\ k_{xt} \end{bmatrix} \qquad \text{(Eqn 3.41)}$$

where t is the thickness of the laminate. These calculations are done by the MA-CLT.BAS program listed in Appendix H and are listed in the section 6.2.

3.6 The Validation Model

Although the accuracy of the Finite Element Method (FEM) has been proven with numerous examples, its application when analysing complicated structures such as a road tanker had to be validated. This is done by experimental studies using a scaled down model of

a road tanker consisting of a filament wound tube in steel supports. These supports attempt to model the effect of a stiff chassis and ring stiffeners on the relatively flexible GRP shell. The experimental results obtained from this model are compared to the output from FEM and a theoretical analysis based on strength of materials. The objectives of this experimental work are as follows:

- to compare the experimental, theoretical and FEM results.
- to determine the stress patterns around the supports.
- to validate the use of FEM for the accurate stress analysis of a GRP road tanker shell.

The model is loaded in combined tension and bending as a result of the offset between the line of action of the force and the neutral axis of the circular tube. From Timoschenko and Gere (1984), the normal stress at any vertical distance y away from the neutral axis can be written in terms of the tensile force F, tube cross-sectional area A and moment of inertia I as follows:

$$\sigma_x = F/A - F.y_e.y/I \qquad \text{(Eqn 3.42)}$$

where $A = \pi/4.(d_o^2 - d_i^2)$

$I = \pi/64.(d_o^4 - d_i^4)$

To calculate the axial strains e_x, use is made of the laminate elastic constants E_x, E_t and ν_{xt} which are obtained from Classical Lamination Theory (Appendix C-5). As a result of the symmetrical $\pm 45^o$ layup of the tubes, $E_x = E_t$. We can approximate the axial strain e_x as follows:

$$e_x = \sigma_x/E_x \qquad \text{(Eqn 3.43)}$$

With the exception of the areas very close to the ring stiffener, the transverse strain e_t can be calculated from the longitudinal strain e_x as follows:

$$e_t = -\nu_{xt}.e_x \qquad \text{(Eqn 3.44)}$$

The bending moment M is uniform beyond the ring stiffeners ie:

$V = dM/dx$ (Eqn 3.45)

and hence the shear force V = 0 . A zero inplane shear strain τ_{xt} is predicted from strength of materials. The inplane moment resultants M_x, M_t and M_{xt} and transverse shear resultants Q_x and Q_t are not calculated theoretically as this will involve many assumptions with respect to the material properties and boundary conditions. These resultants are however obtained from the FEM analysis and are evaluated to calculate the FEM surface strains e_x, e_t and τ_{xt}. The data processing relationships to obtain the strains from the measured voltages are discussed in more detail by Appendix G.

4 FINITE ELEMENTS

4.1 The Road Tanker

4.1.1 General requirements

Experimental studies on the tanker used the Finite Element Method (FEM) as the research tool. This analysis of the expected dynamic loads on the tanker was then compared to strength of materials and theory of elasticity approximations. A finite element model allows for more precise definition of the expected dynamic loads than simulated static tests on an existing tanker. The difficulties associated with simulated testing were clear from the papers by Kenney (1966) and TFM (1986). An experimental study would require the construction of a prototype GRP tanker and involve extensive machinery and instrumentation. Both of these were beyond the scope of this research. For the FEM analysis, the acceleration loadings were modelled by static pressures and body forces which acted on each element of the shell. The accelerations could be applied singly or in combination to simulate a worst case scenario for the tanker. The shell was considered to be of uniform thickness as this allowed more accurate analysis and highlighted the effect of stress concentrations on the shell. Although an operational tanker would have optimally varying thicknesses, this would complicate both the experimental and mathematical analyses. The filament winding of a shell would also result in a uniform thickness as a result of the process requirements. A candidate road tanker was designed to enable a comparison between the various analyses. The design chosen for this research was the filament wound circular shell with circumferential stiffeners. Drawings and a description of this design are presented in Appendix A.

4.1.2 The finite element model of the road tanker

The FEM models of the road tanker and validation model were analysed using the ABAQUS version 4.6 FEM program and run on the IBM 370 mainframe at the University of the Witwatersrand Computer Centre. All input data for the tanker FEM models was generated using the author's pre-processing software which ran on IBM compatible personal computers. These programs are discussed in more detail in section 4.1.3 and were required due to the poor pre-processing facilities available at the time.

The tanker and validation FEM models consist of discrete elements whose geometric outline was defined by nodes. These nodes were points in three dimensional space and were defined in terms of a rectangular coordinate system. The elements were then defined by specifying their constituent nodes. Forces, displacements and pressures were applied at the nodes and elements. Together with the material and thickness properties, the FEM package could then set up a stiffness matrix which was used to solve the systems of equations relating external forces and displacements to internal stresses and strains. The accuracy of the FEM analysis was highly dependent on the shape and density of the element mesh. The element types also differ for various applications. Elements used for the this analysis were three dimensional composite shell elements for the tanker shell and orthotropic beam elements for the tanker ribs.

Sign conventions

The model was generated using a rectangular coordinate system with the origin located on the axis of the cylinder in line with the intersection of the rear dome and the cylinder (rear tan

line). The axial direction was represented by the x or 1 axis and increased towards the front of the tanker. The sideways direction was represented by the y or 2 axis and the vertical direction by the z or 3 axis with all dimensions given in metres. The constraints, boundary conditions, nodal coordinates and displacements were specified relative to this global coordinate system. The material properties were input relative to a local cylindrical coordinate systems. This was established through the use of the "*ORIENTATION" command which defined a cylindrical coordinate system relative to the central axis of the cylinder. The shell stress output was obtained in terms of this local coordinate system, namely axial (1), circumferential (2) and radial (3).

The material orientation for the shell was then defined as an angular rotation around the radial (3) axis of the previous cylindrical coordinate system. This angle corresponds to the winding angles and provides for accurate and convenient definition of the fibre path during filament winding.

Nodes and elements

The FEM model of the tanker was planned to be an accurate representation of a tanker with the cylindrical shell, circumferential ribs and ellipsoidal domes. The entire tanker had to be modelled as the loading conditions made the use of symmetry impossible. The node and element mesh file was generated by the RTBEGIN.BAS program. Further details on this program were provided in section 4.1.3 and Appendix I, and a summarised listing of the ABAQUS mesh file is presented in Appendix J. The elements were grouped in element sets for the cylindrical shell (ECYL), the ribs (RIBS) and the domes (LDOME and RDOME). The domes were further divided into two regions, one constructed of quadratic elements and the other of triangular elements.

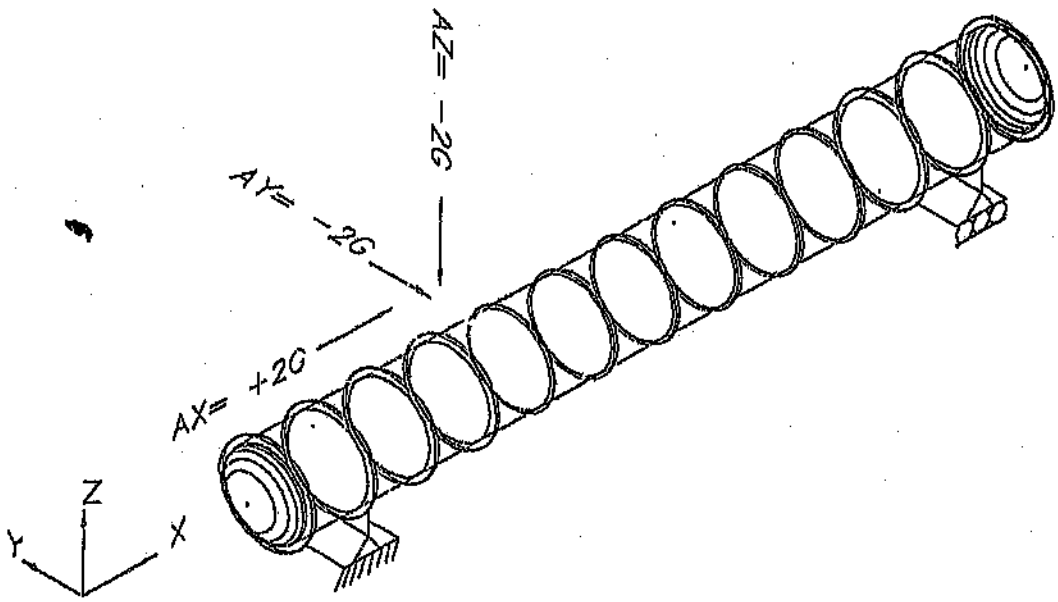

Figure 4.1 Schematic illustrating the loading and supports applied to the road tanker model.

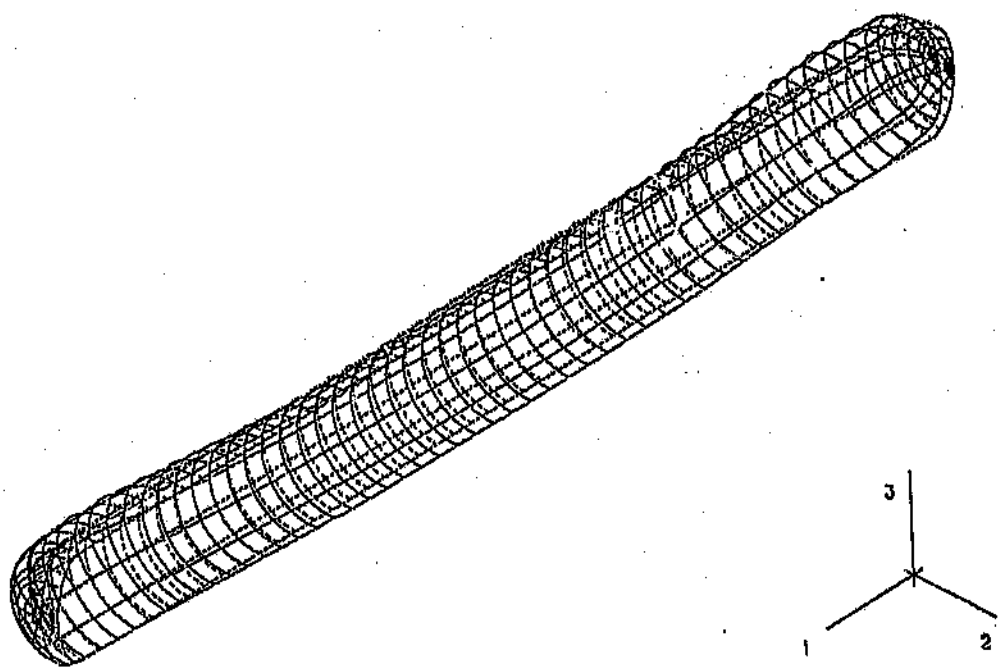

Figure 4.2 The FEM mesh of one half of the road tanker showing the original (dotted) and deflected (solid) shape.

These various elements sets were connected with multi point constraints (MPC) to complete the model as shown in Figure 4.6.

The cylindrical shell consisted of 3D shell elements of the type S8R. This is an eight noded quadrilateral stress/displacement element with four corner nodes and one centre node on each side as shown in Figure 4.3 below. The element uses reduced integration and can be used to define doubly curved shells consisting of anisotropic layers, each with a different orientation, and allowed for transverse shear stiffness. The S8R element uses a quadratic interpolation shape function and is more accurate than a similar density of four noded elements. It has six active degrees of freedom per node and can be used to predict bending effects. Care was taken to ensure that the generated elements had aspect ratios (length/width) as close as possible to unity. High aspect ratios could result in large errors in the analysis and were avoided by careful mesh generation.

The material orientation for the cylinder elements were input relative to the local directions specified using the "*ORIENTATION" command. The lamina properties were then input using the "*ELASTIC,TYPE=LAMINA" option and were typical for the filament wound material used (see Appendix C). The shell definition used the "*SHELL SECTION,ELSET=SHELL,COMPOSITE" option. This command allows the cross section of the shell to be defined by numerical integration of any number of material points through its thickness. Hence different materials at varying orientations can be defined. The shell was modelled by a laminate consisting of a $[\pm 10°/\pm 85°/\pm 10°/\pm 85°/\pm 10°/\pm 85°]_S$ layup. This resulted in a balanced and symmetrical laminate with a thickness of 0,625 mm per layer and a total laminate thickness of 15 mm.

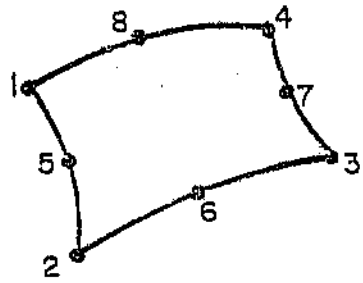

Figure 4.3 Node ordering for an S8R shell element.

One integration point per layer was specified. The transverse shear stiffness of the shell was defined as $K_{13} = G_{13} = 4.14$ GPa and $K_{23} = G_{23} = 3.5$ GPa by using the "*TRANSVERSE SHEAR STIFFNESS" command. This was especially important for the composite shell element as transverse shear effects can be significant.

The ribs consisted of B32 three-dimensional stress/displacement quadratic beam elements. The formulation of these elements includes the effects of transverse deformation and uses Timoshenko beam theory. The rib cross section was a rectangular shape and of two sizes. The thick ribs were assigned to the element set RIBTHICK and were 50 mm wide and 100 mm thick. These provided the attachment points for the fifth wheel (connection to the truck), the landing legs and the rear bogie cradle. The remainder of the ribs (element set RIBTHIN) were thinner with dimensions of 50 mm square. Both sets of ribs were defined by nodes along the neutral axis of the rib. Because of the offset between these nodes and the corresponding cylinder nodes, they were connected by multi-point constraint (MPC) type 7 which connected them in all six degrees of freedom, as shown in Figure 4.4 below.

The "*ORIENTATION" and "*ELASTIC,TYPE=LAMINA" options could not be used for beam elements. The rib material properties were therefore defined as orthotropic by using the "*ELASTIC,TYPE=ORTHOTROPIC" option relative to the neutral axis of the rib for the axial and transverse directions (see Appendix C). The rib was assumed to consist of unidirectional E-glass/polyester (vf = 0.45) and the orthotropic constants required to define this material were obtained from classical lamination theory via the MA-CLT.BAS program (see Appendix H). The transverse shear of the beam was also defined by using the "*TRANSVERSE SHEAR STIFFNESS" command.

The majority of the dome elements were of the quadratic S8R shell type and were assigned to the LDQUA and RDQUA element sets for the back and front dome respectively. At the apex of each dome was a small circle consisting of 24 triangular STRI3 shell elements which were assigned to the LDTRI and RDTRI element sets as shown by Figure 4.6. These elements closed the top of the dome and were connected to the rest of the dome by MPC type 7. The dome material was defined as being isotropic. The ellipsoidal shape did not allow alignment with the cylindrical or spherical co-ordinate systems and in reality, the domes would either be hand laminated or wound as a geodesic isotensoid. The dome material was defined by assuming a quasi-isotropic layup of $[0°/\pm60°]_S$ of E-glass/polyester or vinylester (vf = 0.45) which was 15mm thick. Further details can be obtained from Appendix C. Two load cases were analysed during this research. The first was the pressure case with a uniform internal pressure of 8.4×10^5 Pa to simulate a pressure test with contents of zero density. This case does not relate to the hydrostatic pressure test where the tanker would be tested with water at a pressure of 3.5×10^5 Pa resulting in additional bending stresses due to the density of the water and shell.

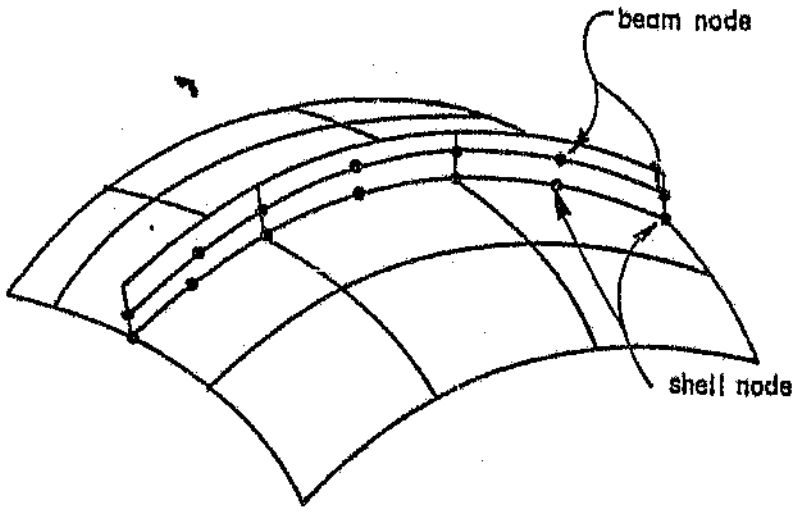

Figure 4.4 Connection of the shell and ribs using multi-point constraint type 7.

Load conditions

The pressure of 8.4×10^5 Pa was chosen to give the same tensile stress levels as a hydrostatic test (see Appendix E). Due to the lack of bending stresses from the cargo, direct comparisons could be made between FEM and a theory of elasticity analysis by Timoshenko (1959). This would serve as a validation of the tanker model and check the accuracy of the method.

The second load case was obtained from requirements to satisfy SABS 1398 (1983). The tanker must sustain the combined effect of 2G accelerations in the axial, vertical and sideways direction. The effect of the accelerations on the cargo and shell of the tanker was modelled by the use of equivalent pressures and body forces. As a result of the acceleration of the cargo the liquid exerts a hydrostatic pressure perpendicular to the inner walls

of the tanker shell. This pressure is a linear function of the head of liquid in the respective direction. By superimposing these pressures for the various directions and applying them on each individual element, it was possible to accurately model the effect of the cargo on the shell. This procedure was used by the RTEND.BAS program (see Appendix J). The effect of the acceleration on the tanker shell was represented by body forces acting on the shell and beam elements. This was input under the "*DLOAD" option where the force per unit volume and force per unit length were specified in the various directions for the shell and beam elements respectively.

Constraints and boundary conditions

The rib nodes which form part of the cradle support were defined by using the "*NSET" command. The included angle for these supports was 120° as recommended by BS4994 (1987). Although the tanker's support would normally be spread over the entire bogie and fifth wheel, only one support was used on each side to facilitate analysis of the load reactions as most of the tanker designers locate these reactions at the centre of the bogie or fifth wheel. In this case the load bearing supports were located at SUPR2 and SUPR12 which were positioned one metre from the back and front of the tanker respectively. This allows the high local loads to be transferred to the shell through the ribs and can be seen as a worst case scenario for the tanker where the entire tanker load is being supported by one rib on each side. This configuration is similar to the support geometry of horizontal tanks and lends itself to more accurate comparison between the FEM and theoretical results.

The boundary conditions vary for each load case. For the internal

load pressure case, both SUPR2 (x = 1) and SUPR12 (x = 11) were constrained in the vertical direction. SUPR2 was constrained in the axial direction but SUPR12 was free to move to allow for elongation of the tanker. The bottom node on each support was also constrained in the sideways direction (nodes 4669 and 5029). There were no angular constraints. For the combined acceleration load case, both SUPR2 and SUPR12 were constrained in the vertical direction. The bottom node on each support was also constrained in the sideways direction (nodes 4669 and 5029). SUPR2 was constrained in the axial direction but SUPR12 was free to move to allow for elongation. There were no angular constraints.

Numerical and graphical output

The FEM output for the shell is presented in terms of the inplane force resultants N_x, N_ϕ and $N_{x\phi}$, the transverse shear force resultants Q_x and Q_ϕ and the inplane moment resultants M_x, M_ϕ and $M_{x\phi}$. The axial (x) and circumferential (ϕ) directions are represented by the 1 and 2 directions in the ABAQUS force resultant output. These force and moment resultants are specified for the integration points on the element. A force resultant is the force in a shell per unit width (N/m width) and is a practical way of representing stresses within composites. This notation is used by Jones (1975) for composites and Timoshenko (1959) for plate theory and allows for easy comparison with the FEM results. Using stresses for comparison would involve calculating the various stress components per layer resulting in considerable amount of data to be processed.

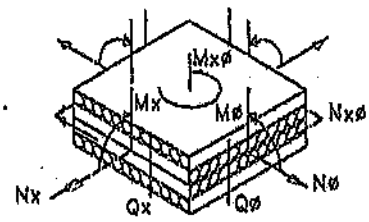

Nx – AXIAL FORCE RESULTANT (N/m width)
Nø – CIRCUMFERENTIAL FORCE RESULTANT (N/m width)
Nxø – INPLANE SHEAR FORCE RESULTANT (N/m width)
Mx – AXIAL MOMENT RESULTANT (Nm/m width)
Mø – CIRCUMFERENTIAL MOMENT RESULTANT (Nm/m width)
Mxø – TWISTING MOMENT RESULTANT (Nm/m width)
Qx – AXIAL TRANSVERSE SHEAR (N/m width)
Qø – CIRCUMFERENTIAL TRANSVERSE SHEAR (N/m width)

Figure 4.5 The applied loads result in force and moment resultants acting on the laminate.

FEM model size

The entire model consisted of 2522 nodes and 900 elements. The original wavefront was estimated on the maximum number of degrees of freedom (DOF) per node and were as follows:

- original maximum DOF wavefront : 2196
- original RMS DOF wavefront : 1254

After computer optimisation of the model, the total number of variables including Lagrange multipliers was 15132. The wavefront was optimised and reduced as follows :

- optimised maximum DOF wavefront : 348
- optimised RMS DOF wavefront : 229

Linear small displacement theory was used. Attempts were made to run these models for non-linear geometry but these were unsuccessful due to the large size of the model.

Finite element analysis

The pre-processing software enabled the generation of course models with each of the load conditions applied separately. The RTBEGIN.BAS and RTEND.BAS programs (Appendix I) produced error free input files according to the loading and mesh density requested. These element meshes were also checked graphically by

the MACONV.BAS and MA3DCAD.BAS programs to ensure that they had been correctly generated. This procedure avoided the use of the mainframe until it was necessary for running the analysis and avoided the delays associated with batch processing.

Once all the load conditions had been run separately and all errors had been corrected in the mesh generation programs, the final fine meshes were generated and checked graphically. These were then down loaded onto the mainframe and run using the batch processing facility. The size of these models often resulted in delays of up to a week before the results became available. The results were then condensed using the post processing ABASAS.WBA program which extracted the required data. This data was then processed using the SAS graphical program to produce the plots of Appendix S and T, and then down loaded onto a personnel computer for further post processing and generation of graphs.

4.1.3 Computer programs

The majority of these programs were written in BASIC and run on personal computers. The ABASAS.WBA program was however written in Waterloo Basic and ran on the IBM 370 mainframe.

MACLT.BAS - Classical lamination theory program

The analysis of composites by classical lamination theory (CLT) was carried out by this program. This theory is discussed in more detail in paragraph 3.1.5. The program allowed for the input of complete laminate data with the lamina properties and angles (lines 100-250). This data was saved to disk for further retrieval (250-300). The program provided the following functions:

- Calculation of the extensional [A] and bending [B] stiffnesses from which the orthotropic properties for the ribs were derived (300-40140).
- Calculation of the equivalent laminate properties which were used for the theoretical analysis and dome properties (40140-60045).
- Calculation of the laminate surface strains and curvatures from the force resultant data obtained from FEM (40140-61530).
- Calculation of the lamina stresses and failure criteria from force resultants included in the laminate data (61530-62720).

The listing of this program is presented in Appendix H.

RTBEGIN.BAS and RTEND.BAS - Preprocessing programs for the tanker FEM model

These programs were used to generate the FEM model of the road tanker. Version 4.6 of ABAQUS did not have pre-processing facilities and the complexity and size of this model requires an accurate method of mesh generation. A listing of the RTBEGIN and RTEND programs were available in Appendix I. The NISA FEM PC Based program available at the time was not able to process this large model due to memory limitations.

Data which completely specified the tanker's dimensions, thicknesses, accelerations, densities, pressures, dome and rib properties was typed into the program (lines 150 - 550). This information was then used to generate the model. The user was then prompted for the element included angle and axial increment (1020 - 1110). Small values resulted in a finer mesh. The program then continued through a sequence of subroutines which generate the nodes and elements for the cylinder, ribs and domes (610 - 790). Subroutines then connect the ribs and domes to the cylinder by

use of a multi-point constraint (830 - 8[illegible]). The positions for the cradle supports were also specified, and the nodal displacements which could model the effect of an angular twist were calculated (869 - 870). This data was then written to sequential files. One became the ABAQUS mesh file and the others were temporary files required by the second part of the model generation contained in the RTEND.BAS program which provided the load history, property and output information required for the FEM analysis. The input section (lines 150-550) of the program were identical to that of RTBEGIN.BAS. The temporary files were reloaded (570-610) and these provided the geometric data for the nodes and elements. The equivalent pressures and body forces which simulate the accelerations imposed on the tanker and its cargo (8910-9540) were then calculated. The material properties for the ring stiffeners, shell and dome were defined (6940-8660), followed by the supports and boundary conditions (8680-8780). The last parts of the program specify the output required from the analysis (9570-10220).

After the files from RTBEGIN and RTEND had been merged into one file, manual changes to the support boundary conditions were necessary, depending on which analysis was being run. The main advantage of having two programs was that many loading conditions could be generated from one mesh file. Any errors picked up during the FEM check runs were corrected in these preprocessing programs to ensure that they were not repeated. The programs allowed for the fault-free generation of the course check models as well as the fine mesh, high accuracy models.

MACONV.BAS - Graphic generation program

This program was written to convert the data from the ABAQUS

input file into graphic data which could be read by the MA3DCAD program. The node and element data from the ABAQUS file was converted into node and line data. Shell, rib and solid elements could be converted in this way. A listing of the MACONV program was given in Appendix M.

MA3DCAD.CAD - Three dimensional mesh preview program

This program was written to facilitate graphic preview of the mesh generated by the MABEGIN and MAVAGEN programs. Due to the complexity of the FEM models used, a graphic check was necessary to ensure that the mesh was correct. Existing PC packages such as NISA were not able to process the large models used for this research. The node and element data from the ABAQUS input file was converted into graphic data by the MACONV program. The MA3DCAD program read this data and then functioned as an interactive three dimensional computer aided design program with many graphic manipulation functions such as scaling, rotating, panning, zooming and change of perspective and viewpoint. An example of the screen display is shown in Figure 4.6. A listing of the program was given in Appendix N.

ABASAS.WBA - WBASIC program to extract geometric, stress and force resultant data from the ABAQUS output file

This program summarised the bulky ABAQUS output file by extracting only that information which was necessary. The element number and co-ordinates of the integration points were first extracted (lines 770-1220). From this data the circumferential arc-length was calculated (650-750). The force and moment resultants at each integration point were then extracted (1240-1780). This data was then written to a separate data file (360-470). These summarised

files were sufficiently reduced to enable them to be down loaded onto a PC for further processing. The program was listed in Appendix O.

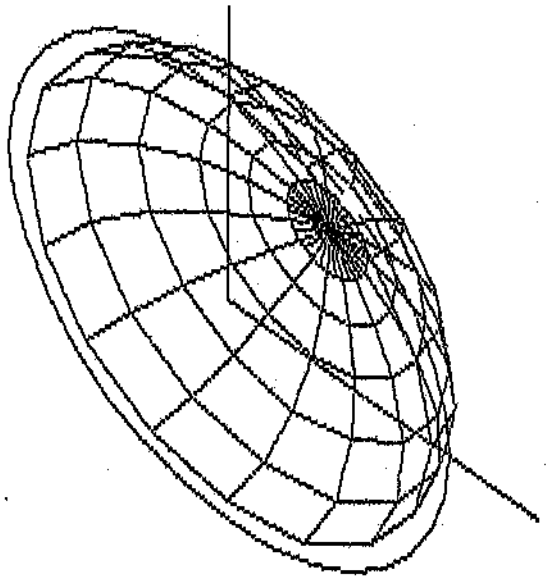

Figure 4.6 Example of the MA3DCAD screen display showing the tanker dome and the first ring.

SAS - Statistical analysis and presentation graphics package.

This package was available on the IBM mainframe and was used to

generate some of the stress maps in Appendices S, T and U. The data is presented in three-dimensional format by using the axial length of the model as the x axis, the arc length or circumferential distance as the sideways axis and the force resultant as the vertical axis. Both contour maps and 3-D grid representations were generated.

PLOT.SAS - Input program for the SAS graphics package

A listing of the input program used to generate the SAS graphics for the road tanker and validation model is presented in Appendix O. The data was read from the summarised ABAQUS output file and then plotted on a Hewlett Packard HP7570 plotter in the prescribed format. A print of this SAS input program is listed in Appendix O.

LOTUS 123 and QUATTRO - Spreadsheet and graphics packages

These PC based programs were used to generate the two-dimensional plots of the FEM and theoretical results which were imported into LOTUS from the output of the MATHEORY program.

The Matheory program

This program was written to allow comparison of the FEM and theoretical predictions of section 3 and Appendix E and F for the road tanker. The load cases which could be analysed were accelerations in the x, y and z directions, internal static pressure and an angular twist of the shell relative to its support. A listing of the program was given in Appendix P. The

program was written in modular form and extensive use was made of subroutines to access each module:

- Lines 3 to 970: define the flowpath of the program.
- 1010 to 1250: Define the loading conditions of the tanker. These are modified by the user to model the various load cases.
- 1265 to 1910: Define the material properties of the tanker's shell, domes and ribs. These were obtained from classical lamination theory using the MA-CLT.BAS program (Appendix H). 1950 to 2750: Define the geometrical dimensions of the tanker.
- 2780 to 3270: Define the input and output of the data files used. The original FEM files were loaded to give the reference x, y and z positions for the theoretical analysis.
- 3310 to 3770: Allow the selection of the position under evaluation. The options were Top/Bottom/Left/Right/Dome.
- 3950 to 4200: Define the shell properties.
- 4290 to 4450: Define the densities of the shell and contents.
- 4490 to 5170: Sectional geometrical properties and volumes.
- 5210 to 5670: The masses of the various components.
- 5710 to 6195: The effects which result from the axial A_x acceleration.
- 6210 to 6229: The variation of the circumferential load from the axial acceleration.
- 6392 to 6377: The effect the axial acceleration has on the ribs, shell and domes of the tanker.
- 6381 to 6510: The total effect of the axial acceleration.
- 7110 to 7710: The effect of the vertical (A_z) acceleration.
- 7110 to 8710: The effect of the sideways (A_y) acceleration.
- 9470 to 9570: The effect of the twisting.
- 9630 to 9890: Membrane stresses in the dome from internal pressure.
- 9910 to 10050: Membrane stresses in the shell from internal pressure.

- 10090 to 10950: Totals of all the force and moment resultants for the various load cases.
- 10990 to 13790: Stresses which result from a shell under internal pressure with circumferential ribs.
- 13840 to 13855: Definition of local variable for the dome analysis.
- 13858 to 14650: Stresses which arise from the discontinuity at the dome to shell junction for a vessel under internal pressure.

The theoretical predictions of the MATHEORY.BAS program were run over a range of values with a small increment to give a more continuous curve for comparison to the FEM gauss point values. These curves were discussed in more detail by section 6.1

4.2 The Validation Model

4.2.1 The validation finite element model

A FEM model of the validation test model was generated to allow comparison of the FEM strain results with the experimental and theoretical analysis.

Sign conventions

The model was generated using a rectangular coordinate system with the x or 1 axis along the axis of the tube, the y or 2 axis vertical and the z or 3 axis in the sideways direction. The material properties were input relative to a local cylindrical coordinate system. This was established through the use of the "*ORIENTATION" command which was first used to define a cylindrical coordinate system relative to the centre of the tube.

The shell output is obtained in terms of this system, namely axial x, circumferential t and radial r. The material axis for the shell was then defined as an angular rotation around the radial r axis of the cylindrical coordinate system. This angle corresponds to the winding angles for the filament wound tube and provides for accurate and convenient definition of the lamina properties. All constraints, boundary conditions, nodes and forces where specified relative to the global rectangular coordinate system.

Nodes and elements

The geometry of the test model was represented as accurately as possible with the tube shell, ribs and connecting shaft being modelled. The FEM model consisted of a half symmetrical representation of the test model, although quarter symmetry could have been used. The tube shell consisted of 240 shell elements of the type S8R and were numbered 1 to 120 and 500 to 619. The material properties were input relative to the local $\pm 45^{\circ}$ directions specified. These were the lamina properties and are typical for filament wound material used (see Appendix C) and input using the "*SHELL SECTION,ELSET=SHELL,COMPOSITE" option. This command allows the cross section of the shell to be defined by numerical integration of any number of material points through its thickness. The manufactured shell consists of three double layers of $\pm 45^{\circ}$ orientation with the -45° and $+45^{\circ}$ fibres interlocked by the method of filament winding which results in a balanced and symmetrical laminate. Attempts to represent the FEM model as a six layer laminate would result in an unsymmetrical and hence unbalanced laminate. The FEM shell was approximated by eight layers with a thickness of 0,23625 per layer and constructed as $[\pm 45/\pm 45]_s$ to avoid this inaccuracy.

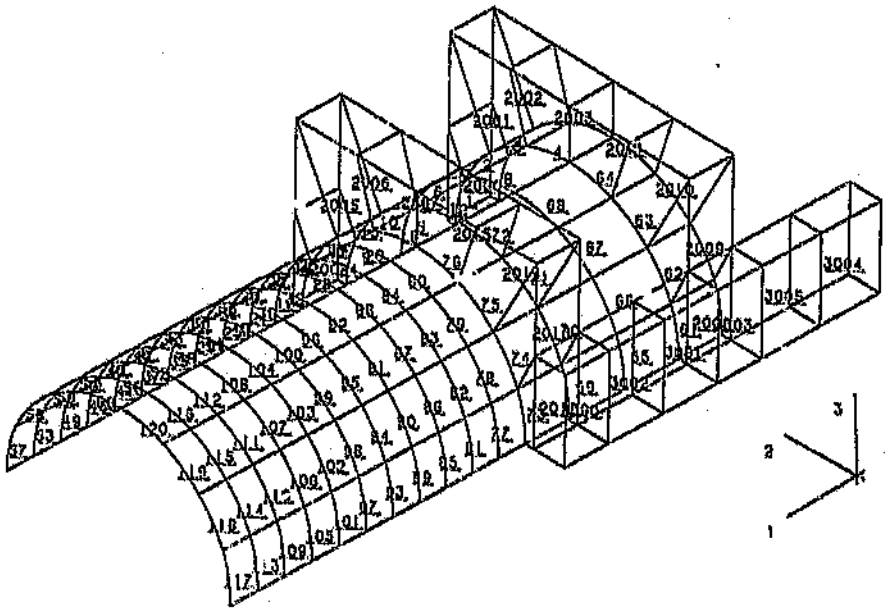

Figure 4.7 One half of the validation finite element model.

Hence the coupling [B] matrix was zero and the laminate is accurately defined. The transverse shear stiffness of the shell was defined as $K_{13} = G_{13} = 4.14$ GPa and $K_{23} = G_{23} = 3.5$ GPa by using the "*TRANSVERSE SHEAR STIFFNESS" command. This is especially important for the composite shell element as transverse shear effects were significant. High element aspect ratios which could have resulted in large errors in the analysis were avoided. This requirement did however limit the use of a graded mesh near the support ribs as the MABEGIN.BAS program could only grade the mesh with respect to the axial x length once the circumferential angle had been defined.

The ribs and shaft were generated using the pre-processor of the NISA FEM program and consist of three dimensional solid elements of the type C3D20 shown in Figure 4.8. These elements are 20 noded, quadratic stress/displacements bricks and have three active degrees of freedom (DOF) per node. The elements were

chosen and positioned so that they would coincide with the shell elements at their nodes. Two methods of FEM model generation were used and both gave identical results. One model was generated using the NISA FEM pre-processing software. The NISA input data was then converted int. ABAQUS data through the use of the NISA-ABA.BAS program (Appendix K). The material, boundary conditions and loading data were then added manually. The use of half symmetry also allowed the use of a mesh generation programs [illegible]V.BAS (Appendix K) to generate the shell elements of an [illegible] model. This program was derived from the RTBEGIN.BAS program used to generate the road tanker model. The rib data was obtained from the NISA data file and connected to the shell with multi-point constraints by using the MAMPC.BAS program. Both of these methods gave the same results. These programs were discussed in more detail in section 4.2.2.

Although the shaft is circular on the test model, it was modelled as a rectangular rod on FEM. This enabled the connection of the shaft to the rectangular rib elements. The stiffness of the rod was adjusted to ensure that the flexural properties of the rod were the same as the shaft with the elastic properties of the rod defined as E = 428 GPa and ν = 0,3. Definition of the ribs and rod properties where defined using the "*SOLID SECTION" command. The properties for steel ribs were E = 200 GPa and ν = 0,3.

Constraints and boundary conditions

Half of the test model was modelled on FEM as a result of both geometric and loading symmetry. All the nodes at the plane of symmetry at x = 0,278 m were constrained by the "XSYMM" option under the "*BOUNDARY" command. This only allows for linear displacement in the z and y directions and rotation about the x

axis. Node number 216 at (0,278 ; 0,0919 ; 0,431) was pinned to prevent any rigid body modes of the entire model.

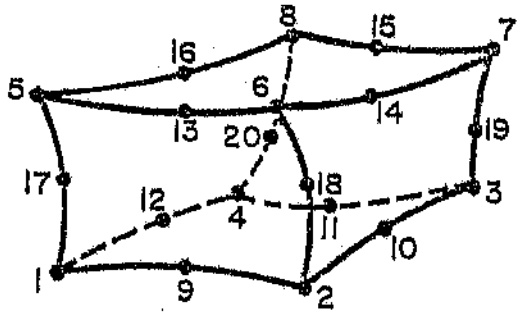

Figure 4.8 A C3D20 three dimensional brick element.

Force and force tolerance

The tensile force of 5 kN was modelled by applying nodal forces to the end of the rod of -3000 N at node 1020 and -1000 N at nodes 1021 and 1066 using the "CLOAD" command. This approximation was acceptable due to the Saint Venant hypotheses, as the area of interest, namely the shell, is remote from the points of the applied load. The force tolerance for convergence of the analysis was set at 1 N.

Numerical and graphical output

The FEM analysis output for the shell was presented in terms of the inplane force resultants N_x, N_ϕ and $N_{x\phi}$, the transverse shear force resultants Q_x and Q_ϕ and the inplane moment resultants M_x, M_ϕ and $M_{x\phi}$. The geometric position of the central points on the element were also obtained. The values of the inplane force and

moment resultants were then evaluated using Classical Lamination Theory to obtain the centreline strains and curvatures. The outer surface strains were then established.

FEM model size

The entire model consisted of 1077 nodes and 284 elements. The original wavefronts as estimated on the maximum number of degrees of freedom (DOF) per node were as follows:

- original maximum DOF wavefront : 1272
- original RMS DOF wavefront : 834

After computer optimisation of the model, the total number of variables including Lagrange multipliers was 5487. The wavefronts had been optimised and reduced as follows :

- optimised maximum DOF wavefront : 848
- optimised RMS DOF wavefront : 376

Linear small displacement theory was used.

The finite element analysis

Two different methods were used to generate the validation FEM models as discussed in paragraph 4.2.1. Once the models had been checked graphically using the MA3DCAD.BAS programs, they were then down-loaded onto the mainframe and run using the ABAQUS FEM package. The results were then condensed using the post processing ABASAS.WBA program which extracted the required data. This data was then processed using the SAS graphical program to produce the plots of Appendix U, and then down-loaded onto a personnel computer for further post processing and generation of graphs.

4.2.2 Computer Programs

The following programs were used in the analysis of the validation model. Several of the programs from the road tanker analysis such as MACONV.BAS, MA3DCAD.BAS, ABASAS.WBA, PLOT.SAS and LOTUS 123 were also used.

NISA - Finite element program

This finite element package was used on a IBM compatible AT-286 PC. Although the memory limitations restricted its use to small sized models, it was sufficient to allow the generation and analysis of the validation model. This was assisted by the powerful pre-processing functions of this package. The entire validation model consisting of the shell, ribs and rod were modelled and then run on NISA to check the accuracy. The mesh (nodes and element) data could then be rewritten in ABAQUS format by the NISA-ABA.BAS program.

MAVAGEN.BAS - Program to generate a FEM mesh of the validation model shell

This program was derived from the RTBEGIN.BAS program for generation of the tanker FEM mesh (see Appendix K). The dimensions of the model were input (lines 250 - 500) after which the nodes and elements were calculated according to the angular (1030 - 1060) and axial increment (1112 - 1113). This node and element data was then written as a mesh data file for further processing.

NISA-ABA.BAS - Program to convert the NISA mesh data into ABAQUS format.

This program converted only the node and element data from the NISA input file into ABAQUS format. The element properties, load and boundary conditions were not included and had to be added manually to the ABAQUS input file.

MPC.BAS - Program to connect the ribs and shell with multi-point constraints.

This program was used to connect the nodes of the ribs and shells by using multi-point constraints. This was only necessary when the shell had been generated by the MAVAGEN.BAS program and needed to be connected to the ribs derived from the NISA data. The nodes were connected in three translational degrees of freedom by using MPC Type 6. The program then wrote a new file to disk which contained the node, element and MPC data in the correct ABAQUS format. The remainder of the loading and property data still had be added manually by using a suitable editor before the model could be run. The listing of the MAMPC program could be found in Appendix K.

MAMERGE.BAS - Program to merge common nodes

This program established which nodes were common between the shell elements generated by the MAVAGEN.BAS program and the solid elements which were obtained from the NISA-ABA.BAS program. The program then merged the common nodes by renumbering the rib nodes. A listing of the MAMERGE program can be found in Appendix K.

SOLIDVAL.WBA - WBASIC program for the estimation of the validation stresses using beam theory.

This program was used to calculate the theoretical stresses from beam theory. The summarised ABAQUS output data file was loaded for the geometric data (lines 370-512) and then the sectional properties were calculated (530-1160). The axial stress resultants were then calculated by superimposing axial force and bending moment components of the stress (1500-1580). The calculated data was then written to a data file for comparison with the ABAQUS results (2240-2260). A listing of this program was given in Appendix K.

LOTUS 123 and QUATTRO - Spreadsheet and graphics package.

This package was also used to generate the two-dimensional plots for comparing the FEM, theoretical and experimental data for the validation model. The summarised ABAQUS output was first converted into strain data by the MA-CLT.BAS program and then imported into the spreadsheet. The experimental voltage data from the strain gauges was entered directly into a spreadsheet and then converted into strain readings to allow for comparison. Theoretical calculations based on beam theory were also done by the spreadsheet.

5 EXPERIMENTAL

5.1 General Requirements

Although the accuracy of the Finite Element Method (FEM) has been proven with numerous examples, its application when analysing complicated structures such as a road tanker has to be validated. This was done by experimental studies using a scale model consisting of a filament wound tube in steel supports. These supports model the effect of a stiff chassis and ring stiffeners on the relatively flexible GRP shell. The experimental results obtained from this model were compared to the output from a FEM analysis and a theoretical analysis based on strength of materials.

The objectives of this experimental work were as follows:
- to compare experimental, theoretical and FEM results.
- to determine the stress patterns around the supports.
- to validate the use of FEM for the accurate stress analysis of
a GRP road tanker shell.

5.2 Description of Experimental Apparatus

The model consists of a filament wound tube and two metal supports which were bonded to each end of the tube. A schematic of the model is shown below in Figure 5.1

A tensile force of 5 kN was applied to the ends of the metal support shaft by mounting the model in a tensile testing machine. Experimental readings were obtained from strain gauges which had been bonded to the tube.

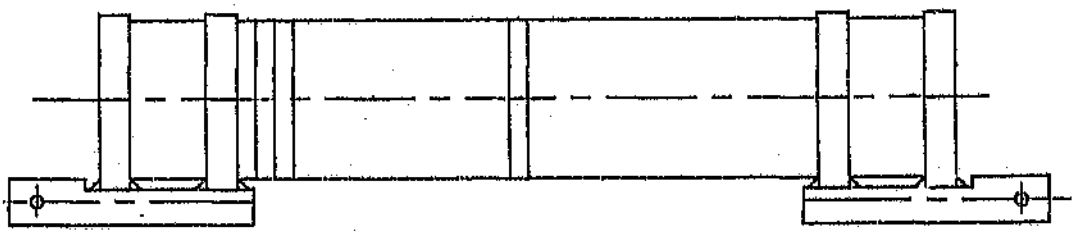

Figure 5.1 Schematic of the validation test model.

A more detailed description of the apparatus is presented in Appendix B. Plates 5.1 and 5.2 show the experimental rig and details of the validation model.

5.2.1 Strain gauges

Resistance foil strain gauges were bonded to the tube to establish the experimental strains. The specification of the chosen gauges were as follows:

- Three gauge rosettes with gauges at angles at 0°, -45° and $+45^{o}$.
- TML Type FRA-5-17
- Gauge Length : 5 mm
- Gauge Resistance : 120 ± .5 Ω
- Gauge Factor F_g : 2.12
- Lot Number : 253631

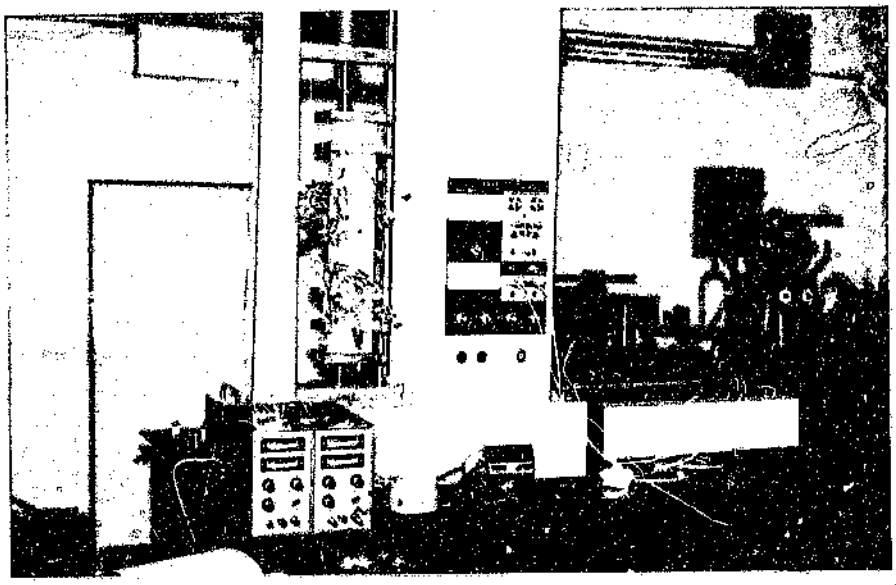

Plate 5.1 The test rig for the validation model showing the tensile test machine, validation model, power supply, temperature compensation, multi-meter and plotter.



Plate 5.2 Detail of the validation model showing the positions of the ribs and strain gauges.

These gauges were considered ideal for this application because their flexibility allowed them to be accurately and securely bonded to the tube's curved surface without affecting the properties of the laminate. The orthotropic nature of the composite involved special precautions and these are discussed in detail by Bert (1985) and Tuttle and Brinson (1984) and summarised in Appendix G. The corrections for transverse sensitivity were also included. The tube could be considered to be homogeneous as a result of the precise control over the filament winding process. By comparing the characteristic fibre dimension (3 to 20 μm) to the gauge length of 5 mm, it is obvious that the heterogeneity of the material is of no great concern. Because the tube had a low coefficient of thermal conductivity and acted as an effective heat and electrical insulator, the gauge excitation voltage was kept low to avoid heating. Tuttle and Brinson (1984) suggested excitation levels ranging from two to four volts. The effect of conducted heat on the laminate would be negligible as the testing was done at room temperature and was of short duration. The maximum anticipated strain levels of 0.002 m/m were far below the maximum allowed for the gauges. Accuracy problems could be expected with the high strain gradients near the ring stiffeners. The gauge length of 5 mm could be too long to accurately predict these exact strains and would give an average over the length of the gauge.

Although the strain fields were largely uni-axial, there were local moments and shear stresses close to the ring stiffener resulting in a more complicated state of strain. This required a three gauge element for complete definition of the inplane state of strain. The chosen gauges had the three elements superimposed on top of each other at positions of -45°, 0° and 45° relative to the longitudinal (x) axis of the tube.

The filament winding left an uneven surface which was abraded to provide a surface appropriate for bonding the gauges by using 400 grit sand paper. With this technique a thin layer was removed from the resin rich surface and care was taken to avoid damaging the fibres of the outer ply of the laminate. The surface was dusted and then cleaned with a solvent before the gauges where bonded. The alignment of the gauges was done by marking their position with a ball point pen. The zero degree direction (x) was established by drawing a line perpendicular to the support for each gauge using a 90° set square placed against the circumferential rib. The gauge was then attached to a piece of sellotape and its position checked under a magnifying glass. Accurate positioning is important for a composite material in order to minimise misalignment errors.The adhesive used to bond the gauges was a commercial cyanoacrylate contact adhesive. A thin layer of adhesive was smeared onto the tube surface and the gauge pressed down with slight pressure until the glue had set. The rosettes were oriented with the centre gauges at 0° and the others at -45° and +45°. This arrangement was necessary in order to obtain the transverse component for all the gauge directions. The rosettes were positioned in four bands of eight gauges each. The first band was positioned close to the ring support and the second and third band next to it. The fourth band was positioned at the centre of the model. Table 5.1 summarises the position of the bands and the respective rosette numbers, listed from the top to bottom of the tube.

A schematic of the rosette positions on the model is shown in Figure 5.2. To avoid overheating of the gauge and the laminate, gauges with attached gauge lead wires were used. The circuit lead wires were soldered after positioning of the gauges and care was taken to avoid damage by soldering the wires away from the tube surface.

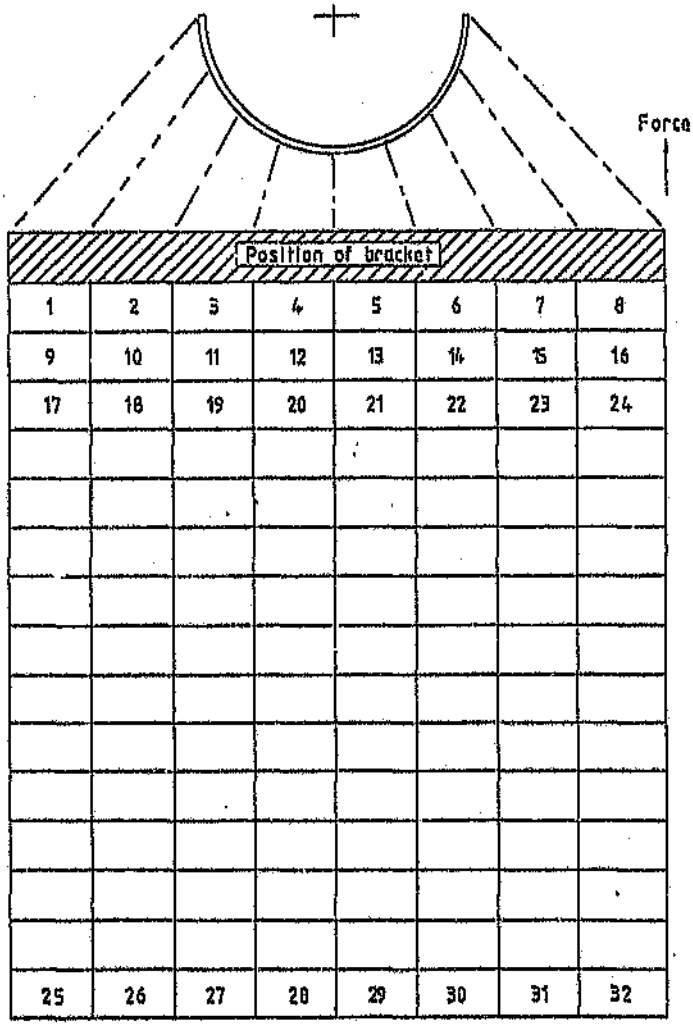

Figure 5.2 Layout of the tube showing the positions of the rosettes.

Band	x co-ord (mm)	Rosette Numbers
1	96	1 to 8
2	108	9 to 16
3	120	17 to 24
4	217.8	25 to 32

Table 5.1 Band positions and rosette numbers.

Contact with the liquid solder or a hot soldering iron could result in broken fibres or a damaged matrix. Care was taken that each gauge and its connecting wires were electrically insulated. Different colours were used for each direction namely blue, red and orange for the 0°, 45° and -45° directions respectively. The wires were then all numbered and labelled to avoid confusion. Crocodile clips were connected to the end of the compensation wires to facilitate convenient changing between gauges. The end of the gauge leads were also soldered to improve the electrical contact with the crocodile clips.

5.2.2 Wheatstone bridge and temperature compensation

The most commonly used method of determining strain gauge readings is by means of a wheatstone bridge circuit. The bridge becomes a direct output device and is shown schematically in Figure 5.3. The excitation voltage V_{in} is applied across AC and the output voltage V_{out} recorded between BD. The active gauge is the one mounted in position on the test piece in the 0°, -45° or 45° direction. The other three arms of this bridge were mounted on an offcut of the tube which are positioned close to the model during testing. These gauges experience the same temperature changes as the active gauges, but none of the mechanical loads. They were oriented in the same direction as the active gauges with separate connections for the 0° and $\pm 45^{o}$ directions. This ensured that the compensation gauges experience the same axial and transverse thermal strains as the active gauge.

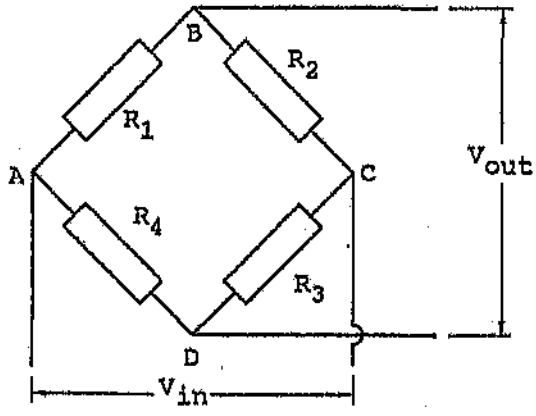

Figure 5.3 Schematic of a wheatstone bridge circuit.

Due to the characteristics of the wheatstone bridge circuit, the apparent strain effects due to the temperature cancel, and the output is due only to the mechanical loading. The excitation voltage for the bridge V_{in} was set to 5 V and current to 0,1 A. This resulted in a gauge excitation voltage of 2.5 V which was within the 2 to 4 V range recommended by Tuttle and Brinson (1984). The wheatstone bridge was often not totally balanced and gave a small non-zero null or unloaded voltage V_{out} across AC. This was recorded and later subtracted from the loaded voltage when the gauge was strained in order to obtain the voltage difference δV_{out}. From this quantity the strain in the gauge could be calculated. The theoretical relationships or the strain gauge, wheatstone bridge and transverse sensitivity are discussed in sections 3.2.3 and Appendix G.

5.2.3 Tensile testing machine

The test model was loaded in tension by mounting it in a JJ Lloyd Instruments T22K tensile testing machine. The machine was fitted with a 20 kN load cell and the applied load of 5 kN was well within its capability. The test model was mounted between the base and the cross-beam by means of two pins. The force and

displacement output was recorded on a JJ Lloyd XY plotter attached to the tensile tester. This was used to check the applied load and any creep or nonlinear effects.

5.2.4 Instrumentation

An Oltronix C40-1 DC power supply was used to energise to wheatstone bridge. The input voltage was set to 5 V and the current to 0,1 A for the test. The gauge connecting leads had been colour coded and labelled and a separate compensation circuit was used for the 0° and $\pm 45^{o}$ directions. The wiring used was single strand telephone wire. Crocodile clips facilitated convenient reconnection between the gauges and compensation circuits. All other connections were soldered. The bridge output voltage V_{out} was read from a Takeda Raiken TR6355 mini multimeter set to the appropriate sensitivity.

5.3 Experimental Procedure

5.3.1 Calibration of the tensile testing machine and plotter

The completed test modal was positioned in the tensile tester and the shafts connected by pins to the bottom and crossbar of the machine. The force calibration dial was set to zero with the force setting at x 0,1 and the extension setting at 2,5/1. These settings are necessary in order to calibrate the XY plotter. The extension calibration dial was also set to zero. The sensitivity on the plotter was then set to zero for the force and extension axis and the pen located at the origin of the calibrated graph paper.

The XY plotter was then calibrated by pressing the "1/2 Load" button for the force axis and then setting the sensitivity so that the pen position was halfway along the axis. The "100 mm Paper Travel" was then pressed for the extension axis and the sensitivity set to position the pen at 100 mm from the origin. This concluded the calibration of the testing machine and XY plotter.

5.3.2 Connection and cycling of the model

The force setting on the tensile tester was changed to x 0,4 which gives a full scale force of 8 kN. The test model was then cycled between 0 and 5 kN to check the gauges and model.

The 0° gauge of rosette 25 was connected with the wheatstone bridge circuit. The bridge voltage V_{in} was set to 5 V and the current to 0,1 A. The multimeter was connected to monitor the voltage reading V_{out} across the bridge. At zero load, the voltage V_{out} was 2,91 mV. The model was then slowly loaded to 5 kN at 4.5 mm/min. The voltage V_{out} was measured at -0,03 mV and remained constant for the duration of the ten minute settling time. The plotter showed a decrease in the measured force from 5000 N to 4914 N during this time. The model was then unloaded back to zero load where the voltage V_{out} was measured at 2,73 mV. This indicated a slight amount of irrecoverable strain. The extension scale was then set to 5:1 and the procedure repeated. The voltage reading at 5 kN was measured at -0,19 mV and remained constant for ten minutes. The tube was then unloaded back to zero load where the voltage was measured as 2.67 mV. This is very close to the initial reading and indicates linearity in the load/unload cycle. This load/unload cycle was then repeated a further five times to remove any residual non-linearities in the model.

5.3.3 Experimental testing

After all the gauges and settings were checked for drift and loss of calibration, the testing commenced by recording the zero load readings for all the gauges. These were necessary as the bridge was not fully balanced and would have some residual resistance at zero load due to the gauges, connections and lead wires. Different compensation circuits were used for the 0°, +45° and -45° directions.

The model was then loaded to 5 kN. After a five minute settling period, the loaded readings for all the gauges were recorded. Both the loaded and unloaded voltage readings V_{out} were required in order to establish the strain induced voltages δV_{out} which were then manipulated by the data reduction equations of Appendix G to calculate the surface strains.

The testing was completed by unloading the model back to zero load. All the final zero load voltage readings were then recorded to allow comparison with the initial zero load voltage readings as a check for non-linearity.

6 RESULTS AND DISCUSSION

6.1 The Road Tanker

6.1.1 Internal pressure

The finite element analysis of the internal pressure load produced the plot shown in Figure 6.1. The original FEM mesh in the undisplaced position is shown as dashed lines. The displaced shape (magnified by 64 times) is plotted in solid lines and shows the deformation of the tanker under the influence of the internal pressure. The rear of the tanker was constrained in the axial direction at the second ring at x = 1 m and this is clear from the limited elongation towards the back of the tanker. The front of the tanker showed significant axial elongation.

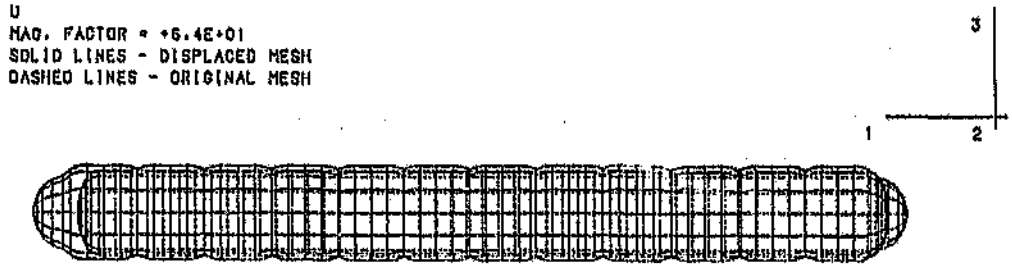

Figure 6.1 Original and displaced mesh of the road tanker FEM model with 8,4 Bar internal pressure.

The effect of the dome to cylinder discontinuity is also shown. The cylinder is more flexible in the circumferential direction and expands more than the ellipsoidal dome. The interaction of these two components results in a transition region between them

with reverse curvature at the knuckle radius. The effect that this has on the force and moment resultants were discussed later. The top or apex of the dome has a low curvature and the pressure results in the considerable axial deformation of this region. The cylindrical section of the tanker expands circumferentially under the influence of the internal pressure. The relatively stiff circumferential rings affect this expansion as is clear from the displaced plot.

Figures 6.2 to 6.9 show the variation of the dimensionless force and moment resultant along the tanker for a pure internal pressure of 8.4 Bar. This represents a gas pressure without the bending effects which result from the acceleration of the shell or its contents. This idealisation allows for the comparison of the FEM, theory of plates and shells (Timoshenko 1959) and a large deformation analysis of ellipsoidal pressure vessel heads by Uddin (1985). Both Uddin and Timoshenko derive their analyses for isotropic materials such as steel. The theoretical predictions from the MATHEORY program used isotropic theory with the engineering constants of the laminate substituted for the moduli, Poisson's ratio and shell flexural rigidity as discussed in Appendix C. The shell and dome laminate were assumed to be orthotropic and quasi-isotropic respectively and this allowed the use of the laminate engineering constants E_x, E_ϕ, $G_{x\phi}$ and $\nu_{x\phi}$ to be used.

The use of the dimensionless force and moment resultants $N_x' = N_x/(p.r_i)$, $N_\phi' = N_\phi/(p.r_i)$, $N_{x\phi}' = N_{x\phi}/(p.r_i)$, $M_x' = M_x/(p.r_i.t)$, $M_\phi' = M_\phi/(p.r_i.t)$, $M_{x\phi}' = M_{x\phi}/(p.r_i.t)$, $Q_x' = Q_x/(p.r_i)$ and $Q_\phi' = Q_\phi/(p.r_i)$ is convenient as it allows comparison of the FEM results to curves produced by Uddin (1987). His research solved the force and moment distributions by non-linear shell equations using the multi-segment method of integra-

tion. However, this tank did not have circumferential rings and could be considered as thin walled with $r_i/t = 100$. The road tanker had r_i/t of 43 and a pressure/modulus ratio of 37×10^{-6} which compared with Uddin's research with a pressure/modulus ratio of 37.6×10^{-6}.

The FEM and theoretical data used below are presented in Appendix Q. Appendix S shows the output of the all the FEM values of axial, circumferential and inplane shear force resultants for the entire cylindrical section of the tanker. This is represented by 'unrolling' the tanker cylinder into a flat plate with the tanker length (x) as the longitudinal axis, the tanker circumference (arc) as the sideways axis and the various force resultants as the vertical axis. The value of arc = 0 corresponds to the top of the tanker. This representation shows all the Gauss point values from FEM between the tan lines of the tanker. The values are plotted in their 'as is' condition without the approximations of any curve fitting or contour mapping routines provided by the ABAQUS post processor.

Non-dimensional axial force resultants (N_x')

This is presented in Figure 6.2 where only one-half of the tanker is shown as the loads were symmetrical with respect to the middle of the tanker. The forces in the domes are also shown to allow comparison of the dome results with literature. The axial force resultants were a function of the axial forces in the shell which result from the pressure acting on the projected area of the dome. This varies with the radius r_i in the dome as shown by the curve $-0,33 \leq x \leq 0$. The N_x' is also relatively unaffected by the dome/cylinder discontinuity and the circumferential stiffeners as shown by both the FEM and theoretical predictions. The two curves

were almost identical over the entire length of the tanker, with the exception of the two FEM values at the apex of the dome.

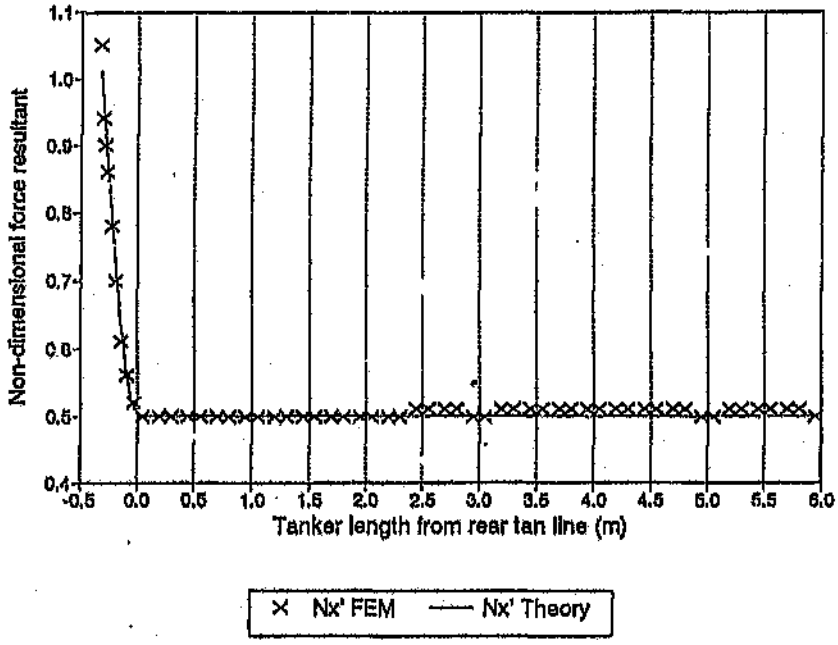

Figure 6.2 Non-dimensional axial force resultants (N_x')

These differences may result from the use of the linear triangular elements in this region which were connected with multi-point constraints. The average error along the cylindrical portion of the tanker varied between one and two percent. This correlation proved the accuracy of the FEM method in predicting the axial force resultants.

The axial force resultants N_x between the tan lines of the tanker were shown in Figures S1 and S2 of Appendix S. These show the influence that the supports and rings have on N_x. The magnitude changes were negligible with the values varying between

270 kN/m and 281 kN/m. The regions between the supports show little variation over the membrane stress prediction (see Eqn 3.1).

Non-dimensional circumferential force resultants (N_ϕ')

Figure 6.3 shows the variation of the non-dimensional circumferential force resultant (N_ϕ') for the back half of the tanker. The FEM prediction for N_ϕ' is identical in shape to the non-linear analysis of Uddin (1985). The value at the apex of the dome (x = 0,325) is predicted by FEM, theory and the Uddin analysis to be 0,99; 1,01 and 0,97 respectively.

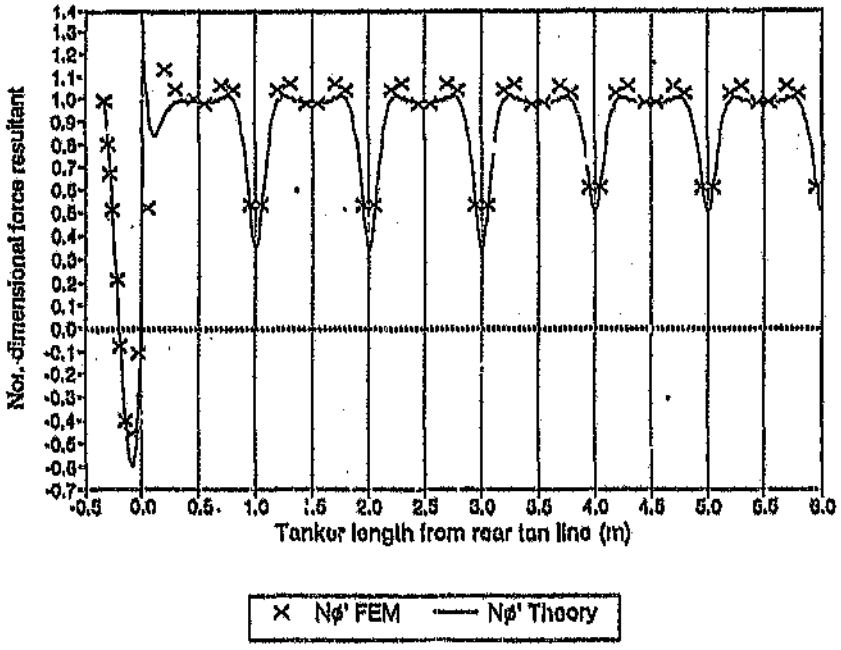

Figure 6.3 Non-dimensional circumferential force resultants (N_ϕ')

As predicted by Timoshenko (1959) and confirmed here, a compressive zone develops near the ellipsoidal dome to cylinder junction. The FEM curve indicates that this compressive force resultant is not as severe as predicted by either Timoshenko or the Uddin analysis with the minimum values of -0.46, -0.59 and -0.6 for the FEM, linear theory and Uddin results at x = - 0,089 m. The FEM, theory and Uddin values were also similar at the maximum value at x = 0,02 with values of 1.13, 1.14 and 1.07 respectively. The maximum for the theory occurred at x = 0,001 with a value of 1,35. The circumferential stiffener at x = 0 had a significant effect on the FEM force resultant at the tan line. The FEM minimum value of 0,52 at x = 0,05 is considerably less than the theoretical prediction of 1,35. The FEM result is however similar to those at the other ring stiffeners at x positions of 1, 2 and 3 m. The supersition of the dome and ring discontinuity stresses by the theory did not predict this value for the tan line, although the values at the remaining stiffeners were accurate.

The influence of the remaining circumferential rings caused significant deviations from the membrane theory (Eqn 3.2) at the regions close to the rings. This effect is proportional to the stiffness of the rings as can be seen by the differences between the stiffer rings at x = 1, 2, 3 m and the more flexible rings at 4, 5, 6 m. The stiffer rings at x = 1, 2, 3 had a section 100 mm high by 50 mm wide and those at x = 4, 5, 6 were of a square 50 mm by 50 mm section. Because the N_ϕ is related to the deflection w by $N_\phi = E.t.w/r$, the force resultant curve had a similar shape to the deflection curve with the minimum deflection and N_ϕ' directly under the ring. The remainder of the shell is able to expand beyond the rings, and for values of $x > 2.\pi/\beta$ i.e. (x > 0,476), the radial deflection and circumferential force resultant could be predicted accurately by Timoshenko's (1959) membrane

theory. The N_ϕ' curve followed the deflection curve of Timoshenko (1959) closely with a decrease which had its minimum under the ring. The theoretical N_ϕ' values corresponded to the FEM predictions for the large and small rings. This represented an unloading of the shell while the circumferential load is absorbed by the stiffer rings. This effect is very localised and predicted by Timoshenko to be significant for $x < \pi/\beta$ (i.e. $x < 0{,}238$). The theory and FEM results were very similar with values of 0,52 and 0,53 for the large ring at distances of 0,05 m from the ring centre-line. The shapes of the curve were also identical. The minimum values occurred under the ring and theory predicted 0,36. The maximum values of N_ϕ' at distances of 0,3 m from the stiffener centre-line were similar with 1,07 for the FEM and 1,02 for the theory.

The circumferential force resultants N_ϕ between the tan lines of the tanker are shown in Figures S3 and S4 of Appendix S. These show the influence that the rings have on N_ϕ. The supports at $x = 1$ and $x = 11$ have no influence on N_ϕ. This may result from the stiff rings at this region which redistribute the forces at the top of the cradle support (or horns) before they can influence the shell. The high local stresses predicted by Zick (1951) result from the tank expanding over the stiff horn of the support, in this case without the circumferential ring. The FEM definition of only a single sideways constraint at nodes 4669 at $x = 1$ and node 5029 at $x = 11$ also allowed for more support flexibility, thus decreasing the discontinuity stresses.

Non-dimensional inplane shear force resultants ($N_{x\phi}'$)

The application of a pure internal pressure in the tanker shell does not result in any significant inplane shear forces. This is

indicated by the theoretical and FEM curves of Figure 6.4 which shows both curves with average values of zero across the entire tanker. The magnitude of the FEM values are small compared to the predictions of axial and circumferential force resultants.

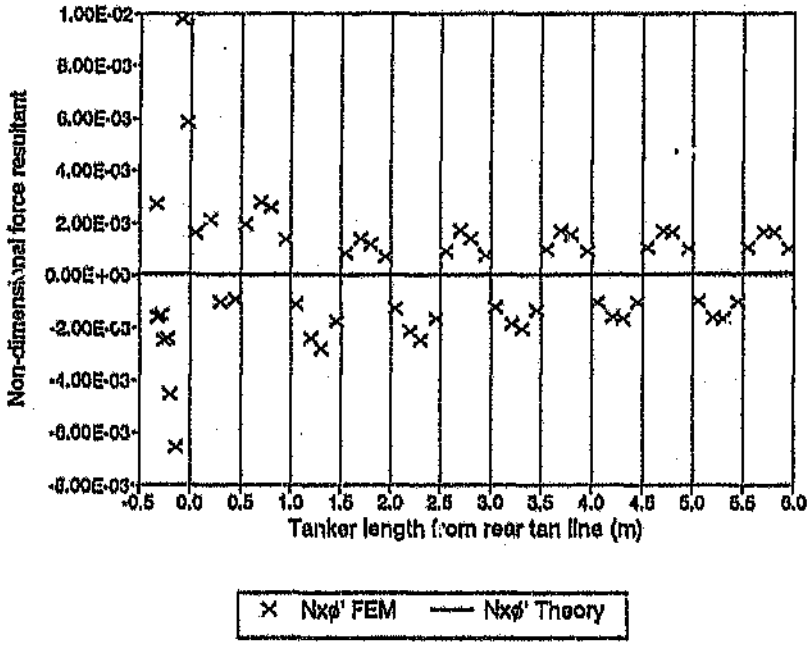

Figure 6.4 Non-dimensional inplane shear force resultants ($N_{x\phi}'$)

Figures S5 and S6 of Appendix S showed the FEM values to be low (between -3153 and 3324 N/m) compared to the values for N_x which averaged at 273000 N/m. These results prove the accuracy of this FEM model for predicting the axial, circumferential and inplane shear force resultants, (N_x, N_ϕ and $N_{x\phi}$).

Non-dimensional axial moment resultants (M_x')

Figure 6.5 shows the variation of the non-dimensional axial moment resultant M_x' for the back half of the tanker. Representing the moments as non-dimensional data is used to allow comparison with the results presented by Uddin (1985). The M_x' are predicted by FEM to be zero at the apex of the dome at x = -0,325m. The FEM curve increased to M_x' = 0,0208 at x = -0,26. The curve continued to a minimum of -0,12 at x = -0,09 and then increased to 0 at x = 0. The FEM curve further increases to 0,0397 at x = 0,2 and then dropped below zero to a value of -0,017 at x = 0,3. The values at x = 0,55 and 0,575 were very close to zero.

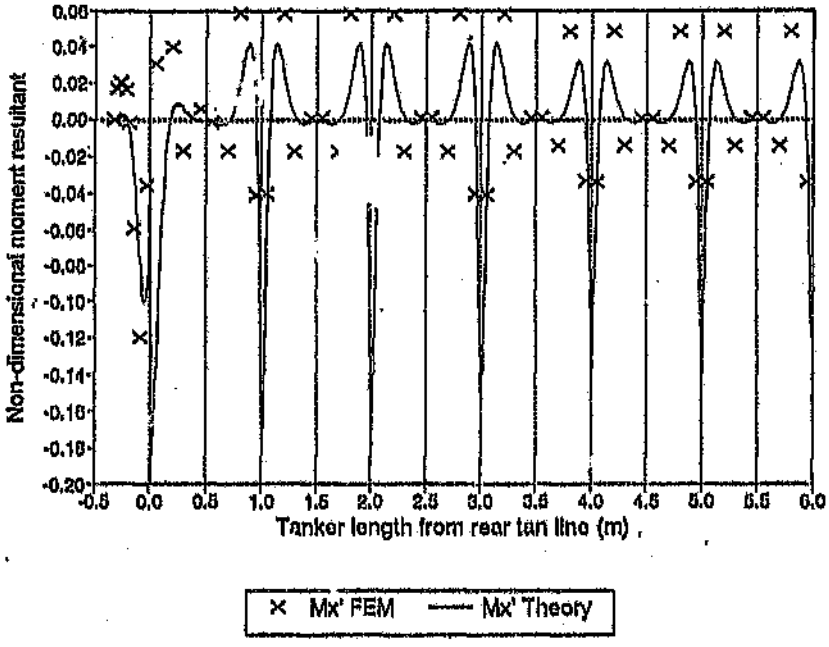

Figure 6.5 Non-dimensional axial moment resultants (M_x')

This result is predicted by the discussion of Appendix E as these moments were of a local nature and the result of the stiffness discontinuity between the cylinder, rings and domes. They will reduce to zero when the section of the uniform cylinder is large enough. The FEM results also show the differences between the moment resultants at the thick and thin rings. The thick rings result in a larger discontinuity and hence cause greater moments.

The theoretical curve of Figure 6.5 also begin at zero, and the values remain very small until x = -0,2. The curve then follows the FEM prediction to value of -0,054 at x = -0,129. The curve then undergoes a discontinuous change from the head to the cylinder. This deviation of the theoretical curve could be explained by the assumptions made to allow the isotropic theory to be applied to the laminated composite. Assumptions were made with respect to the equivalent flexural rigidity and Poisson's ratio of the cylinder and head. Equivalent properties where used in both cases with the cylinder flexural stiffness approximated by D_{11} of the laminate bending stiffness matrix of Appendix D. The sudden change in these properties would result in the discontinuous variation of the theoretical $M_x' = -0,0317$ at $x = -0,009$ (dome) to $M_x' = -0,20$ at $x = 0,001$ (cylinder). The curve between x = 0,025 to 0,45 do however not follow the FEM predictions and this may again result from the previous assumptions. Both the FEM and theoretical values converge to zero at x = 0,55. The magnitudes of the curves at the ring stiffeners also differ. This may again result from the assumptions concerning stiffnesses for the theoretical model. The shape of the curves were similar and particularly the FEM curve closely resemble those presented by Timoshenko (1959) for the bending of a long cylindrical shell by a load uniformly distributed around the cylinder. The predictions by Uddin were however very similar

to the FEM results around the regions of the head and cylinder junction with a minimum value of $M_x' = -0,12$. The value at $x = 0$ of $M_x' = 0$ is identical to the FEM prediction. The maximum value on the cylinder is $M_x' = 0,09$ and then decreased rapidly to zero. Comparison of these curves highlighted the sensitivity of the theoretical solution to the assumptions made in order to accommodate the isotropic theory. It would be possible to derive these relationships specifically for laminated composites, but this is beyond the scope of this research.

Non-dimensional circumferential moment resultants (M_ϕ')

Figure 6.6 shows the moment resultants which arises from the Poisson's effect where $M_\phi = \nu.M_x$ (Eqn E3 of Appendix E). These FEM curves have values at the apex of the dome very similar to M_x'. This was expected due to the geometry of the dome. The curve then dropped to a minimum of -0,036 at $x = -0,9$. Back calculation of the ratio of M_ϕ'/M_x' would indicate the equivalent Poisson's ratio of 0,28 compared to the prediction from CLT (Appendix C-2) of 0,27. The shape of the M_ϕ' followed the shape of the M_x' curve for the FEM prediction. Close correlation is achieved for the curves from Uddin (1985) for dome regions before the dome-cylinder junction.

The theoretical curves were generated from the theory of Appendix E. The magnitude of the theoretical curves did not correlate with the FEM curves for the regions between the apex and the knuckle ($-0,33 < x < -0,14$). The deflection of this region of low curvature is very dependent on the flexural stiffness and the assumption of an equivalant stiffness may be the cause for this disparity. The shape of the FEM and theoretical curves correlate for regions before the junction. The regions after the tan line were

largely influenced by the ring stiffener and were not predicted accurately by the theory. The M_{ϕ}' curves around the remaining ring stiffeners followed a similar trend although the magnitude difference of the FEM and theoretical results is apparent.

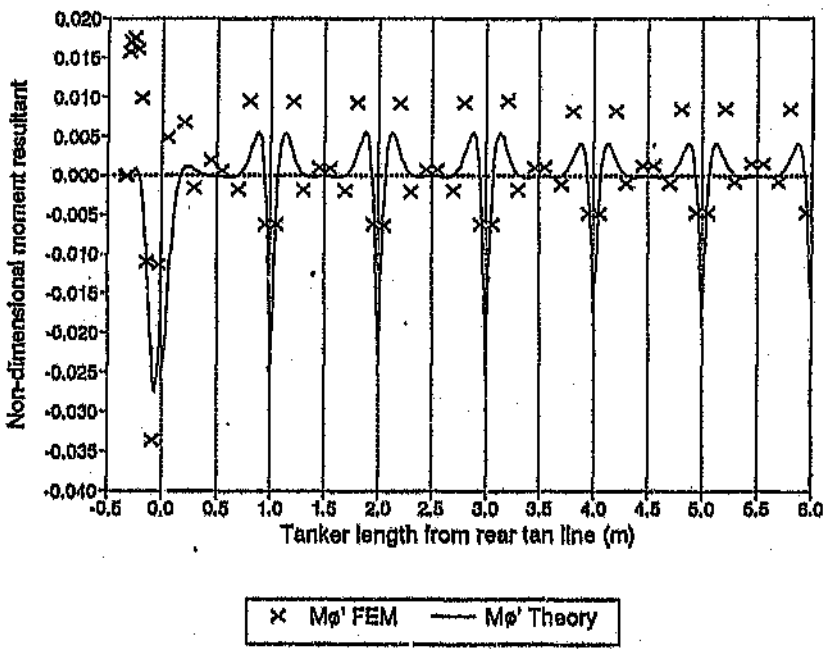

Figure 6.6 Non-dimensional circumferential moment resultants (M_{ϕ}')

Non-dimensional twisting moment resultants ($M_{x\phi}'$)

The FEM and theoretical predictions are shown in Figure 6.7. The FEM prediction mostly averaged around zero with the exception of the regions at the tan line (x = 0), where a maximum of $Mx\phi'$ = 0,00317 is predicted. The theoretical prediction for the entire

length of the tanker is zero and resulted from the absence of any twisting moments or bending induced shear forces on the shell.

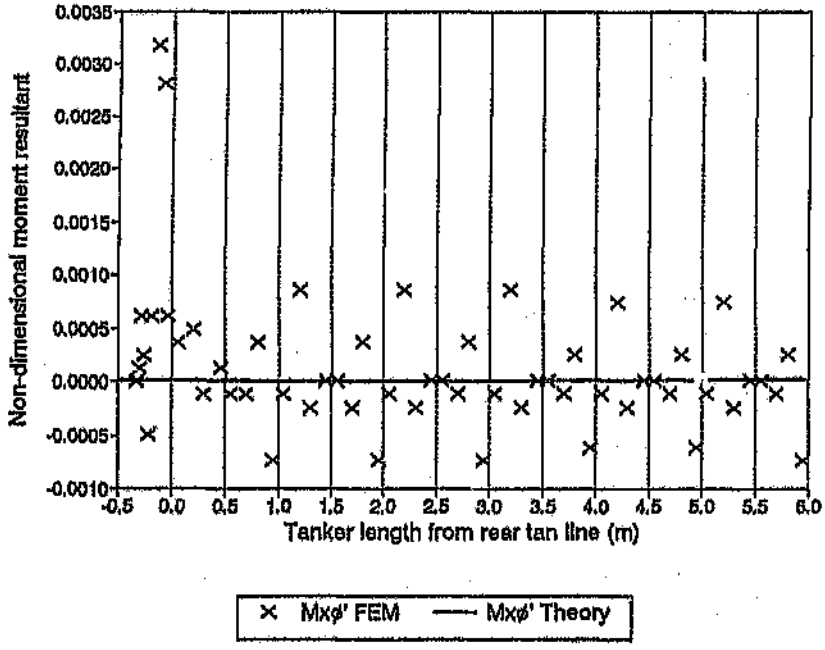

Figure 6.7 Non-dimensional twisting moment resultants ($M_{x\phi}'$)

Non-dimensional axial transverse shear force resultants (Q_x')

These transverse shear force resultants exist at the cylinder/dome junction and rings and were derived theoretically in Appendix E. Figure 6.8 shows the FEM and theoretical predictions along the cylindrical section of the tanker. The two curves correlate at the dome and this can be attributed in the definition of the same isotropic material properties for both the FEM and theoretical analyses. The curves for the cylinder were however very different. The assumptions made to accommodate

isotropic plate theory assumed this stiffness to be equal to the equivalent inplane shear moduli of the dome and shell, which were 7,47 and 4,63 GPa respectively. The lamina or single layer transverse shear moduli where defined in Appendix C as being G_{13} = 4,14 GPa and G_{23} = 3,5 GPa.

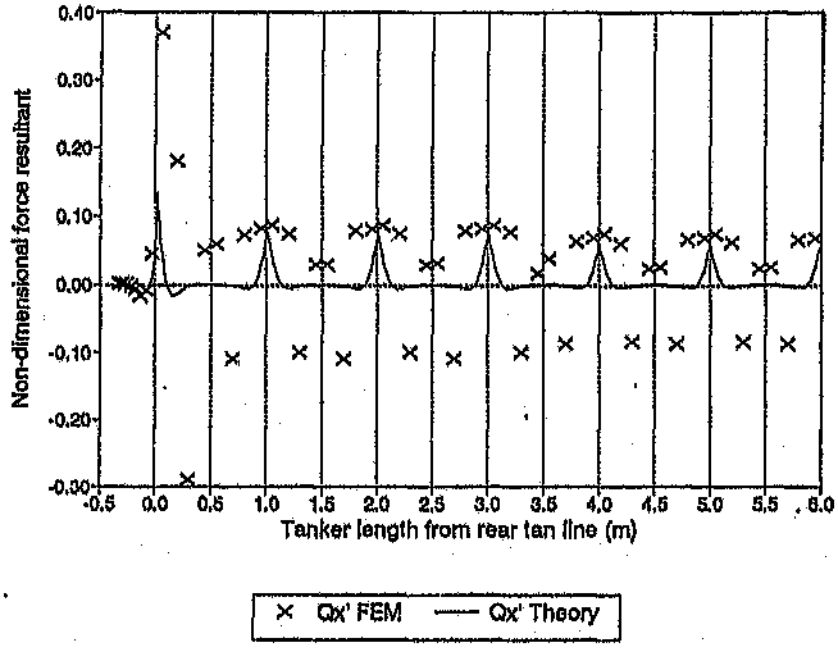

Figure 6.8 Non-dimensional axial transverse shear force resultants (Q_x')

However, the laminate equivalent transverse shear stiffnesses were dependent on the layup orientation. The magnitude of the transverse shear forces were also dependent on the ring circumferential stiffness as these cause the discontinuity which prevents the cylinder from expanding freely from the internal pressure. The combination of these results may explain the lack of correlation between the FEM and theory.

Non-dimensional axial transverse shear force resultants (Q_ϕ')

From the conditions of symmetry (see Appendix E), the Q_ϕ' are predicted as zero. This is shown by the results of Figure 6.9 where the FEM and theory values average around zero. The theoretical prediction for the entire tanker cylinder is $Q_\phi' = 0$.

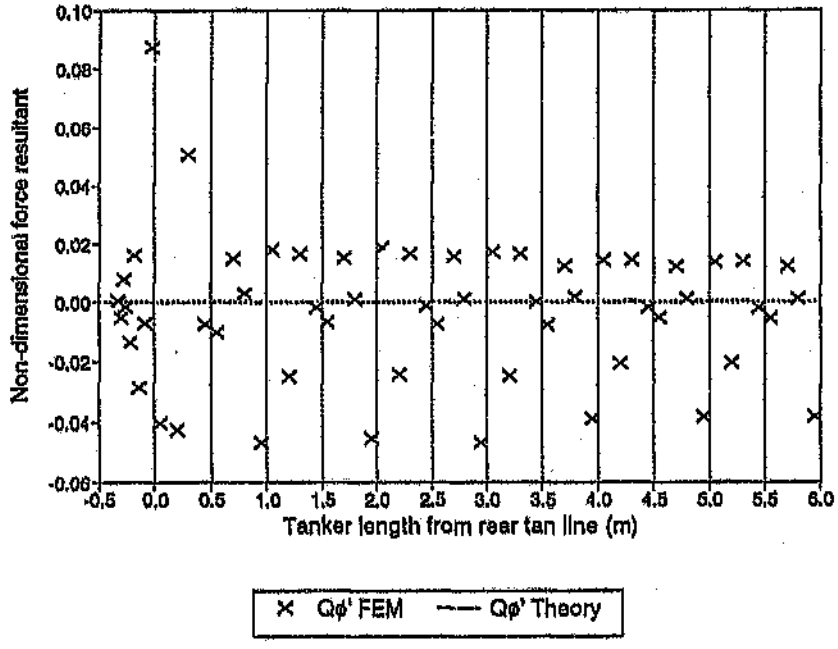

Figure 6.9 Non-dimensional circumferential transverse shear force resultants (Q_ϕ')

6.1.2 Combined accelerations

The FEM analysis of the combined accelerations load case was run once suitable convergence had been achieved with the pressure load case. This served to validate the FEM model. Shown in Figure 6.10 and 6.11 were the output of the combined accelerations deflection plots.

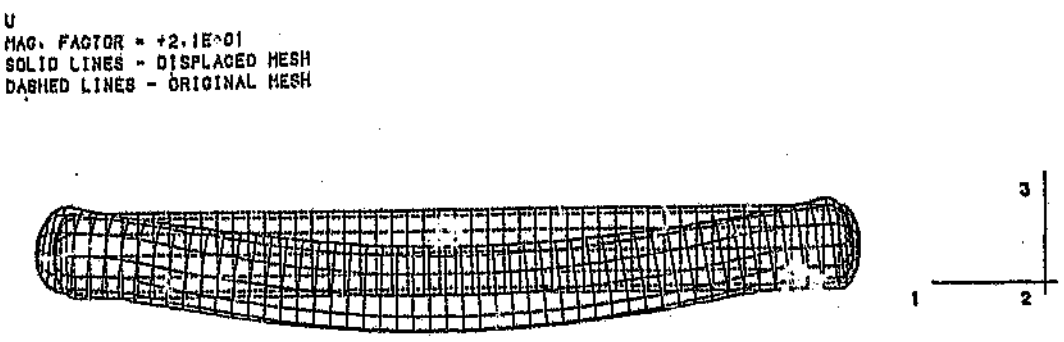

Figure 6.10 FEM plot of the tanker shape resulting from the 2g combined accelerations (side view).

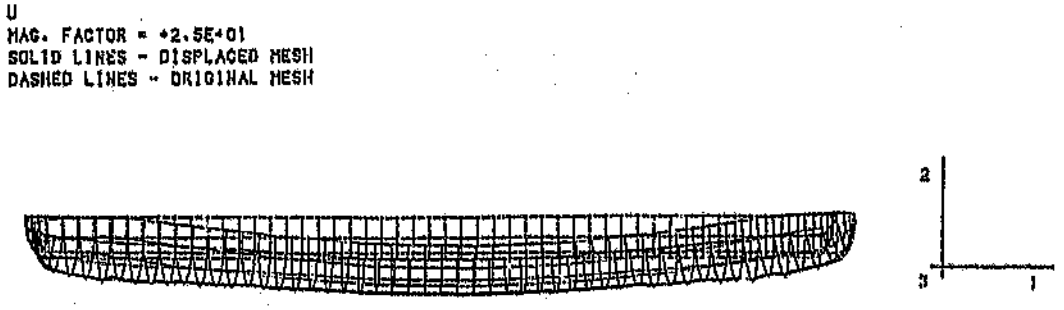

Figure 6.11 FEM plot of the tanker shape resulting from the 2g combined accelerations (top view).

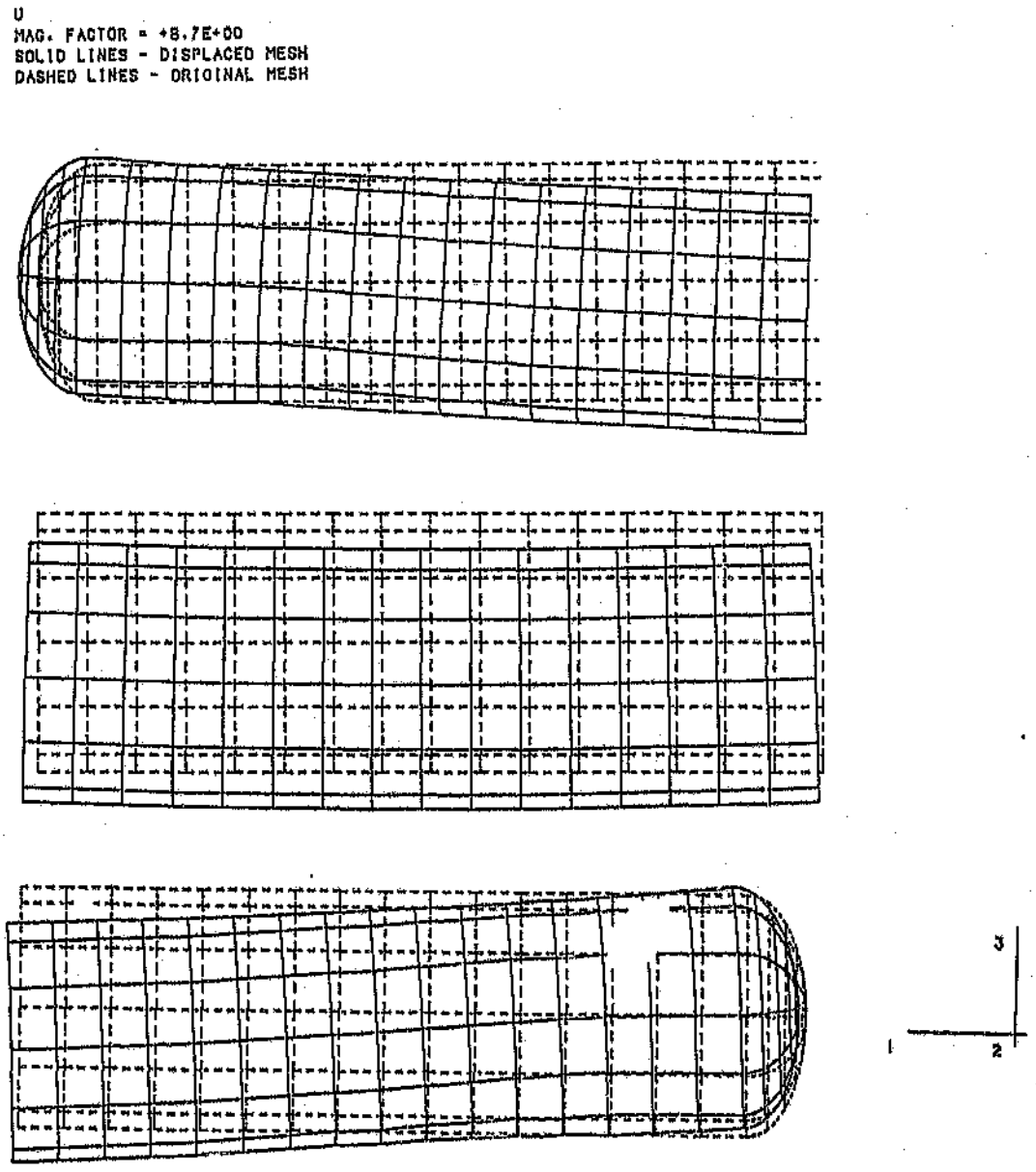

Figure 6.12 Detailed FEM plot of the tanker shape resulting from the 2g combined accelerations (side view).

The undeformed geometry is shown in dashed lines with the deformed geometry superimposed. Both deflected shapes have been exaggerated to show the deflections. The vertical and sideways bending of the shell is apparent in both plots. The effect that the supports at x = 1 and x = 11 have on the shell deformation is shown in more detail in Figure 6.12.

The FEM and theoretical data used below are presented in Appendix R. Appendix T shows the output of the all the FEM values of axial, circumferential and inplane shear force resultants for the entire 'unrolled' tanker. This representation shows all the Gauss point values from FEM between the tan lines of the tanker. From these plots it is clear that the force resultants varybetween different sections and that separate curves are required for the top (+z), bottom (-z), left (+y) and right (-y) of the tanker to allow comparison between the FEM and theory results.

Axial Force Resultants (N_x)

The axial force resultant N_x are dependent on the distribution of axial forces and bending moments along the tanker. Figure T1 and T2 of Appendix T show the variation of N_x over the tanker. The horns of the supports at x = 1 cause considerable peaks as a result of the shell and support interaction. The rest of the shell was uniformly loaded and dependent on the bending and axial loads.

Figure 6.13 shows the variation of N_x along the top of the tanker. The theoretical curve between $0 < x < 1$ is largely dependent on the vertical bending of the rear overhang, with minor effects from hydrostatic pressure and axial force. The axial load which results from the hydrostatic pressure on the front dome is

introduced into the shell at the rear

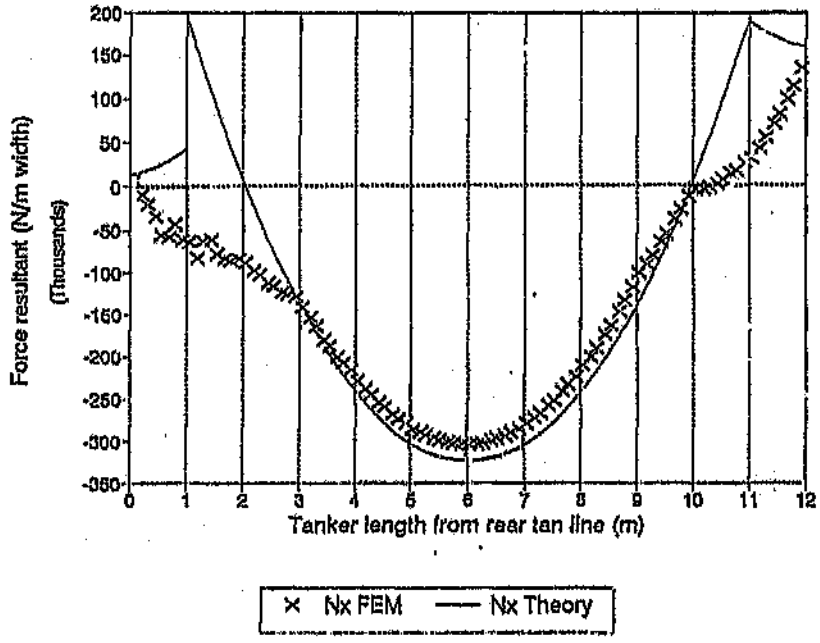

Figure 6.13 Axial force resultant N_x in the top of the tanker (+z).

support and results in the sudden increase in N_x at x = 1 to 185,5 kN/m. The N_x curve then follows the classical simply supported beam with uniformly distributed load typical of a horizontal tank under vertical acceleration. The minimum compressive value is -323,7 kN/m at x = 6. The curve then increases back to 186,3 kN/m at the front support at x = 11. The bending of the front overhang results in a decrease of N_x to the front tan line value of 159 kN/m. The FEM curve drops from 7,3 kN/m at x = 0 to -62,9 kN/m at x = 1. The N_x then decreases parabolically to a minimum of -303 KN/m at x = 6. The value then increases to 31,3

kN/m at x = 11, with a change in slope at x = 10. The tan line value of 134 kN/m at x = 12 is lower than that predicted by theory. The back support has considerable influence on the axial force resultant N_x. The flexibility of the shell above the support also affects the distribution of the load. The FEM results differ considerably from the theoretical curves until x = 3 along the length. This may result from the reduced load transfer along the top of the tank as a result of the flexibility of the shell. This phenomenon was documented by Zick (1951) who found that a considerable section of the area above a saddle support is ineffective in transferring load into the saddle as a result of the material's behaviour under compressive loading. This phenomenon is less problematic in stiffened tanks although its effect on the more flexible composite material is difficult to predict theoretically. From this curve it is clear that the stress concentrations at the top were not as significant as those at the sides and bottom of the tanker. The minimum compressive load of between -303 kN/m is not the minimum for the tanker as a result of the axial tensile component of the hydrostatic pressure on the front dome. The minimum compressive load is obtained for the vertical acceleration of 2G only, and the value of -457 kN/m was used to determine the minimum composite thickness to give a safety factor of four against buckling.

Figure 6.14 shows the variation of N_x along the bottom of the tanker. The tensile component of the bending moment and hydrostatic head combine and result in the maximum tensile N_x in the tanker shell. The effect of the supports is considerably more significant, especially at the back support x = 1 where the axial hydrostatic head component is transferred from the shell. The theoretical curve experiences a sudden jump from the pressure component to 156 kN/m at x = 1, followed by a bending moment distribution typical of a horizontal tank. These values were not

affected significantly by the bending moment of the end overhang as these were relatively short. A large tensile peak of 377 kN/m is predicted by FEM on the dome side of the support, but this drops to a value of -113 kN/m on the cylinder side.

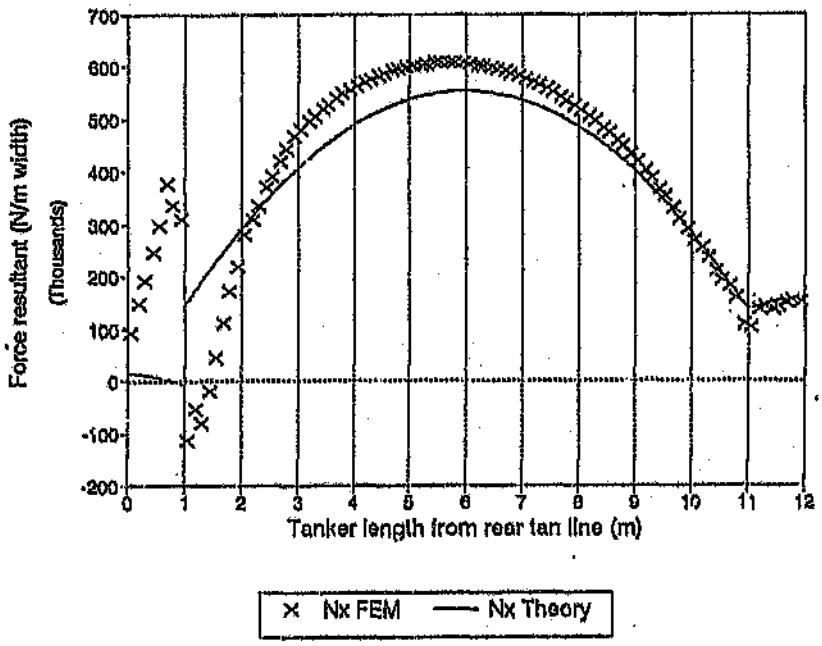

Figure 6.14 Axial force resultant N_x in the bottom of the tanker (-z).

The FEM curve differs considerably at the position of the back support x = 1. The large FEM tensile forces for $0 < x < 1$ most likely result from a stress concentration. The N_x variation then becomes complicated by the load distributed through the rings to the shell, as the ring is constrained to provide an axial (x) and vertical (z) support. The sideways acceleration may also have an effect on these results. From x = 2.3 m, the FEM curve follows

the theoretical curve more closely, showing a typical bending distribution. The FEM and theory curves convergence towards the front of the tanker. The stress concentrations around the front support were negligible as there no axial constraint at this position. The FEM and theory curves were very close for the region of $9 < x < 12$.

Figure 6.15 shows the variation of N_x for the left (+y) and right (-y) of the tanker. The N_x on the sides of the tanker were dependent on the axial force from the hydrostatic pressure and the sideways bending from the acceleration A_y. The theoretical curves for the left (+y) and right (-y) sides were very similar to those for the top and bottom as their only inputs were the axial forces and bending moments resulting from the axial, sideways or vertical acceleration. The theoretical N_x between $0 < x < 1$ were low as the overhanging portion of the shell is relatively small. The back support is constrained in the axial (x) direction and this allows transfer of all the axial force into the shell via the ring stiffener. There is however a significant difference between the theory and FEM curves for both the left and right of the tanker at the back support ($x = 1$), The left (+y) theoretical curve jumps from a low value just before $x = 1$ to the value for the axial pressure load of 185,5 kN/m. The distribution then continues following that expected from a bending analysis for a uniformly distributed load. The FEM prediction for the left (+y) shows a large peak of 594 kN/m at this support. This is approximately three times that predicted by theory. This may result from the application of a completely pinned constraint at the 120° saddle support. The discontinuity of this support (which occurs for the lower 120° of the cylinder) may result in the concentration of stress at the horn or top point of the support. The large sideways movement of the tank centre as a result of the fluid and shell sideways acceleration

would result in a compressive stress resultant in the middle of the tank as shown. However, this displacement of the tank shell away from its unloaded position is constrained by a very rigid support at the horn. This effect further contributes to the high stress concentration at this point. In reality, the support does have some flexibility and a FEM 'improvement on this result would be achieved by modelling the entire support down to the chassis to ensure correct load distribution.

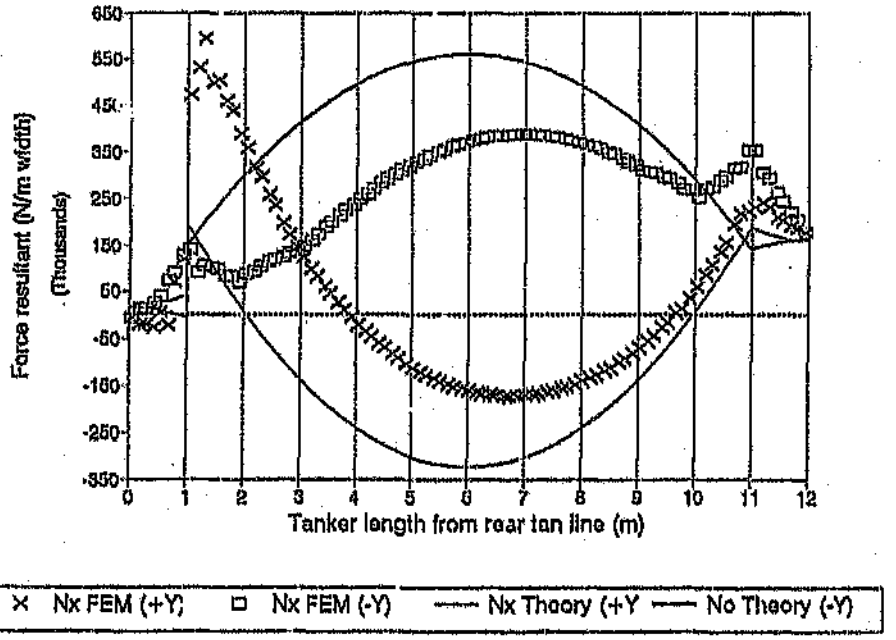

Figure 6.15 Axial force resultant N_x in the left (+y) and right (-y) side of the tanker.

Another reason for the difference between the FEM and theory results is the positioning of the support. Beam theory assumes the support in the middle or across the entire height or width of the beam. For the tanker, the supports span only the bottom 120°

of the shell. This may also contribute to the large differences between the FEM and theory for especially the sides of the tankers, where the supports were not symmetrical and offset with the line of action of the acceleration.

The theoretical curves for the right side (-y) of the tanker were similar to those for the bottom of the tanker. The sideways acceleration results in a largely tensile N_x for this portion of the shell. The FEM results for $0 < x < 1$ increase linearly from $x = 0$ to a peak at $x = 1$. The effect of the support is not as significant as is seen on the left (+y) side of the shell, although the region $1 < x < 10$ also shows considerable differences between the FEM and theory results. The region between $1 <$ and < 2 shows an almost constant N_x which then increases to a maximum of 387 kN/m at $x = 6,8$ m. It is clear from these analyses that the sideways accelerations have not been accurately predicted by theory. The FEM maximum values were lower than the predicted results in regions remote from any stress concentration.

Circumferential force resultants (N_ϕ)

Figures 6.16, 6.17 and 6.18 show the variation of the circumferential force resultant N_ϕ for the top, bottom and sides of the tanker. These force resultants were a result of the internal pressure generated by the acceleration of the liquid towards the front of the tanker. The areas between the rings exhibit a linear increase in N_ϕ which varies in direct proportion to the hydrostatic pressure at that point. The values at the ring stiffeners were lower d: to the unloading effect that the ring stiffeners have on the shell. The relatively stiff rings carry a significant amount of the circumferential load at these positions with the load being transferred from the shell to the stiffener by a

combination of transverse shears and local moments. Due to the similarity of the A_y and A_z accelerations, the only difference between the +z, -z, +y and -y circumferential force resultants ($N\phi$), in areas remote from ends of supports, is the hydrostatic head in the z and y directions respectively. The FEM values for the top (+z) were on average 32 N/m lower than those at the bottom of the shell (-z). This difference is close to the predicted N_ϕ difference of 30,6 N/m as a result of the hydrostatic head difference in the vertical direction. The FEM values differ from the theory at the supports at x = 1 and x = 11. These can be attributed to the stress concentrations which can have a significant effect on N_ϕ as mentioned by Zick (1959).

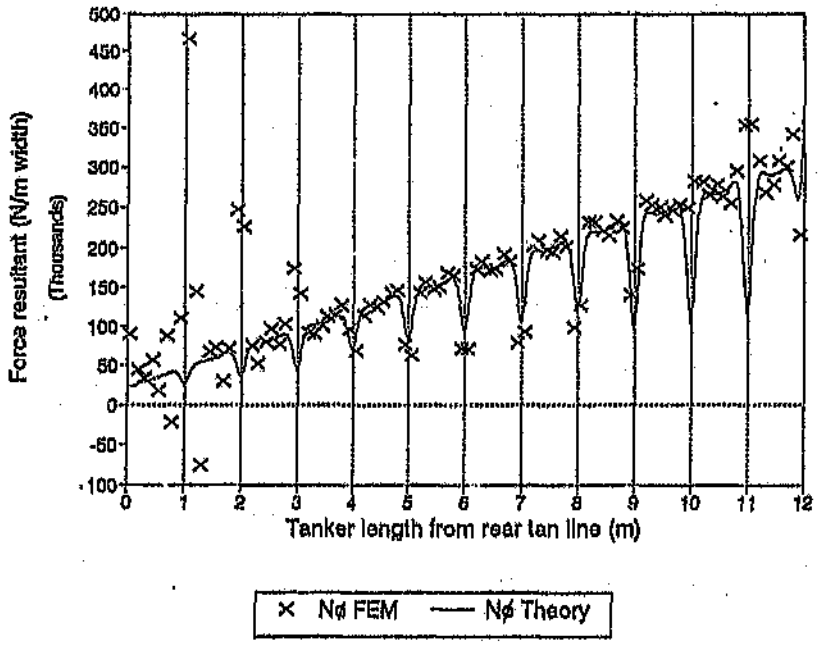

Figure 6.16 Circumferential force resultant N_ϕ in the top (+z) of the tanker.

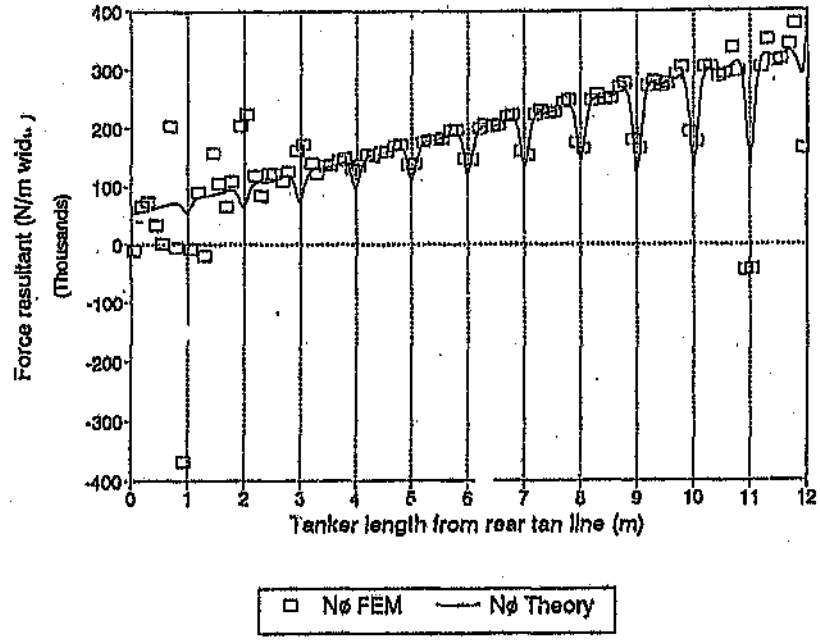

Figure 6.17 Circumferential force resultant N_ϕ in the bottom (-z) of the tanker.

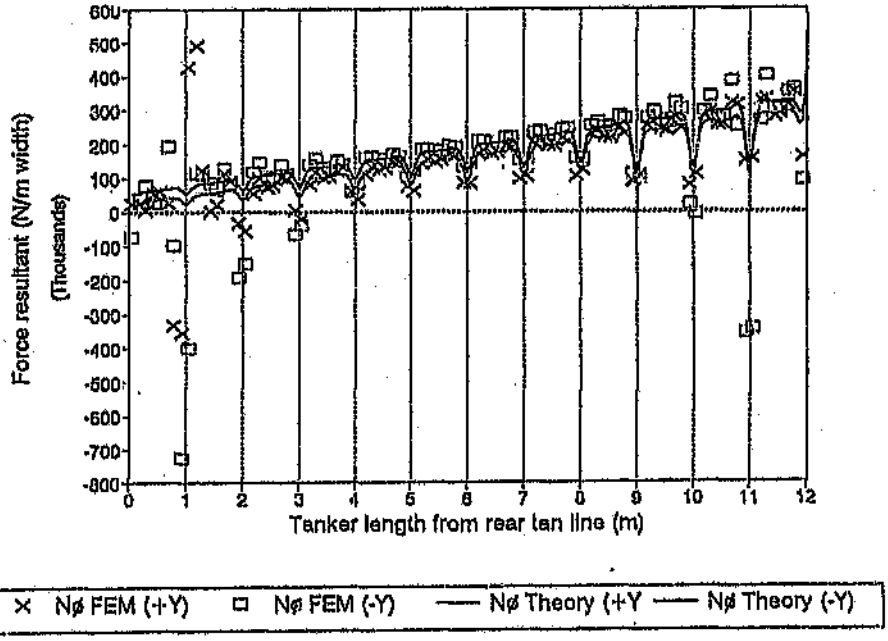

Figure 6.18 Circumferential force resultant N_ϕ in the left (+y) and right side (-y) of the tanker.

Inplane shear force resultants ($N_{x\phi}$)

Inplane shear resultants occur from the effects of shear force and torsion of the shell. The shear forces result from the load transfer of the supports and the loads induced by the accelerations. Due to the cylindrical geometry of the tanker with the thin outer skin, these shear resultants vary sinusoidally, with a maximum at the neutral axis of the shell. If a shearing stress occurs at a given point on a plane in a stressed body, there must exist a shearing stress of equal magnitude at that point on a second plane perpendicular to the first. The theoretical curves of Figure 6.19, 6.20 and 6.21 were based on these assumptions and were calculated from the shear force diagrams.

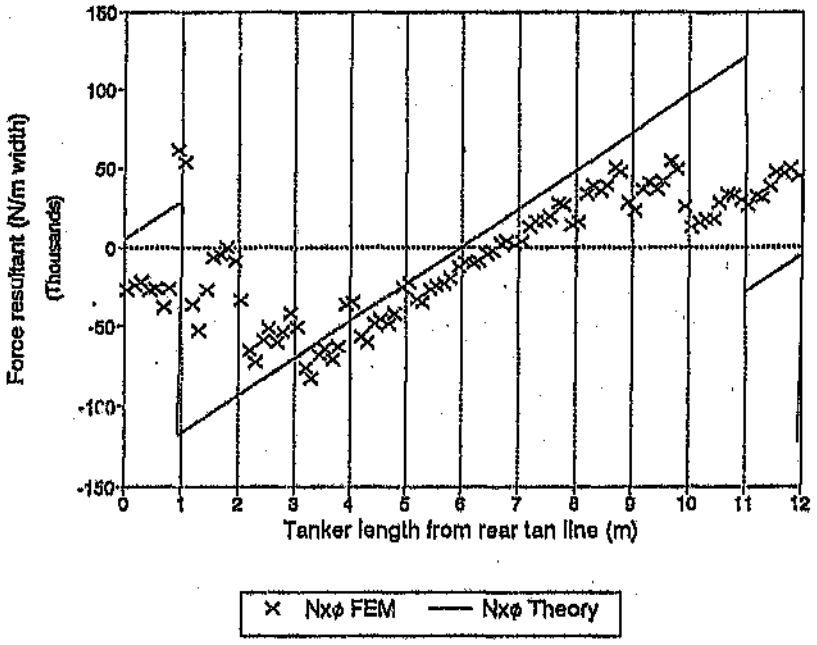

Figure 6.19 Inplane shear force resultant $N_{x\phi}$ in the top (+z) of the tanker.

No account was taken for stress concentrations at the supports because these were not available for such complex loadings on composite tanks.

Figure 6.19 shows the $N_{x\phi}$ for the top of the tanker shell. The theoretical curves follow the shear force distributions which vary lineally as a result of the uniformly distributed load of the cargo and shell. The FEM curves follow the theoretical curves with reasonably accuracy between $3 < x < 8.5$ m. The zero intercept is not however in the same position, and this may be the result of shear forces induced by the axial acceleration, which have not been taken into account in the theoretical analysis. The FEM values between $0 < x < 3$ do however not follow the theoretical curves. This may result from the effect the support geometry has on these shear resultants. The $N_{x\phi}$ at the top is largely influenced by the sideways bending produced by A_y which acts in line with the neutral axis. The vertical acceleration has little influence at this position. The load path for these shear resultants would concentrate towards these supports, hence unloading the upper section as is clear from this plot.

Figure 6.20 indicated the that the $N_{x\phi}$ at the bottom of the tanker were largely influenced by the sideways acceleration A_y and the geometry of the supports. As is found with the $N_{x\phi}$ curves for the top, the zero intercept occurs at a position of $x = 7$ m. This correspondeds to the position of the maximum N_x predicted for the +y and -y sides of the tanker in Figures 6.15. The theoretical $N_{x\phi}$ values were higher than the FEM predictions at the supports. This results from the load path where the shear loads were transferred from the shell into the supports. Although the ring stiffeners do assist in distributing these loads around the shell, the large relative stiffness of the support tended to concentrate the loads in these areas. This is

shown clearly by the peaks at 1 < x <3 and 10 < x < 11.

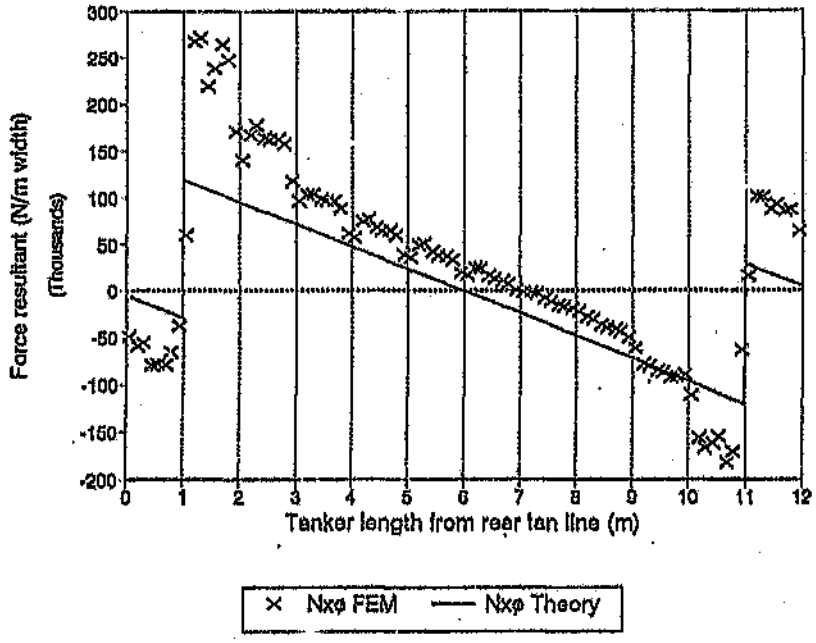

Figure 6.20 Inplane shear force resultant $N_{x\phi}$ in the bottom (-z) of the tanker.

Figure 6.21 shows the variation of the $N_{x\phi}$ for the sides of the tanker. Both the theoretical curves were dependent on the vertical acceleration and resultant bending. The left (+y) and right (-y) theoretical curves were mirror images of each other and plotted as shown to be consistent with the sign convention used by FEM. The intercept with the x axis corresponds with the position of maximum N_x at x = 6 from Figure 6.13. The FEM curve for the left (+y) of the tanker corresponded to the theoretical curve between 3 < x < 9. The FEM values at the rear support x = 1 were very different and this can be attributed to the complex load transfer from the shell to the supports. The FEM values also

undergo a discontinuity at x = 10 where deviations from the theory were apparent.

The FEM curve for the right (-y) of the tanker also correlate closely with the theory prediction between $3 < x < 9$. The intercept with the x axis also occurs at x = 6. The values at the rear support were higher than those predicted. The affect of the support load transfer could result in this increase. The FEM model is representative of the real tanker as the stiffness distribution will determine the load path of the forces. This results in the disparity of the idealised rigid beam theory predictions and the FEM results.

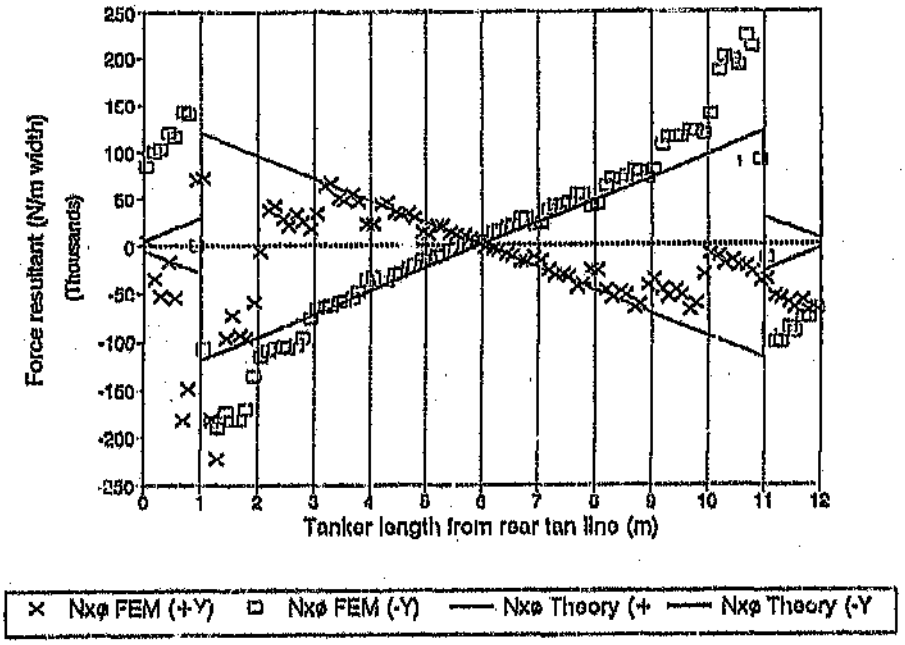

Figure 6.21 Inplane shear force resultant $N_{x\phi}$ in the left (+y) and right side (-y) of the tanker.

The vertical support at x = 11 is constrained in the vertical and sideways direction and will also transfer the shear forces into the shell. The shape of this FEM curve follows that of the theoretical curve, except that the magnitudes of the values differ beyond 3 < x < 9. Another factor which will also affect this load distribution is the effect where the load path of the shear forces is determined by the deflected tanker. It is possible that in this case, the right (-y) side of the deformed tanker has higher shear stiffness than the left (+y) side and hence transfers more of the shear load onto the supports.

Axial (M_x) and circumferential (M_ϕ) moment resultants

Figures 6.22 to 6.25 show the moment resultants for the top, bottom, left and right side of the tanker. From the discussion of paragraph 6.1.1, it is clear that the theoretical prediction of these moments is dependent on the accurate determination of the equivalent flexural stiffnesses of the cylinder. As indicated by Eqn E3, in most cases $M_\phi = \nu . M_x$ and this is shown by the FEM plots. The moment resultants of all the positions have concentrations about the back supports. The bottom and right of the tanker also have high values for the M_ϕ and M_x at the front support.

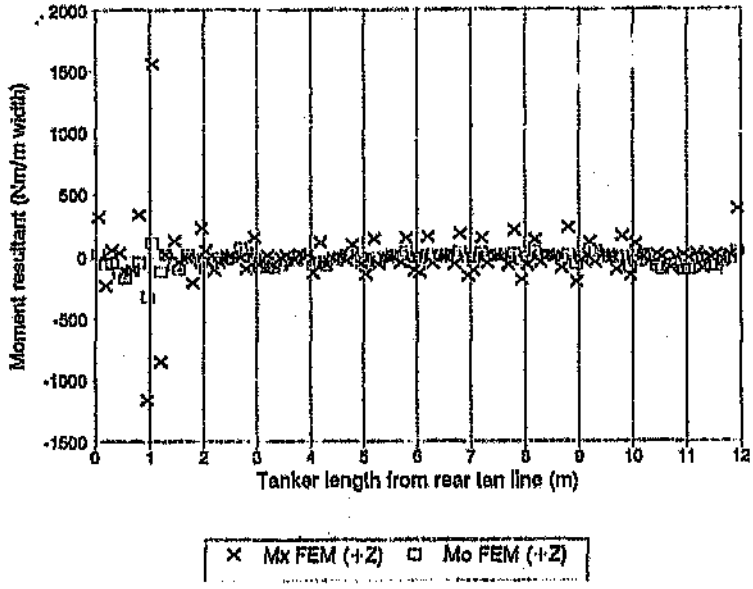

Figure 6.22 Moment resultants in the top (+z) of the tanker.

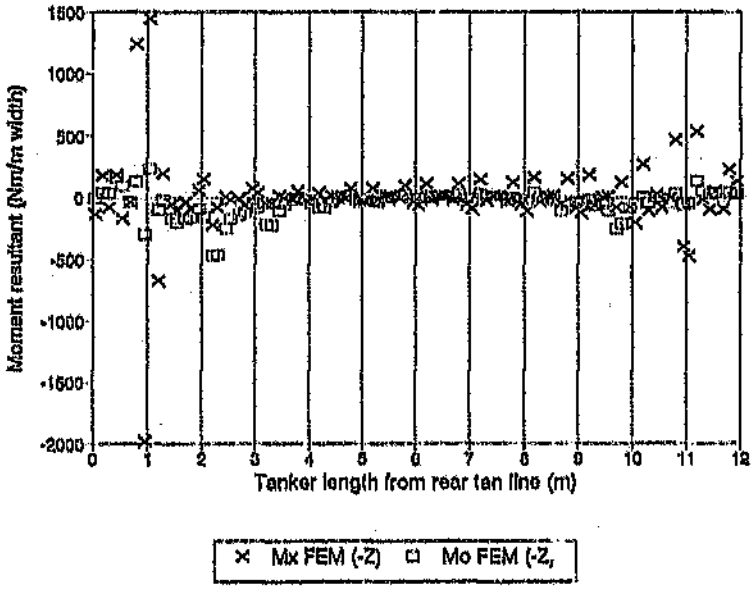

Figure 6.23 Moment resultants in the bottom (-z) of the tanker.

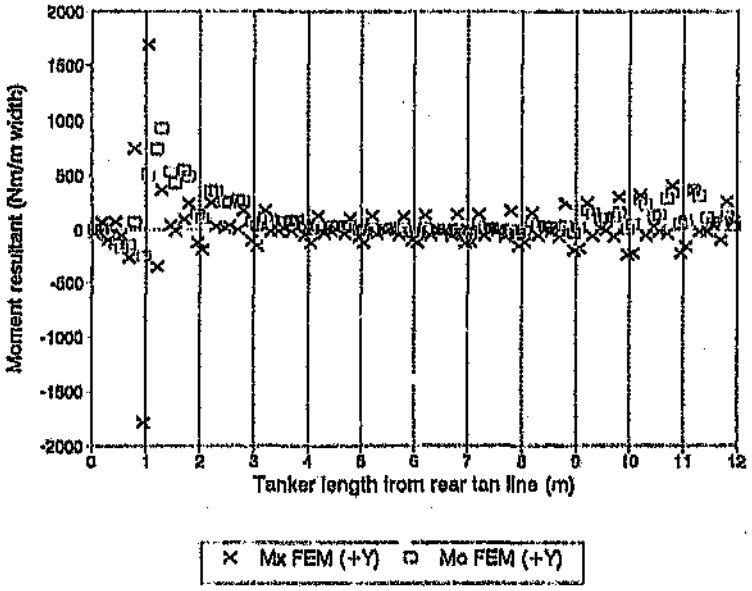

Figure 6.24 Moment resultants in the left (+y) of the tanker.

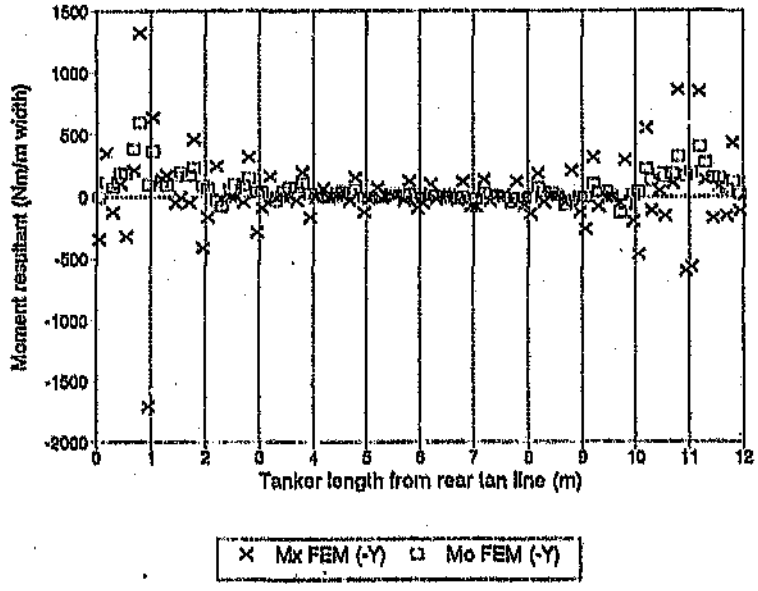

Figure 6.25 Moment resultants in the right (-y) of the tanker.

6.2 The Validation Model

6.2.1 Experimental observations

The data obtained from the experimental procedure discussed in paragraph 5.3 are listed in Table 6.1. The rosette numbers as defined by Figure 5.2 and Table 5.1 are listed with the corresponding FEM element number. The initial zero load voltage readings were taken as the bridge circuit was not totally balanced. These values were subtracted from the loaded voltage readings to determine the strain induced voltages. The final readings of Table 6.1 were the zero load readings taken after the test. These served as a check of any non-linearity within the system. In most cases the final zero load readings where similar to the initial zero load readings. Gauges that showed error had duplicate gauges placed at corresponding positions on the other side of the tube. The experimental procedure was then repeated with all the gauges for the final test. Table 6.2 listed the differences between the initial zero load voltages and the loaded voltages to determine the strain induced voltages. These values where then processed by the strain gauge theory of Appendix G to determine the apparent gauge strains (Eqn G7). Due to the large Poisson's ratio of the tube material ($\nu_{xt} = 0,52$), transverse sensitivity effects where accounted for (Eqn G8) in the calculation of the corrected gauge strains of Table 6.3. The experimental outer layer strains in the tube axial, circumferential and inplane shear directions where then calculated using Eqns G10 to G16 of Appendix G. Table 6.4 listed the x,y and z co-ordinates at the centre of the gauge. This is the position where the three gauges of the rosette overlap and also the centre of the FEM shell element. The beam theory relationships (Eqn 3.42 to 3.45) were then used to determine the theoretical outer layer strains.

Table 6.1 Voltage readings obtained from strain gauge circuit.

Rosette No.	Element No.	Differences (m (Loaded-Initial) (mV)			Apparent Gauge Strains			
		+45	-45	0	+45	-45	0	90
1	17	-9.300E-01	-3.000E-02	-2.580E+00	-2.106E-04	-6.792E-06	-5.842E-04	3.858E-04
2	18	-1.140E+00	-3.000E-01	-1.690E+00	-2.581E-04	-6.792E-05	-3.826E-04	5.660E-05
3	19	-6.500E-01	7.100E-01	-2.000E-01	-1.472E-04	1.608E-04	-4.528E-05	5.887E-05
4	20	-9.600E-01	1.400E+00	1.500E-01	-2.174E-04	3.170E-04	3.396E-05	6.566E-05
5	80	2.120E+00	6.500E-01	2.280E+00	4.800E-04	1.472E-04	5.162E-04	1.109E-04
6	79	2.120E+00	1.360E+00	4.590E+00	4.800E-04	3.079E-04	1.039E-03	-2.513E-04
7	78	1.560E+00	1.820E+00	6.300E+00	3.532E-04	4.121E-04	1.426E-03	-6.611E-04
8	77	2.000E+00	-3.000E-01	7.120E+00	4.528E-04	-6.792E-05	1.612E-03	-1.227E-03
9	21	-8.400E-01	-4.400E-01	-2.270E+00	-1.902E-04	-9.962E-05	-5.140E-04	2.242E-04
10	22	-2.700E-01	-2.900E-01	-1.900E+00	-6.113E-05	-6.566E-05	-4.302E-04	3.034E-04
11	23	-3.600E-01	2.800E-01	-7.300E-01	-8.151E-05	6.340E-05	-1.653E-04	1.472E-04
12	24	-2.000E-01	1.100E-01	5.500E-01	-4.528E-05	2.491E-05	1.245E-04	-1.449E-04
13	84	-5.000E-02	1.400E-01	2.280E+00	-1.132E-05	3.170E-05	5.162E-04	-4.956E-04
14	83	1.150E+00	5.200E-01	5.390E+00	2.604E-04	1.177E-04	1.220E-03	-5.423E-04
15	82	1.050E+00	1.400E+00	8.960E+00	2.377E-04	3.170E-04	2.029E-03	-1.474E-03
16	81	1.390E+00	6.500E-01	9.780E+00	3.147E-04	1.925E-04	2.214E-03	-1.707E-03
17	25	-4.200E-01	-7.100E-01	-3.160E+00	-9.509E-05	-1.608E-04	-7.155E-04	4.596E-04
18	26	-5.600E-01	-1.400E-01	-1.840E+00	-1.268E-04	-3.170E-05	-4.166E-04	2.581E-04
19	27	-3.010E-01	9.000E-02	-1.080E+00	-6.792E-05	2.038E-05	-2.445E-04	1.970E-04
20	28	-6.000E-02	1.800E-01	7.500E-01	-1.358E-05	4.075E-05	1.698E-04	-1.426E-04
21	86	2.800E-01	9.700E-01	3.130E+00	6.340E-05	6.377E-05	7.087E-04	-5.613E-04
22	87	1.810E+00	3.900E-01	5.770E+00	4.098E-04	8.151E-05	1.306E-03	-6.151E-04
23	88	2.130E+00	1.140E+00	9.880E+00	4.823E-04	2.581E-04	2.011E-03	-1.270E-03
24	85	2.090E+00	1.850E+00	9.740E+00	4.732E-04	4.189E-04	2.205E-03	-1.313E-03
25	57	-5.900E-01	-2.800E-01	-3.030E+00	-1.336E-04	-6.340E-05	-6.860E-04	4.891E-04
26	58	-6.400E-01	-4.000E-01	-2.470E+00	-1.449E-04	-9.057E-05	-5.592E-04	3.236E-04
27	59	-8.000E-01	-2.500E-01	-9.700E-01	-1.811E-04	-5.660E-05	-2.196E-04	-1.811E-05
28	60	1.400E-01	1.900E-01	1.490E+00	3.170E-05	4.302E-05	3.374E-04	-2.626E-04
29	120	1.090E+00	6.000E-01	9.200E+00	2.468E-04	1.358E-04	7.245E-04	-3.419E-04
30	1 9	1.490E+00	8.600E-01	6.110E+00	3.374E-04	1.947E-04	1.383E-03	-8.513E-04
31	118	1.540E+00	1.750E+00	7.920E+00	3.487E-04	3.962E-04	1.793E-03	-1.049E-03
32	117	1.820E+00	2.430E+00	9.200E+00	4.121E-04	5.502E-04	2.083E-03	-1.121E-03

Table 6.2 Gauge voltage differences and apparent strains.

Rosette No.	Element No.	Initial readings (mV) +45	-45	0	Loaded readings (mV) +45	-45	0	Final readings (mV) +45	-45	0
1	17	1.76	-0.79	1.85	0.83	-0.82	-0.73	1.73	-0.81	1.39
2	18	5.21	1.31	4.42	4.07	1.01	2.73	5.19	1.34	4.43
3	16	2.83	1.94	2.88	2.18	2.65	2.68	2.84	1.88	2.83
4	20	1.33	1.93	3.22	0.37	3.33	3.37	0.78	2.07	3.17
5	60	1.75	2.24	3.75	3.87	2.89	6.03	2.77	1.97	3.75
6	79	0.66	1.95	2.54	2.78	3.31	7.13	0.76	2.02	2.54
7	78	1.75	2.72	4.34	3.31	4.54	10.64	1.82	2.83	4.65
8	77	3.88	25.80	4.13	5.86	25.50	11.25	3.72	24.20	4.22
9	21	2.01	2.06	3.56	1.17	1.62	1.29	1.99	2.09	2.56
10	22	2.99	3.55	3.16	2.86	3.26	1.26	2.88	3.52	2.99
11	23	2.94	3.21	3.45	2.56	3.49	2.72	2.68	3.25	3.42
12	24	2.87	1.71	2.42	2.67	1.82	2.97	2.83	1.75	2.97
13	84	1.57	3.67	2.95	1.52	3.81	5.23	1.60	3.69	2.97
14	83	1.31	1.76	2.44	2.46	2.30	7.83	1.36	1.82	2.81
15	82	1.41	3.17	3.57	2.46	4.57	12.53	1.39	3.29	3.95
16	81	2.29	2.91	3.38	3.66	3.76	13.16	2.44	1.95	3.78
17	25	1.16	1.84	2.41	0.74	0.63	-0.75	1.16	1.26	2.05
18	26	3.24	2.38	1.97	2.68	2.24	0.16	3.23	2.29	1.93
19	27	3.57	3.72	1.88	3.27	3.81	0.80	3.60	3.73	1.81
20	28	3.46	0.98	1.95	3.40	1.16	2.70	3.38	1.06	1.89
21	88	2.49	3.02	3.14	2.77	3.39	6.27	2.53	3.07	3.25
22	87	4.28	2.73	3.90	6.09	3.09	9.67	4.49	2.77	4.09
23	86	2.68	3.43	4.27	4.61	4.57	13.15	2.54	3.53	4.65
24	85	0.81	2.87	2.47	2.70	4.72	12.21	0.79	3.02	2.86
25	57	3.08	3.45	2.69	2.49	3.17	-0.34	3.04	3.47	2.71
26	58	1.02	3.24	3.74	0.38	2.84	1.27	1.01	3.55	3.42
27	59	3.48	1.95	2.63	2.66	1.70	1.66	3.03	2.08	2.45
28	60	2.57	3.71	3.21	2.71	3.90	4.70	2.55	3.66	3.28
29	120	2.55	3.34	5.02	3.64	3.24	8.22	2.35	3.41	4.96
30	119	2.57	1.24	3.44	4.06	2.10	9.55	2.69	1.31	3.53
31	118	2.77	2.25	2.96	4.31	4.00	10.86	2.85	2.37	2.82
32	117	4.31	0.37	4.19	6.13	2.60	13.33	4.43	0.60	4.53

Table 6.3 Corrected gauge strains.

Rosette No.	Element No.	Corrected Gauge Strains				Experimental Outer Layer Strains		
		+45	-45	0	90	exx	ett	ext
1	17	-2.104E-04	-5.410E-06	-5.845E-04	5.677E-04	-5.845E-04	5.677E-04	-2.040E-04
2	18	-2.579E-04	-6.743E-05	-3.825E-04	5.726E-05	-3.825E-04	5.660E-05	-1.902E-04
3	19	-1.474E-04	1.609E-04	-4.537E-05	5.892E-05	-4.537E-05	5.867E-05	-3.079E-04
4	20	-2.178E-04	3.172E-04	3.383E-05	6.557E-05	3.383E-05	6.566E-05	-5.343E-04
5	80	4.795E-04	1.462E-04	5.158E-04	1.100E-04	5.158E-04	1.109E-04	3.328E-04
6	79	4.792E-04	9.069E-04	1.039E-03	-2.531E-04	1.039E-03	-2.513E-04	1.721E-04
7	78	3.523E-04	4.112E-04	1.427E-03	-6.634E-04	1.427E-03	-6.611E-04	-5.887E-05
8	77	4.527E-04	-6.870E-05	1.619E-03	-1.229E-03	1.619E-03	-1.227E-03	5.206E-04
9	21	-1.899E-04	-9.923E-05	-5.141E-04	2.250E-04	-5.141E-04	2.242E-04	-9.057E-05
10	22	-6.008E-05	-6.552E-05	-4.305E-04	3.040E-04	-4.303E-04	3.034E-04	4.528E-06
11	23	-8.158E-05	6.351E-05	-1.655E-04	1.474E-04	-1.655E-04	1.472E-04	-1.449E-04
12	24	-4.530E-05	2.497E-05	1.247E-04	-1.451E-04	1.247E-04	-1.449E-04	-7.019E-05
13	84	-1.137E-05	3.170E-05	5.169E-04	-4.965E-04	5.169E-04	-4.958E-04	-4.302E-05
14	83	2.600E-04	1.172E-04	1.221E-03	-8.440E-04	1.221E-03	-8.423E-04	1.426E-04
15	82	2.370E-04	3.164E-04	2.030E-03	-1.477E-03	2.030E-03	-1.474E-03	-7.925E-05
16	81	3.142E-04	1.918E-04	2.216E-03	-1.710E-03	2.216E-03	-1.707E-03	1.223E-04
17	25	-9.476E-05	-1.605E-04	-7.159E-04	4.607E-04	-7.159E-04	4.596E-04	6.566E-05
18	26	-1.267E-04	-3.145E-05	-4.169E-04	2.587E-04	-4.169E-04	2.581E-04	-9.509E-05
19	27	-6.793E-05	2.049E-05	-2.449E-04	1.973E-04	-2.448E-04	1.970E-04	-8.830E-05
20	28	-1.365E-05	4.076E-05	1.700E-04	-1.429E-04	1.700E-04	-1.426E-04	-5.434E-05
21	88	6.321E-05	8.962E-05	7.093E-04	-5.825E-04	7.093E-04	-5.815E-04	-2.038E-05
22	87	4.095E-04	8.073E-05	1.307E-03	-8.170E-04	1.307E-03	-8.151E-04	3.263E-04
23	86	4.816E-04	2.571E-04	2.012E-03	-1.273E-03	2.012E-03	-1.270E-03	2.242E-04
24	85	4.722E-04	4.176E-04	2.207E-03	-1.317E-03	2.207E-03	-1.313E-03	5.434E-05
25	57	-1.334E-04	-6.812E-05	-6.866E-04	4.900E-04	-6.866E-04	4.891E-04	-7.019E-05
26	58	-1.447E-04	-9.026E-05	-5.595E-04	3.246E-04	-5.595E-04	3.236E-04	-5.434E-05
27	59	-1.509E-04	-5.829E-05	-2.195E-04	-1.771E-05	-2.195E-04	-1.811E-05	-1.245E-04
28	60	3.160E-05	4.294E-05	3.977E-04	-2.631E-04	3.977E-04	-2.626E-04	-1.132E-05
29	120	2.464E-04	1.353E-04	7.248E-04	-3.430E-04	7.248E-04	-3.419E-04	1.109E-04
30	119	3.368E-04	1.940E-04	1.384E-03	-8.534E-04	1.384E-03	-8.519E-04	1.426E-04
31	118	3.478E-04	3.954E-04	1.794E-03	-1.051E-03	1.794E-03	-1.048E-03	-4.755E-05
32	117	4.109E-04	5.492E-04	2.084E-03	-1.124E-03	2.084E-03	-1.121E-03	-1.381E-04

Table 6.4 Geometrical data and theoretical strains.

Rosette No.	Element No.	Co-ordinates (m) x	y	z	Arc length (m)	Theoretical Outer Layer Strains (m/m) exx	ett	ext
1	17	0.0960	0.0507	0.0102	0.0103	-6.629E-04	3.365E-04	0.000E+00
2	18	0.0960	0.0428	0.0286	0.0306	-4.599E-04	2.334E-04	0.000E+00
3	19	0.0960	0.0286	0.0428	0.0509	-9.276E-05	4.708E-05	0.000E+00
4	20	0.0960	0.0102	0.0507	0.0714	3.843E-04	-1.951E-04	0.000E+00
5	80	0.0960	-0.0102	0.0507	0.0919	9.091E-04	-4.615E-04	0.000E+00
6	79	0.0960	-0.0286	0.0428	0.1120	1.386E-03	-7.036E-04	0.000E+00
7	78	0.0960	-0.0428	0.0286	0.1323	1.753E-03	-8.900E-04	0.000E+00
8	77	0.0960	-0.0507	0.0102	0.1531	1.956E-03	-9.930E-04	0.000E+00
9	21	0.1080	0.0507	0.0102	0.0103	-6.629E-04	3.365E-04	0.000E+00
10	22	0.1080	0.0428	0.0286	0.0306	-4.599E-04	2.334E-04	0.000E+00
11	23	0.1080	0.0286	0.0428	0.0509	-9.276E-05	4.708E-05	0.000E+00
12	24	0.1080	0.0102	0.0507	0.0714	3.843E-04	-1.951E-04	0.000E+00
13	84	0.1080	-0.0102	0.0507	0.0919	9.091E-04	-4.615E-04	0.000E+00
14	83	0.1080	-0.0286	0.0428	0.1120	1.386E-03	-7.036E-04	0.000E+00
15	82	0.1080	-0.0428	0.0286	0.1323	1.753E-03	-8.900E-04	0.000E+00
16	81	0.1080	-0.0507	0.0102	0.1531	1.956E-03	-9.930E-04	0.000E+00
17	25	0.1200	0.0507	0.0102	0.0103	-6.629E-04	3.365E-04	0.000E+00
18	26	0.1200	0.0428	0.0286	0.0306	-4.599E-04	2.334E-04	0.000E+00
19	27	0.1200	0.0286	0.0428	0.0509	-9.276E-05	4.708E-05	0.000E+00
20	28	0.1200	0.0102	0.0507	0.0714	3.843E-04	-1.951E-04	0.000E+00
21	88	0.1200	-0.0102	0.0507	0.0919	9.091E-04	-4.615E-04	0.000E+00
22	87	0.1200	-0.0286	0.0428	0.1120	1.386E-03	-7.036E-04	0.000E+00
23	86	0.1200	-0.0428	0.0286	0.1323	1.753E-03	-8.900E-04	0.000E+00
24	85	0.1200	-0.0507	0.0102	0.1531	1.956E-03	-9.930E-04	0.000E+00
25	57	0.2178	0.0507	0.0102	0.0103	-6.629E-04	3.365E-04	0.000E+00
26	58	0.2178	0.0428	0.0286	0.0306	-4.599E-04	2.334E-04	0.000E+00
27	59	0.2178	0.0286	0.0428	0.0509	-9.276E-05	4.708E-05	0.000E+00
28	60	0.2178	0.0102	0.0507	0.0714	3.843E-04	-1.951E-04	0.000E+00
29	120	0.2178	-0.0102	0.0507	0.0919	9.091E-04	-4.615E-04	0.000E+00
30	119	0.2178	-0.0286	0.0428	0.1120	1.386E-03	-7.036E-04	0.000E+00
31	118	0.2178	-0.0428	0.0286	0.1323	1.753E-03	-8.900E-04	0.000E+00
32	117	0.2178	-0.0507	0.0102	0.1531	1.956E-03	-9.930E-04	0.000E+00

6.2.2 Finite element observations

The FEM plot showing the original FEM model (dashed lines) and displaced model (solid lines) is shown in Figure 6.26. The displacements had been magnified 14 times and show the bending of

the tube relative to the middle of the model. The pinned constraint at the end of the rod corresponds to the point of force application with the result of limited bending of the stiff rod.

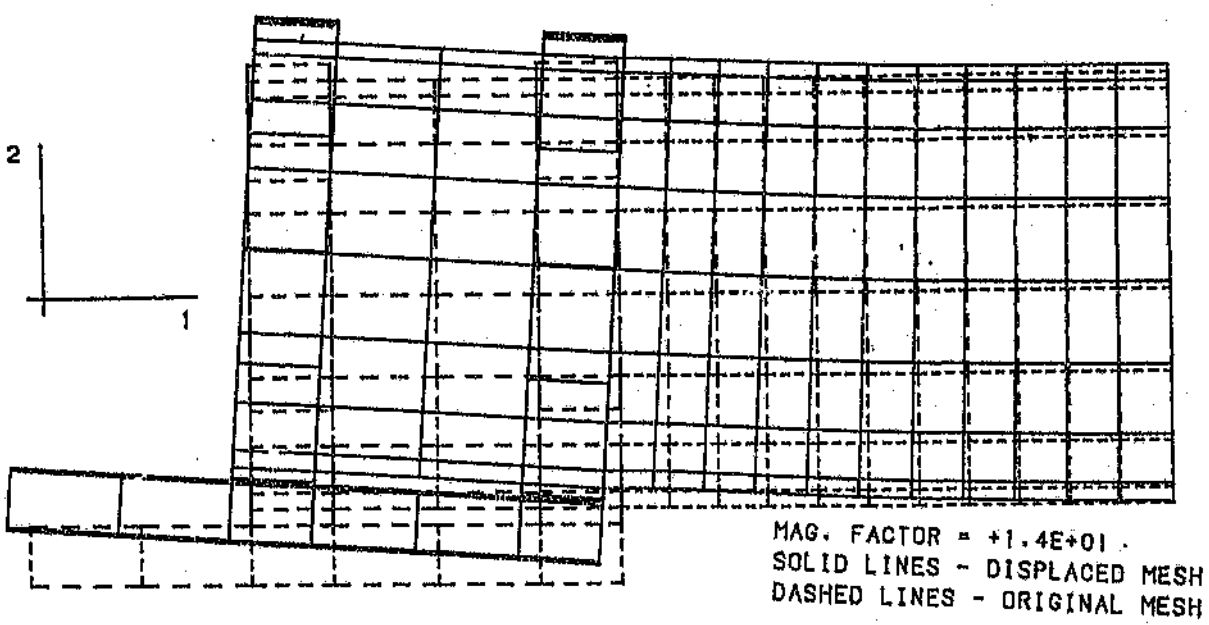

Figure 6.26 Original and displaced mesh of the validation FEM model.

Table 6.5 summarises the force and moment resultant data extracted from the FEM output for the elements at the positions of the gauges. The distribution of the axial, circumferential and in-plane shear moment resultants were shown superimposed on the 'unrolled' tube in Appendix U with the arc value at arc = 0 corresponding to the top of the tube. The effect that the steel ribs have on these forces is clear from these three dimensional represe .ations.

Table 6.5 Finite element force and moment resultants.

Rosette No.	Element No.	FEM: Inplane Forces (N/m width) Nxx	Ntt	Nxt	Transverse Shear (N/m width) Qx	Qt	Inplane Moments (Nm/m width) Mxx	Mtt	Mxt
1	17	-19790.00	-8297.75	618.25	-3561.50	575.25	0.75	0.50	0.00
2	18	-15173.75	-5276.25	413.25	-2663.50	194.00	0.50	0.25	-0.50
3	19	-5650.25	-1494.50	470.75	-1984.75	-825.50	0.00	-0.25	-1.00
4	20	7084.25	3536.00	664.75	-1408.50	-1865.50	-0.50	-0.25	-0.75
5	80	21521.25	8241.50	-53.50	-571.75	1436.25	-0.75	-0.50	-0.75
6	79	35310.75	12346.75	-81.50	-1181.25	2087.00	-1.25	-0.75	-0.50
7	78	46671.50	15055.00	-609.25	-1819.75	1824.75	-1.00	-0.75	-0.50
8	77	52654.50	16801.50	419.50	-1028.00	2620.50	-1.25	-0.50	0.00
9	21	-20048.75	-1470.00	230.25	-106.25	231.50	-0.50	-0.25	0.00
10	22	-14990.00	-743.75	271.00	964.75	967.00	-0.25	-0.25	0.00
11	23	-5696.75	-252.00	186.50	1423.00	955.00	0.00	0.00	0.00
12	24	7172.50	393.00	254.75	1211.00	837.00	0.50	0.25	0.00
13	84	21514.75	762.75	52.75	-1243.50	-856.50	1.00	0.50	0.00
14	83	35580.75	1133.75	-128.25	-776.25	-682.25	1.25	0.75	0.00
15	82	46554.25	1078.75	-230.50	-274.00	-736.50	1.75	1.00	0.25
16	81	52538.25	1165.25	1.50	621.50	-445.75	1.75	0.75	0.00
17	25	-20119.00	341.75	34.50	148.75	-349.00	-0.25	0.00	0.00
18	26	-15025.00	322.25	71.50	195.50	-230.50	-0.25	-0.25	0.00
19	27	-5632.50	210.50	0.75	32.25	-382.00	0.00	0.00	0.00
20	28	7112.50	-72.50	17.50	-307.00	-371.50	0.00	0.00	0.00
21	88	21664.75	-297.25	-130.75	4[illegible]00	309.50	0.00	0.00	0.00
22	87	35653.50	-557.50	-261.75	[illegible]5	236.00	0.25	0.25	0.00
23	86	46503.25	-845.75	-204.50	449.50	-17.75	0.25	0.25	0.00
24	85	52468.50	-1077.50	-104.00	549.25	-141.00	0.25	0.00	0.00
25	57	-20258.00	-68.25	87.50	-88.00	90.50	0.00	-0.75	0.00
26	58	-15193.50	-13.75	113.25	-86.75	83.75	0.00	0.00	0.00
27	59	-5713.25	12.25	87.75	-41.00	105.25	0.00	0.00	0.00
28	60	7173.00	126.00	-1.75	63.25	116.25	0.25	-0.50	0.00
29	120	22347.00	276.50	-786.75	-12.75	52.50	0.00	1.00	0.00
30	119	35832.50	83.75	-1092.25	0.00	124.25	0.00	0.25	0.00
31	118	46200.50	-203.25	-879.50	-26.25	102.50	-0.25	0.00	0.00
32	117	52182.50	-203.75	-257.25	-97.25	62.50	-1.00	-1.00	0.00

Table 6.6 Finite element strains calculated using classical lamination theory.

Rosette No.	Element No.	FEM/CLT : Centreline Strains (m/m)			FEM/CLT : Centreline Curvatures (Rad)			FEM/CLT Outer Layer Strains (m/m)		
		e0xx	e0tt	e0xt	Kx	Kt	Kxt	exx	ett	ext
1	17	-6.447E-04	7.2300E-05	3.0290E-05	7.1690E-02	1.9290E-02	-2.431E-02	-2.075E-04	-5.593E-05	8307E-05
2	18	-5.172E-04	1.0040E-04	2.0250E-05	5.3220E-02	1.0820E-02	-1.021E-01	-2.070E-04	-3.654E-05	-4.668E-05
3	19	-2.025E-04	5.6840E-05	2.3060E-05	3.6550E-02	-1.895E-02	-1.701E-01	-1.414E-04	-3.591E-06	-1.490E-04
4	20	2.189QE-04	-2.389E-06	3.2570E-0	-3.891E-02	1.3490E-02	-1.187E-01	2.1474E-05	1.9437E-06	-6.997E-05
5	80	7.1760E-04	-1.110E-04	-2.621E-06	-5.711E-02	-4.706E-03	-1.069E-01	2.6170E-04	-2.655E-05	-7.344E-05
6	79	1.2020E-03	-2.308E-04	-3.693E-06	-1.155E-01	-1.066E-02	-4.860E-02	5.2995E-04	-8.839E-05	-2.686E-05
7	78	1.6150E-03	-3.573E-04	-2.965E-05	-8.017E-02	-2.777E-02	-5.346E-02	8.8145E-04	-1.672E-04	-8.567E-05
8	77	1.8260E-03	-4.107E-04	2.0550E-05	-1.423E-01	1.4910E-02	3.4030E-02	1.0328E-03	-1.549E-04	-6.724E-06
9	21	-7.9396E-04	3.6030E-04	1.1260E-05	-5.350E-02	-1.095E-03	1.4590E-02	-7.883E-04	3.1950E-04	2.0040E-05
10	22	-6.043E-04	2.8410E-04	1.3260E-05	-1.920E-02	-1.820E-02	9.7240E-03	-7.421E-04	2.1630E-04	8.0339E-06
11	23	-2.505E-04	1.0920E-04	9.2360E-06	0.0000E+00	0.0000E+00	0.0000E+00	-2.903E-04	8.8542E-06	3.2510E-05
12	24	2.8960E-04	-1.344E-04	1.2480E-05	5.3500E-02	1.0950E-03	-1.459E-02	1.2240E-04	-6.716E-05	7.9640E-06
13	84	8.7400E-04	-4.196E-04	2.5850E-06	1.0700E-01	2.1900E-03	-2.917E-02	6.8610E-04	-3.176E-04	-4.651E-06
14	83	1.4490E-03	-7.005E-04	-8.039E-06	1.2520E-01	2.0390E-02	-3.890E-02	1.3349E-03	-5.104E-04	-3.590E-05
15	82	1.9040E-03	-9.333E-04	-1.129E-05	1.7380E-01	1.6620E-02	-8.734E-03	1.9696E-03	-8.127E-04	-7.169E-06
16	81	2.1500E-03	-1.055E-03	7.3490E-06	1.9580E-01	-1.382E-02	-4.862E-02	2.4092E-03	-1.029E-03	-8.416E-06
17	25	-8.396E-04	4.3660E-04	1.6900E-06	-3.630E-02	1.7100E-02	4.8620E-03	-8.688E-04	4.4710E-04	4.6510E-06
18	26	-6.286E-04	3.2900E-04	3.5030E-06	-1.820E-02	-1.820E-02	9.7240E-03	-7.844E-04	2.9670E-04	3.5496E-05
19	27	-2.375E-04	1.2700E-04	3.6750E-06	0.0000E+00	0.0000E+00	0.0000E+00	-3.736E-04	1.9250E-04	-3.969E-05
20	28	2.958QE-04	-1.524E-04	8.5740E-07	0.0000E+00	0.0000E+00	0.0000E+00	1.2920E-04	-6.999E-05	-1.377E-05
21	88	9.0290E-04	-4.674E-04	-6.406E-06	0.0000E+00	0.0000E+00	0.0000E+00	7.2720E-04	-3.826E-04	-1.627E-05
22	87	1.4870E-03	-7.720E-04	-1.292E-05	1.8200E-02	1.8200E-02	-9.724E-03	1.4019E-03	-6.264E-04	-5.720E-05
23	86	1.9420E-03	-1.012E-03	-1.002E-05	1.8200E-02	1.8200E-02	-9.724E-03	1.9099E-03	-8.839E-04	-5.127E-05
24	85	2.1940E-03	-1.147E-03	-5.096E-06	3.5300E-02	-1.710E-02	-4.862E-03	2.2936E-03	-1.196E-03	-2.742E-06
25	57	-8.370E-04	4.2270E-04	4.2870E-06	5.1310E-02	-1.059E-01	1.4590E-02	-8.025E-04	3.0595E-04	1.7233E-05
26	58	-6.260E-04	3.1730E-04	5.5490E-06	0.0000E+00	0.0000E+00	0.0000E+00	-7.152E-04	3.6510E-04	-5.104E-06
27	59	-2.397E-04	1.2050E-04	1.8500E-06	0.0000E+00	0.0000E+00	0.0000E+00	-3.703E-04	1.9030E-04	-4.655E-06
28	60	2.9420E-04	-1.455E-04	-8.574E-06	1.0950E-03	5.3500E-02	-1.459E-02	1.2450E-04	-6.140E-05	-1.990E-07
29	120	9.1910E-04	-4.560E-04	-3.904E-05	-8.641E-02	1.4120E-01	-1.945E-02	6.7385E-04	-2.391E-04	-1.420E-05
30	119	1.4620E-03	-7.513E-04	-5.352E-05	-1.710E-02	3.5300E-02	-4.862E-03	1.2608E-03	-5.485E-04	2.8106E-06
31	118	1.9160E-03	-9.759E-04	-4.309E-05	-3.530E-02	1.7100E-02	4.8620E-03	1.6110E-03	-9.326E-04	1.9750E-05
32	117	2.1630E-03	-1.104E-03	-1.260E-06	-7.279E-02	-7.279E-02	9.8900E-02	2.0591E-03	-1.159E-03	4.6914E-05

The axial moment resultants shown in Figure U1 and U2 of Appendix U where fully developed within a very short distance of the rib. Of particular significance is that the bending load is nearly all distributed by the rear rib onto the tube. This occurred as a result of the high stiffness of the rib and connecting rod relative to the tube. The observation validates the assumption made for the road tanker whereby all of the load is transferred at a single support at each end. If the stiffness of the bogie is high enough, then a large proportion of the axial and bending load would be distributed along the stiffest load path from the bogie into the shell. Figures U3 and U4 of Appendix U show the circumferential loads induced by the rib and tube interaction. These result in stress concentrations at the tube side of the rib, but were localised and dissipate fairly quickly. Figures U5 and U6 show the inplane shear forces induced by the load. These were highest between the two ribs and may have resulted from the skewing or diagonalisation of the rib and rod assembly, thus inducing shear forces in the relatively flexible tube. These inplane shear forces were a maximum at the sides of the tube in line with the tube neutral axis.

The force and moment resultant values from Table 6.5 were then used as inputs for the MACLT.BAS program (Appendix D and H) to determine the outer layer strains as discussed by section 3.6. The centre-line strains and curvatures where then combined by Eqn 3.41 to determine the FEM outer layer strains in the axial, circumferential and inplane shear directions.

6.2.3 Comparison of experimental, theoretical and FEM results.

The results of the various analyses are compared graphically in Figures 6.27 to 6.31 for each of the bands as defined by Table

5.1. Figure 6.27 shows the predictions for the first band at x = 96 mm from the end of the tube. The axial strain (e_x) values all showed the same tendency. The differences in magnitude of the experimental values may have resulted from the strain measurement which were taken over the gauge length of 5 mm, whereas the theoretical and FEM results where point values at the centre of the rosette and element respectively. The experimental circumferential and FEM strains (e_t) were different after arc = 0,06. This may be due to the stress concentration shown in Figures U3 and U4. The FEM and experimental strains correlate over the circumference of the tube.

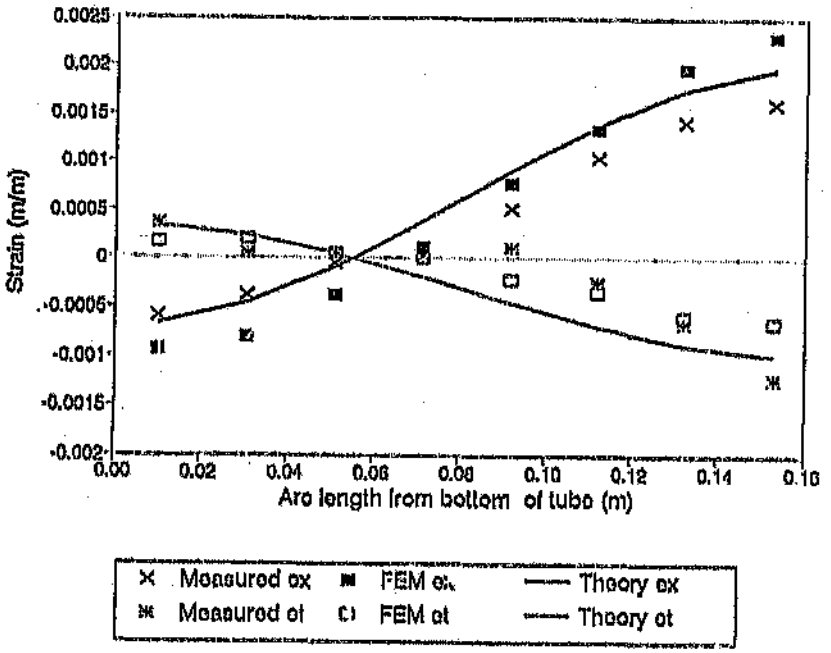

Figure 6.27 Comparison of the experimental, theoretical and FEM axial and circumferential strains for band 1 at x = 96 mm.

Figure 6.28 shows the strain results for the second band at x = 108 mm. The diminishing effect of the support on the e_x is apparent by the closer correlation of these results. The e_t results were almost identical in all three cases except for the two experimental values near the top of the tube.

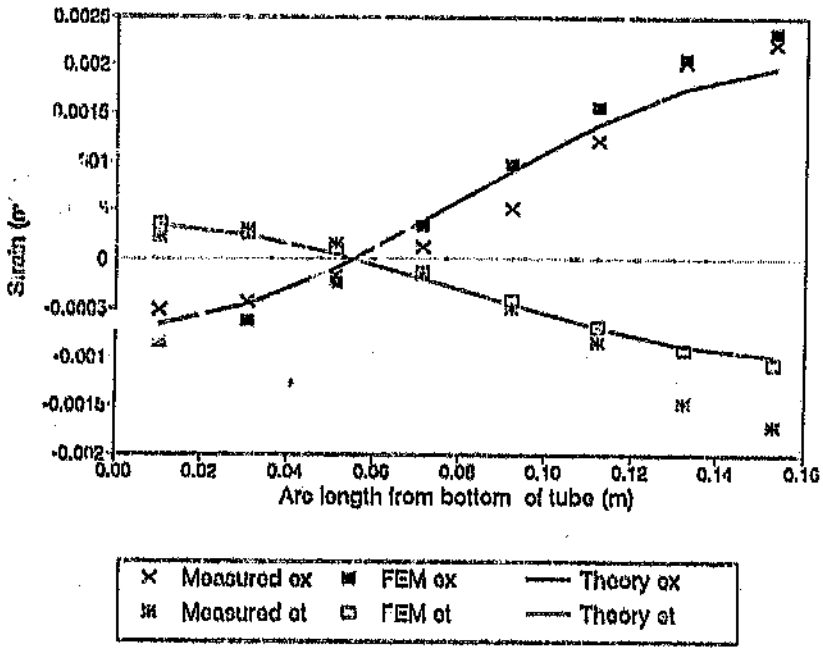

Figure 6.28 Comparison of the experimental, theoretical and FEM axial and circumferential strains for band 2 at x = 108 mm.

Figure 6.29 shows the strain results at the third band at x = 120 mm. All the curves were very similar with minor magnitude differences between the e_x results. The e_t results were all similar until the last two experimental results at the top of the tube.

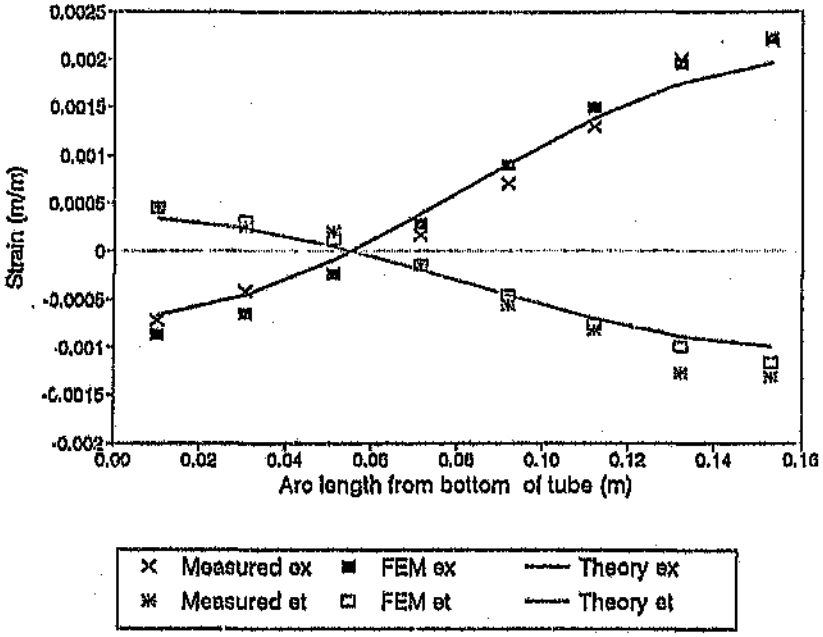

Figure 6.29 Comparison of the experimental, theoretical and FEM axial and circumferential strains for band 3 at x = 120 mm.

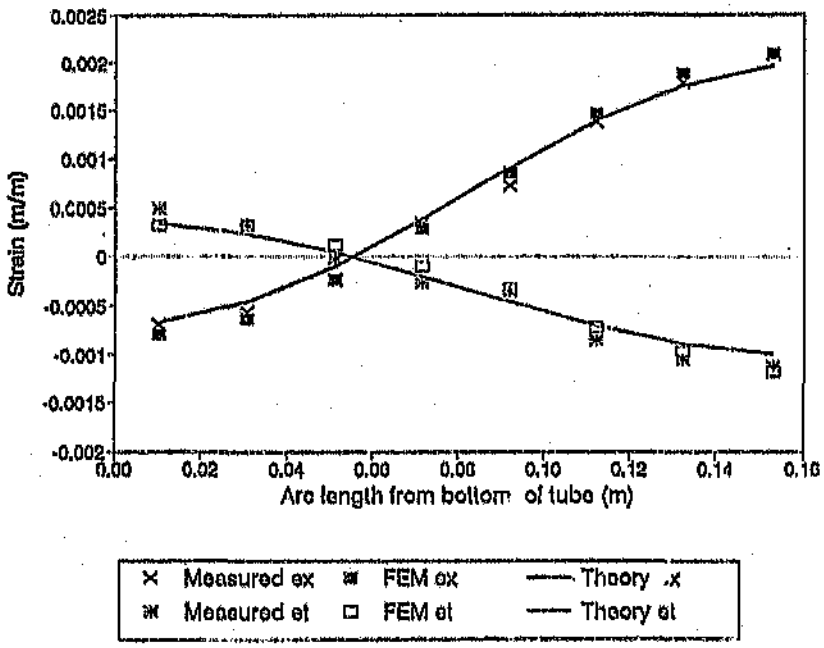

Figure 6.30 Comparison of the experimental, theoretical and FEM axial and circumferential strains for band 4 at x = 217,8 mm in the middle of the tube.

Figure 6.30 shows the strain results for the fourth band at the middle of the tube (x = 217,8 mm). Close correlation of the experimental, theoretical and FEM strains is achieved in the axial and circumferential directions. This position is remote from the discontinuity effect of the ribs and this is further indicated by the accuracy of the theoretical curve in predicting the FEM and experimental results.

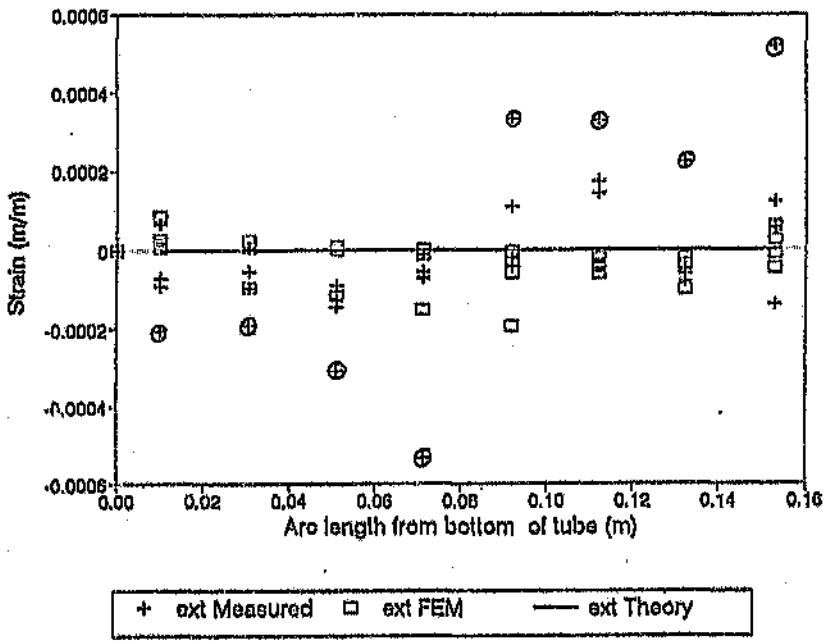

Figure 6.31 Comparison of the experimental, theoretical and FEM inplane shear strains for all the bands.

Figure 6.31 shows the inplane shear strains e_{xt} for all the bands relative to the circumference. The theoretical prediction of zero is similar in most cases to the FEM predictions which were either zero or very small. The experimental e_{xt} values at the first band, shown by the circled crosses did indicate some localised

shear strains near the ribs. This could be the result of the skewing of the ribs, but the effect diminished rapidly as the distance from the rib increased.

This experimental study was successful in providing a comparison of the theoretical, experimental and FEM predictions for the validation model. The results showed that FEM is an accurate method for the prediction of complex stress and strain distributions in a three dimensional, laminated composite structure under the influence of combined axial force and bending. The FEM model is able to take the varying stiffnesses of the tube, ribs and rod into account to accurately predict the strains and deflections. The validity of using one support to model the bogie or fifth wheel of the tanker is also tested. The validation model shows that the load followed the stiffest path. It is assumed that a similar situation would arise in the road tanker as a result of the varying stiffnesses of the shell, ribs, bogie and fifth wheel construction. The redundant supports will contribute to load sharing, although this will depend on the direction and magnitude of the accelerations. A conservative analysis assumes all the load through one support and this is readily calculated by theoretical methods.

7 CONCLUSIONS

- The use of the equivalent engineering constants to represent the composite laminate's extensional moduli is accurate for the beam theory predictions of the inplane force resultants.

- The bending and transverse shear behaviour of the laminate were difficult to predict using isotropic analyses and resulted in significant differences.

- The FEM axial and circumferential force resultants are predicted very accurately by the theory of isotropic shells for the internal pressure loadcase.

- Modelling the effect of the accelerating liquid as equivalent pressures on the elements of the FEM model is an accurate method of analysis.

- Beam and isotropic shell theory give accurate predictions of the inplane force resultants for vertical bending and axial acceleration in the tanker shell, in areas remote from stress concentrations.

- Beam theory does not accurately predict the effect of the sideways acceleration on the tanker. This may result from the offset between the line of action of the acceleration and the position of the supports.

- The FEM analysis of the validation model correlated accurately with the strain gauge results.

- FEM is a more elegant and possibly more accurate method of simulating the effect that accelerations have on the tanker and its contents.

- FEM gave an indication of the stress concentrations around the supports of the tanker. More accurate data could by obtained by further element mesh refinement in regions of high stress gradients.

- FEM is a suitable alternative to the complex theoretical analysis required by the design standards as it takes the exact geometric, laminate and loading configurations into account. The outputs from the FEM program include the evaluation of failure criteria for each layer in the proposed laminate.

- The Finite Element Method is suitable for the analysis of three-dimensional composite structures under complex loading conditions. The ABAQUS FEM program allows the use of various element types and material moduli on the same model.

- The laminate proposed in this research is not the optimum for an production design. The final laminate will depend on buckling, natural frequency and manufacturing considerations and will also contain local reinforcement in the high stress regions.

- The design and construction of a GRP road tanker is feasible. The use of FEM to optimise the laminate orientation and thicknesses can result in a tanker design which uses the composite material as efficiently as possible to fulfil the customer's requirements.

8 RECOMMENDATIONS

- The use of circumferential rings at the supports is highly recommended as they transfer the loads from the supports to the shell over a large area and also assist in stabilising the shell against localised buckling.

- This FEM study can be extended to consider the buckling and natural frequency considerations of the tanker.

- The bogie and suspension could be modelled to determine the exact effect that these features have on the stress distributions around the supports.

- Other load cases such as twisting of the shell and the various crash conditions can also be evaluated using FEM. The FEM model could also be upgraded to include the manhole openings and overturn protection

- More detailed analysis using advanced laminated plate theory could be used to achieve closer correlation to the moment and transverse shear predictions of FEM.

- Further research could focus on the generation of a FEM model of an existing metal or GRP road tanker. This vehicle could then be instrumented with strain gauges and accelerometers to determine the exact relationships that occur.

9 REFERENCES

ASME X (1989), ASME Boiler and Pressure Vessel Code - Fibreglass Reinforced Plastic Pressure Vessels, American Society of Mechanical Engineers, New York.

ANSI/NFPA 385 (1985), Tank Vehicles for Flammable and Combustible Liquids, American National Standards Institute, Washington.

AS2809.1 (1985), Road Tank Vehicles for Dangerous Goods Part 1 - General Requirements, Australian Standard.

AS2809.2 (1985), Road Tank Vehicles for Dangerous Goods Part 2 - Tankers for Flammable Liquids, Australian Standard.

AS2809.3 (1985), Road Tank Vehicles for Dangerous Goods Part 3 - Tankers for Compressed Liquefiable Gasses, Australian Standard.

AS2809.4 (1985), Road Tank Vehicles for Dangerous Goods Part 4 - Tankers for Toxic and Corrosive Cargoes, Australian Standard.

Belanger, A. (1972), Filament Wound, Self-supporting Liquid Transporter Tanker, Proc. 27 SPI Conv. 1972, Section 10A, pp.1-3.

Bert, C.W. (1985), Normal and Shear Stress Gauges and Rosettes for Orthotropic Composites, Experimental Mechanics, Sep.1985, pp.288-293.

Brownell, L.E. and Young, E.H. (1959), Process Equipment Design, John Wily and Sons, New York.

Bruhn, E.F. (1973), Analysis and Design of Flight Vehicle Structures, S.R. Jacobs and Associates Inc.

BS4994 (1987), British Standard Specification for Design and Construction of Vessels and Tanks in Reinforced Plastics, British Standards Institution, London.

BS5500 (1988), British Standard Specification for Unfired Fusion Welded Pressure Vessels, British Standards Institution, London.

Dally, J.W. and Riley, W.F. (1985), Experimental Stress Analysis, 2nd Edition, McGraw Hill Book Company, New York.

DOT (1981), General Design and Structural Requirements, Specification MC 306; Cargo Tanks, Department of Transport.

Hibbitt, Karlsson and Sorenson (1986), Abaqus Reference Manual Version 4.6.

Henred Freuhauf (PTY) LTD (1986), Tender 1090-72943 for a SAR 27500 L Road Tanker.

Henred Freuhauf (PTY) LTD (1986), Specification Sheet for Model T e/k X-F2-R Tanker Semi-Trailer.

Jones, R.M. (1975), Mechanics of Composite Materials, McGraw Hill, Kogakusha.

Kenney, M.E. (1966), Design and Stress Analysis for RP Road and Rail Transport Tanks, SPE Journal, Apr. 1966, pp.57-67.

Ministry of defence (1973), Fire Engulfment Tests on Road Tankers, Transcript of film produced by the Ministry of Defence.

Minsker, J.H. and Triestram, D.E. (1973), Filament Wound Tankers Using Derakane Vinyl Ester Resins, 28th SPI, Washington, DC, Feb 6-9, Section 6-D, pp.1-4.

Peters, S.T. and Humphrey, W.D. (1987), Filament Winding, Engineered Materials Handbook, Composites, ASM International, vol.1, Nov.1987, pp.501-518.

Roark, R.J. and Young, W.C. (1979), Formulas for Stress and Strain", 5th Edition, McGraw-Hill, Tokyo.

Rosen, B.W. and Dow, N.F. (1987), Overview of Composite Materials Analysis and Design, Engineered Materials Handbook, Composites, ASM International, vol.1, Nov.1987, pp.175-180.

SABS 1398 (1983), Standard Specification for Road Tank Vehicles for Flammable Liquids, South African Bureau of Standards, Pretoria.

Swanson, S.R. (1987), Analysis of Structures, Engineered Materials Handbook, Composites, ASM International, vol.1, Nov.1987, pp.458-462.

Szyszkowski, W. and Glockner, P.G. (1987), A Rational Design of Thin Walled Pressure Vessel Ends, ASME Journal of Pressure Vessel Technology, Nov.1987, vol 109, pp.368-373.

Tsai, S.W. (1988), Composites Design, Fourth Edition, Think Composites, Dayton, Ohio.
TFM (PTY) LTD (1978), Specification and Design Method for a 29000 l Stainless Steel Road Tanker", 20 Jul.1978.

TFM (PTY) LTD (1986), Strain/Stress Measurements on 360001 M3 Tanker", 1 Feb.1986, pp.1-12.

Timoshenko, S.P. and Gere, J.M. (1984), Mechanics of Materials, 2nd Ed, California, Wadsworth International.

Timoshenko, S. and Woinowsky-Krieger S. (1959), Theory of Plates and Shells, McCraw Hill Kogakusha Ltd, Tokyo.

Tuttle, M.E. and Brinson, H.F. (1984), Resistance Foil Strain Gauge Technology as Applied to Composite Materials, Experimental mechanics, Mar.1984, pp.55-65.

Uddin, W. (1986), Large Deformation Analysis of Ellipsoidal Head Pressure Vessels, Computers and Structures, vol.23, No.4, pp 487-495.

United Kingdom, Draft Specification Design Notes for Road Tank Wagons Constructed from Glass Reinforced Plastics for Carriage of Dangerous Substances, (1985).

Zick, L.P. (1951), Stresses in Large Horizontal Cylindrical Pressure Vessels on Two Saddle Supports, Weld J. (Research Supplement), Sep.1951

APPENDIX A

SPECIFICATIONS AND DRAWINGS OF THE PROPOSED ROAD TANKER

Shell

A minimum allowable wall thicknesses of 15 mm to allow the transport of 98% sulphuric acid was chosen. This chemical has one of the highest densities of commonly transported liquid cargoes. Special precautions such as thermoplastic liners and extensive resin testing would also be required for a tanker designed to carry this cargo. In practice, the shell may be thicker to comply with local standards requirements or have local thickening around high stress areas. The proposed tanker consisted of a 12 m long, cylindrical, single compartment shell with an inside diameter of 1,3 m and no interior baffles. This tanker was limited to carrying a single cargo per journey and must be either full or empty to avoid surging and sl hing. The reason for avoiding baffles was the difficulty associated with using a thermoplastic liner. A baffle would need to be attached to the structural component of the shell and this could compromise the liner's integrity. The proposed cylindrical shell consisted of a helically wound E-glass polyester or vinylester laminate with a volume fraction vf = 0.45 and consists of a $[\pm 10/\pm 85/...../\pm 10/\pm 85]_s$ layup. This resulted in a balanced and symmetrical laminate with sufficient layers to achieve total laminate thickness of 15 mm.

Domes

The end closures were provided by a 2:1 ellipsoidal dome at either end. The dome laminate thickness was 15 mm.

Ribs

Circumferential stiffeners (ribs) were positioned at 1 m intervals along the length of the tanker to ensure that the circularity of the

shell was maintained during bending. They also provided overturn protection for the shell. Thick ribs were 50 mm wide and 100 mm thick and were positioned at 0,1,2,3,9,10,11 and 12 metres from the rear tan line. These provide the attachment points for the fifth wheel (11 m & 12 m), the landing legs (9 m & 10 m) and the bogie cradle (0,1,2,3 m). The remainder of the ribs were 50 mm wide by 50 mm thick and were positioned at 4,5,6,7 and 8 m from the rear tan line. The ribs were constructed by hoop winding impregnated fibres (vf = 0.45) between two temporary formers to build up the rectangular shape. The domes could be manufactured by either a hand layup moulding which was later bonded to the cylinder or by winding the ellipsoidal domes as geodesic isotensoids. For the FEM analysis the domes were assumed to be isotropic.

Manufacture

The actual manufacture of this tanker would depend on the quantities required and the technology available. For large production runs the manufacture of metal mandrels may be cost justified. Single tankers could be manufactured using a hand layup mandrel over a thermoplastic liner. A compromise solution may be to first manufacture an inner shell consisting of the thermoplastic liner and a hand laminated corrosion barrier. The inside of the shell would be supported by a mandrel and radial spokes. Similar mouldings for the domes would then be attached to the cylinder. Holes at the apex of the domes allow the mandrel to pass through and facilitate removal of the radial spokes and the mandrel after winding. This shell will then be used as a mandrel for filament winding of the structural laminate. The domes could also be wound at this stage and this will result in a seamless monocoque structure. The main advantage of this method was that the mould becomes part of the tanker and potential weaknesses from any seams was avoided. This method would also lend itself to the manufacture of tankers for the transport of liquefied gas. If helical winding

was unavailable then the longitudinal layers could be added manually and then overwound by hoop winding. This construction was mentioned by Belanger (1972) who found only minor property differences between the filament wound hoop and hand layup axial layers.

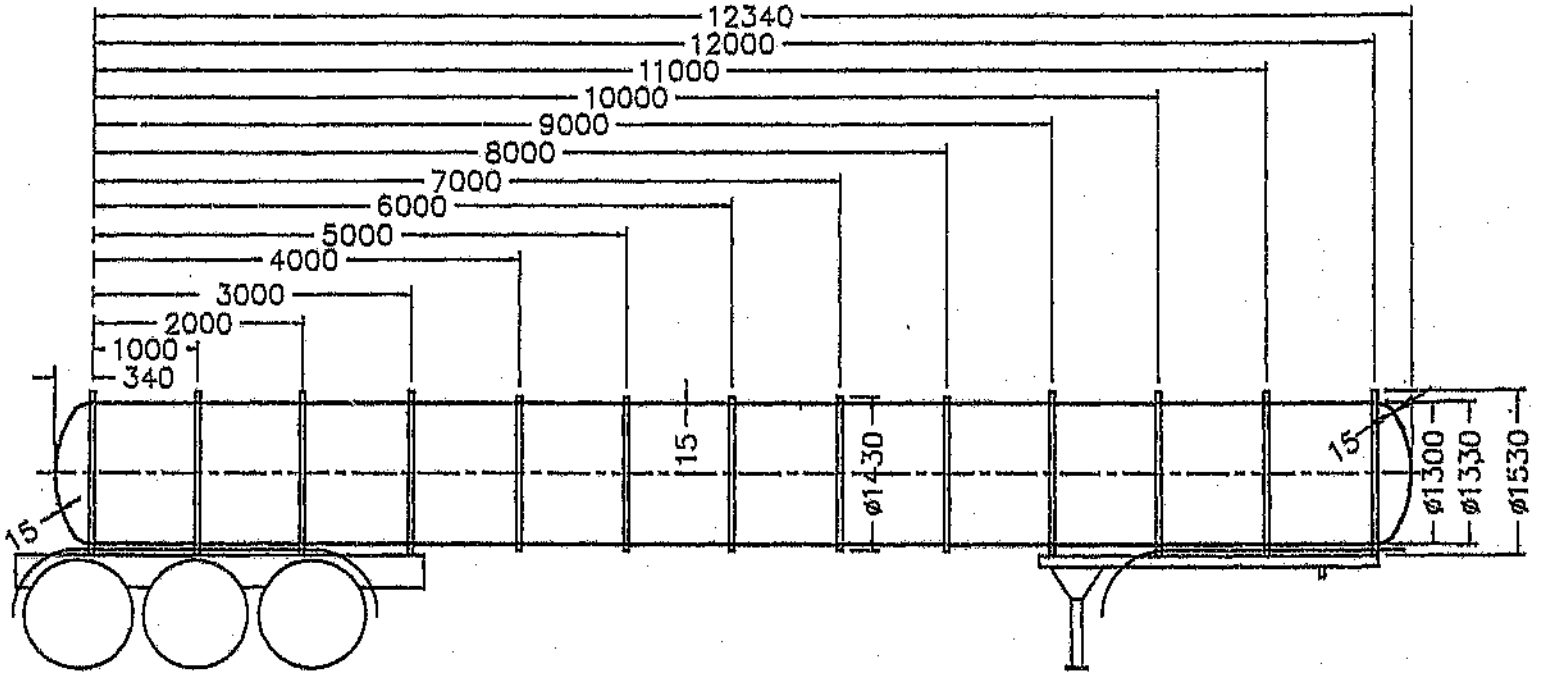

Figure A1 Assembly of the composite road tanker.

APPENDIX B

SPECIFICATIONS AND DRAWINGS OF THE VALIDATION MODEL

The Filament Wound Tube

The tube was manufactured by Aerodyne Technology (Pty) Ltd and a 560 mm length was cut for the validation model. The tube manufacturing specifications were supplied by Aerodyne as follows:

- Inside diameter d_i : 100 mm
- Glass reinforcement : E-glass, 4 rovings, 1200 Tex
- Resin Matrix : Ciba Geigy Epoxy, LY564 & HY2954
- Winding Angle : $\pm 45^{o}$
- Bandwidth : 7,9 mm
- Bands : 28 per layer
- Double Layers : 3
- Cure : Ramp-up, dwell at 125 ^{o}C

The tube was helically wound with 6 layers of 28 bands each.

The average thickness of the tube was measured as 1.89 mm. Hence the outer diameter d_o is 103.78 mm. These values were used for further theoretical calculations. The lamina properties were obtained from Tsai (1986) and were listed in Appendix C. This data was supplied by the manufacturer as being typical for the supplied tubes. Testing for material properties of the tube was not done. Burn off tests were not possible due to the properties of the epoxy resin matrix. The split parallel fibre-reinforced ring (NOL ring) specimen does not give modulus or Poisson's ratio data and was only suitable for comparative purposes as detailed by Peters and Humphrey (1987).

Metal support cradle

Two identical metal support cradles were designed and built to connect the tube to the tensile testing machine. Each consisted of a steel mounting shaft and four steel split rings. Two of the rings were

welded to the shaft. The cradle was then bonded to the tube and the top rings bonded and bolted down for a more exact fit. Araldite AW106 epoxy adhesive was used after suitable surface treatment of the tube and the cradle.

The end of the shaft had been machined to allow attachment to the tensile testing machine. The tolerances were large enough to allow rotational movement and could be considered as a pinned constraint. The manufacturing drawings for the cradle were presented in below. The support was an attempt to model the effect of a stiff chassis on a flexible GRP shell. They also allowed for an effective transfer of the tensile force to the tube, as well as inducing a uniform bending moment between the supports. This resulted from the offset between the line of action of the force and the neutral axis of the tube.

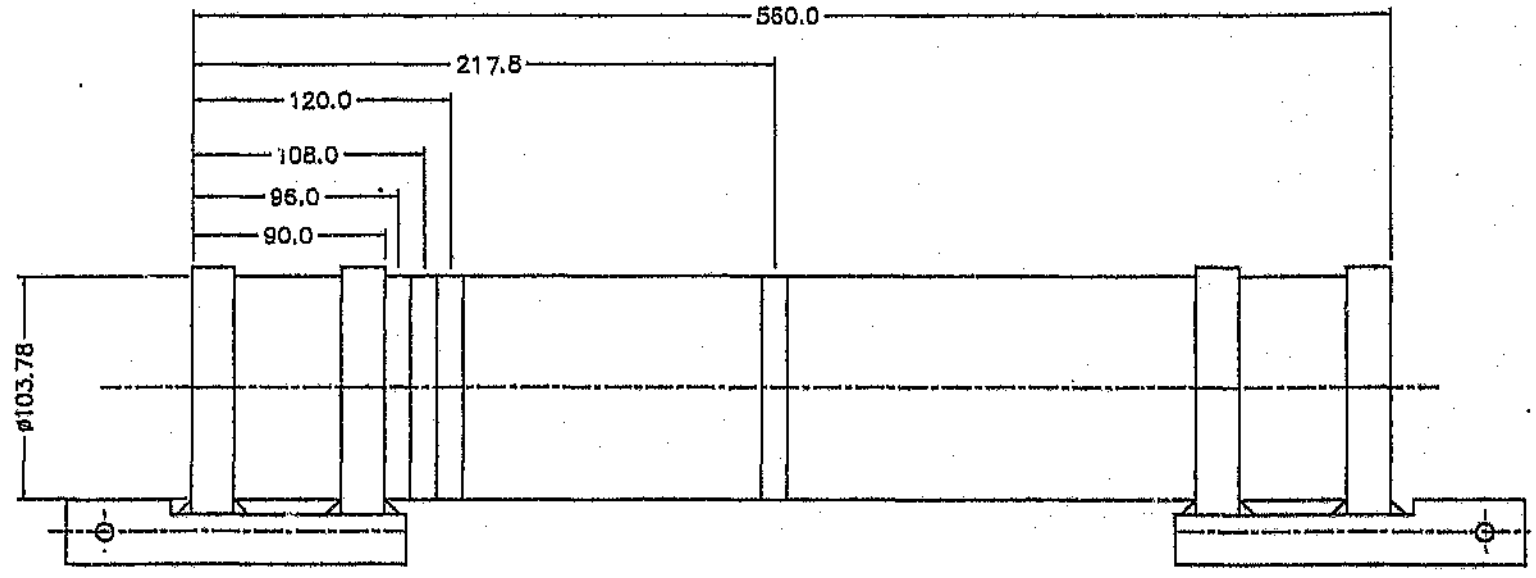

Figure B1 Validation model assembly with the position of the strain gauges at x = 96, 108, 120 and 217,8 mm.

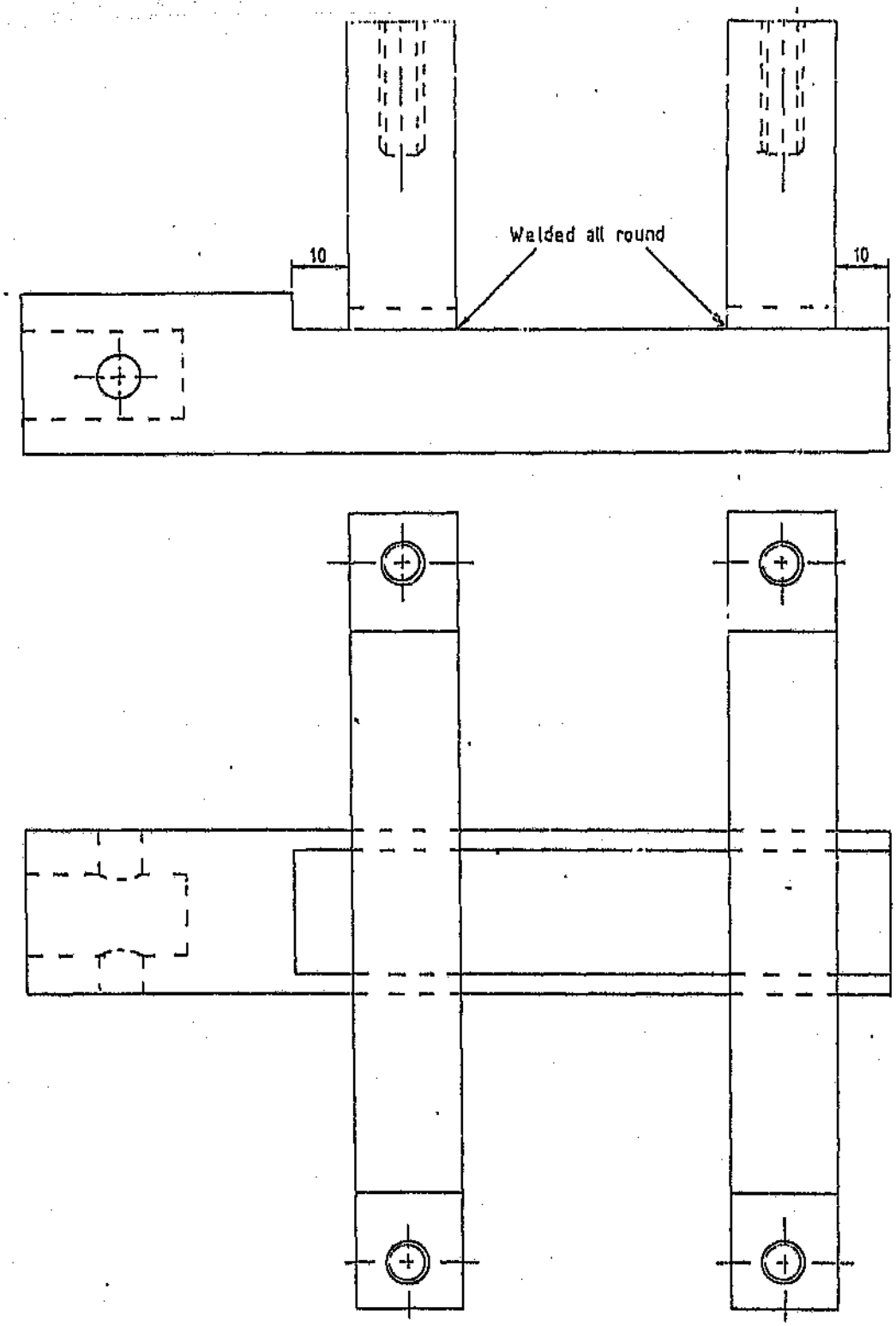

Figure B2 Welded assembly of the ribs and rod.

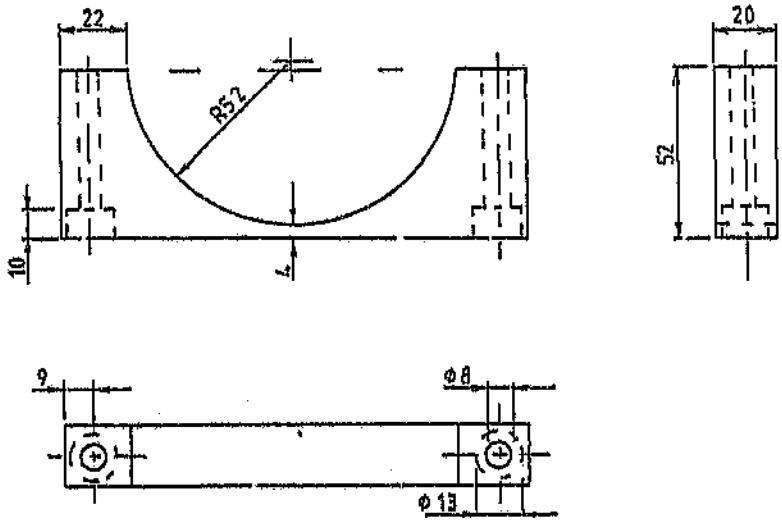

Figure B3 Top bracket for ribs.

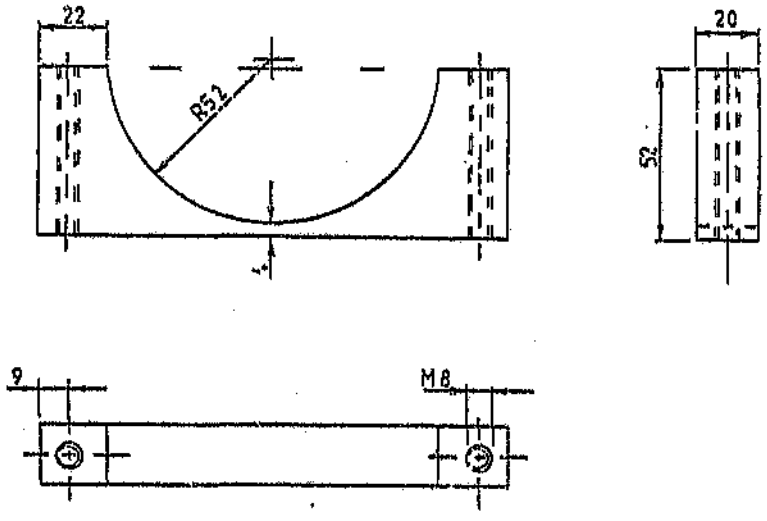

Figure B4 Bottom bracket for ribs.

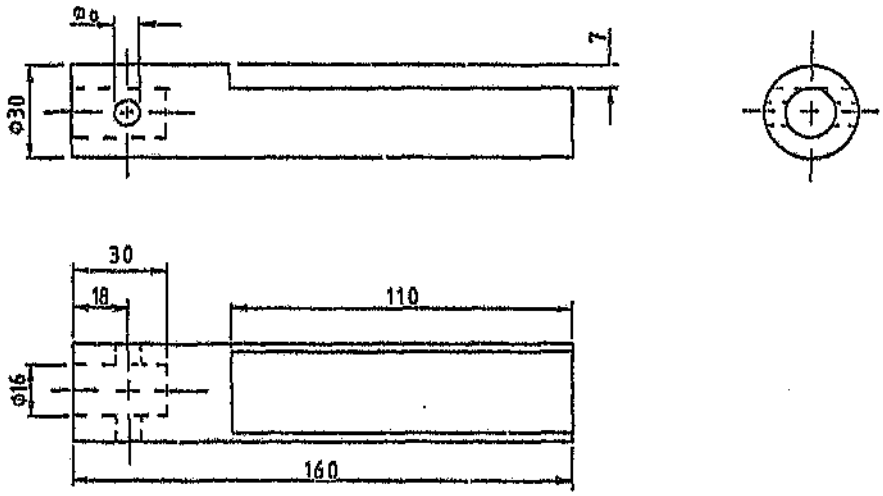

Figure B5 Mounting shaft.

APPENDIX C

MATERIAL PROPERTIES FOR THE ROAD TANKER AND VALIDATION MODEL

C-1 Lamina Properties of E-glass/polyester or E-glass/Vinylester

The final resin system selected for the tanker would typically be determined by its strength, processing and corrosive properties and cost. A PVC lined tanker carrying sulphuric acid would typically use a vinylester resin. The winding and corrosion requirements would limit the winding tension and typical values for a filament wound laminate were obtained for E-glass/epoxy from Tsai (1986) as follows:

E_1 = 38,6 GPa
E_2 = 8,27 GPa
ν_{12} = 0,26 GPa
G_{12} = 4,14 GPa
vf = 0,45
mf = 0,62
p = 1800 kg/m^3

These properties would not vary significantly between the various resin systems and were used for the FEM and theoretical predictions. The shear stiffnesses for the laminate were calculated at $G_{12} = G_{13}$ = 4.14 GPa. The remaining transverse shear stiffnesses was calculated at G_{23} = 3,5 GPa.

C-2 Laminate properties for the Tanker Dome

The composite road tanker is an assembly of three types of structural members namely a cylindrical shell, two elliptical domes (or ta.. ends) and 13 circumferential ribs or rings. Due to the nature of the Finite Elements and their material definitions, three types of materials were used to model the tanker namely:
- cylinder : laminated composite
- domes : isotropic

- ribs : orthotropic

The definition of a material as isotropic is the simplest of the three cases and was used to model the 2:1 ellipsoidal domes. The shape of the dome did not allow alignment with either the cylindrical or the spherical coordinate system, as the shape deviated from both. This would result in the incorrect definition of the material. For the complicated geometry of winding of an geodesic isotensoid, the prediction of the path of the fibres would vary over the ellipsoid and was difficult to predict accurately using ABAQUS. As the domes were included in the FEM model to ensure the correct distribution of load onto the cylinder, little improvement in accuracy would be achieved over using the quasi-isotropic assumption. The domes were therefore modelled as isotropic. This was a variation from inplane quasi-isotropic because the through thickness modulus E_z was the same as the circumferential and meridianal inplane moduli. Although this would have little influence on the axial, meridianal and circumferential membrane forces, the domes would also be loaded by local moments and transverse shear forces at the intersection to the cylinder (tan line). These were more dependent on the through thickness stiffness which in the isotropic case were equal to $G_{12} = G_{13} = G_{23} = E/(2.(1+\nu))$.

The values of E and v were obtained as the equivalent engineering constants from the lamination theory analysis of Appendix D and the MA-CLT.BAS program of Appendix H. The layup was assumed to consist of a quasi-isotropic layup of $[0°/\pm60°]_s$ with a volume fraction vf = 0,45 for E-glass/polyester. The thickness of the dome was equal to that of the shell at 15 mm. Hence from MA-CLT.BAS:

RT27DO60.CLT:- RT27 DOME [0/-60/+60]4s
Total laminate thickness = 15 mm
[A B] MATRIX
[B D]

3.068E+08	8.267E+07	0	0	0	0
8.267E+07	3.067E+08	0	0	0	0
0	0	1.120E+08	0	0	0
0	0	0	6.428E+03	1.430E+03	8.121E+01
0	0	0	1.430E+03	5.316E+03	2.051E+02
0	0	0	8.121E+01	2.051E+02	1.980E+03

E_θ (GPa)	E_ϕ (GPa)	$G_{\theta\phi}$ (GPa)	$\nu_{\theta\phi}$
18.96	18.96	7.47	0.2695

C-3 Laminate properties for the cylindrical tanker shell

The road tanker under evaluation would typically be manufactured by filament winding. This process was well established in the composite industry and documented (see Appendix V). The shell was modelled for FEM by using the laminated 3D composite option for the shell element S8R. The theoretical background used for this element was based on laminated plate theory covered in Appendix D. Further details can be obtained from the ABAQUS V4.6 reference manuals.

The laminate chosen for this analysis consisted of the following: $[\pm 10°/\pm 85°/\pm 10°/\pm 85°/\pm 10°/\pm 85°]_s$. This was represented for the CLT and FEM analysis by a total of 24 layers, each with 0,625 mm thickness to give a total laminate thickness of 15 mm. This laminate was analysed by the MA-CLT.BAS program (Appendix H) and the results were as follows:

RT27.CLT:- RT27 CYLINDER $[\pm 10°/\pm 85°/\pm 10°/\pm 85°/\pm 10°/\pm 85°]_S$
Total laminate thickness = 15 mm
[A B] MATRIX
[B D]

3.441E+08	4.008E+07	0	0	0	0
4.008E+07	3.545E+08	0	0	0	0
0	0	6.945E+08	0	0	0
0	0	0	7.473E+03	7.717E+02	8.121E+01
0	0	0	7.717E+02	5.586E+03	-0.262E+02
0	0	0	9.496E+01	-0.262E+02	1.322E+03

E_x (GPa)	E_ϕ (GPa)	$G_{x\phi}$ (GPa)	$\nu_{x\phi}$
22.64	22.64	4.63	0.1130

The laminate is balanced and symmetrical, with low inplane shear stiffness. This was important to decrease the torsional stresses which result from the tanker interaction with the road.

C-4 Laminate properties for the tanker ribs

The circumferential rings would be wound onto the tanker shell once the laminate had cured. The ring laminate would consist purely of hoop windings which were positioned between two formers until cure. The FEM representation of these ribs was achieved through the use of orthotropic beam elements (B32) which were connected to the shell with a multi-point constraint type 7. The material properties were evaluated by the MA-CLT.BAS program of Appendix D and H and were used for the theoretical analysis.

RT27RIB.CLT:- RT27 RIB LAMINATE [90°]
Total laminate thickness = 50 mm
[A B] MATRIX
[B D]

1.958E+09	1.091E+08	0	0	0	0
1.091E+08	4.196E+08	0	0	0	0
0	0	2.070E+08	0	0	0
0	0	0	4.080E+05	2.273E+04	0
0	0	0	2.273E+04	8.741E+04	0
0	0	0	0	0	4.013E+04

E_x (GPa)	E_ϕ (GPa)	$G_{x\phi}$ (GPa)	$\nu_{x\phi}$
38.60	8.27	4.14	0.26

The definition of the orthotropic constants for the B32 element was covered by the ABAQUS v4.6 Reference Manual. These coefficients where derived using the lamina properties of Appendix C1 from the reduced lamina stiffnesses $[Q_{ij}]$ of Appendix D as follows :

$Q_{11} = D_{1111} = 39.170E+09$
$Q_{12} = D_{1122} = 2.182E+09$
$Q_{22} = D_{2222} = 8.392E+09$
$Q_{14} = D_{1133} = 2.182E+09$
$Q_{24} = D_{2233} = 2.182E+09$
$Q_{44} = D_{3333} = 8.392E+09$
$Q_{33} = D_{1212} = 4.140E+0$
$Q_{55} = D_{1313} = 4.140E+09$
$Q_{66} = D_{2323} = 3.500E+09$

C-5 Laminate Properties for Validation Model

The validation model was manufactured by filament winding a tube from E-glass/epoxy. The layup directions consisted of double layers, each either at +45° or -45° to the tubes longitudinal axis. The properties of Appendix C1 were provided by the supplier of the tube as being typical for the laminate. Although the actual tube consisted of three -45° and three +45° layers which where interwoven, the FEM and CLT analysis assumed the layup to consist of eight layers to allow for the modelling of the laminate balance and symmetry. The material definition of the FEM model was based on the laminated 3D shell composite element and was described in more detail in paragraph 3.2.3.

The stiffness matrix for this tube was determined from the MA-CLT.bas program (see Appendix D and H) and were as follows:

VALIDAT.CLT:- VALIDATION LAMINATE $[\pm 45]_{2S}$
Total laminate thickness = 1.89 mm
[A B] MATRIX
[B D]

3.236E+07	1.671E+07	0	0	0	0
1.671E+07	3.236E+07	0	0	0	0
0	0	2.041E+07	0	0	0
0	0	0	9.632E+00	4.974E+00	1.623E+00
0	0	0	4.974E+00	9.632E+00	1.623E+00
0	0	0	1.623E+00	1.623E+00	6.075E+00

E_x (GPa)	E_ϕ (GPa)	$G_{x\phi}$ (GPa)	$\nu_{x\phi}$
12.56	12.56	10.80	0.5164

APPENDIX D

CLASSICAL LAMINATION THEORY

Stress-Strain Relations for a Lamina (Jones 1975)

The elastic stress-strain relations for the lamina will be expressed in matrix form using the following notation:
1 - longitudinal in the fibre direction,
2 - transverse to the fibres in the plane of the lamina,
3 - transverse to the fibres normal to the plane of the lamina
x, ϕ, r - laminate or arbitary co-ordinates.

For an orthotropic lamina we can represent the material properties as follows:

$E_1 = E_L$ (longitudinal Young's modulus)
$E_2 = E_3 = E_T$ (transverse Young's modulus)
$G_{12} = G_L$ (longitudinal shear modulus)
$G_{23} = G_T$ (transverse shear modulus) (Eq D1)
$\nu_{12} = \nu_L$ (longitudinal Poisson's ratio)
$\nu_{23} = \nu_T$ (transverse Poisson's ratio)

For a lamina treated as an effectivly homogenous and transversly isotropic materials, the stress σ and strain ϵ relationships can be written as

$$\begin{bmatrix} \epsilon_1 \\ \epsilon_2 \\ \epsilon_3 \\ \gamma_{23} \\ \gamma_{13} \\ \gamma_{12} \end{bmatrix} = \begin{bmatrix} \frac{1}{E_1} & \frac{-\nu_{21}}{E_2} & \frac{-\nu_{31}}{E_1} & 0 & 0 & 0 \\ \frac{-\nu_{12}}{E_1} & \frac{1}{E_2} & \frac{-\nu_{32}}{E_3} & 0 & 0 & 0 \\ \frac{-\nu_{13}}{E_1} & \frac{-\nu_{23}}{E_2} & \frac{1}{E_3} & 0 & 0 & 0 \\ 0 & 0 & 0 & \frac{1}{G_{23}} & 0 & 0 \\ 0 & 0 & 0 & 0 & \frac{1}{G_{31}} & 0 \\ 0 & 0 & 0 & 0 & 0 & \frac{1}{G_{12}} \end{bmatrix} \begin{bmatrix} \sigma_1 \\ \sigma_2 \\ \sigma_3 \\ \tau_{23} \\ \tau_{13} \\ \tau_{12} \end{bmatrix} \quad \text{(Eq D2)}$$

Account has been taken of the symmetry relations:

$\nu_{12}/E_2 = \nu_{12}/E_1 = \nu_{31}/E_3 = \nu_{13}/E_1$ and $\nu_{23}/E_2 = \nu_{32}/E_3$

and as is common in laminate analysis, use is made of the engineering shear strain γ.

For the tanker analysis, the loadings generally result in a plane state of stress hence

$$\sigma_{13} = \sigma_{23} = \sigma_3 = 0 \qquad \text{(Eq D3)}$$

and this applies for both plane stress and bending at sufficient distance from the laminate edges. Hence the above relation can be written as

$$\begin{bmatrix} \epsilon_1 \\ \epsilon_2 \\ \gamma_{12} \end{bmatrix} = \begin{bmatrix} \frac{1}{E_1} & \frac{-\nu_{12}}{E_1} & 0 \\ \frac{-\nu_{12}}{E_1} & \frac{1}{E_2} & \frac{-\nu_{23}}{E_2} \\ 0 & 0 & \frac{1}{G_{12}} \end{bmatrix} \begin{bmatrix} \sigma_1 \\ \sigma_2 \\ \tau_{12} \end{bmatrix} \qquad \text{(Eq D4)}$$

or $\{\epsilon_k\} = [S]\{\sigma_k\}$

where [S] is the compliance matrix which relates the stress and strain components in the principal material directions for the lamina (k). For the plane stress state, the additional strains can be found to be $\epsilon_{23} = \epsilon_{13} = 0 \quad \epsilon_3 = -\sigma_1 \cdot \nu_{12}/E_1 = -\sigma_2 \cdot \nu_{23}/E_2$ and this completely defines the state of stress and strain. Relations from Eqn D4 can be inverted to yield

$$\{\sigma_k\} = [S]^{-1}\{\epsilon_k\}$$
$$= [Q]\{\epsilon_k\} \qquad \text{(Eq D5)}$$

where [Q] is inverse of the compliance matrix and is known as the reduced lamina stiffness matrix given by

$$[Q] = \begin{bmatrix} Q_{11} & Q_{12} & 0 \\ Q_{12} & Q_{22} & 0 \\ 0 & 0 & Q_{66} \end{bmatrix}$$

where $Q_{11} = E_1/(1-\nu_{12}\cdot\nu_{21})$

$Q_{22} = E_2/(1-\nu_{12}\cdot\nu_{21})$

$Q_{12} = \nu_{12}\cdot E_2/(1-\nu_{12}\cdot\nu_{21})$

$Q_{66} = G_{12}$

and $\nu_{12}/E_1 = \nu_{21}/E_2 \qquad \text{(Eq D6)}$

These reduced stiffness and compliance matrix relate stresses and strains in the principal directions of the material. To define material responce in other directions, transformation relations must be developed by refering to Fig D1 and the analysis below.

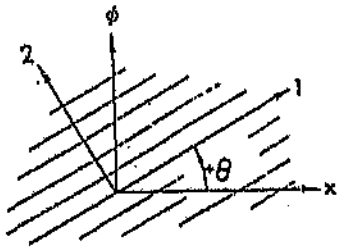

Fig D1 Coordinate systems: 1,2 are principal material coordinates; x,ϕ are laminate or arbitary coordinates.

The angle θ is defined as the rotation from the arbitary x,ϕ axis to the material 1,2 system (positive counter-clockwise).

The transformation from the 1,2 system to the x,ϕ system is accomplished by the following

$$\begin{bmatrix} \sigma_x \\ \sigma_\phi \\ \tau_{x\phi} \end{bmatrix} = \begin{bmatrix} c^2 & s^2 & -2cs \\ s^2 & c^2 & 2cs \\ cs & -cs & c^2-s^2 \end{bmatrix} \begin{bmatrix} \sigma_1 \\ \sigma_2 \\ \tau_{12} \end{bmatrix} \qquad \text{(Eq D7)}$$

or $\{\sigma_x\} = [T]^{-1}\{\sigma_x\}$ where $c = \cos\theta$ and $s = \sin\theta$.

The same technique can also be used to relate the shear strains

$$\begin{bmatrix} \epsilon_x \\ \epsilon_\phi \\ \frac{\gamma_{x\phi}}{2} \end{bmatrix} = [T]^{-1} \begin{bmatrix} \epsilon_1 \\ \epsilon_2 \\ \frac{\gamma_{12}}{2} \end{bmatrix} \qquad \text{(Eq D8)}$$

where the division of the engineering strain be two is necessary as only the tensor definition applies in this case.(tensor shear strain is equivalent to the eng. shear strain divided by two). The superscript -1 denotes the matrix inverse and the [T] matrix is defined as

$$[T] = \begin{bmatrix} c^2 & s^2 & 2cs \\ s^2 & c^2 & -2cs \\ -cs & cs & c^2-s^2 \end{bmatrix} \qquad \text{(Eq D9)}$$

If we introduce the so called Reuter matrix [R]

$$[R] = \begin{bmatrix} 1 & 0 & 0 \\ 0 & 1 & 0 \\ 0 & 0 & 2 \end{bmatrix} \qquad \text{(Eq D10)}$$

then the more natural strain vectors can be written as

$$\begin{bmatrix} \epsilon_1 \\ \epsilon_2 \\ \gamma_{12} \end{bmatrix} = [R] \begin{bmatrix} \epsilon_1 \\ \epsilon_2 \\ \frac{\gamma_{12}}{2} \end{bmatrix} \quad \text{and} \quad \begin{bmatrix} \epsilon_x \\ \epsilon_\phi \\ \gamma_{x\phi} \end{bmatrix} = [R] \begin{bmatrix} \epsilon_x \\ \epsilon_\phi \\ \frac{\gamma_{x\phi}}{2} \end{bmatrix} \qquad \text{(Eq D11)}$$

Accordingly we can use the above strain transformations and manipulate

$$\begin{bmatrix}\sigma_1\\ \sigma_2\\ \tau_{12}\end{bmatrix} = [Q]\begin{bmatrix}\epsilon_1\\ \epsilon_2\\ \gamma_{12}\end{bmatrix}$$

to obtain

$$\begin{bmatrix}\sigma_x\\ \sigma_\phi\\ \tau_{x\phi}\end{bmatrix} = [T]^{-1}\begin{bmatrix}\sigma_1\\ \sigma_2\\ \tau_{12}\end{bmatrix} = [T]^{-1}[Q][R][T][R]^{-1}\begin{bmatrix}\epsilon_x\\ \epsilon_\phi\\ \gamma_{x\phi}\end{bmatrix} \qquad \text{(Eq D12)}$$

however $[R][T][R]^{-1}$ can be shown to be $[T]^{-T}$ where the superscript T denotes the matrix transpose. Then if we use the abbreviation

$$[\bar{Q}] = [T]^{-1}[Q][T]^{-T}$$

the stress-strain relations in x,ϕ coordinates are

$$\begin{bmatrix}\sigma_x\\ \sigma_\phi\\ \tau_{x\phi}\end{bmatrix} = [\bar{Q}]\begin{bmatrix}\epsilon_x\\ \epsilon_\phi\\ \gamma_{x\phi}\end{bmatrix} = \begin{bmatrix}\bar{Q}_{11} & \bar{Q}_{12} & \bar{Q}_{16}\\ \bar{Q}_{12} & \bar{Q}_{22} & \bar{Q}_{26}\\ \bar{Q}_{16} & \bar{Q}_{26} & \bar{Q}_{66}\end{bmatrix}\begin{bmatrix}\epsilon_x\\ \epsilon_\phi\\ \gamma_{x\phi}\end{bmatrix} \qquad \text{(Eq D13)}$$

where the transformed reduced stiffnesses $\bar{Q}_{ij}$ are given in terms of the reduced stiffnesses Q_{ij} from Eq D6 as follows:

$$\begin{aligned}
\bar{Q}_{11} &= Q_{11}.c^4 + 2.c^2.s^2.(Q_{12} + 2.Q_{66}) + Q_{22}.s^4\\
\bar{Q}_{12} &= (Q_{11} + Q_{22} - 4.Q_{66}).s^2.c^2 + Q_{12}.(s^4 + c^4)\\
\bar{Q}_{22} &= Q_{11}.s^4 + 2.(Q_{12} + 2.Q_{66}).s^2.c^2 + Q_{22}.c^4 \qquad \text{(Eq D14)}\\
\bar{Q}_{16} &= (Q_{11} - Q_{12} - 2.Q_{66}).s.c^3 + (Q_{12} - Q_{22} + 2.Q_{66}).s^3.c\\
\bar{Q}_{26} &= (Q_{11} - Q_{12} - 2.Q_{66}).s^3.c + (Q_{12} - Q_{22} + 2Q_{66}).s.c^3\\
\bar{Q}_{66} &= (Q_{11} + Q_{22} - 2.Q_{12} - 2.Q_{66}).s^2.c^2 + Q_{66}.(s^4 + c^2)
\end{aligned}$$

Stress and Strain Variation in a Laminate

This analysis of stresses and deformations of laminates is very dependant on the fact that the thickness of the laminate is so much smaller than the inplane dimensions and can be analysed on the basis of the usual simplifications of plate theory. These are as follows:

- The plate thickness is much smaller than the inplane dimensions.
- The strains in the deformed plate are small compared to unity.
- Normals to the undeformed plate remain normal to the deformed plate surface ie $Y_{xr} = Y_{\phi r} = 0$, where r is the direction of the normal to the middle surface shown in Fig D2.
- Vertical deflection does not vary through the thickness ie ($\epsilon_r = 0$).
- Stress normal to the plate is negligable.
- The laminate consists of perfectly bonded laminae connected by bonds which are infinitesimally thin and non-shear-deformable.

Accordingly, a normal originally straight and perpendicular to the middle surface of the laminate is assumed to remain straight and perpendicular to the middle surface when the laminate is extended and bent.

The foregoing collection of assumptions constitues the Kirchoff-Love hypothesis for shells and applies to flat or curved laminates. We can therefore derive the displacements u,v and w in the x,ϕ and r directions by considering a laminate cross section in the $x\phi$ plane shown in Fig D2.

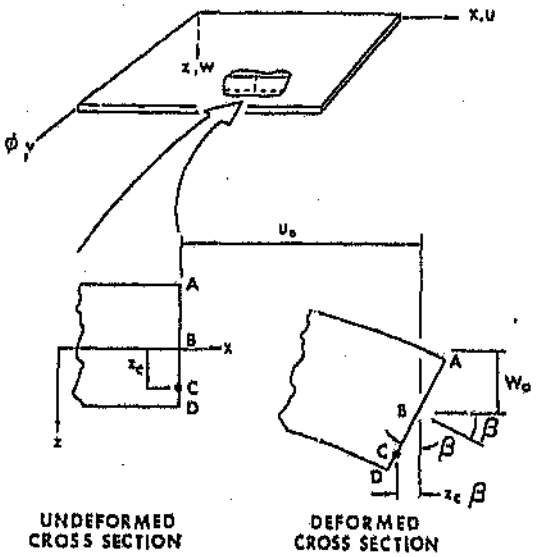

Figure D2. Geometry of deformation in the xϕ plane.

The displacement of a point C on the laminate can be written as

$u_C = u_o - r_C.\beta$ (Eq D15)

where u_o is the x displacement of the laminate middle surface

β is the slope of the laminate middle surface = $\delta w_o/\delta x$

Hence the displacement u at any point r through the laminate thickness is

$u = u_o + r.\delta w_o/\delta x$ (Eq D16)

By similar reasoning, we find the displacement v in the ϕ direction is

$v = v_o + r.\delta w_o/\delta \phi$ (Eq D17)

The laminate strains have been reduced to only ϵ_x, ϵ_ϕ and ϵ_r by the Kirchoff-Love hypothesis ie $\gamma_{xr} = \gamma_{\phi r} = \epsilon_r = 0$. For small strains and linear elasticity, the remaining strains in a plate can be calculated in terms of the displacements as

$$\epsilon_x = \delta u/\delta x$$
$$\epsilon_\phi = \delta u/\delta \phi \quad \text{(Eq D18)}$$
$$\gamma_{x\phi} = \delta u/\delta \phi + \delta v/\delta x$$

Hence we can write the strains in terms Eq D16 and D17 as follows:

$$\begin{bmatrix}\epsilon_x\\ \epsilon_\phi\\ \gamma_{x\phi}\end{bmatrix} = \begin{bmatrix}\epsilon_x^{\,o}\\ \epsilon_\phi^{\,o}\\ \gamma_{x\phi}^{\,o}\end{bmatrix} + r.\begin{bmatrix}k_x\\ k_\phi\\ k_{x\phi}\end{bmatrix} \qquad \text{(Eq D19)}$$

where

$$\begin{bmatrix}\epsilon_x^{\,o}\\ \epsilon_\phi^{\,o}\\ \gamma_{x\phi}^{\,o}\end{bmatrix} = \begin{bmatrix}\delta u_o/\delta_x\\ \delta u_o/\delta_x\\ \delta u_o/\delta_\phi + \delta v_o/\delta_x\end{bmatrix} \quad \text{and} \quad \begin{bmatrix}k_x\\ k_\phi\\ k_{x\phi}\end{bmatrix} = -\begin{bmatrix}\delta^2 w_o/\delta_x{}^2\\ \delta^2 w_o/\delta_\phi{}^2\\ 2.\delta^2 w_o/(\delta_x.\delta_\phi)\end{bmatrix}$$

(Eq D20)

The Kirchoff-Love hypothesis hence implies a linear variation of strain through the laminate thickness. The stress-displacement relations in Eq D18 are only valid for plates. For circular cylindrical shells, the ϵ_ϕ term in Eq D18 must be supplemented by w_o/r_c where r_c is the radius of the shell. Other shells have more complicated strain-displacement relations.

By substitution of the strain variation through the thickness (Eq D20) into the stress-strain relations (Eq D13), the stresses in the k_{th} layer be expressed in terms of the laminate middle surface strains and curvatures as

$$\begin{bmatrix}\sigma_x\\ \sigma_\phi\\ \tau_{x\phi}\end{bmatrix} = \begin{bmatrix}\bar{Q}_{11} & \bar{Q}_{12} & \bar{Q}_{16}\\ \bar{Q}_{12} & \bar{Q}_{22} & \bar{Q}_{26}\\ \bar{Q}_{16} & \bar{Q}_{26} & \bar{Q}_{66}\end{bmatrix}_k \cdot \left[\begin{bmatrix}\epsilon_x^{\,o}\\ \epsilon_\phi^{\,o}\\ \gamma_{x\phi}^{\,o}\end{bmatrix} + r.\begin{bmatrix}k_x\\ k_\phi\\ k_{x\phi}\end{bmatrix}\right] \qquad \text{(Eq D21)}$$

Since the $\bar{Q}_{ij}$ can be different for each layer k of the laminate, the stress variation is not necessarily linear even though the strain

is linear.

Resultant Laminate Forces and Moments.

The forces and moment resultants acting on a laminate are obtained by intergration of the stresses in each layer through the laminate thickness, for example

$$N_x = \int_{-t/2}^{t/2} \sigma_x . dr \quad \text{and} \quad M_x = \int_{-t/2}^{t/2} \sigma_x . r . dr \qquad \text{(Eq D21)}$$

N_x is a force per unit width of the cross section of the laminate and M_x is the moment per unit width as shown in Figure D3 below.

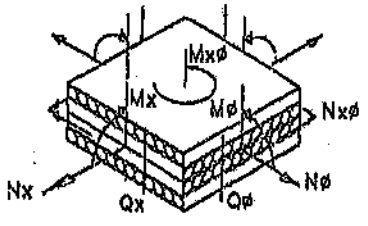

Nx – AXIAL FORCE RESULTANT (N/m width)
Nø – CIRCUMFERENTIAL FORCE RESULTANT (N/m width)
Nxø – INPLANE SHEAR FORCE RESULTANT (N/m width)
Mx – AXIAL MOMENT RESULTANT (Nm/m width)
Mø – CIRCUMFERENTIAL MOMENT RESULTANT (Nm/m width)
Mxø – TWISTING MOMENT RESULTANT (Nm/m width)
Qx – AXIAL TRANSVERSE SHEAR (N/m width)
Qø – CIRCUMFERENTIAL TRANSVERSE SHEAR (N/m width)

Figure D3 In-plane force and moment resultants on a flat plate.

All the force and moment resultants for an N-layered laminate can be defined as

$$\begin{bmatrix} N_x \\ N_\phi \\ N_{x\phi} \end{bmatrix} = \int_{-t/2}^{t/2} \begin{bmatrix} \sigma_x \\ \sigma_\phi \\ \tau_{x\phi} \end{bmatrix} .dr = \sum_{k=1}^{N} \int_{r_{k-1}}^{r_k} \begin{bmatrix} \sigma_x \\ \sigma_\phi \\ \tau_{x\phi} \end{bmatrix} .dr \qquad \text{(Eq D22)}$$

and

$$\begin{bmatrix} M_x \\ M_\phi \\ M_{x\phi} \end{bmatrix} = \int_{-t/2}^{t/2} \begin{bmatrix} \sigma_x \\ \sigma_\phi \\ \tau_{x\phi} \end{bmatrix} .r.dr = \sum_{k=1}^{N} \int_{r_{k-1}}^{r_k} \begin{bmatrix} \sigma_x \\ \sigma_\phi \\ \tau_{x\phi} \end{bmatrix} .r.dr \qquad \text{(Eq D23)}$$

where r_k and r_{k-1} are defined below in Figure D4 and $r_o = -t/2$. These force and moment resultants do not depend on r after intergration, but are functions of x and ϕ, the coordinates of the laminate middle surface.

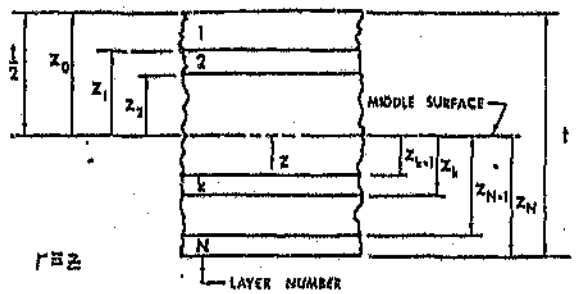

Figure D4. Geometry of an N layered plate.

Taking advantage of the fact that the stiffness matrix is constant within the lamina, we can rearrange Eqn D22 and D23 by taking the stiffness matrix outside the intergration for each layer but within the summation of force and moment resultants.

$$\begin{bmatrix} N_x \\ N_\phi \\ N_{x\phi} \end{bmatrix} = \sum_{k=1}^{N} \begin{bmatrix} \bar{Q}_{11} & \bar{Q}_{12} & \bar{Q}_{16} \\ \bar{Q}_{12} & \bar{Q}_{22} & \bar{Q}_{26} \\ \bar{Q}_{16} & \bar{Q}_{26} & \bar{Q}_{66} \end{bmatrix}_k \cdot \left[\int_{r_{k-1}}^{r_k} \begin{bmatrix} \epsilon_x^{\,o} \\ \epsilon_\phi^{\,o} \\ \gamma_{x\phi}^{\,o} \end{bmatrix} .dr + \int_{r_{k-1}}^{r_k} . \begin{bmatrix} k_x \\ k_\phi \\ k_{x\phi} \end{bmatrix} .r.dr \right]$$

(Eq D24)

$$\begin{bmatrix} M_x \\ M_\phi \\ M_{x\phi} \end{bmatrix} = \sum_{k=1}^{N} \begin{bmatrix} \bar{Q}_{11} & \bar{Q}_{12} & \bar{Q}_{16} \\ \bar{Q}_{12} & \bar{Q}_{22} & \bar{Q}_{26} \\ \bar{Q}_{16} & \bar{Q}_{26} & \bar{Q}_{66} \end{bmatrix}_k \cdot \left[\int_{r_{k-1}}^{r_k} \begin{bmatrix} \epsilon_x^{\,o} \\ \epsilon_\phi^{\,o} \\ \gamma_{x\phi}^{\,o} \end{bmatrix} .r.dr + \int_{r_{k-1}}^{r_k} . \begin{bmatrix} k_x \\ k_\phi \\ k_{x\phi} \end{bmatrix} .r^2.dr \right]$$

(Eq D25)

The strains $\epsilon_x^{\,o}$, $\epsilon_\phi^{\,o}$,$\epsilon_{x\phi}^{\,o}$, k_x, k_ϕ and $k_{x\phi}$ are not functions of r but middle surface values and can also be removed from under the summation signs. After simplifying we get

$$\begin{bmatrix} N_x \\ N_\phi \\ N_{x\phi} \end{bmatrix} = \begin{bmatrix} A_{11} & A_{12} & A_{16} \\ A_{12} & A_{22} & A_{26} \\ A_{16} & A_{26} & A_{66} \end{bmatrix} \cdot \begin{bmatrix} \epsilon_x^{\,o} \\ \epsilon_\phi^{\,o} \\ \gamma_{x\phi}^{\,o} \end{bmatrix} + \begin{bmatrix} B_{11} & B_{12} & B_{16} \\ B_{12} & B_{22} & B_{26} \\ B_{16} & B_{26} & B_{66} \end{bmatrix} \cdot \begin{bmatrix} k_x \\ k_\phi \\ k_{x\phi} \end{bmatrix}$$

(Eq D26)

$$\begin{bmatrix} M_x \\ M_\phi \\ M_{x\phi} \end{bmatrix} = \begin{bmatrix} B_{11} & B_{12} & B_{16} \\ B_{12} & B_{22} & B_{26} \\ B_{16} & B_{26} & B_{66} \end{bmatrix} \cdot \begin{bmatrix} \epsilon_x{}^o \\ \epsilon_\phi{}^o \\ \gamma_{x\phi}{}^o \end{bmatrix} + \begin{bmatrix} D_{11} & D_{12} & D_{16} \\ D_{12} & D_{22} & D_{26} \\ D_{16} & D_{26} & D_{66} \end{bmatrix} \cdot \begin{bmatrix} k_x \\ k_\phi \\ k_{x\phi} \end{bmatrix} \qquad \text{(Eq D27)}$$

where

$$A_{ij} = \sum_{k=1}^{N} (\bar{Q}_{ij})_k \cdot (r_k - r_{k-1}) \qquad \text{(Eq D28)}$$

$$B_{ij} = 1/2 \cdot \sum_{k=1}^{N} (\bar{Q}_{ij})_k \cdot (r_k{}^2 - r_{k-1}{}^2) \qquad \text{(Eq D29)}$$

$$D_{ij} = 1/3 \cdot \sum_{k=1}^{N} (\bar{Q}_{ij})_k \cdot (r_k{}^3 - r_{k-1}{}^3) \qquad \text{(Eq D30)}$$

A_{ij} are called extensional stiffnesses, the B_{ij} are called coupling stiffnesses and the D_{ij} are called bending stiffnesses. The presence of B_{ij} implies coupling between bending and extension.

The analysis of isotropic plates is well established and involves All the seperate analysis of the inplane loading and bending moments, the results then being superimposed. This occurs because the two loadings are uncoupled. For anisotopic laminates, coupling does occur and the inplane loading and bending are treated together. It is only for a symmetrical laminate sequences that uncoupling occurs.

APPENDIX E

THEORY FOR INTERNAL PRESSURE

E-1 Theory of plates and shells applied to internal pressure loadcase

Consider a cylindrical shell loaded symmetrically with respect to its axis. A segment of this shell is shown below in Figure E1.

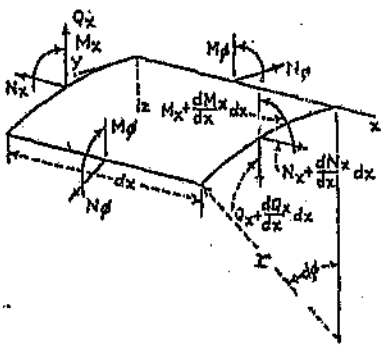

Figure E1 Segment of the tanker shell.

It can be concluded from symmetry that the membrane shearing forces $N_{x\phi} = N_{\phi x}$ are zero and that the forces N_ϕ are constant along the circumference. From symmetry considerations, the transverse shearing forces Q_ϕ are also zero. The moments acting on the element are also affected by symmetry which results in the twisting moments $M_{x\phi} = M_{\phi x} = 0$, and the circumfential bending moments M_ϕ are constant along the circumference. These conditions simplify the equations of equilibrium considerably. Assuming that the external forces consist only of pressure normal to the surface, it was indicated that the forces N_x remain constant across the segment, and are taken as zero. Non-zero forces and their associated deformations can easily be calculated and superimposed onto the stresses and deformations produced by lateral loads.

The expression for the strain components can be written as follows:

$e_x = du/dx \qquad e_\phi = w/r$ (Eqn E1)

By applying Hooke's law, we can conclude that

$du/dx = \nu.w/a$ and $N_\phi = -E.t.w/r$ (Eqn E2)

Considering the bending moments, we can conclude from symmetry that there is no change in curvature in the circumfential direction. The curvature in the x direction is equal to $-d^2w/dx^2$. Using the equations derived by Timoshenko (1959) for plates, we obtain

$$M_\phi = \nu.M_x$$
$$M_x = -D\cdot d^2w/dx^2 \quad \text{(Eqn E3)}$$
$$Q_x = -D\cdot d^3w/dx^3$$

where $D = E\cdot t^3/(12.(1-\nu^2))$ is the flexural rigidity of the shell for an isotropic material.

By eliminating Q_x from the equation, the equations of equilibrium can be simplified (for symmetrical deformation of circular cylindrical shells of constant thickness) in the simplified form as follows:

$d^4w/dx^4+4.\beta^4.w = p/D$ (Eqn E4)

where $\beta^4 = E.t/(4.r^2.D) = 3.(1-\nu^2)/(r^2.t^2)$

The general solution of this equation is

$w = e^{\beta.x}.(C_1.\cos \beta.x + C_2.\sin \beta.x)+e^{-\beta.x}.(C_3.\cos \beta.x + C_4.\sin \beta.x)+f(x)$ (Eqn E5)

where f(x) is the particular solution and C_1, C_2, C_3, C_4 are the constants of integration which are determined from the conditions at the ends of the cylinder.

Consider the sections of the road tanker as a long circular pipe submitted to the action of the bending moments M_o and the shearing

forces Q_o, both uniformly distributed along the edge x' = 0 shown below. Note that the deflection w is taken positive towards the axis of the cylinder. Both M_o, Q_o are shown below as positive.

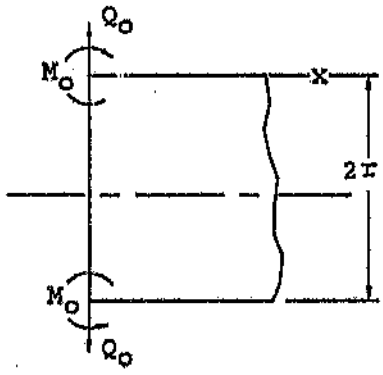

Figure E2 Section of a long circular pipe under the action of bending moments M_o and shearing forces Q_o.

In this case the effect of the forces M_o, Q_o are only considered. Assume for the moment that the pressure p distributed over the surface is not included at this stage but that it will be taken into account later by supersition. By considering the boundary conditions and eliminating all those that are zero, Timoshenko (1959) obtains the following expression:

$$w = e^{-\beta.x}/(2\cdot\beta^3\cdot D).[\beta.M_o.(\sin \beta.x - \cos \beta.x) - Q_o.\cos \beta.x] \qquad \text{(Eqn E6)}$$

The slope can be obtained by differentiating the above equation. By introducing the notation:

$$\text{phi}(\beta.x) = e^{-\beta.x}.(\cos \beta.x + \sin \beta.x)$$
$$\text{psi}(\beta.x) = e^{-\beta.x}.(\cos \beta.x - \sin \beta.x) \qquad \text{(Eqn E7)}$$
$$\text{theta}(\beta.x) = \theta(\beta.x) = e^{-\beta.x}.\cos \beta.x$$
$$\text{zeta}(\beta.x) = e^{-\beta.x}.\sin \beta.x$$

The expressions for deflection and its consecutive derivatives can be represented as follows:

$$w = -1/(2.\beta^3.D).[\beta.M_o.psi(\beta.x) + Q_o.\theta(\beta.x)]$$
$$dw/dx = 1/(2.\beta^2.D).[2.\beta.M_o.\theta(\beta.x) + Q_o.phi(\beta.x)]$$
$$d^2w/dx^2 = -1/(2.\beta.D).[2.\beta.M_o.phi(\beta.x) + 2.Q_o.zeta(\beta.x)]$$
$$d^3w/dx^3 = 1/D.[2.\beta.M_o.zeta(\beta.x) - Q_o.psi(\beta.x)]$$

(Eqn E8)

These effects are of a local character, because the functions defining the bending of the shell approach zero as the quantity βx becomes large. Hence the moments M_x and M_ϕ and the deflection w can be determined from equation E3 and N_ϕ from equation E2. What are however unknown are the Moment M_o and transverse force Q_o which the rings exert on the shell when they tend to expand under pressure.

Timoshenko (1959) mentions that the bending of a shell by a load uniformly distributed along a circular section is of a local nature, and that the bending is small for $x > \pi/\beta$. This corresponds to a value of $x > 0{,}238$m for the road tanker in question. This indicates that this bending is localized and that a shell of length $l = 2.\pi/\beta$ (i.e. $l = 0{,}476$m) loaded at the middle w ll have practically the same deflection and same maximum stress as a very long shell. For the ring stiffener spacing of 1m, the above relationships will therefore be able to predict the effect with sufficient accuracy, as the shell on either side of the stiffener can be considered as being a long shell.

The calculation of the moment M_o and forces Q_o is calculated by Timeschenko (1959) for a cylindrical shell bent by forces and moments distributed along the edges. This solution is extended to evaluate the stresses in a long pipe reinforced by equidistant rings and submitted to the action of a uniform internal pressure of p as shown below.

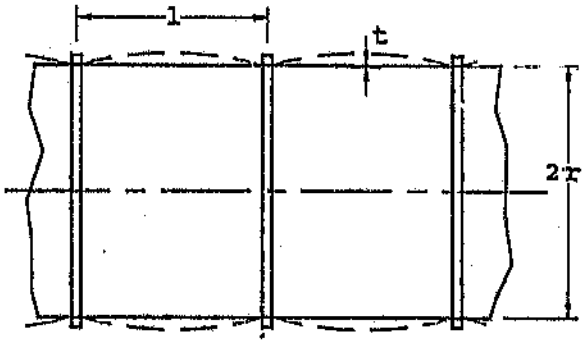

Figure E3 Portion of the tanker between two adjacent rings.

By defining chi_1, chi_2 and chi_3 as follows:

$$chi_1(2.\alpha) = (\cosh 2.\alpha + \cos 2.\alpha)/(\sinh 2.\alpha + \sin 2.\alpha)$$
$$chi_2(2.\alpha) = (\sinh 2.\alpha - \sin 2.\alpha)/(\sinh 2.\alpha + \sin 2.\alpha)$$
$$chi_3(2.\alpha) = (\cosh 2.\alpha - \cos 2.\alpha)/(\sinh 2.\alpha + \sin 2.\alpha)$$
(Eqn E9)

where $\alpha = \beta.l/2$ and l is the distance between the rings

The moment M_o can be approximated for infinitely stiff rings by

$$_o = p/(2.\beta^2).chi_2(2\cdot\alpha)$$ (Eqn E10)

and taking into account the flexibility of the rings, we observe that the reactive forces P (where $Q_o = -1/(2\cdot P)$ produce a tensile force P.r in the ring and the corresponding increase in the inner radius of the ring is

$$\delta_1 = P\cdot r^2/(A_r\cdot E)$$ (Eqn E11)

where A_r is the cross sectional area of the ring. Taking this into

account, the force P can be obtained from

$$P.\beta.[chi_1(2.\alpha)-chi_2^2(2.\alpha)/(2\cdot chi_3(2.\alpha)] = p'-P.t/A_r \quad \text{(Eqn E12)}$$

and the moment from

$$M_o = (p' - (P.t/A_r)/(2.\beta^2)\cdot chi_2(2\alpha) \quad \text{(Eqn E13)}$$

However, the pressure p acts not only on the cylindrical shell but also on the ends, producing longitudinal forces in the shell:

$$N_x = p.r/2 \quad \text{(Eqn E14)}$$

This produces an extension in the radius of the cylinder of

$$\delta' = p.r^2/(E.t).(1-\nu/2) \quad \text{(Eqn E15)}$$

and hence $p' = p.(1-\nu/2)$ (Eqn E16)

This analysis can also be used to evaluate the stresses arising from the discontinuity between the 2:1 ellipsoidal domes and the cylinder. Expressions have been derived by Timoshenko (1959) for the membrane stresses in a shell in the form of an ellipsoid of revolution as shown below in Figure E4. The 2:1 ellipsoidal dome or head is an efficient pressure vessel closure with regards to space allocation and stresses. This dome shape provides tangential meridional forces at the seam.

The membrane and bending stresses in an ellipsoidal dome under internal pressure loading are derived from analyses by Timoshenko (1959) and Bruhn (1973). The meridianal (θ) and tangential (ϕ) stresses can be written as follows:

$N_\theta = p.r_2/2$ and

$$N_\phi = p.r_2.(1-r_2^2/(2.r_1)) \quad \text{(Eqn E17)}$$

where

$a = r$ and $b = r/2$

$r_2 = (a^4\cdot y'^2+b^4.x'^2)^{(1/2)}/b^2$

$r_1 = r_2^3.b^2/a^4$

y' and x' are local dome variables in the circumferential and meridional directions.

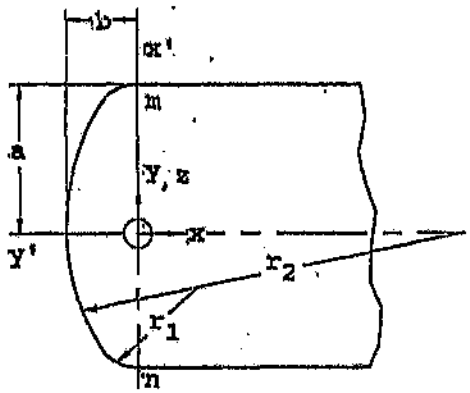

Figure E4 Schematic of a 2:1 ellipsoidal dome showing the radii (a,b), local (x',y') and global (x,y,z) co-odinates.

At the join mn at the equator of the ellipsoid shown in Figure E4, the force resultants in the meridional (N_θ) and circumfential directions (N_ϕ) are as follows:

$N_\theta = p.r/2$

$N_\phi = p.r.(1-r^2/(2.b^2))$ (Eqn E18)

The extension of the radius of the cylindrical shell under the action of the internal pressure is

$\delta_1 = p.r^2/(E.t).1-v/2)$ (Eqn E19)

The extension of the radius at the equator of a 2:1 ellipsoid is

$\delta_2' = r/E.(N_\theta/t-v.N_\theta/t)$

$= pr^2/(E.t).(1-r^2/(2.b^2)-v/2)$ (Eqn E20)

By substituting this into a derived equation for the shearing force Q_o we find

$$\delta_1-\delta_2' = p.r^4/(2.E.t.b^2) \qquad \text{(Eqn E21)}$$

and hence obtain

$$Q_o = p.r^2/(8.\beta.b^2) \qquad \text{(Eqn E22)}$$

This can then be substituted into equation E8 to determine w, dw/dx, dw^2/dx^2 and d^3w/dx^3 and hence M_x, M_ϕ, N_x and Q_x for the dome/shell junction.

E-2 Calculation of equivalent design pressure

A pressure of 8,4 Bar with no gravity load is used for the first tanker loadcase. This pressure will result in the same maximum tensile stress in the tanker as can be expected from a hydrostatic pressure test with water at 3,5 Bar and allows comparison between FEM and the theory from Timoshenko (1959). The equivalent pressure of 8,4 Bar also corresponds to six times 1.4 Bar, which was the maximum operating pressure recommended by Kenney (1966), and conforms to a requirement from ASME X (1990) that the burst pressure be six times the design pressure. The analysis shown below is based on an analysis from BS5500 (1988).

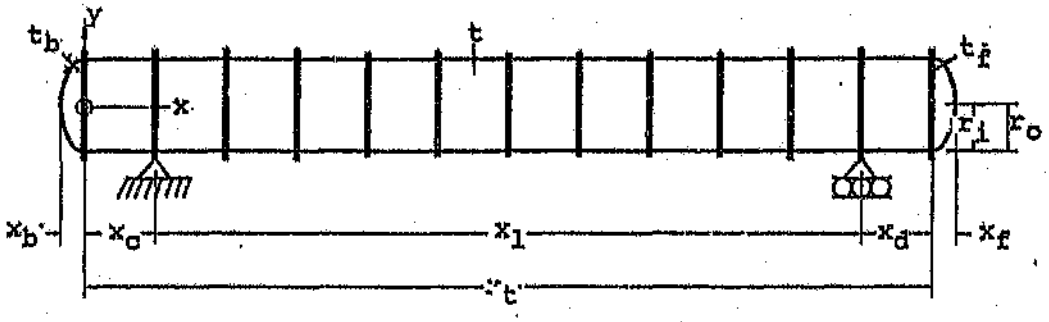

Figure E5 Schematic of the road tanker.

The principal dimensions are given as follows

$x_f = x_b = 0,325$ m

$x_o = x_d = 1$ m

$x_1 = 10$ m

$r_i = 0,650$ m; $r_o = 0,665$ m

$t = 15$ mm

To estimate the bending stresses due to a 1g vertical loading from the tanker and content weight, we can use the approach from Brownell (1959):

The tanker is treated as an equivalent cylinder having an equivalent length L_e as follows:

$L_e = (x_c + x_l + x_d) + 2/3.(x_b) + 2/3.(x_f)$
$= 12.43m$

The weight of the fluid and tanker may then be considered to be a uniform load equal to the total weight divided by the equivalent length L_e.

The masses of the various components can be calculated as follows:
Volume of cylindrical contents $(V_c)_c = \pi.r_i^2.l = 15,928\ m^3$

Volume of cylindrical shell $(V_s)_c = \pi.(r_o^2-r_i^2).l = 0,743\ m^3$
Volume of dome contents $(V_c)_d = 1/3.\pi.r_i^3 = 0,288\ m^3$
Volume of dome shell $(V_s)_d = 1/3.\pi.(r_o^3-r_i^3) = 0,02\ m^3$
Volume of ribs $V_r = \{no.\pi.[(r_o+b)^2-r_o^2)].a\}_{thick} + \{no.\pi.[(r_o+b)^2-r_o^2)].a\}_{thin} = 0,2289\ m^3$

For $(density)_s = 1900\ kg/m^3$ and $(density)_c = 1000\ kg/m^3$
Total mass of shell $= (V_r + 2.(V_s)_d + (V_s)_c).(density)_s = 1922\ kg$
Total mass of contents $= 2.(V_c)_d + (V_c)_c).(density)_c = 16504\ kg$
Total mass of tanker $m_t = 1922 + 16504 = 18428\ kg$

The equivalent loading is obtained from Brownell (1959) as
$w = g.m_t/L_e = 14542\ N/m$ where $g = 9.81\ m/s^2$.

For For $l = 10\ m$, $c = 1,215$ and $c_1 = 1,215\ m$; the reactions $(R_z)^b$ and $(R_z)_f$ are found as follows:

$(R_z)_b = w.[(c + l)^2 - c_1^2]/(2.l) = 90739$ N
$(R_z)_f = w.[(c_1 + l)^2 - c^2]/(2.l) = 90739$ N
This checks with the total weight of the tanker of 180757 N

The maximum bending moment about the y axis is
$(M_y)_{max} = (R_z)_b.[(R_z)_b/(2.w) - c] = 171,043$ kNm

The maximum tensile bending stress
$\sigma = M.z/I$
where z is vertical distance from the neutral axis. Hence the maximum force resultant from bending
$(N_x)_b = M.z.t/I$
where $I = \pi/4.(r_o^4 - r_i^4) = 1,0717*10^{-2}$ m^2
and occurs at the outer surface of the shell at z = 0,665 m hence:
$(N_x)_b = 159201$ N/m width

The analysis for internal pressure is based on Timoshenko (1984) who gives the longitudinal stress (membrane stress ignoring edge effects) resulting from internal pressure as
$\sigma_x = p.r_i/(2.t)$
Hence for membrane stresses, we can calculate the force resultant (force per unit width) from
$(N_x)_p = p.r_i/t$

For a pressure of 3,5 Bar this results in
$(N_x)_p = 113750$ N/m

Hence the maximum tensile stress due to bending and pressure
$(N_x)_{max} = 159201 + 113750 = 272951$ N/m width

The equivalent pressure which will give rise to the same tensile force resultant is given by
$p_{equiv} = (N_x)_{max}.2/r_i = 8.4*10^5$ N/m^2 = 8,4 Bar

APPENDIX F

THEORY FOR COMBINED ACCELERATIONS

F-1 Theory for stresses arising from acceleration in the axial direction (A_x).

F-1.1 Axial elongation and bending forces from hydrostatic pressure.

The hydrostatic pressure p(x) results from the axial acceleration (A_x) of the liquid and varies linearly in x. Since the tank is full, we can assume that surging is eliminated as the flow of the liquid is limited. To determine the force F_x which the front dome exerts on the cylindrical shell, we refer to Figure F1.1.

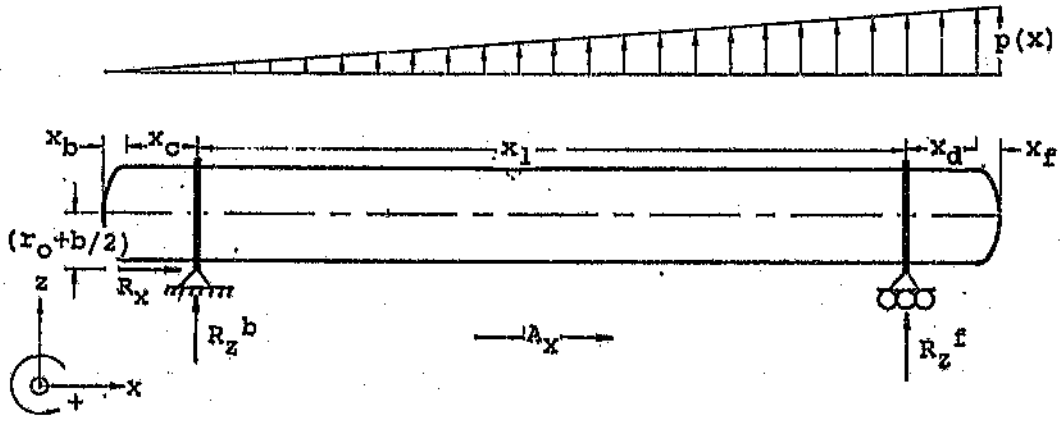

Figure F1.1 Variation of hydrostatic pressure from axial acceleration

The average pressure in the front dome p_{ave} can be approximated by

$$p_{ave} = p_c \cdot A_x \cdot h_{ave} \qquad \text{(Eqn F1.1)}$$

where p_c = density of contents
A_x = axial acceleration
h_{ave} = average head in the front dome

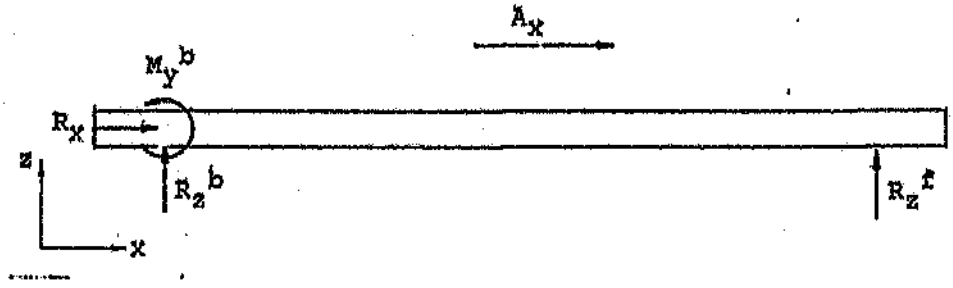

Figure F1.2 Beam theory idealisation of A_x acceleration

The centroid of the ellipsoid was given as 3/8 x_f by Meriam (1980) where x_f is the inside depth of the front dome. For 2:1 ellipsoidal domes

$x_b = x_f = r_i/2.$

hence we have the average head in the front dome

$h_{ave} = r_i/2 + x_t + 3/8.(r_i/2)$ (Eqn F1.2)

This pressure exerts a force equivalent to F_x on the dome:

$F_x = p_{ave}.A_p$ (Eqn F1.3)

where A_p = projected area of dome

$= \pi.r_i^2$

Beam theory can be used for the tanker geometry by representing the axial reaction at the bottom of the tank into an axial reaction R_x and a moment M_y^b at the tanker centreline. For static equilibrium [$\Sigma F_x = 0$] hence:

$F_x + R_x = 0$ hence $R_x = -F_x$ (Eqn F1.4)

Taking moments about the back support b; [$\Sigma M_b = 0$]

$M_y^b + R_z^f.x_1 = 0$

hence $R_z^f = -M_y^b/x_1$

But $M_y^b = F_x.(r_o+b/2)$

hence $R_z^f = F_x.(r_o+b/2)/x_1$ (Eqn F1.5)

Summation of forces in the vertical direction [$\Sigma F_z = 0$]

$R_z^b + R_z^f = 0$

hence $R_z^b = - R_z^f$

$= - F_x.(r_o+b/2)/x_1$ (Eqn F1.6)

The quantity $r_o+b/2$ is the offset between the tanker neutral axis and the position of the support reaction. This theory assumed that the location of the axial support had a significant influence on the reaction R_z^f and the moment M_y^b. If the reaction of the constraint was in line with the neutral axis of the tanker shell, then the moment M_y^b and the reaction R_z^f are both equal to zero. For this analysis however, they were still considered as non-zero and their effect evaluated later. From the evaluation of free body, axial and shear force and bending moment diagrams, refer to paragraph 3.1.2

F-1.2 Elongation and bending from the acceleration of the shell.

The mass of the shell, ribs and domes also affect the stresses when the tanker decelerates due to the density and inertia of the shell. This acceleration acts as a body force on each of the components which constitute the tanker shell. These stresses can be calculated from Newton II i.e. $\Sigma F_x = \Sigma m.A_x$. Consider the free body diagram for a section at an arbitrary position x shown in Figure F1.7. For the section $x_o < x \leq x_t$, this force would be equal to the mass of the tank to the right of the section multiplied by the acceleration A_x:

$\Sigma F_x = \Sigma m.A_x$

$F_x = \Sigma m.A_x$ (Eqn F1.7)

hence $F_x = \Sigma m.A_x$ where $A_x = -2 \times 9.81$ m/s^2

$= -19.6$ m/s^2

and Σm is the summation of mass forward of section at x.

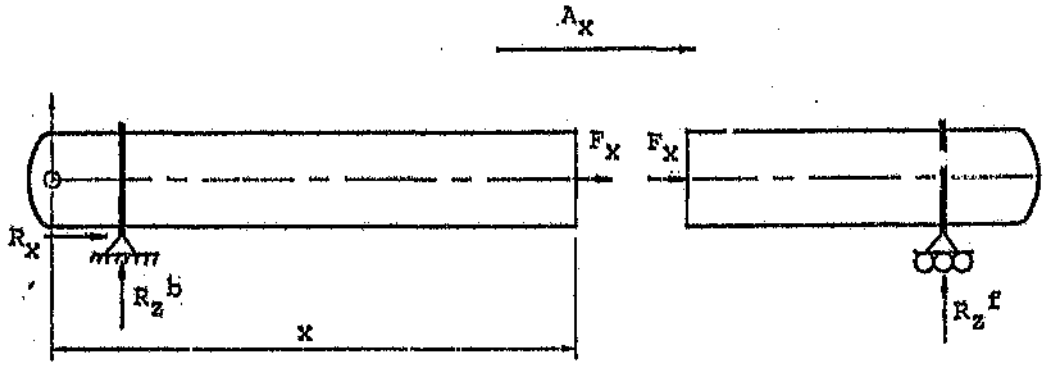

Figure F1.3 Schematic showing the acceleration of the shell and ribs.

For $x \geq x_c$, this can be approximated by:

$\Sigma m = p_s.A.(x_t-x) + {}_x\Sigma^{xt}m_r + m_s{}^d$ (Eqn F1.8)

where p_s = density of the shell

A = cross sectional area of the shell

${}_x\Sigma^{xt}m_r$ = sum of rib masses forward of section x

$m_s{}^d$ = mass of front dome

For $x < x_c$ this can be approximated by:

$\Sigma F_x = \Sigma m.A_x$ (Eqn F1.9)

$F_x = [m_s{}^d + p_s\ A.x + m_r{}^1].A_x$

Hence for $A_x = -2g$, F_x is negative and hence compressive. Due to the support being offset from the beam, the force configuration from Figure F1.3 can be simplified as shown in Figure F1.4 below. The effect the offset between the tanker centre-line and the axial reaction R_x line of action was not easy to predict from theoretical methods. Hence the configuration shown in Figure F1.4 assumed that the reaction was offset from the tanker centre-line. The validity of this

assumption will be checked against the FEM results.

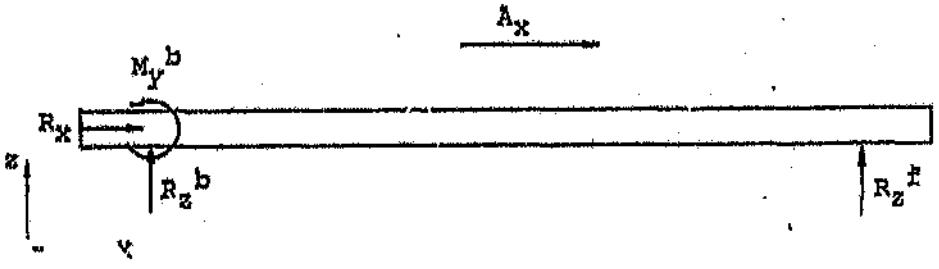

Figure F1.4 Free body diagram showing the effect of an offset between the reaction line of action and the tanker centre-line.

The axial reaction is

$$R_x = \Sigma^{all}m.A_x \qquad \text{(Eqn F1.10)}$$
$$= [m_s^d + p_s.A.x_t + \Sigma m_r + m_s^d].A_x$$
$$= (2 \times m_s^d + p_s.A.x_t + N_r^l.m_r^l + N_r^s.m_r^s).A_x$$

For vertical reactions $[\Sigma M^b = 0]$

$$M_y^b - R_z^f.x_1 = 0$$
$$\Rightarrow R_z^f = M_y^b/x_1 \qquad \text{(Eqn F1.11)}$$

and $[\Sigma F_z = 0]$ hence

$$R_z^b + R_z^f = 0$$
$$\Rightarrow R_z^b = - R_z^f \qquad \text{(Eqn F1.12)}$$

For the free body, axial force, shear force and bending moment diagrams, refer to paragraph 3.1.2.

APPENDIX G

THEORY FOR STRAIN GAUGES

G-1 Strain Gauge Theory

A strain gauge will be affected by strain in the axial and transverse directions. Modern foil gauges have enlarged end loops and are considerably less sensitive to transverse strain effects than early gauges. Some amount of transverse strain will still be monitored by the axial segments of the gauge grid pattern due to the large width t thickness ratio. This will produce a strain in addition to the axial strain. This transverse sensitivity of the gauge can be a problem wit laminated composite materials due to their orthotropic nature.

A $\pm 45^{\circ}$ E-glass/epoxy laminate has a Poisson's ratio of 0,5164 which i higher than that of steel. In the case of uniaxial loading, the trans verse strains largely result from the Poisson's effect. The strain gauge relations are discussed in detail by Tuttle and Brinson (1984) and are summarized below.

When a strain gauge is exposed to a strain field, a small change is grid resistance occurs given by:

$$\delta R/R = F_a \cdot e_a + F_t \cdot e_t \qquad \text{(Eqn G1)}$$

where δR = change in gauge resistance
R = original gauge resistance
e_a = strain parallel to the major gauge axis
e_t = strain perpendicular to major gauge axis
F_a = axial gauge factor
F_t = transverse gauge factor

The transverse sensitivity coefficient K is defined by:

$$K = F_t/F_a \qquad \text{(Eqn G2)}$$

and is normally supplied by the manufacturer. This value varies between -0,05 to 0,05 for most gauges. Equation (Eqn G1) then becomes

$$\delta R/R = F_a.(e_a + K.e_t) \qquad \text{(Eqn G3)}$$

During the manufacturer's calibration of the gauge, it is mounted on standard calibration material ($\nu_o = 0{,}285$) and subjected to a uniaxia stress field with the major axis of the gauge parallel to the stress field. Hence the transverse strain is due to the poissions effect and equal to :

$$e_t = -\nu_o.e_a \qquad \text{(Eqn G4)}$$

Eqn G3 then becomes :

$$\delta R/R = F_a.(1 - \nu_o.K).e_a \qquad \text{(Eqn G5)}$$

The gauge factor F_g supplied by the manufacturer is defined as :

$$F_g = F_a.(1 - \nu_o.K) \qquad \text{(Eqn G6)}$$

For conditions where the transver se sensitivity is negligible, strain measured e_m by the gauge is given by :

$$e_m = \delta R/(R.F_g) \qquad \text{(Eqn G7)}$$

for significant transverse effects, the use of Eqn G7 can result in incorrect results as a result of ignoring transverse sensitivity.

The two measured apparent strains e_{mx} and e_{mt} are obtained from equation Eqn G7. Hence the true strains e_x and e_t are obtained by relations taking the transverse sensitivity into account :

$$e_x = (1 - \nu_o.K).(e_{mx} - K.e_{mt})/(1 - K^2)$$

$$e_t = (1 - \nu_o.K).(e_{mt} - K.e_{mx})/(1 - K^2) \qquad \text{(Eqn G8)}$$

These equations are used with rosettes where the axial and transverse readings are known. The error resulting from ignoring transverse sensitivity effects is given by :

error = $K.(e_t/e_x + \nu_o)/(1 - \nu_o.K)$ * 100 percent (Eqn G9)

As a general rule, the transverse sensitivity errors are most severe for unidirectional composites when gauges are mounted close to parallel to the fibres. For the validation model the errors would be less severe due to the orthotropic nature of the ±45° laminate. However, the high Poisson's ratio of 0,5164 produces significant transverse strain and therefore these effects will be considered when calculatin the gauge strains of e_0, e_{-45} and e_{45}.

To calculate the inplane strains e_x, e_t and Y_{xt} for the test model, w derive equations relating these in terms of the measured gauge strain e_0, e_{-45} and e_{45}. Consider a three gauge rosette with the gauges aligned in the 0°, -45° and 45° directions as shown schematically in Figure G1 below.

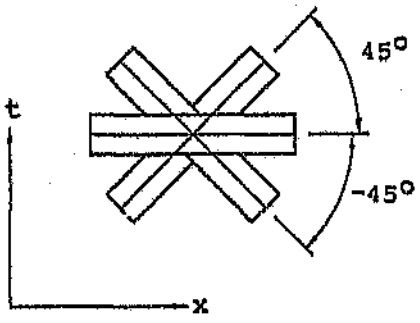

Figure G1 Orientation of the gauges on the validation model.

Dally and Riley (1978) present relations between these strains as follows :

$e_{-45} = e_x.\cos(-45)^2 + e_t.\sin(-45)^2 + Y_{xt}.\sin(-45).\cos(-45)$

$$= 1/2.(e_x + e_t - \gamma_{xt}) \qquad \text{(Eqn G10)}$$

$$e_0 = e_x.\cos(0)^2 + e_t.\sin(0)^2 + Y_{xt}.\sin(0).\cos(0)$$

$$= e_x \qquad \text{(Eqn G11)}$$

$$e_{45} = e_x.\cos(45)^2 + e_t.\sin(45)^2 + Y_{xt}.\sin(45).\cos(45)$$

$$= 1/2.(e_x + e_t + \gamma_{xt}) \qquad \text{(Eqn G12)}$$

Simplifying (Eqn G11) :

$$e_x = e_0 \qquad \text{(Eqn G13)}$$

Adding Eqn G11 and Eqn G12 :

$$e_t = e_{45} + e_{-45} - e_0 \qquad \text{(Eqn G14)}$$

Subtracting Eqn 12 and Eqn 10 :

$$Y_{xt} = e_{45} - e_{-45} \qquad \text{(Eqn G15)}$$

To evaluate the transverse sensitivity effects, we need to know the axial e_{mx} and transverse e_{mt} measured apparent strains for each gauge as shown below.

-45° Direction : $e_{mx} = e_{m-45}$
$e_{mt} = e_{m+45}$

$+45^o$ Direction : $e_{mx} = e_{m+45}$ (Eqn G16)
$e_{mt} = e_{m-45}$

0° Direction : $e_{mx} = e_{m0}$
$e_{mt} = e_{m90}$

$$= e_{m+45} - e_{m-45} - e_0$$

where e_{m-45}, e_{m+45} and e_{m0} are the measured apparent gauge strains ar obtained from the wheatstone bridge relations. The appropriate values of e_{mx} and e_{mt} from Eqn G16 are then substituted into Eqn G8 to determine the corrected gauge strains e_{-45}, e_{45} and e_0. These are then substit ted into equations Eqn G13, Eqn G14 and Eqn G15 to calculate the global model strains e_x, e_t and Y_{xt}. These values are then compared to similar strains from the FEM and beam theory.

G-2 Wheatstone Bridge Theory

This circuit is used to determine the static strain gauge reading. Th bridge is used as a direct readout device where the output voltage V_{out} is measured and related to strain. Consider a schematic of the circuit shown in Figure G2 below :

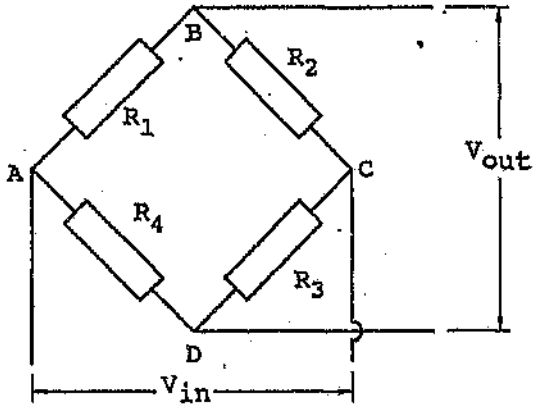

Figure G2 Schematic of the wheatstone bridge circuit

The voltage drop V_{AB} across R_1 is :

$$V_{AB} = R_1 \cdot V_{in} / (R_1 + R_2) \qquad \text{(Eqn G17)}$$

The voltage drop V_{AD} across R_4 is :

$$V_{AD} = R_4 \cdot V_{in} / (R_3 + R_4) \qquad \text{(Eqn G18)}$$

The output voltage from the bridge V_{out} is equivalent to V_{BD} :

$$V_{out} = V_{BD} = V_{AB} - V_{AD} \qquad \text{(Eqn G19)}$$

Substituting and simplifying Eqn G17, G18 and G19 :

$$V_{out} = (R_1.R_3 - R_2.R_4).V_{in}/[(R_1 + R_2).(R_3 + R_4)] \quad \text{(Eqn G20)}$$

The output voltage V_{out} will be zero and the bridge balanced when $R_1.R_3 = R_2.R_4$

Consider an initially balanced bridge when $R_1.R_3 = R_2.R_4$ such that $V_{out} = 0$ when the active gauge is unloaded. The strain induced output voltage δV_{out} for the loaded circuit can be written in terms of the resistances R_1, R_2, R_3 and R_4, and the changes in resistance δR_1, δR_2 δR_3 and δR_4 as follows:

$$\delta V_{out} = \frac{\begin{vmatrix} R_1 + \delta R_1 & R_2 + \delta R_2 \\ R_4 + \delta R_4 & R_3 + \delta R_3 \end{vmatrix}}{\begin{vmatrix} R_1 + \delta R_1 + R_2 + \delta R_2 & 0 \\ 0 & R_3 + \delta R_3 + R_4 + \delta R_4 \end{vmatrix}} . V_{in}$$

$$= (A/B).V_{in} \quad \text{(Eqn G21)}$$

A is the determinant of the numerator and B the determinant of the denominator. By expanding these determinants, neglecting second order terms and noting that $R_1.R_3 = R_2.R_4$ we get :

$$A = R_1.R_3.(\delta R_1/R_1 - \delta R_2/R_2 + \delta R_3/R_3 - \delta R_4/R_4) \quad \text{(Eqn G22)}$$

$$B = (R_1.R_3.(R_1 + R_2)^2)/(R_1.R_2) \quad \text{(Eqn G23)}$$

Combining equations Eqn G21, G22 and G23 :

$$\delta V_{out} = V_{in}.R_1.R_2/(R_1 + R_2)^2.(\delta R_1/R_1 - \delta R_2/R_2 + \delta R_3/R_3 - \delta R_4/R_4) \quad \text{(Eqn G24)}$$

For similar gauges used for the compensation arms of the bridge and

the active gauge, $R_1 = R_3 = R_2 = R_4 = R$. Due to the temperature compensation, only the R_1 gauge is sensitive to the strain and a net change in resistance ie : $\delta R_1 = \delta R$ and $\delta R_1 = \delta R_2 = \delta R_3 = 0$. Eqn G24 can then be simplified as :

$$\delta V_{out} = (V_{in}/4).(\delta R/R) \qquad \text{(Eqn G25)}$$

For the chosen gauges, R = 120 Ω. The change in resistance is proportional the measured strain from Eqn G25, substituting Eqn G23 into Eq G25 we can relate the measured strain to the voltage change as follows:

$$\delta V_{out}/V_{in} = F_g.e_m/4 \qquad \text{(Eqn G26)}$$

For the constructed circuit, V_{out} is not equal to zero when the activ gauges are unloaded. This is the result of the different resistances of the gauges, connections and lead wires. These values were noted fo all the gauges in their unloaded state and later subtracted from the loaded value of V_{out} to obtai the voltage difference δV_{out}, the strain induced output voltage.

The gauge excitement voltage V_{AB} can be derived from V_{in} from Eqn G17 For $R_1 = R_3 = R_2 = R_4 = R$:

$$V_{AB} = R/(2.R).V_{in} \qquad \text{(Eqn G27)}$$

Hence $V_{AB} = V_{in}/2$ and for $V_{in} = 5$ V, the gauge excitement voltage V_{AB} = 2,5 V.

APPENDIX H

LISTING OF MACLT CLASSICAL LAMINATION THEORY PROGRAM

```
  ' MA-CLT5.BAS     2/6/1991
    PI=3.1415597654
      CLEAR
     DEFDBL A-E,G-H,O-R,T-Z
' *** MAIN MENU FOR PROGRAM*********
10    CLS:CLOSE
11    CLS:PI=3.1415592654
      LOCATE 1,20:PRINT "CLASSICAL LAMINATION THEORY"
      LOCATE 2,20:PRINT "--------------------------"
      LOCATE 6,30:PRINT "OPTIONS MENU"
      LOCATE 7,30:PRINT "------------"
      LOCATE 10,20:PRINT "1 - LOAD DATA"
      LOCATE 11,20:PRINT "2 - EDIT DATA"
      LOCATE 12,20:PRINT "3 - RUN PROGRAM"
      LOCATE 13,20:PRINT "4 - PRINT RESULTS"
      LOCATE 14,20:PRINT "5 - EXIT TO OPERATING SYSTEM"
      LOCATE 18,10:INPUT "Selection (1--> 5) ?",SEL
      ON SEL GOTO 100,103,300,500,500
      GOTO 11

500   close:SYSTEM

'************************************
'** input the stress resultant as stresses for later inclusion
'************************************
'    GET #2,1:ANS$=B$
'          IF ANS$="F" OR ANS$="f" GOTO 2615
'           GET #1,2001:SXX1=CVD(A$)
'           GET #1,2002:SYY1=CVD(A$)
'           GET #1,2003:SXY1=CVD(A$)
'           NXX=SXX1*LW*TLT
'           NYY=SYY1*LW*TLT
'           NXY=SXY1*LW*TLT
'           MXX=0
'           MYY=0
'           MXY=0


'*********************************************
'**** routine to enter existing laminate data
'*********************************************'
100 CLOSE:CLEAR
    FLAG=0
    CLS:PRINT "LOAD DATA"
    LOCATE 4,1:INPUT "Input name of materials file (excl extension)
";NA$
    IF NA$="" THEN RETURN
     LAMDATA$=NA$+".CLT"
     SIGMA$=NA$+".STR"
    ON ERROR GOTO 101
```

```
     ' *** determine wether file exists
     OPEN LAMDATA$ FOR INPUT AS#1

IF FLAG=0 THEN
   ' *** load existing data if file exists
 ON ERROR GOTO 102
 LOCATE 6,20:PRINT "Loading existing file:- ";LAMDATA$
 LOCATE 24,10:INPUT "                Press enter to Continue";a$

  INPUT#1,LAMDESC$:'*** laminate description
  INPUT#1,NOM:' *** number of materials

  IF DI1=0 THEN
     ' *** routine to avoid double definition
    DIM
MDESC$(NOM),E1(NOM),E2(NOM),V12(NOM),V12T(NOM),V12C(NOM),G12(NOM),G13
    DIM
FXT(NOM),FYT(NOM),FXC(NOM`,FYC(NOM),FSXY(NOM),FSXZ(NOM),FSYZ(NOM)
    DI1=1
  END IF

 FOR I = 1 TO NOM
  INPUT#1,DUM,MDESC$(I):' *** material description
  INPUT#1,E1(I),E2(I),V12T(I),V12C(I),G12(I),G13(I),G23(I)
   INPUT#1,FXT(I),FYT(I),FXC(I),FYC(I),FSXY(I),FSXZ(I),FSYZ(I)
 NEXT I

INPUT#1,NOL:'*** number of layers
     IF DI2=0 THEN
     ' *** routine to avoid double definition
      DIM LNO(NOL),MNO(NOL),ANG(NOL),ANGR(NOL),PLTM(NOL)
      DIM SXY(3,NOL),S12(3,NOL),EXYK(3,NOL)
      DIM Q(3,3,NOL),QB(3,3,NOL),ZC(NOL),AD(6,6),A(6,6),B(6,6)
      DIM EK(6),CN(6),E0(3),CK(3),TS(3,3,NOL)
     DI2=1
    END IF


    FOR I=1 TO NOL
     INPUT#1,LNO(I),MNO(I),ANG(I),PLTM(I)
      LNO(I)=I
    NEXT I

   INPUT#1,NXX,NYY,NXY,MXX,MYY,MXY,QXX,QYY:'*** stress and moment
resultants
  CLOSE#1
 GOTO 11
END IF
```

```
101 IF ERR=53 OR ERR=62 THEN
    LOCATE 6,20:PRINT "Loading new file:- ";LAMDATA$
    LOCATE 24,1:INPUT "                  Press enter to Continue";a$
    GOTO 11
      ELSE:ON ERROR GOTO 102
 102 CLS:LOCATE 19,28:PRINT"ERROR ";ERR;:INPUT DUM$:CLOSE:GOTO 11
    END IF
  '*** if file not exist then selection = new file
     ' *** determine wether file exists


'*****************************************************
'****** DATA EDIT MENU
'*****************************************************

103 IF LAMDATA$="" THEN GOTO 11
 CLS:LOCATE 1,20:PRINT "CLASSICAL LAMINATION THEORY"
     LOCATE 2,20:PRINT "--------------------------"
     LOCATE 4,30:PRINT "INPUT MENU"
     LOCATE 5,30:PRINT "----------"
     LOCATE 7,10:PRINT "SELECT ITEM TO BE CHANGED"
     PRINT
     PRINT TAB(2) "1 - Change laminate description "
     PRINT TAB(2) "2 - Lamina material properties "
     PRINT TAB(2) "3 - Number of lamina or layers"
     PRINT TAB(2) "4 - Material type per lamina"
     PRINT TAB(2) "5 - Lamina angles"
     PRINT TAB(2) "6 - Lamina thicknesses"
     PRINT TAB(2) "7 - Force and moment resultants"
     PRINT:PRINT TAB(1) "8 - EXIT"
     PRINT:INPUT "Selection (1--> 8) ?",SEL
 IF SEL=0 THEN 103
 IF SEL<1 OR SEL>7 THEN GOSUB 250:GOTO 11
  ' *** save new file
 ON SEL GOSUB  105,110,120,130,140,150,160
   GOTO 103

'*****************************************************************
'*** Change laminate description"
105 CLS:LOCATE 1,1:PRINT "Laminate description.-"
LOCATE 2,1:PRINT LAMDESC$
LOCATE 3,1:INPUT DUM$
  IF DUM$<>"" THEN LAMDESC$=DUM$
  IF LAMDESC$="" THEN LAMDESC$=LAMDATA$
  ' *** assign filename if empty string
RETURN

'*** routine to input material properties
110 CLS:LOCATE 1,1:PRINT "Enter Number of Different Materials in the
```

```
laminate"
 LOCATE 1,60:PRINT USING"###";NOM;:INPUT DUM$
  IF DUM$<>"" THEN NOM=VAL(DUM$)
  IF NOM<1 THEN RETURN

    IF DI1=0 THEN
     DIM
MDESC$(NOM),E1(NOM),E2(NOM),V12(NOM),V12T(NOM),V12C(NOM),G12(NOM),G13
     DIM
FXT(NOM),FYT(NOM),FXC(NOM),FYC(NOM),FSXY(NOM),FSXZ(NOM),FSYZ(NOM)

     DI1=1
    END IF
   ' *** dim for new data only

   FOR I=1 TO NOM
   CLS
    LOCATE 1,1:PRINT "For material number"
    LOCATE 1,20:PRINT USING "###";I;
    LOCATE 2,1:PRINT "Description:- ";MDESC$(I);:INPUT DUM$
    IF DUM$<>"" THEN MDESC$(I)=DUM$
    DUM$=""
    LOCATE 4,1:PRINT "Longitudinal Modulus E1 [";:PRINT USING
"####.###";E1(I)/1E9;
    PRINT " GPa] ";:INPUT DUM$
    IF DUM$<>"" THEN E1(I)=VAL(DUM$)*1E9
    DUM$=""
    LOCATE 5,1:PRINT "Transverse Modulus E2 [";:PRINT USING
"####.###";E2(I)/1E9;
    PRINT " GPa] ";:INPUT DUM$
    IF DUM$<>"" THEN E2(I)=VAL(DUM$)*1E9
    DUM$=""
    LOCATE 6,1:PRINT "Tensile Poissions Ratio V12 [";:PRINT USING
"#.###";V12C(I);
    PRINT "] ";:INPUT DUM$
    IF DUM$<>"" THEN V12C(I)=VAL(DUM$)
    DUM$=""
    LOCATE 7,1:PRINT "Compressive Poissions Ratio V12 [";:PRINT USING
"#.###";V12T(I);
    PRINT "] ";:INPUT DUM$
    IF DUM$<>"" THEN V12T(I)=VAL(DUM$)
    DUM$=""
    LOCATE 9,1:PRINT "Inplane shear modulus G12 [";:PRINT USING
"####.###";G12(I)/1E9;
    PRINT " GPa] ";:INPUT DUM$
    IF DUM$<>"" THEN G12(I)=VAL(DUM$)*1E9
    DUM$=""
    LOCATE 10,1:PRINT "Transverse shear modulus G13 [";:PRINT USING
"####.###";G13(I)/1E9;
    PRINT " GPa] ";:INPUT DUM$
```

```
    IF DUM$<>"" THEN G13(I)=VAL(DUM$)*1E9
    DUM$=""
    LOCATE 11,1:PRINT "Transverse shear modulus G23 [";:PRINT USING
"####.###";G23(I)/1E9;
    PRINT " GPa] ";:INPUT DUM$
    IF DUM$<>"" THEN G23(I)=VAL(DUM$)*1E9
    DUM$=""
    LOCATE 13,1:PRINT "Longitudinal Tensile Strength  Xt [";:PRINT
USING "####.###";FXT(I)/1E6;
    PRINT " MPa] ";:INPUT DUM$
    IF DUM$<>"" THEN FXT(I)=VAL(DUM$)*1E6
    DUM$=""
    LOCATE 14,1:PRINT "Transverse Tensile Strength Yt [";:PRINT USING
"####.###";FYT(I)/1E6;
    PRINT " MPa] ";:INPUT DUM$
    IF DUM$<>"" THEN FYT(I)=VAL(DUM$)*1E6
    DUM$=""
    LOCATE 16,1:PRINT "Longitudinal Compressive Strength Xc [";:PRINT
USING "####.###";FXC(I)/1E6;
    PRINT " MPa] ";:INPUT DUM$
    IF DUM$<>"" THEN FXC(I)=VAL(DUM$)*1E6
    DUM$=""
    LOCATE 17,1:PRINT "Transverse Compressive Strength  Yc [";:PRINT
USING "####.###";FYC(I)/1E6;
    PRINT " MPa] ";:INPUT DUM$
    IF DUM$<>"" THEN FYC(I)=VAL(DUM$)*1E6
    DUM$=""
    LOCATE 19,1:PRINT "Inplane Shear Strength S12 [";:PRINT
USING"####.###";FSXY(I)/1E6;
    PRINT " MPa] ";:INPUT DUM$
    IF DUM$<>"" THEN FSXY(I)=VAL(DUM$)*1E6
    DUM$=""
    LOCATE 20,1:PRINT "Transverse Shear Strength S13 [";:PRINT USING
"####.###";FSXZ(I)/1E6;
    PRINT " MPa] ";:INPUT DUM$
    IF DUM$<>"" THEN FSXZ(I)=VAL(DUM$)*1E6
    DUM$=""
    LOCATE 21,1:PRINT "Transverse Shear Strength S23 [";:PRINT USING
"####.###";FSYZ(I)/1E6;
    PRINT " MPa] ";:INPUT DUM$
    IF DUM$<>"" THEN FSYZ(I)=VAL(DUM$)*1E6
  NEXT I
 RETURN

'*****************************************************************
'*** routine to input number of lamina
120 CLS:LOCATE 1,1:PRINT "Enter Number Of Layers in the laminate "
 LOCATE 1,60:PRINT USING"###";NOL;:INPUT DUM$
  IF DUM$<>"" THEN NOL=VAL(DUM$)
```

```
      IF DI2=0 THEN
      ' *** routine to avoid double definition
       DIM LNO(NOL),MNO(NOL),ANG(NOL),ANGR(NOL),PLTM(NOL)
       DIM SXY(3,NOL),S12(3,NOL),EXYK(3,NOL)
       DIM Q(3,3,NOL),QB(3,3,NOL),ZC(NOL),AD(6,6),A(6,6),B(6,6)
       DIM EK(6),CN(6),E0(3),CK(3),TS(3,3,NOL)
       DI2=1
      END IF

 RETURN


'*** routine to input material type per lamina
130 CLS:DEFAULT=MNO(1):DUM$="N"
    IF NOL=0 THEN RETURN
    FOR I=1 TO NOL
     LOCATE 1,1:PRINT USING"Enter Material Number for layer #### :-";I
      LOCATE 1,50:PRINT "                    "
     LOCATE 1,50:PRINT USING"###";MNO(I)
     LOCATE 10,10:PRINT "CHANGE DEFAULT Y/N ?"
     LOCATE 11,10:PRINT "KEEP SAME FOR ALL LAYERS: TYPE K ?"
     DUM1$=DUM$:LOCATE 13,25:PRINT DUM$
     LOCATE 13,25:INPUT DUM$
     IF DUM$="" THEN DUM$=DUM1$


       IF DUM$="Y" OR DUM$="y" THEN
        LOCATE 1,50:INPUT D$
        IF D$<>"" THEN MNO(I)=VAL(D$)
        DEFAULT=MNO(I)
       END IF

       IF DUM$="K" OR DUM$="k" THEN
         FOR J=I TO NOL
          MNO(J)=DEFAULT
         NEXT J
         GOTO 131
       END IF

     NEXT I
131 RETURN

'*** routine to input material angle per lamina
140 CLS:DEFAULT=ANG(1):DUM$="N"
    FOR I=1 TO NOL
   LOCATE 1,1:PRINT USING"Enter lamina angle in degrees for layer ####
:-";I
    LOCATE 1,60:PRINT "                    "
    LOCATE 1,60:PRINT USING"###";ANG(I)
    LOCATE 10,10:PRINT "CHANGE DEFAULT Y/N ?"
```

```
   LOCATE 11,10:PRINT "KEEP SAME FOR ALL LAYERS: TYPE K ?"
   DUM1$=DUM$:LOCATE 13,25:PRINT DUM$
   LOCATE 13,25:INPUT DUM$
    IF DUM$="" THEN DUM$=DUM1$

      IF DUM$="Y" OR DUM$="y" THEN
       LOCATE 1,60:INPUT D$
       IF D$<>"" THEN ANG(I)=VAL(D$)
       DEFAULT=ANG(I)
      END IF

      IF DUM$="K" OR DUM$="k" THEN
        FOR J=I TO NOL
         ANG(J)=DEFAULT
        NEXT J
       GOTO 141
      END IF

     NEXT I
141 RETURN


'*********************************************
'*** routine to input thickness per lamina
'*********************************************
150 CLS:DEFAULT=PLTM(1):DUM$="N"
   FOR I=1 TO NOL
   LOCATE 1,1:PRINT USING"Enter lamina thickness in mm for layer ####
:-";I
   LOCATE 1,50:PRINT "                    "
   LOCATE 1,50:PRINT USING"  ###.###";PLTM(I)*1000
   LOCATE 10,10:PRINT "CHANGE DEFAULT Y/N ?"
   LOCATE 11,10:PRINT "KEEP SAME FOR ALL LAYERS: TYPE K ?"
   DUM1$=DUM$:LOCATE 13,25:PRINT DUM$
   LOCATE 13,25:INPUT DUM$
    IF DUM$="" THEN DUM$=DUM1$

      IF DUM$="Y" OR DUM$="y" THEN
       LOCATE 1,50:INPUT D$
       IF D$<>"" THEN PLTM(I)=VAL(D$)/1000
       DEFAULT=PLTM(I)
      END IF

      IF DUM$="K" OR DUM$="k" THEN
        FOR J=I TO NOL
         PLTM(J)=DEFAULT
        NEXT J
       GOTO 151
      END IF
     NEXT I
```

```
151 RETURN

'***********************************
'** input the stress resultant data
'***********************************
160 CLS:LOCATE 1,1:PRINT"Enter stress and moment resultants"
     LOCATE 3,1:PRINT "Nxx [";:PRINT USING "+#####.####";NXX/1E3;
     PRINT " N/mm width] ";:INPUT D$
     IF D$<>"" THEN NXX=VAL(D$)*1E3
     DUM$=""
     LOCATE 4,1:PRINT "Nyy [";:PRINT USING "+#####.####";NYY/1E3;
     PRINT " N/mm width] ";:INPUT D$
     IF D$<>"" THEN NYY=VAL(D$)*1E3
     DUM$=""
     LOCATE 5,1:PRINT "Nxy [";:PRINT USING "+#####.####";NXY/1E3;
     PRINT " N/mm width] ";:INPUT D$
     IF D$<>"" THEN NXY=VAL(D$)*1E3
     DUM$=""
     LOCATE 7,1:PRINT "Mxx [";:PRINT USING "+#####.####";MXX/1E3;
     PRINT " Nm/mm width] ";:INPUT D$
     IF D$<>"" THEN MXX=VAL(D$)*1E3
     DUM$=""
     LOCATE 8,1:PRINT "Myy [";:PRINT USING "+#####.####";MYY/1E3;
     PRINT " Nm/mm width] ";:INPUT D$
     IF D$<>"" THEN MYY=VAL(D$)*1E3
     DUM$=""
     LOCATE 9,1:PRINT "Mxy [";:PRINT USING "+#####.####";MXY/1E3;
     PRINT " Nm/mm width] ";:INPUT D$
     IF D$<>"" THEN MXY=VAL(D$)*1E3
     DUM$=""
     LOCATE 11,1:PRINT "Qxx [";:PRINT USING "+#####.####";QXX/1E3;
     PRINT " N/mm width] ";:INPUT D$
     IF D$<>"" THEN QXX=VAL(D$)*1E3
     DUM$=""
     LOCATE 12,1:PRINT "Qyy [";:PRINT USING "+#####.####";QYY/1E3;
     PRINT " N/mm width] ";:INPUT D$
     IF D$<>"" THEN QYY=VAL(D$)*1E3
   RETURN


'*********************************************
'**** routine to SAVE existing laminate data
'*********************************************
250 CLS:LOCATE 1,1:PRINT "Type name of materials file to be saved
(excl extension) [";LAMDATA$;"]:- ";
    INPUT NA$
   IF NA$<>"" THEN LAMDATA$=NA$+".CLT"
  CLOSE:OPEN LAMDATA$ FOR OUTPUT AS #1

 PRINT#1,LAMDESC$
```

```
 PRINT#1,NOM

 FOR I = 1 TO NOM
  PRINT#1,I;MDESC$(I);' *** material description
  PRINT#1,USING "##.###^^^^ ";E1(I);E2(I);
  PRINT#1,USING "#.### ";V12T(I);V12C(I);
  PRINT#1,USING "##.###^^^^ ";G12(I);G13(I);G23(I)
  PRINT#1,USING "##.###^^^^
";FXT(I);FYT(I);FXC(I);FYC(I);FSXY(I);FSXZ(I);FSYZ(I)
 NEXT I

PRINT#1,NOL:'*** number of layers
 FOR I=1 TO NOL
  PRINT#1,I;MNO(I);ANG(I);PLTM(I)
 NEXT I

PRINT#1,USING "+##.###^^^^ ";NXX;NYY;NXY;MXX;MYY;MXY;QXX;QYY:'***
stress and moment resultants

CLOSE
RETURN

'*************************************************
300 ' cls:PRINT "** calculate average thicknesses **"
'*************************************************
cls
INPUT "Do you want a display of the intermediate results (N/Y)
[N]";DUMDIS$
 IF DUMDIS$="y" THEN DUMDIS$="Y"
 FLAGFILE$=""

IF LAMDATA$="" OR NOL=0 THEN 11
TLT=0
 FOR I=1 TO NOL
  TLT=PLTM(I)+TLT
 NEXT I
PLT=TLT/NOL
'*********************************************************************
'CLS:PRINT "** CALCULATE Q MATRIX **"
'*********************************************************************

PI=3.1415592654
FOR I=1 TO NOL
 ANGR(I)=ANG(I)/180*PI
NEXT I
'*** convert angles to radians

FOR I=1 TO NOL
 V12(MNO(I))=(V12T(MNO(I))+V12C(MNO(I)))/2
 V21=V12(MNO(I))*E2(MNO(I))/E1(MNO(I))
```

```
 Q(1,1,I)=E1(MNO(I))/(1-V12(MNO(I))*V21)
 Q(1,2,I)=(V12(MNO(I))*E2(MNO(I)))/(1-V12(MNO(I))*V21)
 Q(2,2,I)=E2(MNO(I))/(1-V12(MNO(I))*V21)
 Q(3,3,I)=G12(MNO(I))
 Q(1,3,I)=0
 Q(2,1,I)=Q(1,2,I)
 Q(2,3,I)=0
 Q(3,1,I)=0
 Q(3,2,I)=0
NEXT I

IF DUMDIS$="Y"THEN
CLS:PRINT "** CALCULATE Q MATRIX **"
   FOR I=1 TO 3
     FOR J=1 TO 3
      PRINT USING "#.###^^^^ ";Q(I,J,1);
      IF ABS(Q(I,J,1)) > 1E20  THEN PRINT I;J:INPUT A$
     NEXT J
    PRINT
   NEXT I
  INPUT A$
 END IF

'*********************************************************************
'cls:PRINT "** CALCULATE QBAR MATRIX **"
'*********************************************************************
FOR J=1 TO NOL
 QS=SIN(ANGR(J))
 QC=COS(ANGR(J))
 QB(1,1,J)=Q(1,1,J)*QC^4+2*(Q(1,2,J)+2*Q(3,3,J))*QS^2*QC^2+Q(2,2,J)*QS
 QB(1,2,J)=(Q(1,1,J)+Q(2,2,J)-
4*Q(3,3,J))*QS^2*QC^2+Q(1,2,J)*(QS^4+QC^4)
 QB(2,2,J)=Q(1,1,J)*QS^4+2*(Q(1,2,J)+2*Q(3,3,J))*QS^2*QC^2+Q(2,2,J)*QC
 QB(1,3,J)=(Q(1,1,J)-Q(1,2,J)-2*Q(3,3,J))*QS*QC^3+(Q(1,2,J)-
Q(2,2,J)+2*Q(3,3,J))*QS^3*QC
 QB(2,3,J)=(Q(1,1,J)-Q(1,2,J)-2*Q(3,3,J))*QS^3*QC+(Q(1,2,J)-
Q(2,2,J)+2*Q(3,3,J))*QS*QC^3
 QB(3,3,J)=(Q(1,1,J)+Q(2,2,J)-2*Q(1,2,J)-
2*Q(3,3,J))*QS^2*QC^2+Q(3,3,J)*(QS^4+QC^4)
 QB(2,1,J)=QB(1,2,J)
 QB(3,1,J)=QB(1,3,J)
 QB(3,2,J)=QB(2,3,J)
NEXT J


IF DUMDIS$="Y"THEN
PRINT "** CALCULATE QBAR MATRIX **"
   FOR K=1 TO NOL
    PRINT "For Layer No.";K;" at ";ANG(K);" Degrees"
     FOR I=1 TO 3
```

```
      FOR J=1 TO 3
       PRINT USING "#.###^^^^^ ";QB(I,J,K);
      NEXT J
      PRINT
     NEXT I
    INPUT A$
   NEXT K
 END IF

'*********************************************************************
'REM THIS SUBROUTINE CALCULATES ZC(K)
'*********************************************************************

TOTALZ=0
IF CINT(NOL/2)-NOL/2=0.5 THEN
   END
    ELSE
     ZC(0)=-TLT/2
     COUNT=0

     FOR I=1 TO NOL/2
      COUNT=COUNT+PLTM(I)
      ZC(I)=-(TLT/2-COUNT)
     NEXT I
    COUNT=0

    FOR I=NOL/2+1 TO NOL
     COUNT=COUNT+PLTM(I)
     ZC(I)=COUNT
    NEXT I

   FOR I=1 TO NOL
    TOTALZ=TOTALZ+PLTM(I)
   NEXT I
CLS:PRINT LAMDATA$;":- ";LAMDESC$
PRINT "Total laminate thickness= ";TOTALZ*1000;" mm"
 END IF
'*********************************************************************
REM THIS SUBROUTINE CALCULATES AD(I,J)
'*********************************************************************
FOR I=0 TO 3
 FOR J= 0 TO 3
  AD(I,J)=0
 NEXT J
NEXT I
'*** reset values to zero

FOR I=1 TO 3
FOR J=1 TO 3
  AD(I,J)=0
```

```
  FOR L=1 TO NOL
   AD(I,J)=AD(I,J)+QB(I,J,L)*(ZC(L)-ZC(L-1))
  NEXT L
 NEXT J
NEXT I

FOR I=4 TO 6
 FOR J=4 TO 6
  AD(I,J)=0
  FOR L=1 TO NOL
   AD(I,J)=AD(I,J)+1/3*(QB(I-3,J-3,L))*(ZC(L)^3-ZC(L-1)^3)
  NEXT L
 NEXT J
NEXT I

FOR I=1 TO 3
 FOR J=4 TO 6
  FOR L=1 TO NOL
   AD(I,J)=AD(I,J)+1/2*(QB(I,J-3,L))*(ZC(L)^2-ZC(L-1)^2)
  NEXT L
 NEXT J
NEXT I

FOR I=4 TO 6
 FOR J=1 TO 3
  FOR L=1 TO NOL
   AD(I,J)=AD(I,J)+1/2*(QB(I-3,J,L))*(ZC(L)^2-ZC(L-1)^2)
  NEXT L
 NEXT J
NEXT I

       '*** eliminate small numbers
         FOR I=1 TO 6
          FOR J=1 TO 6
           IF ABS(AD(I,J))<1e-5 THEN LET AD(I,J)=0
          NEXT J
         NEXT I

           PRINT "[ A B ]  MATRIX
           PRINT "[ B D ]"
           PRINT
       FOR I=1 TO 6
         FOR J=1 TO 6
          PRINT USING "#.###^^^^ ";AD(I,J);
         NEXT J
        PRINT
       NEXT I

'*************************************************************************
' REM THIS SUBROUTINE CALCULATES ABD'S INVERSE-ABDI
```

```
'*************************************************************************
FOR I=1 TO 6
 FOR J=1 TO 6
  B(I,J)=0
 NEXT J
NEXT I
'*** reset values to zero

FOR I=1 TO 6
 FOR J=1 TO 6
  A(I,J)=AD(I,J)
 NEXT J
NEXT I

FOR I=1 TO 6
 B(I,I)=1
NEXT I

FOR J=1 TO 6
 FOR I=J TO 6
  IF A(I,J)<> 0 THEN 40130
 NEXT I
 PRINT "ERROR IN MATRIX":INPUT A$:GOTO 11

  40130 FOR H=1 TO 6
        T=A(J,H)
        A(J,H)=A(I,H)
        A(I,H)=T
        M=B(J,H)
        B(J,H)=B(I,H)
        B(I,H)=M
       NEXT H
       D=A(J,J)
        FOR H=1 TO 6
         A(J,H)=A(J,H)/D
         B(J,H)=B(J,H)/D
        NEXT H

        FOR H = 1 TO 6
         IF J=H THEN 40140
         D=A(H,J)
          FOR K=1 TO 6
           A(H,K)=A(H,K)-A(J,K)*D
           B(H,K)=B(H,K)-B(J,K)*D
          NEXT K
40140     NEXT H
NEXT J

'*************************************************************************
'Print out equivalent laminate properties Ex,Ey,Gxy,Vxy
```

```
'*****************************************************************
PRINT "Exx(GPa)         Eyy(GPa)          Gxy(GPa)         Vxy"

EXX=CSNG((AD(1,1)-AD(1,2)^2/AD(2,2))/(TLT)/10^9)
EYY=CSNG((AD(2,2)-AD(1,2)^2/AD(1,1))/(TLT)/10^9)
GXY=CSNG(AD(3,3)/(TLT)/10^9)
VXY=CSNG(AD(1,2)/AD(2,2))
PRINT USING " ####.##         ";EXX;EYY;GXY;
PRINT USING " ##.####         ";VXY

'*****************************************************************
'*** THIS SUBROUTINE PRINTS [ABD] inverse
'*****************************************************************
CLS
            PRINT "        -1"
            PRINT "[ A B ]   MATRIX
            PRINT "[ B D ]
            PRINT
        FOR I=1 TO 6
          FOR J=1 TO 6
           PRINT USING "#.###^^^^ ";B(I,J);
          NEXT J
         PRINT
        NEXT I
60100 IF INKEY$="" THEN 60100

'*****************************************************************
'*** STRESS RESULTANTS Nxx,Nyy,Nxy,Mxx,Myy,Mxy
'*****************************************************************
N(1)=NXX
N(2)=NYY
N(3)=NXY
N(4)=MXX
N(5)=MYY
N(6)=MXY
'*****************************************************************
'" THIS SUBROUTINE CALCULATES [To]=[ADI][N]"
'*****************************************************************
 FOR I=1 TO 6
  FOR J=1 TO 6
   EK(I)=0
  NEXT J
 NEXT I


 FOR I=1 TO 6
  FOR J=1 TO 6
   EK(I)=EK(I)+B(I,J)*N(J)
  NEXT J
 NEXT I
```

```
IF DUMDIS$="Y" THEN
 CLS: print  " *** calculate centreline strains [Eo]=[ADI][N]"
  FOR I=1 TO 6
   PRINT EK(I)
   NEXT I
  input a$
 END IF


'*****************************************************************

CLS:LOCATE 1,1:INPUT"Enter [R] to load resultants off ABAQUS output
file";RES$
IF RES$="R" OR RES$="r" THEN
      RESFLAG$="R"
         PRINT:PRINT "Type the stress resultant input filename.ext"
         INPUT IN$
         OPEN IN$ FOR INPUT AS #3
        PRINT:PRINT"Select type of output for resultant input "
        PRINT:PRINT"[E] for centreline strains and curvatures , [T] fo
Tsai-Wu"
901      INPUT OUTFLAG$
         IF OUTFLAG$="" THEN GOTO 11
'*****************************************************************
  IF  OUTFLAG$="E" OR OUTFLAG$="e" THEN
         ' ***  write a file of centreline strains and curvature for
resultants file
         PRINT :PRINT "Type  the calculated strain output filename.ext
         INPUT FUT$
         OPEN FUT$ FOR OUTPUT AS #4
         WHILE NOT EOF(3)
            FOR I=1 TO 6
             EK(I)=0
            NEXT I
            '    *** reset values to 0

             INPUT#3,REL,RX,RY,RZ,RARC,N(1),N(2)
             INPUT#3,N(3),QX,QY,N(4),N(5),N(6)
             ' *** input values from abaqus file

             FOR I=1 TO 6
              FOR J=1 TO 6
               EK(I)=EK(I)+B(I,J)*N(J)
              NEXT J
             NEXT I

             PRINT#4,USING "#### ";REL;
             PRINT#4,USING "###.### ";RX;RY;RZ;RARC;
             print#4,N(1);N(2);N(3);QX;QY;N(4);N(5);N(6);
```

```
            PRINT#4,USING "#.###^^^^^
";EK(1);EK(2);EK(3);EK(4);EK(5);EK(6)
         WEND
        GOTO 11
    END IF
'*****************************************************************
        IF OUTFLAG$="T" OR OUTFLAG$="t" THEN
         ' ***  write a file of tsai hill factor for chosen resultant
file
         PRINT :PRINT "Type the Tsai Hill output filename.ext"
         INPUT FUT$
        OPEN FUT$ FOR OUTPUT AS #4
        FS=1:PRINT:PRINT "Factor of safety for Tsai Hill [";FS;"]"
        INPUT dum
        IF DUM<>0 THEN FS=DUM

     TSHFLAG$="A":PRINT:INPUT "Choose All data or Failed only data
(A/F)";DUM$
     IF DUM$<>"" THEN TSHFLAG$=DUM$

   GOSUB 62740:' headings

          COUNT=0: ' *** counter of number of lines
      ' *** input values from abaqus file
         WHILE NOT EOF(3)
          INPUT#3,REL,RX,RY,RZ,RARC,N(1),N(2)
          INPUT#3,N(3),QX,QY,N(4),N(5),N(6)
        '    *** reset values to 0
           FOR I=1 TO 6
            EK(I)=0
           NEXT I
       ' *** local strain and stress values
           FOR I=1 TO 6
            FOR J=1 TO 6
             EK(I)=EK(I)+B(I,J)*N(J)
            NEXT J
           NEXT I
           GOSUB 61530
'*************************************************
        IF TSHFLAG$="F" OR TSHFLAG$="f" THEN
         ' *** routine to print failed values only
         FSMINLAM=10000:' fs min for entire laminate

' run through all layers and check for failure
         FOR J=1 TO NOL
           GOSUB 1010 : ' FAILURE CRITERIA
          IF FSMIN<FSMINLAM THEN FSMINLAM=FSMIN
'         PRINT "E ";REL;"LAYER ";J;"FSMIN ";FSMIN
         NEXT J
```

```
        IF FSMINLAM>=FS THEN 61040

' if failure then repeat process and print failed values
      PRINT#4,USING "#### ";REL;
      PRINT#4,USING " ###.###";RX;RY;RZ;
      PRINT#4," ";
        FOR J=1 TO NOL
           GOSUB 1010 : ' FAILURE CRITERIA
            IF FSMIN>=FS THEN PRINT#4,USING " #.#^^^^";ABS(FSMIN);
            IF FSMIN<FS THEN PRINT#4,USING " ###.## ";ABS(FSMIN);
         NEXT J
          PRINT#4,USING "###.##  ";FSMINLAM
          COUNT=COUNT+1
       '    IF COUNT=25 THEN GOSUB 62740:COUNT=0
       ' *** print header every 25 lines
   END IF

61040  WEND
     PRINT "COMPLETED WRITING FILES"
     CLOSE#3
     CLOSE#4
    GOTO 11
   END IF
  END IF

REM ************************************************************************
'   cls:print "SUBROUTINE CALCULATES [Ek]xy"
REM ************************************************************************
61530 FOR J=1 TO NOL
       FOR K=1 TO 3
        EXYK(K,J)=0
       NEXT K
      NEXT J

      ' assign 0 to avoid summation errors

      FOR J=1 TO 3
       E0(J)=EK(J)
      NEXT J

      FOR J=1 TO 3
       CK(J)=EK(J+3)
      NEXT J

     FOR J=1 TO NOL
      FOR K=1 TO 3
       EXYK(K,J)=E0(K)+ZC(J)*CK(K)
      NEXT K
     NEXT J
```

```
IF DUMDIS$="Y" THEN
 cls:print "PER LAYER STRAINS [Ek]xy"
     FOR J=1 TO NOL
      FOR K=1 TO 3
       PRINT EXYK(K,J);
      NEXT K
      print
     NEXT J
    input a$
   END IF

REM ************************************************
REM THIS SUBROUTINE CALCULATES SIGMAkxy AND SIGMAk12
REM ************************************************
FOR J=1 TO NOL
 FOR K=1 TO 3
   SXY(K,J)=0:S12(K,J)=0
 NEXT K
NEXT J

FOR J=1 TO NOL
 TS=SIN(ANGR(J))
 TC=COS(ANGR(J))
 TS(1,1,J)=TC^2
 TS(1,2,J)=TS^2
 TS(1,3,J)=2*TS*TC
 TS(2,1,J)=TS(1,2,J)
 TS(2,2,J)=TS(1,1,J)
 TS(2,3,J)=-TS(1,3,J)
 TS(3,1,J)=-TS*TC
 TS(3,2,J)=TS*TC
 TS(3,3,J)=TC^2-TS^2
NEXT J

IF RESFLAG$="R" AND OUTFLAG$="T" THEN
'** DO NOT PROVIDE SCREEN INFO FOR RESULTANT FILE
 FOR J=1 TO NOL
  FOR K=1 TO 3
   FOR L=1 TO 3
    SXY(K,J)=SXY(K,J)+QB(K,L,J)*EXYK(L,J)
   NEXT L
  NEXT K
 NEXT J

 FOR J=1 TO NOL
  FOR K=1 TO 3
   FOR L=1 TO 3
    S12(K,J)=S12(K,J)+TS(K,L,J)*SXY(L,J)
   NEXT L
  NEXT K
```

```
 NEXT J

 RETURN
END IF

CLS:PRINT "GLOBAL XY STRESSES (MPa)"
PRINT " NO    LAYER ANGLE     SX          SY          SXY"
FOR J=1 TO NOL
   IF INT(J/21)=J/21 THEN
   INPUT "                        Press Return to Continue";A$
  END IF


 PRINT USING "#### ";J;
 PRINT USING "+###.##    ";ANGR(J)/3.1415*180;
 FOR K=1 TO 3
  FOR L=1 TO 3
   SXY(K,J)=SXY(K,J)+QB(K,L,J)*EXYK(L,J)
  NEXT L
PRINT USING " +####.## ";SXY(K,J)/1E6;
 NEXT K
PRINT " "
NEXT J

PRINT:INPUT "PRESS RETURN TO CONTINUE";A$

PRINT:PRINT "LAYER lt STRESSES (MPa) "
PRINT " NO    LAYER ANGLE     Sl          St          Slt"

FOR J=1 TO NOL
   IF INT(J/21)=J/21 THEN
   INPUT "                        Press Return to Continue";A$
  END IF

 PRINT USING "#### ";J;
 PRINT USING "+###.##    ";ANGR(J)/3.1415*180;
 FOR K=1 TO 3
  FOR L=1 TO 3
   S12(K,J)=S12(K,J)+TS(K,L,J)*SXY(L,J)
  NEXT L
  PRINT USING " +####.## ";S12(K,J)/1E6;
 NEXT K
PRINT " "
NEXT J

PRINT:INPUT "PRESS RETURN TO CONTINUE";A$


' ************************************************************
' THIS SUBROUTINE INVOKES TSAI-HILL FAILURE CRITERION
```

```
' ************************************************************

FS=1:PRINT "Input required minimum factor of safety [FS= ";FS;"]"
INPUT dum
IF DUM<>0 THEN FS=DUM
CLS
PRINT:PRINT "STRENGTH/STRESS RATIO (CHOSEN FACTOR OF SAFTEY MIN=
";FS;")"
' PRINT "From Tsai, Composites design, Pg 11-5):PRINT

IF N(4)=0 AND N(5)=0 THEN
 A$="LAYER  ANGLE THICK    STATUS      TSAI-WU  HILL-HOFFMAN"
 B$="               (mm)                FS       FS"
 PRINT A$:PRINT B$
END IF

IF N(4)<>0 OR N(5)<>0 THEN
 A$="LAYER  ANGLE THICK    STATUS    TSAI-WU     HILL-HOFF   TWAI-WU
HILL-HOFF"
 B$="               (mm)              FS (+Z)     FS (+Z)     FS (-Z)     F
(-Z)
 PRINT A$:PRINT B$
END IF
FOR J=1 TO NOL

  IF INT(J/21)=J/21 THEN
   INPUT "                        Press Return to Continue";A$
  PRINT A$:PRINT B$
  END IF

' '** Modified Tsai-Hill using strength for correct stresses (T or C)
' IF S12(1,J)<=0  'HEN XTSI(J)=FXC(MNO(J))
'  ELSE: XTSI(J)= FXT(MNO(J))
' END IF
' IF S12(2,J)<=0 THEN YTSI(J)=FYC(MNO(J))
'  ELSE:YTSI(J)=FYT(MNO(J))
' END IF
'  PART1=S12(1,J)^2/XTSI(J)^2-S12(1,J)*S12(2,J)/XTSI(J)^2
'  PART2=S12(2,J)^2/YTSI(J)^2+S12(3,J)^2/FSXY(MNO(J))^2
'   ' PART1=S12(1,J)^2/FXT(MNO(J))^2-S12(1,J)*S12(2,J)/FXT(MNO(J))^2
'   ' PART2=S12(2,J)^2/FYT(MNO(J))^2+S12(3,J)^2/FSXY(MNO(J))^2
'  TSAIHILL=PART1+PART2
' FSTH=1/(TSH)^.5

' ********** Quadratic failure criteria ***** TSAI:Composites Design
pg 11-5
'** strength parameters
1010 'come here for per layer ABAQUS analysis
FSMIN=10000
F1=1/FXT(MNO(J))-1/FXC(MNO(J))
```

```
F2=1/FYT(MNO(J))-1/FYC(MNO(J))
F11=1/(FXT(MNO(J))*FXC(MNO(J)))
F22=1/(FYT(MNO(J))*FYC(MNO(J)))
F66=1/FSXZ(MNO(J))^2
' ** 3D TERMS TO BE INCORPARATED LATER
F3=0: '** 3D TERM: F3=1/FZT(MNO(J))-1/FZC(MNO(J))
F33=0:'** 3D TERM: F33=1/(FZT(MNO(J))*FZC(MNO(J)))
F44=0:'** 3D TERM: F44=1/FSYZ(MNO(J))^2
F55=0:'** 3D TERM: F55=1/FSXZ(MNO(J))^2
F23=0:'** 3D TERM: F23= FYZ*(F22*F33)^.5
F13=0:'** 3D TERM: F23= FXZ*(F11*F33)^.5

  '1- *  Tsai-Wu Quadratic failure criteria FXY*=-.5
  ' also known as the Generalised Von Mises Criteria
  ' INCORPORATE Fxy* INTO THE INPUT DATA AT A LATER STAGE"
    FXY=-.5
    FYZ=0:'** 3D TERM: FYZ=-.5
    FXZ=0:'** 3D TERM: FXZ=-.5
     F12= FXY*(F11*F22)^.5
     F23=0:'** 3D TERM: F23= FYZ*(F22*F33)^.5
     F13=0:'** 3D TERM: F23= FXZ*(F11*F33)^.5
      DUM1=F11*S12(1,J)^2 + F22*S12(2,J)^2 + F66*S12(3,J)^2
       '** 3D TERM: DUM1=DUM1+ F33*SZZ^2 + F44* SYZ^2+ F55* SXZ^2
      DUM2=F12*S12(1,J)*S12(2,J)
       '** 3D TERM: DUM2=DUM2+ F13*SXXSZZ + F23* SYY*SZZ
      DUM3=F1*S12(1,J)+F2*S12(2,J)
       '** 3D TERM: DUM3=DUM3+ F3*SZZ
      TSAIWU=DUM1+DUM2+DUM3

  ' ** CALCULATE STRENGTH TO STRESS RATIO ***
  ADUM=DUM1+DUM2:BDUM=DUM3
   FSTWPL=-(BDUM/2/ADUM)+((BDUM/2/ADUM)^2+1/ADUM)^.5
   IF FSTWPL<FSMIN THEN FSMIN=FSTWPL
   IF N(4)<>0 OR N(5)<>0 THEN
    FSTWMI=ABS(-(BDUM/2/ADUM)-((BDUM/2/ADUM)^2+1/ADUM)^.5)
   IF FSTWMI<FSMIN THEN FSMIN=FSTWMI
   END IF

'2- *********  Hill-Hoffman failure criteria FXY*=0
    F12=0:F23=0: F13=0
      ADUM=F11*S12(1,J)^2 + F22*S12(2,J)^2 + F66*S12(3,J)^2
      '** 3D TERM: DUM1=DUM1+ F33*SZZ^2 + F44* SYZ^2+ F55* SXZ^2
      BDUM=F1*S12(1,J)+F2*S12(2,J)
      '** 3D TERM: DUM3=DUM3+ F3*SZZ
      HILLHOF = ADUM+BDUM
 ' ** CALCULATE STRENGTH TO STRESS RATIO ***
   FSHHPL=-(BDUM/2/ADUM)+((BDUM/2/ADUM)^2+1/ADUM)^.5
   IF FSHHPL<FSMIN THEN FSMIN=FSHHPL
   IF N(4)<>0 OR N(5)<>0 THEN
    FSHHMI=ABS(-(BDUM/2/ADUM)-((BDUM/2/ADUM)^2+1/ADUM)^.5)
```

```
   IF FSHHMI<FSMIN THEN FSMIN=FSHHMI
   END IF
IF RESFLAG$="R" AND OUTFLAG$="T" THEN RETURN:' ** return to abaqus
number cruching"

    PRINT USING "##,# ";J;
    PRINT USING "+###.## ";ANGR(J)/3.1415*180;
    PRINT USING "###.###";PLTM(J)*1000;

   IF N(4)=0 AND N(5)=0 THEN
    IF FSTWPL>=FS AND FSHHPL>=FS THEN
     PRINT " SAFE      ";:PRINT USING " ###.##   ";FSTWPL;FSHHPL
    END IF
    IF FSTWPL<FS OR FSHHPL<FS  THEN
     PRINT " FAILED    ";:PRINT USING " ###.##   ";FSTWPL;FSHHPL
    END IF
END IF

   IF N(4)<>0 OR N(5)<>0 THEN
    STATUS$=" SAFE   "
    IF FSTWPL<FS OR FSHHPL<FS THEN  STATUS$=" FAILED "
    IF FSTWMI<FS OR FSHHMI<FS THEN  STATUS$=" FAILED "
   PRINT STATUS$;:PRINT USING "###.###
";FSTWPL;FSHHPL;FSTWMI;FSHHMI
   END IF
NEXT J

 PRINT:INPUT "                    Press any key to Continue";A$

GOTO 11


' ********************************************************************
' ***** write header consisting of layer number and orientation
' ********************************************************************
62740       PI=3.1415592654
              PRINT#4,"ELEM      X         Y         Z     ";
                   FOR LAYERNO=1 TO NOL
                     PRINT#4,USING "####     ";LAYERNO;
                    NEXT LAYERNO
                     PRINT#4,""
              PRINT#4,"                                      ";
                FOR LAYERNO =1 TO NOL
                 PRINT#4,USING "+###.#   ";ANGR(LAYERNO)*180/PI;
                NEXT LAYERNO
                 PRINT#4,""
                RETURN
```

APPENDIX I

LISTING OF THE RTBEGIN AND RTEND PREPROCESSING PROGRAM

```
5 ' *** RTBEGIN.BAS   27/5/1989
10 N=10000:  DIM NO(N),X(N),Y(N),Z(N)
20 ' DEFSNG A-H,O-Z
30 DIM ELSETRIB(13,16)
40 DIM NODE(8),XR(13),XFD(13)
50 DIM A(13),B(13)
60 KEY OFF:CLS
70 DIM XS(13):'*** x location of support
80 DIM NNSS(20):'*** node number support shell
90 DIM NNSR(20):'*** node number support rib
100 LOCATE 10,35:PRINT "MAGENABA"
110 LOCATE 12,20:PRINT "ABAQUS MESH GENERATION FOR ROAD TANKERS"
120 INPUT A$
130 PI=3.141592654#
140 DECPLACE=4
150 G=9.810001:'*** gravitational acceleration
160 XACC=2:' *** forward acceleration of tanker
170 YACC=-2:' *** sideways acceleration of tanker
180 ZACC=-2:' *** upwards acceleration of tanker
200 TWIST=6:TWIST=TWIST*PI/180:'*** twist of the tanker in radians
210 PP=8.4E5:' *** internal pressure in tanker
220 RI=.650:'***    inside radius
230 TS=.015:'***   thickness of shell
240 RO=RI+TS:' *** outside radius of the tanker
250 RS=RI+TS/2:' *** radius of centreline of the shell
260 CJ=PI/2*(RO^4-RI^4):'*** torsional constant of rigidity
270 DENLIQ=1850:' *** liquid or content density
280 DENSHELL=1900:' *** shell material density
290 DENRIBS=1900:'*** DENSITY OF THE RIBS
300 XSTART=0:'*** start of cylindrical section of tanker
320 XSTOP=12:'*** stop of cylindrical section of tanker
330 XLD=RS/2:'*** depth of left dish to shell centreline 2:1 ellip
    soidal
340 TLD=TS:'*** thickness of left dome
350 TRD=TS:'*** thickness of right dome
360 XRD=XLD:'*** depth of right dish
370 XC=XSTOP:'*** length of cylindrical part of the tanker
380 XT=XC+XLD+XRD+TS/2:'*** total length of the tanker
390 NRIBS=13:'*** number of ribs
400 XR(1)=0:XR(2)=1:XR(3)=2:XR(4)=3:XR(5)=4:XR(6)=5:XR(7)=6:XR(8)=7
:XR(9)=8
405 XR(10)=9:XR(11)=10:XR(12)=11:XR(13)=12:' rib x positions
410 A1=.05:A2=.05:A1$=STR$(A1):A2$=STR$(A2):'*** width of ribs
420 B1=.05:B2=.1:B1$=STR$(B1):B2$=STR$(B2):' *** depth of ribs
430 A(1)=A2:A(2)=A2:A(3)=A2:A(4)=A2:A(5)=A1:A(6)=A1:A(7)=A1
440 A(8)=A1:A(9)=A1:A(10)=A2:A(11)=A2:A(12)=A2:A(13)=A2:' *** width
 per rib
450 B(1)=B2:B(2)=B2:B(3)=B2:B(4)=B2:B(5)=B1:B(6)=B1:B(7)=B1:B(8)=B1
460 B(9)=B1:B(10)=B2:B(11)=B2:B(12)=B2:B(13)=B2:'*** depth per rib
470 MPLTHIN=DENRIBS*A1*B1:'*** mass per unit length of thin rib
```

```
480 MPLTHICK=DENRIBS*A2*B2:'*** mass per unit lenght of thick rib
490 NTOL=.05: ' *** tolerance on node distances for *MPC
500 DTOL=.01: ' *** tolerance on node distance for shell dome MPC
510 NODOCON=6:XFD(1)=.02:XFD(2)=.05:XFD(3)=.10:XFD(4)=.19:XFD(5)=.28
    :XFD(6)=.36
520 NOSUP=12:XS(1)=0:XS(2)=1:XS(3)=2:XS(4)=3::XS(10)=9:XS(11)=10
    :XS(12)=11:XS(13)=0:'*** support locations
530 FOR I=5 TO 9:XS(I)=0:NEXT I:'*** locations of no supports
    equel zero
540 ANGSU=60:ANGSU=ANGSU/180*PI:'** angle of the support
550 ' *** number of dome contours:dome contour x fractions
560'************************************************************
570 CLS:LOCATE  1,1:INPUT "Name of ABAQUS file ";NAMEFILE$
580 OPEN  NAMEFILE$ FOR OUTPUT AS #1
590 OPEN "DUMMYC" FOR OUTPUT AS #2
600 OPEN "DUMMYR" FOR OUTPUT AS #3
605 OPEN "NODES" FOR OUTPUT AS #4
610 GOSUB 930:' *** intro section
620 GOSUB 1030:' *** calculate cylinder nodes
630 GOSUB 3470:' *** write cylinder nodes
640 GOSUB 1470:' *** calculate rib nodes
650 GOSUB 3590:' *** write ribs nodes
660 GOSUB 1810:' *** calculate left dome triangular nodes
670 GOSUB 2130:' *** calculate left dome quadratic nodes
680 GOSUB 2630:' *** calculate right dome triangular nodes
690 GOSUB 2970:' *** calculate right dome quadratic nodes
700 GOSUB 3890:' *** write left dome triangular nodes
710 GOSUB 4000:' *** write left dome quadratic nodes
720 GOSUB 4110:' *** write right dome triangular nodes
730 GOSUB 4220:' *** write right dom- quadratic nodes
740 GOSUB 4340:' *** write cylinder elements
750 GOSUB 4510:' *** write rib elements
760 GOSUB 5080:' *** write triangular elements for left dome
770 GOSUB 4900:' *** write quadratic elements for left dome
780 GOSUB 5440:' *** write triangular elements for right dome
790 GOSUB 5260:' *** write quadratic elements for right dome
830 GOSUB 6050:' *** MPC connect left dome to shell
840 GOSUB 6240:' *** MPC connect triangular to left dome
850 GOSUB 6590:' *** MPC connect right dome to shell
860 GOSUB 6410:' *** MPC connect triangular to right dome
865 GOSUB 5620:' *** MPC connect shell to ribs
867 GOSUB 4720:' *** write element sets for individual ribs
869 GOSUB 10580:' *** Nsets for cradle supports
870 GOSUB 11160:' *** twisting boundary conditions
880 CLOSE
900 PRINT "          EXECUTION COMPLETE    ":CLOSE:STOP:END
910'************************************************************
920 '
930 PRINT "Writing introduction section"
940 '
```

```
950 PRINT#1,"*HEADING,CORE=320000"
960 'HEADING$=" RT14ALL"+" AX= "+STR$(XACC)+" AY= "+STR$(YACC)+" AZ=
"+STR$(ZACC)+" PINT= "+STR$(PP)+" TWIST= "+LEFT$(STR$(TWIST),5)
965 HEADING$="RT25ALL 30 DEG,.33M,OVERHANG,ID=1.3m,L=12"
970 PRINT#1,HEADING$
980 PRINT#1,"*DATA CHECK"
990 PRINT#1,"*PREPRINT,ECHO=NO,HISTORY=NO,MODEL=NO"
1000 RETURN
1010'************************************************************
1020 '
1030 PRINT "Calculating cylinder nodes"
1040 '
1050 STARTANGD=0:ENDANGD=360:INPUT "Element angle= ";ELANGD
1060 NEPR=ENDANGD/ELANGD:' *** number of elements per ring
1070 R=RS
1080 ESCYL=1:'*** element start cylinder
1090 ELANG=ELANGD*PI/180
1100  NO=0:NONODE=0
1110 INPUT "X step between elements= ";XSTEP
1120 FOR XLEFT =XSTART TO XSTOP-XSTEP STEP XSTEP
1130  XRIGHT=XLEFT+XSTEP
1140   FOR BOTANGD=STARTANGD TO ENDANGD-ELANGD STEP ELANGD
1150     BOTANG=BOTANGD*PI/180
1160     TOPANG =BOTANG+ELANG
1170   FOR POINTNO =NO+1 TO NO+8:NO(POINTNO)=POINTNO:NEXT POINTNO
1180    X(NO+1)=XLEFT:Z(NO+1)=R *SIN(TOPANG):Y(NO+1)=-R *COS(TOPANG)
1190    X(NO+2)=XLEFT:Z(NO+2)=R *SIN(BOTANG):Y(NO+2)=-R *COS(BOTANG)
1200    X(NO+3)=XRIGHT:Z(NO+3)=R *SIN(BOTANG):Y(NO+3)=-R *COS(BOTANG)
1210    X(NO+4)=XRIGHT:Z(NO+4)=R *SIN(TOPANG):Y(NO+4)=-R*COS(TOPANG)
1220    X(NO+5)=XLEFT:Z(NO+5)=R *SIN((TOPANG+BOTANG)/2)
        :Y(NO+5)=-R*COS((TOPANG+BOTANG)/2)
1230      X(NO+6)=(XLEFT+XRIGHT)/2:Z(NO+6)=R *SIN(BOTANG)
          :Y(NO+6)=-R*COS(BOTANG)
1240      X(NO+7)=XRIGHT:Z(NO+7)=R *SIN((BOTANG+TOPANG)/2)
          :Y(NO+7)=-R*COS((BOTANG+TOPANG)/2)
1250      X(NO+8)=(XLEFT+XRIGHT)/2:Z(NO+8)=R *SIN(TOPANG)
          :Y(NO+8)=-R*COS(TOPANG)
1260 ' *** routine to eliminate small numbers
1270        FOR I= 1 TO 8
1280         IF ABS(X(NO+I))<.00001 THEN LET X(NO+I)=0
1290         IF ABS(Y(NO+I))<.00001 THEN LET Y(NO+I)=0
1300         IF ABS(Z(NO+I))<.00001 THEN LET Z(NO+I)=0
1310 '*** truncate numbers according to decplace
1320             TRUNC=X(NO+I):GOSUB 10430:X(NO+I)=TRUNC
1330             TRUNC=Y(NO+I):GOSUB 10430:Y(NO+I)=TRUNC
1340             TRUNC=Z(NO+I):GOSUB 10430:Z(NO+I)=TRUNC
1350        NEXT I
1360    NONODE=NONODE+8
1370    NO=NO+ 8
1380   NEXT BOTANGD
```

```
1390 NEXT XLEFT
1400 'define cylinder start and end nodes  : NSCYL and NECYL
1410 NSCYL=1:NECYL=NONODE
1420 STNODE=NSCYL:ENNODE=NECYL :'*** parameters for eliminate routine
1430 GOSUB 10270:' *** routine to eliminate duplicate numbers
1440 RETURN
1450'*************************************************************
1460 '
1470 PRINT "Calculating rib nodes"
1480 '
1490 STARTANGD=0:ENDANGD=360
1500 NO=NECYL
1510 NSRIBS=NECYL+1:' *** node start number for ribs
1520 FOR I=1 TO NRIBS
1530 R=RI+TS+B(I)/2:'*** centroidal radius of rib
1540   FOR BOTANGD=STARTANGD TO ENDANGD-ELANGD STEP ELANGD
1550     BOTANG=BOTANGD*PI/180
1560     TOPANG =BOTANG+ELANG
1570   FOR POINTNO =NO+1 TO NO+3:NO(POINTNO)=POINTNO:NEXT POINTNO
1580    X(NO+1)=XR(I):Z(NO+1)=R *SIN(TOPANG):Y(NO+1)=-R *COS(TOPANG)
1590    X(NO+3)=XR(I):Z(NO+3)=R *SIN(BOTANG):Y(NO+3)=-R *COS(BOTANG)
1600    X(NO+2)=XR(I):Z(NO+2)=R *SIN((TOPANG+BOTANG)/2)
          :Y(NO+2)=-R*COS((TOPANG+BOTANG)/2)
1610 ' *** routine to eliminate small numbers
1620        FOR J= 1 TO 3
1630         IF ABS(X(NO+J))<.00001 THEN LET X(NO+J)=0
1640         IF ABS(Y(NO+J))<.00001 THEN LET Y(NO+J)=0
1650         IF ABS(Z(NO+J))<.00001 THEN LET Z(NO+J)=0
1660 '*** truncate numbers according to decplace
1670            TRUNC=X(NO+J):GOSUB 10430:X(NO+J)=TRUNC
1680            TRUNC=Y(NO+J):GOSUB 10430:Y(NO+J)=TRUNC
1690            TRUNC=Z(NO+J):GOSUB 10430:Z(NO+J)=TRUNC
1700        NEXT J
1710    NONODE=NONODE+3
1720    NO=NO+3
1730   NEXT BOTANGD
1740 NEXT I
1750 NERIBS=NONODE
1760 STNODE=NSRIBS:ENNODE=NERIBS
1770 GOSUB 10270:' *** routine to eliminate duplicate numbers
1780 RETURN
1790 '*************************************************************
1800 '
1810 PRINT "Calculating LHS dome triangular nodes"
1820 '
1830 NSLDTRI=NERIBS+1:'*** node start left dome
1840 NO=NERIBS:STARTANGD=0
1850   FOR BOTANGD=STARTANGD TO ENDANGD-ELANGD STEP ELANGD
1860     BOTANG=BOTANGD*PI/180
1870     TOPANG =BOTANG+ELANG
```

```
1880     MIDANG=(BOTANG+TOPANG)/2
1890 N=NO+1:NO(N)=N
1900 X(N)=-XLD:Y(N)=0:Z(N)=0
1910  XR=-XLD+XLD*XFD(1)
1920 X=XR:GOSUB 10550:RR=R:' *** routine containing equation of dome
1930  N=NO+2:NO(N)=N:X(N)=XR:Y(N)=RR*COS(MIDANG):Z(N)=RR*SIN(MIDANG)
1940  N=NO+3:NO(N)=N:X(N)=XR:Y(N)=RR*COS(BOTANG):Z(N)=RR*SIN(BOTANG)
1950  N=NO+4:NO(N)=N:X(N)=XR:Y(N)=RR*COS(TOPANG):Z(N)=RR*SIN(TOPANG)
1960 ' *** routine to eliminate small numbers
1970        FOR I= 1 TO 4
1980         IF ABS(X(NO+I))<.00001 THEN LET X(NO+I)=0
1990         IF ABS(Y(NO+I))<.00001 THEN LET Y(NO+I)=0
2000         IF ABS(Z(NO+I))<.00001 THEN LET Z(NO+I)=0
2010 '*** truncate numbers according to decplace
2020            TRUNC=X(NO+I):GOSUB 10430:X(NO+I)=TRUNC
2030            TRUNC=Y(NO+I):GOSUB 10430:Y(NO+I)=TRUNC
2040            TRUNC=Z(NO+I):GOSUB 10430:Z(NO+I)=TRUNC
2050        NEXT I
2060   NO=NO+4:NONODE=NONODE+4
2070  NEXT BOTANGD
2080  NELDTRI=NONODE
2090 STNODE=NSLDTRI:ENNODE=NELDTRI :'*** parameters for eliminate
routine
2100 GOSUB 10270:' *** routine to eliminate duplicate numbers
2110 RETURN
2120'************************************************************
2130 PRINT "Calculate LHS dome quadratic nodes"
2140 NsLDQUA=NELDTRI+1:'*** node start left dome
2150 NO=NSLDQUA-1:STARTANGD=0
2160   FOR BOTANGD=STARTANGD TO ENDANGD-ELANGD STEP ELANGD
2170     BOTANG=BOTANGD*PI/180
2180     TOPANG =BOTANG+ELANG
2190     MIDANG=(BOTANG+TOPANG)/2
2200   FOR  K=1 TO NODOCON-1
2210     XL=-XLD
2220      FOR L =1 TO K
2230       XL=XL+XLD*XFD(L):' *** find left x for element
2240      NEXT L
2250         XR=-XLD
2260          FOR  L=1 TO K+1
2270           XR=XR-XLD*XFD(L):' *** right x for element
2280          NEXT L
2290        XM=(XL+XR)/2:' *** middle x for element
2300 X=XL:GOSUB 10550:RL=R
2310 X=XR:GOSUB 10550:RR=R
2320 X=XM:GOSUB 10550:RM=R
2330 ' *** assign node numbers
2340 FOR P=NO+1 TO NO+8:NO(P)=P:NEXT P
2350 N=NO
2360 X(N+1)=XL:Z(N+1)=RL*SIN(TOPANG):Y(N+1)=RL*COS(TOPANG)
```

```
2370 X(N+2)=XL:Z(N+2)=RL*SIN(BOTANG):Y(N+2)=RL*COS(BOTANG)
2380 X(N+3)=XR:Z(N+3)=RR*SIN(BOTANG):Y(N+3)=RR*COS(BOTANG)
2390 X(N+4)=XR:Z(N+4)=RR*SIN(TOPANG):Y(N+4)=RR*COS(TOPANG)
2400 X(N+5)=XL:Z(N+5)=RL*SIN(MIDANG):Y(N+5)=RL*COS(MIDANG)
2410 X(N+6)=XM:Z(N+6)=RM*SIN(BOTANG):Y(N+6)=RM*COS(BOTANG)
2420 X(N+7)=XR:Z(N+7)=RR*SIN(MIDANG):Y(N+7)=RR*COS(MIDANG)
2430 X(N+8)=XM:Z(N+8)=RM*SIN(TOPANG):Y(N+8)=RM*COS(TOPANG)
2440 ' *** routine to eliminate small numbers
2450       FOR I= 1 TO 8:' *** to include triangular elements
2460        IF ABS(X(N+I))<.00001 THEN LET X(N+I)=0
2470        IF ABS(Y(N+I))<.00001 THEN LET Y(N+I)=0
2480        IF ABS(Z(N+I))<.00001 THEN LET Z(N+I)=0
2490 '*** truncate numbers according to decplace
2500           TRUNC=X(N+I):GOSUB 10430:X(N+I)=TRUNC
2510           TRUNC=Y(N+I):GOSUB 10430:Y(N+I)=TRUNC
2520           TRUNC=Z(N+I):GOSUB 10430:Z(N+I)=TRUNC
2530       NEXT I
2540  NO=NO+8:NONODE=NONODE+8
2550  NEXT K
2560  NEXT BOTANGD
2570  NELDQUA=NONODE
2580 STNODE=NSLDQUA:ENNODE=NELDQUA:'*** parameters for eliminate
routine
2590 GOSUB 10270:' *** routine to eliminate duplicate numbers
2600 RETURN
2610 '*************************************************************
2620 '
2630 PRINT "Calculating RHS dome triangular nodes"
2640 '
2650 NSRDTRI=NELDQUA+1:'*** node start left dome
2660 NO=NELDQUA:STARTANGD=0
2670   FOR BOTANGD=STARTANGD TO ENDANGD-ELANGD STEP ELANGD
2680     BOTANG=BOTANGD*PI/180
2690     TOPANG =BOTANG+ELANG
2700     MIDANG=(BOTANG+TOPANG)/2
2710 '*** generate triangular element
2720 N=NO+1:NO(N)=N
2730 X(N)=XRD+XSTOP:Y(N)=0:Z(N)=0
2740  XR=XSTOP+XRD-XRD*XFD(1)
2750  X=-XSTOP+XR
2760  GOSUB 10550:RR=R:' *** routine containing equation of dome
2770  N=NO+2:NO(N)=N:X(N)=XR:Y(N)=RR*COS(MIDANG):Z(N)=RR*SIN(MIDANG)
2780  N=NO+3:NO(N)=N:X(N)=XR:Y(N)=RR*COS(BOTANG):Z(N)=RR*SIN(BOTANG)
2790  N=NO+4:NO(N)=N:X(N)=XR:Y(N)=RR*COS(TOPANG):Z(N)=RR*SIN(TOPANG)
2800 ' *** routine to eliminate small numbers
2810       FOR I= 1 TO 4
2820        IF ABS(X(NO+I))<.00001 THEN LET X(NO+I)=0
2830        IF ABS(Y(NO+I))<.00001 THEN LET Y(NO+I)=0
2840        IF ABS(Z(NO+I))<.00001 THEN LET Z(NO+I)=0
2850 '*** truncate numbers according to decplace
```

```
2860              TRUNC=X(NO+I):GOSUB 10430:X(NO+I)=TRUNC
2870              TRUNC=Y(NO+I):GOSUB 10430:Y(NO+I)=TRUNC
2880              TRUNC=Z(NO+I):GOSUB 10430:Z(NO+I)=TRUNC
2890          NEXT I
2900 NO=NO+4:NONODE=NONODE+4
2910  NEXT BOTANGD
2920  NERDTRI=NONODE
2930 STNODE=NSRDTRI:ENNODE=NERDTRI :'*** parameters for eliminate
routine
2940 GOSUB 10270:' *** routine to eliminate duplicate numbers
2950 RETURN
2960'************************************************************
2970 PRINT "Calculate RHS dome quadratic nodes"
2980 NSRDQUA=NERDTRI+1:'*** node start left dome
2990 NO=NERDTRI:STARTANGD=0
3000   FOR BOTANGD=STARTANGD TO ENDANGD-ELANGD STEP ELANGD
3010     BOTANG=BOTANGD*PI/180
3020     TOPANG =BOTANG+ELANG
3030     MIDANG=(BOTANG+TOPANG)/2
3040   FOR  K=1 TO NODOCON-1
3050     XL=XRD+XSTOP
3060      FOR L =1 TO K
3070       XL=XL-XRD*XFD(L):' *** find left x for element
3080      NEXT L
3090         XR=XRD+XSTOP
3100          FOR  L=1 TO K+1
3110           XR=XR-XRD*XFD(L):' *** right x for element
3120          NEXT L
3130 XM=(XL+XR)/2:' *** middle x for element
3140 DCX=1:DCY=COS(THETA):DCZ=COS(PI-THETA)
3150 X=-XSTOP+XL:GOSUB 10550:RL=R
3160 X=-XSTOP+XR:GOSUB 10550:RR=R
3170 X=-XSTOP+XM:GOSUB 10550:RM=R
3180 ' *** assign node numbers
3190 FOR P=NO+1 TO NO+8:NO(P)=P:NEXT P
3200 N=NO
3210 X(N+1)=XL:Z(N+1)=RL*SIN(TOPANG):Y(N+1)=RL*COS(TOPANG)
3220 X(N+2)=XL:Z(N+2)=RL*SIN(BOTANG):Y(N+2)=RL*COS(BOTANG)
3230 X(N+3)=XR:Z(N+3)=RR*SIN(BOTANG):Y(N+3)=RR*COS(BOTANG)
3240 X(N+4)=XR:Z(N+4)=RR*SIN(TOPANG):Y(N+4)=RR*COS(TOPANG)
3250 X(N+5)=XL:Z(N+5)=RL*SIN(MIDANG):Y(N+5)=RL*COS(MIDANG)
3260 X(N+6)=XM:Z(N+6)=RM*SIN(BOTANG):Y(N+6)=RM*COS(BOTANG)
3270 X(N+7)=XR:Z(N+7)=RR*SIN(MIDANG):Y(N+7)=RR*COS(MIDANG)
3280 X(N+8)=XM:Z(N+8)=RM*SIN(TOPANG):Y(N+8)=RM*COS(TOPANG)
3290 ' *** routir  to eliminate small numbers
3300         FOR I= 1 TO 8:' *** to include triangular elements
3310          IF ABS(X(N+I))<.00001 THEN LET X(N+I)=0
3320          IF ABS(Y(N+I))<.00001 THEN LET Y(N+I)=0
3330          IF ABS(Z(N+I))<.00001 THEN LET Z(N+I)=0
3340 '*** truncate numbers according to decplace
```

```
3350              TRUNC=X(N+I):GOSUB 10430:X(N+I)=TRUNC
3360              TRUNC=Y(N+I):GOSUB 10430:Y(N+I)=TRUNC
3370              TRUNC=Z(N+I):GOSUB 10430:Z(N+I)=TRUNC
3380           NEXT I
3390  NO=NO+8:NONODE=NONODE+8
3400  NEXT K
3410  NEXT BOTANGD
3420  NERDQUA=NONODE
3430 STNODE=NSRDQUA:ENNODE=NERDQUA :'*** parameters for eliminate
3440 GOSUB 10270:' *** routine to eliminate duplicate numbers
3450 RETURN
3460'************************************************************
3470 PRINT "Writing cylinder nodes"
3480 PRINT#1,"*NODE,NSET=NCYL"
3490    FOR I=NSCYL TO NECYL
3500      IF I<>NO(I) THEN GOTO 3550
3510      PRINT#1,NO(I);",";
3520      PRINT#1,USING"#####.####";X(I);:PRINT#1,",";
3530      PRINT#1,USING"#####.####";Y(I);:PRINT#1,",";
3540      PRINT#1,USING"#####.####";Z(I);:PRINT#1,""

          PRINT#4,NO(I);",";
          PRINT#4,USING"#####.####";X(I);:PRINT#4,",";
          PRINT#4,USING"#####.####";Y(I);:PRINT#4,",";
          PRINT#4,USING"#####.####";Z(I);:PRINT#4,""


3550    NEXT I
3560 RETURN
3570'************************************************************
3580 '
3590 PRINT "Writing ribs nodes"
3600 '
3610 RIBNODS=0
3620 PRINT#1,"*NODE,NSET=NRIBS"
3630    FOR I=NSRIBS TO NERIBS
3640      IF I<>NO(I) THEN GOTO 3860
3650         YS=Y(I):ZS=Z(I)
3660         IF YS=0 AND ZS=0 THEN THETY=0:THETZ=0:GOTO 3750
3670         IF ZS=0 AND YS>=0 THEN THETZ=PI/2:THETY=0:GOTO 3750
3680       IF ZS=0 AND YS<=0 THEN THETZ=-PI/2:THETY=PI:GOTO 3750
3690         IF YS=0 AND ZS>0 THEN THETY=PI/2:THETZ=0:GOTO 3750
3700         IF YS=0 AND ZS<0 THEN THETY=-PI/2:THETZ=PI:GOTO 3750
3710     IF YS>0 AND ZS>0 THEN THETY=ATN(ZS/YS):THETZ=ATN(YS/ZS)
3720         IF YS<0 AND ZS>=0 THEN THETY=ATN(ZS/YS)-PI
             :THETZ=ATN(YS/ZS)-PI
3730         IF YS<0 AND ZS<=0 THEN THETY=ATN(ZS/YS)-PI
             :THETZ=ATN(YS/ZS)-PI
3740         IF YS>0 AND ZS<=0 THEN THETY=ATN(ZS/YS)
             :THETZ=ATN(YS/ZS)
```

```
3750    DCX=0:DCY=COS(THETY):DCZ=COS(THETZ)
        :'***direction cosines of normal
3760     IF ABS(DCY)<.00001 THEN DCY=0
3770     IF ABS(DCZ)<.00001 THEN DCZ=0
3780       PRINT#1,NO(I);",";
3790       PRINT#1,USING"#####.####";X(I);:PRINT#1,",";
3800       PRINT#1,USING"#####.####";Y(I);:PRINT#1,",";
3810       PRINT#1,USING"#####.####";Z(I);:PRINT#1,",";
3811       PRINT#4,NO(I);",";
3812       PRINT#4,USING"#####.####";X(I);:PRINT#4,",";
3814       PRINT#4,USING"#####.####";Y(I);:PRINT#4,",";
3816       PRINT#4,USING"#####.####";Z(I);:PRINT#4,",";
3820       PRINT#1,USING"#####.####";DCX; :PRINT#1,",";
3830       PRINT#1,USING"#####.####";DCY; :PRINT#1,",";
3840       PRINT#1,USING"#####.####";DCZ; :PRINT#1,""
3850       RIBNODS=RIBNODS+1
3860     NEXT I
3870   RETURN
3880'*************************************************************
3890 PRINT "Writing LHS dome triangular nodes"
3900 PRINT#1,"*NODE,NSET=NLDTRI"
3910     FOR I=NSLDTRI TO NELDTRI
3920       IF I<>NO(I) THEN GOTO 3970
3930       PRINT#1,NO(I);",";
3940       PRINT#1,USING"#####.####";X(I);:PRINT#1,",";
3950       PRINT#1,USING"#####.####";Y(I);:PRINT#1,",";
3960       PRINT#1,USING"#####.####";Z(I);:PRINT#1,""

           PRINT#4,NO(I);",";
           PRINT#4,USING"#####.####";X(I);:PRINT#4,",";
           PRINT#4,USING"#####.####";Y(I);:PRINT#4,",";
           PRINT#4,USING"#####.####";Z(I);:PRINT#4,""


3970     NEXT I
3980 RETURN
3990'*************************************************************
4000 PRINT "Writing LHS dome quadratic nodes"
4010 PRINT#1,"*NODE,NSET=NLDQUA"
4020     FOR I=NSLDQUA TO NELDQUA
4030       IF I<>NO(I) THEN GOTO 4080
4040       PRINT#1,NO(I);",";
4050       PRINT#1,USING"#####.####";X(I);:PRINT#1,",";
4060       PRINT#1,USING"#####.####";Y(I);:PRINT#1,",";
4070       PRINT#1,USING"#####.####";Z(I);:PRINT#1,""

           PRINT#4,NO(I);",";
           PRINT#4,USING"#####.####";X(I);:PRINT#4,",";
           PRINT#4,USING"#####.####";Y(I);:PRINT#4,",";
           PRINT#4,USING"#####.####";Z(I);:PRINT#4,""
```

```
4080     NEXT I
4090 RETURN
4100'*************************************************************
4110 PRINT "Writing RHS dome triangular nodes"
4120 PRINT#1,"*NODE,NSET=NRDTRI"
4130     FOR I=NSRDTRI TO NERDTRI
4140       IF I<>NO(I) THEN GOTO 4190
4150       PRINT#1,NO(I);",";
4160       PRINT#1,USING"#####.####";X(I);:PRINT#1,",";
4170       PRINT#1,USING"#####.####";Y(I);:PRINT#1,",";
4180       PRINT#1,USING"#####.####";Z(I);:PRINT#1,""

           PRINT#4,NO(I);",";
           PRINT#4,USING"#####.####";X(I);:PRINT#4,",";
           PRINT#4,USING"#####.####";Y(I);:PRINT#4,",";
           PRINT#4,USING"#####.####";Z(I);:PRINT#4,""


4190     NEXT I
4200 RETURN
4210'*************************************************************
4220 PRINT "Writing RHS dome quadratic nodes"
4230 PRINT#1,"*NODE,NSET=NRDQUA"
4240     FOR I=NSRDQUA TO NERDQUA
4250       IF I<>NO(I) THEN GOTO 4300
4260       PRINT#1,NO(I);",";
4270       PRINT#1,USING"#####.####";X(I);:PRINT#1,",";
4280       PRINT#1,USING"#####.####";Y(I);:PRINT#1,",";
4290       PRINT#1,USING"#####.####";Z(I);:PRINT#1,""

           PRINT#4,NO(I);",";
           PRINT#4,USING"#####.####";X(I);:PRINT#4,",";
           PRINT#4,USING"#####.####";Y(I);:PRINT#4,",";
           PRINT#4,USING"#####.####";Z(I);:PRINT#4,""


4300     NEXT I
4310 RETURN
4320'*************************************************************
4330 '
4340 PRINT "Writing cylinder elements"
4350 '
4360 PRINT#1,"*ELEMENT,TYPE=S8R,ELSET=ECYL"
4370 NO=NSCYL-1
4380    ECYL=(NECYL-NSCYL+1)/8:'*** number of elements
4390    ESCYL=1:' *** element start cylinder
4400     FOR I=1 TO ECYL
4410        WRITE#1,I,NO(NO+1),NO(NO+2),NO(NO+3),NO(NO+4),NO(NO+5)
```

```
        ,NO(NO+6),NO(NO+7),NO(NO+8)
4420        WRITE#2,I,NO(NO+1);NO(NO+2);NO(NO+3);NO(NO+4);NO(NO+5)
        ;NO(NO+6);NO(NO+7);NO(NO+8)
4430 ' DUMMY FILE TO STORE ELEMENTS FOR LATER CENTRIOD CALCULATION
4440        NO=NO+8
4450      NEXT I
4460     EECYL=I-1:'*** element end cylinder
4470    CLOSE #2
4480 RETURN
4490'************************************************************
4500 '
4510 PRINT "Writing rib elements"
4520 '
4530 PRINT#1,"*ELEMENT,TYPE=B32,ELSET=RIBS"
4540 RC=1:'  *** rib counter
4550 RDUM=0:J=0:' *** variables for ELSET
4560 ESRIBS=EECYL+1
4570 NO=NSRIBS-1
4580 ERIBS=(NERIBS-NSRIBS+1)/3 :' *** number of rib beam elements'
4590     FOR I=ECYL+1 TO ERIBS+ECYL:' *** node numbers sequential to
        cylinder
4600        WRITE#1,I,NO(NO+1),NO(NO+2),NO(NO+3)
4610        WRITE#3,I,NO(NO+1),NO(NO+2),NO(NO+3)
4620           RDUM=RDUM+1:J=J+1
4630            ELSETRIB(RC,J)=I:' *** load element into ELSET
4640           IF RDUM=NEPR*RC THEN LET RC=RC+1:J=0:' *** check if
               element in ring RC
4650        NO=NO+3
4660      EERIBS=I:' *** element end ribs number
4670     NEXT I
4680   CLOSE #3
4690 RETURN
4700'************************************************************
4710 '
4720 PRINT "Writing element set for ribs"
4730 '
4740 ERIBS=0:ESRT$="":' ***number of rib elements
4750 FOR I = 1 TO NRIBS
4760 B$=STR$(I)
4770 A$="*ELSET,ELSET=RIB"+RIGHT$(B$,LEN(B$)-1)
4780  PRINT#1,A$
4790   FOR J=1 TO NEPR
4800        RS$=STR$(ELSETRIB(I,J)):LRS=LEN(RS$):'*** method to
           elimiate spaces
4810          ESRT$=ESRT$+RIGHT$(RS$,LRS-1)
4820     IF J<>NEPR THEN LET ESRT$=ESRT$+","
4830    NEXT J
4840     PRINT#1,ESRT$
4850     ESRT$=""
4860  NEXT I
```

```
4870 RETURN
4880'*************************************************************
4890 '
4900 PRINT "Writing LHS dome quadratic elements"
4910 OPEN "DUMMYLDQ" FOR OUTPUT AS #2
4920 ELNUM=EELDTRI+1:N=NSLDQUA-1
4930 ESLDQUA=ELNUM
4940 PRINT#1,"*ELEMENT,TYPE=S8R,ELSET=LDQUA"
4950 FOR I =1 TO NEPR:'*** load triangular elements into dummy file
     and add later00
4960    FOR J=1 TO NODOCON-1
4970      WRITE#1,ELNUM,NO(N+1),NO(N+4),NO(N+3),NO(N+2),NO(N+8)
          ,NO(N+7),NO(N+6),NO(N+5)
4980      WRITE#2,ELNUM,NO(N+1);NO(N+4);NO(N+3);NO(N+2);NO(N+8)
          ;NO(N+7);NO(N+6);NO(N+5)
4990       EELDQUA=ELNUM
5000       EELD=ELNUM:' *** element end right dome
5010       ELNUM=ELNUM+1
5020        N=N+8
5030    NEXT J
5040   NEXT I
5050   CLOSE #2:CLOSE #3
5060  RETURN
5070'*************************************************************
5080 PRINT "Write LHS triangular elements"
5090 OPEN "DUMMYLDT" FOR OUTPUT AS #3
5100 ELNUM=EERIBS+1:N=NSLDTRI-1
5110 ESLDTRI=ELNUM:ESLD=ERIBS+1
5120 PRINT#1,"*ELEMENT,TYPE=STRI3,ELSET=LDTRI"
5130  FOR I=1 TO NEPR
5140    WRITE#1,ELNUM;NO(N+1);NO(N+2);NO(N+3)
5150    WRITE#3,ELNUM;NO(N+1);NO(N+2);NO(N+3)
5160      ELNUM=ELNUM+1
5170    WRITE#1,ELNUM;NO(N+1);NO(N+4);NO(N+2)
5180    WRITE#3,ELNUM;NO(N+1);NO(N+4);NO(N+2)
5190      EELDTRI=ELNUM:' *** element end triangle left
5200      ELNUM=ELNUM+1:N=N+4
5210  NEXT I
5220 CLOSE #3
5230 RETURN
5240 '*************************************************************
5250 '
5260 PRINT "Writing RHS dome quadratic elements"
5270 OPEN "DUMMYRDQ" FOR OUTPUT AS #2
5280 ELNUM=EERDTRI+1:N=NSRDQUA-1
5290 ESRDQUA=ELNUM
5300 PRINT#1,"*ELEMENT,TYPE=S8R,ELSET=RDQUA"
5310 FOR I =1 TO NEPR:'*** load triangular elements into
      dummy file and add later00
5320    FOR J=1 TO NODOCON-1
```

```
5330        WRITE#1,ELNUM,NO(N+1),NO(N+2),NO(N+3),NO(N+4),NO(N+5)
            ,NO(N+6),NO(N+7),NO(N+8)
5340        WRITE#2,ELNUM,NO(N+1);NO(N+2);NO(N+3);NO(N+4);NO(N+5)
            ;NO(N+6);NO(N+7);NO(N+8)
5350         EERDQUA=ELNUM
5360         EERD=ELNUM:' *** element end right dome
5370         ELNUM=ELNUM+1
5380          N=N+8
5390      NEXT J
5400    NEXT I
5410   CLOSE #2:CLOSE #3
5420   RETURN
5430'*************************************************************
5440 PRINT "Write RHS triangular elements"
5450 OPEN "DUMMYRDT" FOR OUTPUT AS #3
5460 ELNUM=EELDQUA+1:N=NSRDTRI-1
5470 ESRDTRI=ELNUM:ESRD=EELDQUA+1
5480 PRINT#1,"*ELEMENT,TYPE=STRI3,ELSET=RDTRI"
5490  FOR I=1 TO NEPR
5500     WRITE#1,ELNUM;NO(N+1);NO(N+3);NO(N+2)
5510     WRITE#3,ELNUM;NO(N+1);NO(N+3);NO(N+2)
           ELNUM=ELNUM+1
5530     WRITE#1,ELNUM;NO(N+1);NO(N+2);NO(N+4)
5540     WRITE#3,ELNUM;NO(N+1);NO(N+2);NO(N+4)
           EERDTRI=ELNUM:' *** element end triangle right
           ELNUM=ELNUM+1:N=N+4
5570  NEXT I
5580 CLOSE #3
5590 RETURN
5600 '*************************************************************
5610 '
5620 PRINT "Writing MPC's for shell to ribs coupling"
5630 '
5640 PRINT#1,"*MPC"
5650 PRINT#1,"*** MPC CYLINDER TO RIBS"
5660 MPCOUNT=0:' number of nodes connected in MPC
5670  FOR NR=1 TO NRIBS:' number of rib
5680   FOR I=1 TO NEPR*3:' for i= 1 to no of calculated nodes per rib
5690    NO=NSRIBS-1  +(NR-1)*NEPR*3 +I
5700    IF NO<>NO(NO) THEN GOTO 6000
5710         XR=X(NO):YR=Y(NO):ZR=Z(NO)
5720      FOR K=NSCYL TO NECYL
5730       IF K<>NO(K) THEN GOTO 5990
5740       IF ABS(XR-X(K))>PTOL THEN GOTO 5990
5750         YS=Y(K):ZS=Z(K)
5760         IF YS=0 AND ZS=0 THEN THETA=0:GOTO 5860
5770         IF YS=0 AND ZS>0 THEN THETA=PI/2:GOTO 5860
5780         IF YS=0 AND ZS<0 THEN THETA=-PI/2:GOTO 5860
5790 '    EELD=ELNUM-1
5800 ' *** calculate relative distance between shell and beam
```

```
5810          IF YS>0 AND ZS>=0 THEN THETA=ATN(ZS/YS)
5820          IF YS<0 AND ZS>=0 THEN THETA=ATN(ZS/YS)-PI
5830          IF YS<0 AND ZS<=0 THEN THETA=ATN(ZS/YS)-PI
5840          IF YS>0 AND ZS<=0 THEN THETA=ATN(ZS/YS)
5850 '        PRINT THETA
5860        DELTAR=.5*(TS+B(NR))
5870        DELTAY=DELTAR*COS(THETA)
5880        DELTAZ=DELTAR*SIN(THETA)
5890        Y=YS+DELTAY
5900        Z=ZS+DELTAZ
5910 ' *** routine to eliminate small numbers
5920          IF ABS(Z)<.00001 THEN LET Z=0
5930          IF ABS(Y)<.00001 THEN LET Y=0
5940 '*** truncate numbers according to decplace
5950              TRUNC=Y:GOSUB 10430:Y=TRUNC
5960              TRUNC=Z:GOSUB 10430:Z=TRUNC
5970 '*** compare shell to rib co-ordinates
5980        IF ABS(YR-Y)<NTOL AND ABS(ZR-Z)<NTOL THEN WRITE#1,7;NO(K)
            ;NO:MPCOUNT=MPCOUNT+1:GOTO 6000
5990       NEXT K
6000     NEXT I
6010    NEXT NR
6020    PRINT "RIBNODS;MPCOUNT ";NEPR*2*NRIBS;MPCOUNT
6030 RETURN
6040'*************************************************************
6050 PRINT "Writing MPC's for shell to left dome coupling"
6060 '
6070 PRINT#1,"*MPC"
6080 PRINT#1,"*** MPC CYLINDER TO LEFT DOME"
6090 MPCOUNT=0:' number of nodes connected in MPC
6100  FOR I=NSLDQUA TO NELDQUA
6110    IF I<>NO(I) THEN GOTO 6190
6120   FOR J=NSCYL TO NECYL
6130    IF J<>NO(J) THEN GOTO 6180
6140       IF ABS(X(I)-X(J))>DTOL THEN GOTO 6180
6150       IF ABS(Y(I)-Y(J))>DTOL THEN GOTO 6180
6160       IF ABS(Z(I)-Z(J))>DTOL THEN GOTO 6180
6170         WRITE#1,7;NO(I);NO(J):MPCOUNT=MPCOUNT+1
6180    NEXT J
6190  NEXT I
6200 PRINT "NNPR;MPCOUNT ";NEPR*2;MPCOUNT
6210 RETURN
6220 '
6230'*************************************************************
6240 PRINT "Writing MPC's for LHS dome to triangle coupling"
6250 PRINT#1,"*MPC"
6260 PRINT#1,"***MPC LEFT TRI TO LEFT QUA"
6270 MPCOUNT=0:' number of nodes connected in MPC
6280  FOR I=NSLDTRI TO  NELDTRI
6290    IF I<>NO(I) THEN GOTO 6370
```

```
6300    FOR J=NSLDQUA TO NELDQUA
6310     IF J<>NO(J) THEN GOTO 6360
6320        IF ABS(X(I)-X(J))>DTOL THEN GOTO 6360
6330        IF ABS(Y(I)-Y(J))>DTOL THEN GOTO 6360
6340        IF ABS(Z(I)-Z(J))>DTOL THEN GOTO 6360
6350          WRITE#1,7;NO(I);NO(J):MPCOUNT=MPCOUNT+1
6360     NEXT J
6370   NEXT I
6380 PRINT "NNPR;MPCOUNT ";NEPR*2;MPCOUNT
6390 RETURN
6400'*************************************************************
6410 PRINT "Writing MPC's for RHS dome to triangle coupling"
6420 PRINT#1,"*MPC"
6430 PRINT#1,"*** MPC RIGHT TRI TO RIGHT QUA"
6440 MPCOUNT=0:' number of nodes connected in MPC
6450  FOR I=NSRDTRI TO NERDTRI
6460    IF I<>NO(I) THEN GOTO 6540
6470   FOR J=NSRDQUA TO NERDQUA
6480    IF J<>NO(J) THEN GOTO 6530
6490       IF ABS(X(I)-X(J))>DTOL THEN GOTO 6530
6500       IF ABS(Y(I)-Y(J))>DTOL THEN GOTO 6530
6510       IF ABS(Z(I)-Z(J))>DTOL THEN GOTO 6530
6520         WRITE#1,7;NO(I);NO(J):MPCOUNT=MPCOUNT+1
6530    NEXT J
6540  NEXT I
6550 PRINT "NNPR;MPCOUNT ";NEPR*2;MPCOUNT
6560 RETURN
6570 '
6580'*************************************************************
6590 PRINT "Writing MPC's for shell to right dome coupling"
6600 '
6610 PRINT#1,"*MPC"
6620 PRINT#1,"***MPC CYLINDER TO RIGHT DOME"
6630 MPCOUNT=0:' number of nodes connected in MPC
6640  FOR I=NSRDQUA TO NERDQUA
6650    IF I<>NO(I) THEN GOTO 6730
6660   FOR J=NSCYL TO NECYL
6670    IF J<>NO(J) THEN GOTO 6720
6680       IF ABS(X(I)-X(J))>DTOL THEN GOTO 6720
6690       IF ABS(Y(I)-Y(J))>DTOL THEN GOTO 6720
6700       IF ABS(Z(I)-Z(J))>DTOL THEN GOTO 6720
6710         WRITE#1,7;NO(I);NO(J):MPCOUNT=MPCOUNT+1
6720    NEXT J
6730  NEXT I
6740 PRINT "NNPR;MPCOUNT ";NEPR*2;MPCOUNT
6750 RETURN
6760 '
10240'************************************************************
10250 '*** routine to eliminate duplicate nodes  E
10260 '
```

```
10270 PRINT "Eliminate duplicate nodes"
10280 '
10290 FOR I= STNODE TO ENNODE
10300  X=X(I):Y=Y(I):Z=Z(I)
10310   FOR J=STNODE TO ENNODE
10320    IF  J=I THEN GOTO 10380
10330    IF ABS(X-X(J)) > DTOL  THEN 10380
10340    IF ABS(Y-Y(J)) > DTOL  THEN 10380
10350    IF ABS(Z-Z(J)) > DTOL  THEN 10380
10360  IF NO(J)>NO(I) THEN LET NO(J)=NO(I):GOTO 10390
10370  IF NO(J)<=NO(I) THEN LET NO(I)=NO(J):GOTO 10390
10380   NEXT J
10390  NEXT I
10400 RETURN
10410'*************************************************************
10420  '****   routine to truncate numbers
10430   TRUNC=TRUNC*10^DECPLACE
10440   TRUNC=INT(TRUNC)
10450 '      TRUNC$=STR$(TRUNC)
10460 '       TRLE=LEN(TRUNC$)
10470 '        FOR IC = 1 TO TRLE
10480 '           A$=MID$(TRUNC$,IC,1):IF A$="." THEN
                  LET TRUNC$=LEFT$(TRUNC$,IC+DECPLACE)
10490 '          NEXT IC
10500   TRUNC=TRUNC/10^DECPLACE
10510  '      TRUNC=VAL(TRUNC$)
10520   RETURN
10530 ' ***************************************
10540  '*** routine containing equation of dome
10550   R=SQR((1-X^2/XLD^2)*(RI+TS/2)^2)
10560   RETURN
10570 '***************************************
10580 PRINT "Define cradle supports"
10590 NCS=1:NCR=1:'*** node counters
10600 RS=RI+TS/2:'***RS radius of shell nodes
10610 B$=""
10620 FOR I=1 TO NOSUP
10630  IF XS(I)=0 AND I>1 THEN 11130
10640   NCS=1:NCR=1
10650   A$="*NSET,NSET=SUPS"+RIGHT$(STR$(I),LEN(STR$(I))-1)
10660    PRINT#1,A$:'*** for shell support set
10670     YMAX=RS*SIN(ANGSU):YMIN=-YMAX
10680     ZMAX=-RS*COS(ANGSU):ZMIN=-RS
10690      FOR J=NSCYL TO NECYL
10700       IF J<>NO(J) THEN 10770
10710        IF ABS(XS(I)-X(J))>PTOL THEN 10770
10720        IF  Y(J)<=YMAX AND Y(J)>=YMIN THEN 10740
10730       GOTO 10770
10740        IF Z(J)<=ZMAX AND Z(J)>=ZMIN THEN 10760
10750       GOTO 10770
```

```
10760       NNSS(NCS)=NO(J):NCS=NCS+1
10770      NEXT J
10780     NCS=NCS-1
10790 '*** write individual node numbers
10800     B$=""
10810       FOR K =1 TO NCS
10820        DUM$=STR$(NNSS(K)):DUML=LEN(DUM$)
10830        DUM$=RIGHT$(DUM$,DUML-1)
10840         B$=B$+DUM$
10850         IF K<>NCS THEN B$=B$+","
10860       NEXT K
10870      PRINT#1,B$
10880 '*** support for ring
10890   A$="*NSET,NSET=SUPR"+RIGHT$(STR$(I),LEN(STR$(I))-1)
10900    PRINT#1,A$:'*** for rib support node set
10910 '*** support for ring
10920     RR=RI+TS+B(I)/2
10930     YMAX=RR*SIN(ANGSU):YMIN=-YMAX
10940     ZMAX=-RR*COS(ANGSU):ZMIN=-RR
10950      FOR J=NSRIBS TO NERIBS
10960        IF J<>NO(J) THEN 11030
10970        IF ABS(XS(I)-X(J))>PTOL THEN 11030
10980        IF  Y(J)<=YMAX AND Y(J)>=YMIN THEN 11000
10990        GOTO 11030
11000         IF Z(J)<=ZMAX AND Z(J)>=ZMIN THEN 11020
11010        GOTO 11030
11020         NNSR(NCR)=NO(J):NCR=NCR+1
11030       NEXT J
11040  NCR=NCR-1
11050   B$=""
11060  FOR K=1 TO NCR
11070   DUM$=STR$(NNSR(K)):DUML=LEN(DUM$)
11080    DUM$=RIGHT$(DUM$,DUML-1)
11090    B$=B$+DUM$
11100   IF K<>NCR THEN B$=B$+","
11110  NEXT K
11120  PRINT#1,B$
11130 NEXT I
11140 RETURN
11150'*************************************************************
11160 PRINT "Twisting displacements of cradle"
11170 PRINT#1,"*BOUNDARY,OP=MOD"
11180       FOR K=1 TO NCR:'*** constrain the rib nodes
11190        NO=NNSR(K)
11200         Y=Y(NO):Z=Z(NO)
11202          IF Y=0 AND Z<0 THEN THETA=PI:GOTO 11280
11250          IF Z<0 AND Y>0 THEN THETA=ATN(Y/Z)+PI
11260          IF Z<0 AND Y<0 THEN THETA=ATN(Y/Z)+PI
11280         PRINT NO;THETA*180/PI
11285        R=SQR(Z^2+Y^2)
```

```
11290        ZD=R*COS(THETA+TWIST)
11300        YD=R*SIN(THETA+TWIST)
11310        DY=YD-Y
11320        DZ=ZD-Z
11330  ' *** routine to eliminate small numbers
11340          IF ABS(DZ)<.00001 THEN LET DZ=0
11350          IF ABS(DY)<.00001 THEN LET DY=0
11360       PRINT#1,NO;",2,,";:PRINT#1,USING "##.####";DY
11370       PRINT#1,NO;",3,,";:PRINT#1,USING "##.####";DZ
11380     NEXT K
11390   RETURN
```

```
5 ' *** RTEND.BAS   27/5/1989
10 N=11000:  DIM NO(N),X(N),Y(N),Z(N)
20 ' DEFSNG A-H,O-Z
30 DIM ELSETRIB(13,16)
40 DIM NODE(8),XR(13),XFD(13)
50 DIM A(13),B(13)
60 KEY OFF:CLS
70 DIM XS(13):'*** x location of support
80 DIM NNSS(20):'*** node number support shell
90 DIM NNSR(20):'*** node number support rib
100 LOCATE 10,35:PRINT "MAGENE"
110 LOCATE 12,20:PRINT "ABAQUS MESH GENERATION END FOR ROAD TANKERS"
120 INPUT A$
130 PI=3.141592654#
140 DECPLACE=4
150 G=9.810001:'*** gravitational acceleration
160 XACC=2:' *** forward acceleration of tanker
170 YACC=-2:' *** sideways acceleration of tanker
180 ZACC=-2:' *** upwards acceleration of tanker
200 TWIST=6:TWIST=TWIST*PI/180:'*** twist of the tanker in radians
210 PP=8.4E5:' *** internal pressure in tanker
220 RI=.650:'***    inside radius
230 TS=.015:'***   thickness of shell
240 RO=RI+TS:' *** outside radius of the tanker
250 RS=RI+TS/2:' *** radius of centreline of the shell
270 DENLIQ=1850:' *** liquid or content density
280 DENSHELL=1900:' *** shell material density
290 DENRIBS=1900:'*** DENSITY OF THE RIBS
300 XSTART=0:'*** start of cylindrical section of tanker
320 XSTOP=12:'*** stop of cylindrical section of tanker
330 XLD=RS/2:'*** depth of left dish to shell centreline for 2:1
    ellipsoidal
340 TLD=TS:'*** thickness of left dome
350 TRD=TS:'*** thickness of right dome
360 XRD=XLD:'*** depth of right dish
370 XC=XSTOP:'*** length of cylindrical part of the tanker
380 XT=XC+XLD+XRD+TS:'*** total length of the tanker
390 NRIBS=13:'11*** number of ribs
400 XR(1)=0:XR(2)=1:XR(3)=2:XR(4)=3:XR(5)=4:XR(6)=5:XR(7)=6
    :XR(8)=7:XR(9)=8
405 XR(10)=9:XR(11)=10:XR(12)=11:XR(13)=12:' rib x positions
410 A1=.05:A2=.05:A1$=STR$(A1):A2$=STR$(A2):'*** width of ribs
420 B1=.05:B2=.1:B1$=STR$(B1):B2$=STR$(B2):' *** depth of ribs
430 A(1)=A2:A(2)=A2:A(3)=A2:A(4)=A2:A(5)=A1:A(6)=A1:A(7)=A1
440 A(8)=A1:A(9)=A1:A(10)=A2:A(11)=A2:A(12)=A2:A(13)=A2:' *** width
per rib
450 B(1)=B2:B(2)=B2:B(3)=B2:B(4)=B2:B(5)=B1:B(6)=B1:B(7)=B1:B(8)=B1
460 B(9)=B1:B(10)=B2:B(11)=B2:B(12)=B2:B(13)=B2:'*** depth per rib
470 MPLTHIN=DENRIBS*A1*B1:'*** mass per unit length of thin rib
480 MPLTHICK=DENRIBS*A2*B2:'*** mass per unit lenght of thick rib
```

```
490 NTOL=.05: ' *** tolerance on node distances for *MPC
500 DTOL=.01: ' *** tolerance on node distance for shell dome MPC
510 NODOCON=6:XFD(1)=.02:XFD(2)=.05:XFD(3)=.10:XFD(4)=.19
:XFD(5)=.28:XFD(6)=.36
520 NOSUP=12:XS(1)=0:XS(2)=1:XS(3)=2:XS(4)=3::XS(10)=9:XS(11)=10
:XS(12)=11:XS(13)=00:'*** support locations
530 FOR I=5 TO 9:XS(I)=0:NEXT I:'*** locations of no supports equel
zero
540 ANGSU=60:ANGSU=ANGSU/180*PI:'** angle of the support
545 R=RS
547 HEADING$=" RT26ZT 30DEG,.25M,OVERHANG,ID=1.3m,L=12m"
550 ' *** number of dome contours:dome contour x fractions
560'************************************************************
570 CLS:LOCATE  1,1:INPUT "Name of ABAQUS end file ";NAMEFILE$
580 OPEN  NAMEFILE$ FOR OUTPUT AS #1
605 OPEN "NODES" FOR INPUT AS #4
610 GOSUB 3470:'***input dummy node
870 GOSUB 6780:' *** material definitions
880 'KILL "DUMMYC":KILL"DUMMYLDT":KILL "DUMMYLDQ":KILL"DUMMYR"
890 'KILL"DUMMYRDT":KILL "DUMMYRDQ"
900 PRINT "          EXECUTION COMPLETE    ":CLOSE:STOP:END
910'************************************************************
3470 PRINT "Input nodes from dummy file"
3480 WHILE NOT EOF(4)
3510       INPUT#4,NO(I),X(NO(I)),Y(NO(I)),Z(NO(I))
3520 WEND
3540 RETURN
3570'************************************************************
6770'************************************************************
6780 PRINT#1,"*ELSET,ELSET=RIBTHICK"
6790 PRINT#1,"RIB1,RIB2,RIB3,RIB4,RIB10,RIB11,RIB12,RIB13"
6800 PRINT#1,"*ELSET,ELSET=RIBTHIN"
6810 PRINT#1,"RIB5,RIB6,RIB7,RIB8,RIB9"
6820 PRINT#1,"*ELSET,ELSET=LDOME"
6830 PRINT#1,"LDQUA,LDTRI"
6840 PRINT#1,"*ELSET,ELSET=RDOME"
6850 PRINT#1,"RDQUA,RDTRI"
6860 PRINT#1,"*ELSET,ELSET=ENDS"
6870 PRINT#1,"LDOME,RDOME"
6880 PRINT#1,"*ELSET,ELSET=SHELL"
6890 PRINT#1,"ECYL,ENDS"
6900 PRINT#1,"*ELSET,ELSET=ALL"
6910 PRINT#1,"SHELL,RIBS"
6920'************************************************************
6930 '
6940 PRINT "Define beam properties"
6950 PRINT#1,"*BEAM
SECTION,ELSET=RIBTHIN,MATERIAL=ORTHRIB,SECTION=RECT"
6960 PRINT#1,USING "#.###^^^^";A1;:PRINT#1,",";:PRINT#1,USING
"#.###^^^^";B1
```

```
6970 PRINT#1,"1,0,0"
6980 PRINT#1,"*TRANSVERSE SHEAR STIFFNESS"
6990 PRINT#1,"4.14E9,3.5E9"
7000 PRINT#1,"*BEAM
SECTION,ELSET=RIBTHICK,MATERIAL=ORTHRIB,SECTION=RECT"
7010 PRINT#1,USING "#.###^^^^";A2;:PRINT#1,",";:PRINT#1,USING
"#.###^^^^^";B2
7020 PRINT#1,"1.0,0"
7030 PRINT#1,"*TRANSVERSE SHEAR STIFFNESS"
7040 PRINT#1,"4.14E9,3.5E9"
7050'************************************************************
7060 PRINT "Define orientations"
7070 PRINT#1,"*ORIENTATION,NAME=CYL0,SYSTEM=C"
7080 PRINT#1,"0,0,0,8,0,0"
7090 PRINT#1,"1,0"
7100 PRINT#1,"*ORIENTATION,NAME=CYL+10,SYSTEM=C"
7110 PRINT#1,"0,0,0,8,0,0"
7120 PRINT#1,"1,10"
7130 PRINT#1,"*ORIENTATION,NAME=CYL-10,SYSTEM=C"
7140 PRINT#1,"0,0,0,8,0,0"
7150 PRINT#1,"1,-10"
7160 PRINT#1,"*ORIENTATION,NAME=CYL+85,SYSTEM=C"
7170 PRINT#1,"0,0,0,8,0,0"
7180 PRINT#1,"1,85"
7190 PRINT#1,"*ORIENTATION,NAME=CYL-85,SYSTEM=C"
7200 PRINT#1,"0,0,0,8,0,0"
7210 PRINT#1,"1,-85"
7220 PRINT#1,"*ORIENTATION,NAME=SPH+10L,SYSTEM=S"
7230 PRINT#1,"0,0,0,0,0,1"
7240 PRINT#1,"1,10"
7250 PRINT#1,"*ORIENTATION,NAME=SPH-10L,SYSTEM=S"
7260 PRINT#1,"0,0,0,0,0,1"
7270 PRINT#1,"1,-10"
7280 PRINT#1,"*ORIENTATION,NAME=SPH+85L,SYSTEM=S"
7290 PRINT#1,"0,0,0,0,0,1"
7300 PRINT#1,"1,85"
7310 PRINT#1,"*ORIENTATION,NAME=SPH-85L,SYSTEM=S"
7320 PRINT#1,"0,0,0,0,0,1"
7330 PRINT#1,"1,-85"
7340 PRINT#1,"*ORIENTATION,NAME=SPH+10R,SYSTEM=S"
7350 PRINT#1,"10,0,0,10,0,1"
7360 PRINT#1,"1,10"
7370 PRINT#1,"*ORIENTATION,NAME=SPH-10R,SYSTEM=S"
7380 PRINT#1,"10,0,0,10,0,1"
7390 PRINT#1,"1,-10"
7400 PRINT#1,"*ORIENTATION,NAME=SPH+85R,SYSTEM=S"
7410 PRINT#1,"10,0,0,10,0,1"
7420 PRINT#1,"1,85"
7430 PRINT#1,"*ORIENTATION,NAME=SPH-85R,SYSTEM=S"
7440 PRINT#1,"10,0,0,10,0,1"
```

```
7450 PRINT#1,"1,  85"
7460'************************************************************
7470 PRINT "Define material properties
7480 PRINT#1,"*MATERIAL,NAME=LAMCYL"
7490 PRINT#1,"*ELASTIC,TYPE=LAMINA"
7500 PRINT#1,"38.6E9,8.27E9,.26,4.14E9,4.14E9,3.5E9"
7510 PRINT#1,"*DENSITY"
7520 PRINT#1,DENSHELL
7530 PRINT#1,"*MATERIAL,NAME=ORTHRIB"
7540 PRINT#1,"*ELASTIC,TYPE=ORTHOTROPIC"
7550 PRINT#1,"39.17E9,2.182E9,8.39E9,2.182E9,2.182E9,8.392E9
,4.14E9,4.14E9"
7560 PRINT#1,"3.5E9"
7570 PRINT#1,"*DENSITY"
7580 PRINT#1,DENSHELL
7590 PRINT#1,"*MATERIAL,NAME=ISODOM"
7600 PRINT#1,"*ELASTIC"
7610 PRINT#1,"18.96E9,.27"
7620 PRINT#1,"*DENSITY"
7630 PRINT#1,DENSHELL
7640'************************************************************
7650 PRINT "Define shell sections"
7660 PRINT#1,"*SHELL SECTION,ELSET=ECYL,COMPOSITE"
7670 PRINT#1,".625E-3,1,LAMCYL,CYL+10"
7680 PRINT#1,".625E-3,1,LAMCYL,CYL-10"
7690 PRINT#1,".625E-3,1,LAMCYL,CYL-85"
7700 PRINT#1,".625E-3,1,LAMCYL,CYL+85"
7710 PRINT#1,".625E-3,1,LAMCYL,CYL+10"
7720 PRINT#1,".625E-3,1,LAMCYL,CYL-10"
7730 PRINT#1,".625E-3,1,LAMCYL,CYL-85"
7740 PRINT#1,".625E-3,1,LAMCYL,CYL+85"
7750 PRINT#1,".625E-3,1,LAMCYL,CYL+10"
7760 PRINT#1,".625E-3,1,LAMCYL,CYL-10"
7770 PRINT#1,".625E-3,1,LAMCYL,CYL-85"
7780 PRINT#1,".625E-3,1,LAMCYL,CYL+85"
7790 PRINT#1,"**** MIDDLE OF LAMINATE"
7800 PRINT#1,".625E-3,1,LAMCYL,CYL+85"
7810 PRINT#1,".625E-3,1,LAMCYL,CYL-85"
7820 PRINT#1,".625E-3,1,LAMCYL,CYL-10"
7830 PRINT#1,".625E-3,1,LAMCYL,CYL+10"
7840 PRINT#1,".625E-3,1,LAMCYL,CYL+85"
7850 PRINT#1,".625E-3,1,LAMCYL,CYL-85"
7860 PRINT#1,".625E-3,1,LAMCYL,CYL-10"
7870 PRINT#1,".625E-3,1,LAMCYL,CYL+10"
7880 PRINT#1,".625E-3,1,LAMCYL,CYL+85"
7890 PRINT#1,".625E-3,1,LAMCYL,CYL-85"
7900 PRINT#1,".625E-3,1,LAMCYL,CYL-10"
7910 PRINT#1,".625E-3,1,LAMCYL,CYL+10"
7920 PRINT#1,"*TRANSVERSE SHEAR STIFFNESS"
7930 PRINT#1,"4.14E9,3.5E9"
```

```
8510  PRINT#1,"*SHELL SECTION,ELSET=LDQUA,MATERIAL=ISODOM"
8520  PRINT#1,USING "#.###";TLD;:PRINT#1,",3"
8530  PRINT#1,"*TRANSVERSE SHEAR STIFFNESS"
8540  PRINT#1,"4.14E9,3.5E9"
8550  PRINT#1,"*SHELL SECTION,ELSET=LDTRI,MATERIAL=ISODOM"
8560  PRINT#1,USING "#.###";TLD;:PRINT#1,",3"
8570  PRINT#1,"*TRANSVERSE SHEAR STIFFNESS"
8580  PRINT#1,"4.14E0,3.5E9"
8590  PRINT#1,"*SHELL SECTION,ELSET=RDQUA,MATERIAL=ISODOM"
8600  PRINT#1,USING "#.###";TRD;:PRINT#1,",3"
8610  PRINT#1,"*TRANSVERSE SHEAR STIFFNESS"
8620  PRINT#1,"4.14E9,3.5E9"
8630  PRINT#1,"*SHELL SECTION,ELSET=RDTRI,MATERIAL=ISODOM"
8640  PRINT#1,USING "#.###";TRD;:PRINT#1,",3"
8650  PRINT#1,"*TRANSVERSE SHEAR STIFFNESS"
8660  PRINT#1,"4.14E9,3.5E9"
8670'*************************************************************
8680 PRINT "Define boundary conditions"
8690 PRINT#1,"*NSET,NSET=BOGIE"
8700 PRINT#1,"SUPR1,SUPR2,SUPR3,SUPR4"
8710 PRINT#1,"*NSET,NSET=LAND"
8720 PRINT#1,"SUPR10,SUPS11"
8723 PRINT#1,"*NSET,NSET=FIFTH"
8727 PRINT#1,"SUPR12"
8730 PRINT#1,"*BOUNDARY"
8740 PRINT#1,"SUPR2,3"
8750 PRINT#1,"SUPR2,1"
8760 PRINT#1,"???,2"
8770 PRINT#1,"**SUPR12,3"
8780 PRINT#1,"**?????,2"
8790 ' ************************************.*****************
8800 PRINT#1,"*PLOT,PLOTSIZE=3"
8810 PRINT#1,HEADING$
8820 PRINT#1,"*VIEWPOINT"
8830 PRINT#1,"1,1,1"
8840 PRINT#1,"***SHRINK,FACTOR=.2"
8850 PRINT#1,"*DETAIL"
8860 PRINT#1,"-1,-1,-1,2.1,1,1
8870 PRINT#1,"*DRAW,ELNUM"
8880 PRINT#1,"*DETAIL"
8890 PRINT#1,"8.9,-1,-1,11,1,1"
8900 PRINT#1,"*DRAW,ELNUM"
8910 ' ***********************************************************
8920 '*** calculate pressure on element as a function of X,Y,Z
8930 PRINT#1,"*STEP,AMP=RAMP"
8940 PRINT#1,"***STEP,LINEAR=NEW,AMP=RAMP"
8950 PRINT#1,"*STATIC, PTOL=1.E2"
8960 PRINT#1,"*DLOAD"
8970 ' ************************************************
8980 ' ************* routine to calculate pressures on S8R elements
```

```
8990 OPEN "DUMMYC" FOR INPUT AS #2:FILE$="CYL":EN=EECLY:GOTO 9020
9000 OPEN "DUMMYLDQ" FOR INPUT AS #2:FILE$="LDOME":EN=EELDQUA:GOTO
9020
9010 OPEN "DUMMYRDQ" FOR INPUT AS #2:FILE$="RDOME":EN=EERDQUA
9020  WHILE NOT EOF(2)
9030 INPUT#2,ELNO,NODE(1),NODE(2),NODE(3),NODE(4),NODE(5),NODE(6)
,NODE(7),NODE(8):' *** calculate centroids of the elements
9050      CENTX    =.25*(X(NODE(1))+X(NODE(2))+X(NODE(3))+X(NODE(4)))
9060      CENTY    =.25*(Y(NODE(1))+Y(NODE(2))+Y(NODE(4))+Y(NODE(3)))
9070      CENTZ    =.25*(Z(NODE(1))+Z(NODE(2))+Z(NODE(4))+Z(NODE(3)))
9100      PX=DENLIQ*G*ABS(XACC)*(CENTX+RI/2)
9110      PY=DENLIQ*G*ABS(YACC)*(RI-CENTY)
9120      PZ=DENLIQ*G*ABS(ZACC)*(RI-CENTZ)
9130      PT=PP+PX+PY+PZ
9190 IF PT<>0 THEN PRINT#1,ELNO;",P,";:PRINT#1,USING"#.###^^^^^";PT
9200 WEND:' IF ELNO<>EN THEN GOTO 9720
9210 CLOSE#2
9220  IF FILE$="CYL" THEN 9000
9230  IF FILE$="LDOME" THEN 9010
9240 ' ************************************************
9250 ' ************* routine to calculate pressures on STRI3 elements
9260 OPEN "DUMMYLDT" FOR INPUT AS #2:FILE$="LDOME":EN=EELDTRI:GOTO
9280
9270 OPEN "DUMMYRDT" FOR INPUT AS #2:FILE$="RDOME":EN=EERDTRI
    WHILE NOT EOF(2)
9280  INPUT#2,ELNO,NODE(1),NODE(2),NODE(3): ' *** calculate centroids
of the elements
9300      CENTX    =1/3*(X(NODE(1))+X(NODE(2))+X(NODE(3)))
9310      CENTY    =1/3*(Y(NODE(1))+Y(NODE(2))+Y(NODE(3)))
9320      CENTZ    =1/3*(Z(NODE(1))+Z(NODE(2))+Z(NODE(3)))
9330      PX=DENLIQ*G*XACC*(CENTX+RI/2)
9340      PY=DENLIQ*G*ABS(YACC)*(RI-CENTY)
9350      PZ=DENLIQ*G*ABS(ZACC)*(RI-CENTZ)
9360      PT=PP+PX+PY+PZ
9370 IF PT<>0 THEN PRINT#1,ELNO;",P,";:PRINT#1,USING "#.###^^^^^";PT
9380  WEND
9390 CLOSE#2
9400  IF FILE$="LDOME" THEN 9270
9410 '*************************************************
9420 '*** body force for whole shell
9430 BX=DENSHELL*G*XACC:' *** use denshell as approx  density
9440 BY=DENSHELL*G*YACC
9450 BZ=DENSHELL*G*ZACC
9460 IF BX<>0 THEN PRINT#1,"SHELL,BX,";BX
9470 IF BY<>0 THEN PRINT#1,"SHELL,BY,";BY
9480 IF BZ<>0 THEN PRINT#1,"SHELL,BZ,";BZ
9490 IF XACC<>0 THEN PRINT#1,"RIBTHIN,PX,";MPLTHIN*G*XACC
9500 IF XACC<>0 THEN PRINT#1,"RIBTHICK,PX,";MPLTHICK*G*XACC
9510 IF YACC<>0 THEN PRINT#1,"RIBTHIN,PY,";MPLTHIN*G*YACC
9520 IF YACC<>0 THEN PRINT#1,"RIBTHICK,PY,";MPLTHICK*G*YACC
```

```
9530 IF ZACC<>0 THEN PRINT#1,"RIBTHIN,PZ,";MPLTHIN*G*ZACC
9540 IF ZACC<>0 THEN PRINT#1,"RIBTHICK,PZ,";MPLTHICK*G*ZACC
9560 '*** determine output parameters
9565 GOTO 10220
9570 PRINT#1,"*EL PRINT,ELSET=SHELL"
9580 PRINT#1,"COORD,S11,S22,S12"
9590 PRINT#1,"*EL PRINT,ELSET=SHELL"
9600 PRINT#1,"SF"
9610 PRINT#1,"*EL PRINT,ELSET=RIBS"
9620 PRINT#1,"COORD"
9630 PRINT#1,"*EL PRINT,ELSET=RIBS"
9640 PRINT#1,"SF"
9650 PRINT#1,"*PLOT,PLOTSIZE=4"
9660 PRINT#1,"*DETAIL,ELSET=SHELL"
9670 PRINT#1,"-1,-1,-1,13,0,1"
9680 PRINT#1,"*VIEWPOINT"
9690 PRINT#1,"0,1,0"
9700 PRINT#1,"*DISPLACED"
9710 PRINT#1,"U"
9720 PRINT#1,"*PLOT,PLOTSIZE=3"
9730 PRINT#1,"*DETAIL,ELSET=SHELL"
9740 PRINT#1,"-1,-1,-1,13,0,1"
9750 PRINT#1,"*VIEWPOINT"
9760 PRINT#1,"1,1,1"
9770 PRINT#1,"*DISPLACED"
9780 PRINT#1,"U"
9790 PRINT#1,"*PLOT,PLOTSIZE=3"
9800 PRINT#1,"*DETAIL,ELSET=SHELL"
9810 PRINT#1,"-1,-1,-1,4,0,1"
9820 PRINT#1,"*VIEWPOINT"
9830 PRINT#1,"0,1,0"
9840 PRINT#1,"*DISPLACED"
9850 PRINT#1,"U"
9860 PRINT#1,"*PLOT,PLOTSIZE=3"
9870 PRINT#1,"*DETAIL,ELSET=SHELL"
9880 PRINT#1,"8,-1,-1,13,0,1"
9890 PRINT#1,"*VIEWPOINT"
9900 PRINT#1,"0,1,0"
9910 PRINT#1,"*DISPLACED"
9920 PRINT#1,"U"
9930 PRINT#1,"*PLOT,PLOTSIZE=3"
9940 PRINT#1,"SF1";HEADING$;" -1M-0M"
9950 PRINT#1,"*DETAIL,ELSET=SHELL"
9960 PRINT#1,"-1,-1,-1,0,0,1
9970 PRINT#1,"*CONTOUR,DEFORM"
9980 PRINT#1,"SF1"
9990 PRINT#1,"*PLOT,PLOTSIZE=3"
10000 PRINT#1,"SF2";HEADING$;" -1M-0M"
10010 PRINT#1,"*CONTOUR"
10020 PRINT#1,"SF2"
```

```
10030 PRINT#1,"*PLOT,PLOTSIZE=3"
10040 PRINT#1,"SF3";HEADING$;" -1M-0M"
10050 PRINT#1,"*CONTOUR"
10060 PRINT#1,"SF3"
10070 PRINT#1,"*PLOT,PLOTSIZE=3"
10080 PRINT#1,"SF1";HEADING$
10090 PRINT#1,"*DETAIL,ELSET=SHELL"
10100 PRINT#1,"0,-1,-1,2.1,0,1
10110 PRINT#1,"*CONTOUR"
10120 PRINT#1,"SF1"
10130 PRINT#1,"*PLOT,PLOTSIZE=3"
10140 PRINT#1,"SF2";HEADING$
10150 PRINT#1,"*CONTOUR"
10160 PRINT#1,"SF2"
10170 PRINT#1,"*PLOT,PLOTSIZE=3"
10180 PRINT#1 "SF3";HEADING$
10190 PRINT#1,"*CONTOUR,DEFORM"
10200 PRINT#1,"SF3"
10201 PRINT#1,"*PLOT,PLOTSIZE=3"
10202 PRINT#1,"SF1";HEADING$
10203 PRINT#1,"*DETAIL,ELSET=SHELL"
10204 PRINT#1,"0,-1,-1,12.1,0,1
10205 PRINT#1,"*CONTOUR,DEFORM"
10206 PRINT#1,"SF1"
10207 PRINT#1,"*PLOT,PLOTSIZE=3"
10208 PRINT#1,"SF2";HEADING$
10209 PRINT#1,"*CONTOUR,DEFORM"
10210 PRINT#1,"SF2"
10211 PRINT#1,"*PLOT,PLOTSIZE=3"
10212 PRINT#1,"SF3";HEADING$
10213 PRINT#1,"*CONTOUR,DEFORM"
10214 PRINT#1,"SF3"
10215 PRINT#1,"*END STEP"
10220 CLOSE#1
10230 RETURN
```

APPENDIX J

SUMMARIZED LISTING OF ROAD TANKER FEM MODELS

```
** LOADCASE 2: COMBINED AXIAL 2G, VERTICAL 2G AND SIDEWAYS 2G ACCELER-
ATION
*HEADING,CORE=320000
RT27AA 30 DEG,.25M,OVERHANG,ID=1.3m,L=12
*DATA CHECK
*PREPRINT,ECHO=NO,HISTORY=NO,MODEL=NO
*NODE,NSET=NCYL
 1 ,    0.0000,    -0.5695,     0.3287
  ..
 1012 ,     2.7500,     0.5694,    -0.3288
 1020 ,     2.7500,     0.3287,    -0.5695
 1023 ,     2.7500,     0.4649,    -0.4650
 1108 ,     3.0000,     0.5694,    -0.3288
 1112 ,     2.8750,     0.5694,    -0.3288
 1116 ,     3.0000,     0.3287,    -0.5695
 1119 ,     3.0000,     0.4649,    -0.4650
 1120 ,     2.8750,     0.3287,    -0.5695
  ..
 4607 ,    12.0000,    -0.6351,    -0.1702
*NODE,NSET=NRIBS
 4609 ,  0.0000,    -0.6193,     0.3574,     0.0000,    -0.8661,    -0.4998
  ..
 5075 , 12.0000,    -0.6907,    -0.1851,     0.0000,    -0.9659,    -0.2589
*NODE,NSET=NLDTRI
 5077 ,    -0.3288,     0.0000,     0.0000
  ..
 5603 ,     0.0000,     0.6350,    -0.1702
*NODE,NSET=NRDTRI
 5605 ,    12.3287,     0.0000,     0.0000
  ..
 5650 ,    12.3221,     0.1263,    -0.0339
*NODE,NSET=NRDQUA
 5653 ,    12.3221,     0.1133,     0.0654
  ..
 6131 ,    12.0000,     0.6350,    -0.1702
*ELEMENT,TYPE=S8R,ELSET=ECYL
1,1,2,3,4,5,6,7,8
  ..
140,1020,1012,1108,1116,1023,1112,1119,1120
  ..
576,4419,4500,4596,4515,4511,4600,4607,4518
*ELEMENT,TYPE=B32,ELSET=RIBS
577,4609,4610,4611
  ..
732,5043,5075,5071
*ELEMENT,TYPE=STRI3,ELSET=LDTRI
733,5077,5078,5079
  ..
756,5077,5079,5122
*ELEMENT,TYPE=S8R,ELSET=LDQUA
```

```
757,5125,5128,5127,5126,5132,5131,5130,5129
 ..
816,5151,5159,5560,5552,5162,5603,5564,5595
*ELEMENT,TYPE=STRI3,ELSET=RDTRI
817,5605,5607,5606
 ..
840,5605,5650,5607
*ELEMENT,TYPE=S8R,ELSET=RDQUA
841,5653,5654,5655,5656,5657,5658,5659,5660
 ..
900,5679,6080,6088,5687,6123,6092,6131,5690*MPC
*** MPC CYLINDER TO LEFT DOME
7,5159,41
 ..
7,5603,53
*MPC
***MPC LEFT TRI TO LEFT QUA
7,5078,5129
 ..
7,5122,5569
*MPC
***MPC CYLINDER TO RIGHT DOME
7,5687,4556
 ..
7,6131,4567
*MPC
*** MPC RIGHT TRI TO RIGHT QUA
7,5606,5657
 ..
7,5650,6097
*MPC
*** MPC CYLINDER TO RIBS
7,1,4609
 ..
7,4607,5075
*ELSET,ELSET=RIB1
577,578,579,580,581,582,583,584,585,586,587,588
*ELSET,ELSET=RIB2
589,590,591,592,593,594,595,596,597,598,599,600
*ELSET,ELSET=RIB3
601,602,603,604,605,606,607,608,609,610,611,612
*ELSET,ELSET=RIB4
613,614,615,616,617,618,619,620,621,622,623,624
*ELSET,ELSET=RIB5
625,626,627,628,629,630,631,632,633,634,635,636
*ELSET,ELSET=RIB6
637,638,639,640,641,642,643,644,645,646,647,648
*ELSET,ELSET=RIB7
649,650,651,652,653,654,655,656,657,658,659,660
*ELSET,ELSET=RIB8
```

```
661,662,663,664,665,666,667,668,669,670,671,672
*ELSET,ELSET=RIB9
673,674,675,676,677,678,679,680,681,682,683,684
*ELSET,ELSET=RIB10
685,686,687,688,689,690,691,692,693,694,695,696
*ELSET,ELSET=RIB11
697,698,699,700,701,702,703,704,705,706,707,708
*ELSET,ELSET=RIB12
709,710,711,712,713,714,715,716,717,718,719,720
*ELSET,ELSET=RIB13
721,722,723,724,725,726,727,728,729,730,731,732
*NSET,NSET=SUPS1
49,57,61,69,73,77,85
*NSET,NSET=SUPR1
4627,4630,4631,4633,4634,4636,4637,4640
*NSET,NSET=SUPS2
340,348,351,359,364,367,375
*NSET,NSET=SUPR2
4663,4666,4667,4669,4670,4672,4673,4676
*NSET,NSET=SUPS3
724,732,735,743,748,751,759
*NSET,NSET=SUPR3
4699,4702,4703,4705,4706,4708,4709 4712
*NSET,NSET=SUPS4
1108,1116,1119,1127,1132,1135,1143
*NSET,NSET=SUPR4
4735,4738,4739,4741,4742,4744,4745,4748
*NSET,NSET=SUPS10
3412,3420,3423,3431,3436,3439,3447
*NSET,NSET=SUPR10
4951,4954,4955,4957,4958,4960,4961,4964
*NSET,NSET=SUPS11
3796,3804,3807,3815,3820,3823,3831
*NSET,NSET=SUPR11
4987,4990,4991,4993,4994,4996,4997,5000
*NSET,NSET=SUPS12
4180,4188,4191,4199,4204,4207,4215
*NSET,NSET=SUPR12
5023,5026,5027,5029,5030,5032,5033,5036
*ELSET,ELSET=RIBTHICK
RIB1,RIB2,RIB3,RIB4,RIB10,RIB11,RIB12,RIB13
*ELSET,ELSET=RIBTHIN
RIB5,RIB6,RIB7,RIB8,RIB9
*ELSET,ELSET=LDOME
LDQUA,LDTRI
*ELSET,ELSET=RDOME
RDQUA,RDTRI
*ELSET,ELSET=ENDS
LDOME,RDOME
*ELSET,ELSET=SHELL
```

```
ECYL,ENDS
*ELSET,ELSET=ALL
SHELL,RIBS
*BEAM SECTION,ELSET=RIBTHIN,MATERIAL=ORTHRIB,SECTION=RECT
5.000E-02, 5.000E-02
1,0,0
*TRANSVERSE SHEAR STIFFNESS
4.14E9,3.5E9
*BEAM SECTION,ELSET=RIBTHICK,MATERIAL=ORTHRIB,SECTION=RECT
5.000E-02, 1.000E-01
1,0,0
*TRANSVERSE SHEAR STIFFNESS
4.14E9,3.5E9
*ORIENTATION,NAME=CYL0,SYSTEM=C
0,0,0,8,0,0
1,0
*ORIENTATION,NAME=CYL+10,SYSTEM=C
0,0,0,8,0,0
1,10
*ORIENTATION,NAME=CYL-10,SYSTEM=C
0,0,0,8,0,0
1,-10
*ORIENTATION,NAME=CYL+85,SYSTEM=C
0,0,0,8,0,0
1,85
*ORIENTATION,NAME=CYL-85,SYSTEM=C
0,0,0,8,0,0
1,-85
*MATERIAL,NAME=LAMCYL
*ELASTIC,TYPE=LAMINA
38.6E9,8.27E9,.26,4.14E9,4.14E9,3.5E9
*DENSITY
 1900
*MATERIAL,NAME=ORTHRIB
*ELASTIC,TYPE=ORTHOTROPIC
39.17E9,2.182E9,8.39E9,2.182E9,2.182E9,8.392E9,4.14E9,4.14E9
3.5E9
*DENSITY
 1900
*MATERIAL,NAME=ISODOM
*ELASTIC
18.96E9,.27
*DENSITY
 1900
*SHELL SECTION,ELSET=ECYL,COMPOSITE
 .625E-3,1,LAMCYL,CYL+10
 .625E-3,1,LAMCYL,CYL-10
 .625E-3,1,LAMCYL,CYL-85
 .625E-3,1,LAMCYL,CYL+85
 .625E-3,1,LAMCYL,CYL+10
```

```
 .625E-3,1,LAMCYL,CYL-10
 .625E-3,1,LAMCYL,CYL-85
 .625E-3,1,LAMCYL,CYL+85
 .625E-3,1,LAMCYL,CYL+10
 .625E-3,1,LAMCYL,CYL-10
 .625E-3,1,LAMCYL,CYL-85
 .625E-3,1,LAMCYL,CYL+85
**** MIDDLE OF LAMINATE
 .625E-3,1,LAMCYL,CYL+85
 .625E-3,1,LAMCYL,CYL-85
 .625E-3,1,LAMCYL,CYL-10
 .625E-3,1,LAMCYL,CYL+10
 .625E-3,1,LAMCYL,CYL+85
 .625E-3,1,LAMCYL,CYL-85
 .625E-3,1,LAMCYL,CYL-10
 .625E-3,1,LAMCYL,CYL+10
 .625E-3,1,LAMCYL,CYL+85
 .625E-3,1,LAMCYL,CYL-85
 .625E-3,1,LAMCYL,CYL-10
 .625E-3,1,LAMCYL,CYL+10
*TRANSVERSE SHEAR STIFFNESS
4.14E9,3.5E9
*SHELL SECTION,ELSET=LDQUA,MATERIAL=ISODOM
0.015,3
*TRANSVERSE SHEAR STIFFNESS
4.14E9,3.5E9
*SHELL SECTION,ELSET=LDTRI,MATERIAL=ISODOM
0.015,3
*TRANSVERSE SHEAR STIFFNESS
4.14E0,3.5E9
*SHELL SECTION,ELSET=RDQUA,MATERIAL=ISODOM
0.015,3
*TRANSVERSE SHEAR STIFFNESS
4.14E9,3.5E9
*SHELL SECTION,ELSET=RDTRI,MATERIAL=ISODOM
0.015,3
*TRANSVERSE SHEAR STIFFNESS
4.14E9,3.5E9
*NSET,NSET=BOGIE
SUPR1,SUPR2,SUPR3,SUPR4
*NSET,NSET=LAND
SUPR10,SUPS11
*NSET,NSET=FIFTH
SUPR12
*BOUNDARY
SUPR2,3
SUPR2,1
4669,2
SUPR12,3
5029,2
```

```
*PLOT,PLOTSIZE=3
 RT27AA 30DEG,.25M,OVERHANG,ID=1.3m,L=12m
*VIEWPOINT
1,1,1
***SHRINK,FACTOR=.2
*DETAIL
-1,-1,-1,2.1,1,1
*DRAW,ELNUM
*DETAIL
8.9,-1,-1,11,1,1
*DRAW,ELNUM
*STEP,AMP=RAMP
***STEP,LINEAR=NEW,AMP=RAMP
*STATIC, PTOL=1.E2
*DLOAD
 1 ,P, 7.996E+04
  ..
 140 ,P, 1.635E+05
  ..
 840 ,P, 5.038E+04
SHELL,BX, 37278.00390625
SHELL,BY,-37278.00390625
SHELL,BZ,-37278.00390625
RIBTHIN,PX, 93.19501304626465
RIBTHICK,PX, 186.3900260925293
RIBTHIN,PY,-93.19501304626465
RIBTHICK,PY,-186.3900260925293
RIBTHIN,PZ,-93.19501304626465
RIBTHICK,PZ,-186.3900260925293
*EL PRINT,ELSET=SHELL
COORD,S11,S22,S12
*EL PRINT,ELSET=SHELL
SF
*EL PRINT,ELSET=RIBS
COORD
*EL PRINT,ELSET=RIBS
SF
*PLOT,PLOTSIZE=4
*DETAIL,ELSET=SHELL
-1,-1,-1,13,0,1
*VIEWPOINT
0,1,0
*DISPLACED
U
*PLOT,PLOTSIZE=3
*DETAIL,ELSET=SHELL
-1,-1,-1,13,0,1
*VIEWPOINT
1,1,1
*DISPLACED
```

```
U
*PLOT,PLOTSIZE=3
*DETAIL,ELSET=SHELL
-1,-1,-1,4,0,1
*VIEWPOINT
0,1,0
*DISPLACED
U
*PLOT,PLOTSIZE=3
*DETAIL,ELSET=SHELL
8,-1,-1,13,0,1
*VIEWPOINT
0,1,0
*DISPLACED
U
*PLOT,PLOTSIZE=3
SF1 -1M-0M
*DETAIL,ELSET=SHELL
-1,-1,-1,0,0,1
*CONTOUR,DEFORM
SF1
*PLOT,PLOTSIZE=3
SF2 -1M-0M
*CONTOUR
SF2
*PLOT,PLOTSIZE=3
SF3 -1M-0M
*CONTOUR
SF3
*PLOT,PLOTSIZE=3
SF1
*DETAIL,ELSET=SHELL
0,-1,-1,2.1,0,1
*CONTOUR
SF1
*PLOT,PLOTSIZE=3
SF2
*CONTOUR
SF2
*PLOT,PLOTSIZE=3
SF3
*CONTOUR,DEFORM
SF3
*PLOT,PLOTSIZE=3
SF1
*DETAIL,ELSET=SHELL
0,-1,-1,12.1,0,1
*CONTOUR,DEFORM
SF1
*PLOT,PLOTSIZE=3
```

```
SF2
*CONTOUR,DEFORM
SF2
*PLOT,PLOTSIZE=3
SF3
*CONTOUR,DEFORM
SF3
*END STEP
```

APPENDIX K

LISTINGS OF PREPROCESSING PROGRAMS FOR THE VALIDATION FEM MODEL

K1: MAVAGEN.BAS - Program to generate FEM model of validation tube

```
5 'MAVAGEN.BAS
10 N=7000:  DIM NO(N),X(N),Y(N),Z(N)
20 ' DEFSNG A-H,O-Z
30 DIM ELSETRIB(10,36)
40 DIM NODE(8),XR(11),XFD(11)
60 KEY OFF:CLS
100 LOCATE 10,35:PRINT "MAVAGEN"
110 LOCATE 12,20:PRINT "ABAQUS MESH GENERATION FOR VALIDATION MODEL"
120 INPUT A$
130 PI=3.141592654#
140 DECPLACE=4
250 RS=.0519:' *** radius of centreline of the shell
260 YOFF=.0631:'*** y offset for centreline of shell
390 NXVALS=2:'16*** number of x stations
400 DATA .054,.074,.099,.1240,.1440,.1560,.1680,.1800,.1923,.2045
,.2168,.2290,.2413,.2535,.2657,.2780
450 NTOL=.05: ' *** tolerance on node distances for *MPC
500 DTOL=.01: ' *** tolerance on node distance for shell dome MPC
560'************************************************************
570 CLS:LOCATE  1,1:INPUT "Name of ABAQUS file ";NAMEFILE$
580 OPEN  NAMEFILE$ FOR OUTPUT AS #1
620 GOSUB 1030:' *** calculate cylinder nodes
630 GOSUB 3470:' *** write cylinder nodes
740 GOSUB 4340:' *** write cylinder elements
900 PRINT "          EXECUTION COMPLETE   ":CLOSE:STOP:END
910'*********************************************************
1010'*********************************************************
1020 '
1030 PRINT "Calculating cylinder nodes"
1040 '
1050 STARTANGD=0:ENDANGD=360:
1055 ELANGD=22.5:'**Element angle increment
1060 NEPR=ENDANGD/ELANGD:' *** number of elements per ring
1070 R=RS
1080 ESCYL=1:'*** element start cylinder
1090 ELANG=ELANGD*PI/180
1095  RESTORE 400:READ XLEFT
1100  NO=499:NONODE=0
1112  FOR NX=1 TO NXVALS-1
1113  READ XRIGHT:PRINT XRIGHT;
1140   FOR BOTANGD=STARTANGD TO ENDANGD-ELANGD STEP ELANGD
1150     BOTANG=BOTANGD*PI/180
1160     TOPANG =BOTANG+ELANG
1170   FOR POINTNO =NO+1 TO NO+8:NO(POINTNO)=POINTNO:NEXT POINTNO
1180     X(NO+1)=XLEFT:Z(NO+1)=R *SIN(TOPANG):Y(NO+1)=-R *COS(TOPANG)
1190     X(NO+2)=XLEFT:Z(NO+2)=R *SIN(BOTANG):Y(NO+2)=-R *COS(BOTANG)
1200     X(NO+3)=XRIGHT:Z(NO+3)=R *SIN(BOTANG):Y(NO+3)=-R *COS(BOTANG)
1210     X(NO+4)=XRIGHT:Z(NO+4)=R *SIN(TOPANG):Y(NO+4)=-R*COS(TOPANG)
```

```
1220      X(NO+5)=XLEFT:Z(NO+5)=R *SIN((TOPANG+BOTANG)/2)
:Y(NO+5)=-R*COS((TOPANG+BOTANG)/2)
1230      X(NO+6)=(XLEFT+XRIGHT)/2:Z(NO+6)=R *SIN(BOTANG)
:Y(NO+6)=-R*COS(BOTANG)
1240      X(NO+7)=XRIGHT:Z(NO+7)=R *SIN((BOTANG+TOPANG)/2)
:Y(NO+7)=-R*COS((BOTANG+TOPANG)/2)
1250      X(NO+8)=(XLEFT+XRIGHT)/2:Z(NO+8)=R *SIN(TOPANG)
:Y(NO+8)=-R*COS(TOPANG)
1260 ' *** routine to eliminate small numbers
1270        FOR I= 1 TO 8
1280         IF ABS(X(NO+I))<.00001 THEN LET X(NO+I)=0
1290         IF ABS(Y(NO+I))<.00001 THEN LET Y(NO+I)=0
1300         IF ABS(Z(NO+I))<.00001 THEN LET Z(NO+I)=0
1310 '*** truncate numbers according to decplace
1320            TRUNC=X(NO+I):GOSUB 10430:X(NO+I)=TRUNC
1330            TRUNC=Y(NO+I):GOSUB 10430:Y(NO+I)=TRUNC
1340            TRUNC=Z(NO+I):GOSUB 10430:Z(NO+I)=TRUNC
1350        NEXT I
1360    NONODE=NONODE+8
1370    NO=NO+ 8
1380   NEXT BOTANGD
1385  XLEFT=XRIGHT
1390 NEXT NX
1400 'define cylinder start and end nodes  : NSCYL and NECYL
1410 NSCYL=500:NECYL=NONODE+500:PRINT NSCYL;NECYL
1420 STNODE=NSCYL:ENNODE=NECYL :'*** parameters for eliminate routine
1430 GOSUB 10270:' *** routine to eliminate duplicate numbers
1440 RETURN
3460'************************************************************
3470 PRINT "Writing cylinder nodes"
3480 PRINT#1,"*NODE,NSET=NSHELL"
3490    FOR I=NSCYL TO NECYL
3500      IF I<>NO(I) THEN GOTO 3550
3510      PRINT#1,NO(I);",";
3520      PRINT#1,USING"#####.####";X(I);:PRINT#1,",";
3530      PRINT#1,USING"#####.####";Y(I)+YOFF;:PRINT#1,",";
3540      PRINT#1,USING"#####.####";Z(I);:PRINT#1,""
3550    NEXT I
3560 RETURN
4320'************************************************************
4330 '
4340 PRINT "Writing cylinder elements"
4350 '
4360 PRINT#1,"*ELEMENT,TYPE=S8R,ELSET=SHELL"
4370 NO=NSCYL-1
4380   ECYL=(NECYL-NSCYL+1)/8:'*** number of elements
4390   ESCYL=1:' *** element start cylinder
4400    FOR I=1 TO ECYL
4410       WRITE#1,I,NO(NO+1),NO(NO+2),NO(NO+3),NO(NO+4),NO(NO+5)
,NO(NO+6),NO(NO+7),NO(NO+8)
```

```
4440        NO=NO+8
4450      NEXT I
4460     EECYL=I-1:'*** element end cylinder
4470    CLOSE #2
4480 RETURN
10240'*************************************************************
10250 '*** routine to eliminate duplicate nodes
10260 '
10270 PRINT "Eliminate duplicate nodes"
10280 '
10290 FOR I= STNODE TO ENNODE
10300  X=X(I):Y=Y(I):Z=Z(I)
10310   FOR J=STNODE TO ENNODE
10315   LOCATE 10,1:PRINT NSCYL,I,NECYL,J
10320    IF  J=I THEN GOTO 10380
10330    IF X<>X(J) THEN  GOTO 10380
10340    IF Y<>Y(J) THEN  GOTO 10380
10350    IF Z<>Z(J) THEN  GOTO 10380
10360  IF NO(J)>NO(I) THEN LET NO(J)=NO(I):GOTO 10390
10370  IF NO(J)<=NO(1) THEN  LET NO(I)=NO(J):GOTO 10390
10380   NEXT J
10390  NEXT I
10400 RETURN
10410'*************************************************************
10420  '****   routine to truncate numbers
10430   TRUNC=TRUNC*10^DECPLACE
10440   TRUNC=INT(TRUNC)
10450 '      TRUNC$=STR$(TRUNC)
10460 '       TRLE=LEN(TRUNC$)
10470 '         FOR IC = 1 TO TRLE
10480 '            A$=MID$(TRUNC$,IC,1):IF A$="." THEN LET
TRUNC$=LEFT$(TRUNC$,IC+DECPLACE)
10490 '           NEXT IC
10500   TRUNC=TRUNC/10^DECPLACE
10510  '      TRUNC=VAL(TRUNC$)
10520   RETURN
10530 ' ****************************************
```

K2 : NISA-ABA.BAS - Program to convert NISA FEM input data into ABAQUS input format

```
5 CLOSE
10 DIM N(21)
20 CLS:PRINT "NISA-ABA : PROGRAM TO CONVERT NISA TO ABAQUS INPUT
FILES"
30 PRINT
40 '*** dummy variables for *element headings
50 DUMSH$="N":BRICK$="N":BEAM$="N"
60 '************************************************************
70 '*** start file open *****
80 INPUT "INPUT FILENAME :";INFILE$
90 INPUT "OUTPUT FILENAME :";OUTFILE$
100   OPEN INFILE$ FOR INPUT AS #1
110   OPEN "TEMPORAR" FOR OUTPUT AS #2
120   OPEN OUTFILE$ FOR OUTPUT AS #3
122 HEADING$="VALID4-1 VALIDATION MODEL EX NISA"
124 PRINT#3,"*HEADING"
126 PRINT#3,HEADING$
128 PRINT#3,"*DATA CHECK"
130 PRINT#3,"*PREPRINT,ECHO=YES,HISTORY=YES,MODEL=YES"
132 '************************************************************
140 '*** search for *ELTYPE
150 I=0
160 LINE INPUT#1,A$
170   WHILE LEFT$(A$,7)<>"*ELTYPE"
180     LINE INPUT#1,A$
190   WEND
200'************************************************************
210 ' *** load element id index, type number and order
215      I=I+1:INPUT#1,NSRL$(I)
220     IF LEFT$(NSRL$(I),8)= "*RCTABLE"  THEN GOTO 260
230        INPUT#1,NKTP(I),NORDR(I)
240     GOTO 215
250 '** rewrite element id index as a number
260   FOR J=1 TO I-1:NSRL(J)=VAL(NSRL$(J)):NEXT J
270 A$=""
280 '** search for elements
290   WHILE LEFT$(A$,8)<>"*ELEMENT"
300   LINE INPUT#1,A$
320   WEND
330'************************************************************
340 ' *** search for nodes
350 INPUT#1,NELID$
360   IF LEFT$(NELID$,6)= "*NODES"  THEN CLOSE#2:GOTO 450
363 INPUT#1,MATID,NSRL,IDRC,KISO
370 NELID=VAL(NELID$)
380 IF NKTP(NSRL)=20 AND NORDR(NSRL)=2 THEN GOSUB 720
390 IF NKTP(NSRL)=4 AND NORDR(NSRL)=2 THEN GOSUB 620
```

```
400 IF NKTP(NSRL)=12 AND NORDR(NSRL)=1 THEN GOSUB 830
410   GOTO 350
430'************************************************************
440 ' *** input and rewrite nodes
450 PRINT#3,"*NODE"
451 '     INPUT#1,DUM1$,DUM2$
452       INPUT#1,ND$
460    IF LEFT$(ND$,9) ="*MATERIAL"  THEN GOTO 520
470      INPUT#1,IDCSYS,INDEX,NSET,X,Y,Z,IDDSYS
472       ND=VAL(ND$)
473 IF ABS(X)<.000001 THEN LET X=0
474 IF ABS(Y)<.000001 THEN LET Y=0
475 IF ABS(Z)<.000001 THEN LET Z=0
476 U$="##.####"
480       PRINT#3, ND;
482       PRINT#3, ",";:PRINT#3, USING U$;X;
484       PRINT#3, ",";:PRINT#3, USING U$;Y;
486       PRINT#3, ",";:PRINT#3, USING U$;Z
490   GOTO 452
500'************************************************************
510 ' *** read element data  from temporary file and merge with nodes
520 OPEN "TEMPORAR" FOR INPUT  AS #2
530  WHILE NOT EOF(2)
540    LINE INPUT#2,A$
550    PRINT #3,A$
560  WEND
570 CLOSE
580 STOP
590 CLOSE
600'************************************************************
610 '***  read and write brick elements *****
620 INPUT#1,N(7),N(1),N(3),N(5),N(19),N(13),N(15),N(17),N(8),N(2)
,DUM,N(4),N(6),N(20),N(14),N(16),N(18),N(12),N(9),N(10),N(11),A$
630  IF BRICK$="N" THEN PRINT #2,"*ELEMENT,TYPE=C3D20,
ELSET=BRICK":BRICK$="Y"
640 WRITE#2,NELID,N(19),N(12),N(10),N(15),N(3),N(16),N(20)
,N(7),N(4),N(9),N(6),N(13),N(2),N(14),N(8)
655 WRITE#2,N(1),N(5),N(18),N(11),N(17)
660 RETURN
700'************************************************************
710 '***  read and write shell elements *****
720 INPUT#1,N(1),N(3),N(5),N(7),N(2),N(4),N(6),N(8),A$
740  IF DUMSH$="N" THEN PRINT #2,"*ELEMENT,TYPE=S8R,ELSET=SHELL"
:DUMSH$="Y"
770      WRITE#2,NELID,N(1),N(6),N(2),N(5),N(8),N(4),N(7),N(3)
800 RETURN
810'************************************************************
820 '***  read and write beam elements *****
830 CLS:PRINT "not yet available on this version":RETURN
```

K3 : MAMPC.BAS - Program to connect the ribs to the shell and write this data in ABAQUS format

```
5 CLOSE
20 CLS:PRINT "MAMPC  :  PROGRAM TO CONNECT RIBS TO SHELL AND WRITE
ABAQUS FILE FOR VALIDATION MODEL"
30 PRINT
60 '************************************************************
63 PTOL=.003
65 NR=500:DIM RNO(NR),RX(NR),RY(NR),RZ(NR)
66 NS=1500:DIM SNO(NS),SX(NS),SY(NS),SZ(NS)
70 '*** start file open *****
75  INPUT "INPUT NAME OF ABAQUS.INP FILE ";ABA$
77   OPEN ABA$ FOR OUTPUT AS #1
78     GOSUB 132:'***write intro for abaqus
80     GOSUB 145:'*** rib nodes
82     GOSUB 245:'*** shell nodes
85     GOSUB 540:'*** write elements
90     GOSUB 360:'*** write *MPC
100    GOSUB 1245:'*** write history data
110  CLOSE#1
120 PRINT "Program complete":STOP:END
130 '************************************************************
132 PRINT "Writing input section"
134 PRINT#1,"*HEADING,CORE=320000"
136 PRINT#1,"VALIDATION MODEL 5-1"
138 PRINT#1,"*DATA CHECK"
139 PRINT#1,"*PREPRINT,ECHO=YES,HISTORY=YES,MODEL=YES"
140 RETURN
143 '************************************************************
145 PRINT "*** Load the rib nodes"
150 OPEN "NORIBS" FOR INPUT AS #2
170 LINE INPUT#2,A$
180 PRINT#1,A$
185 NNR=0
190  WHILE NOT EOF(2)
191    NNR=NNR+1:INPUT#2,RNO(NNR),RX(NNR),RY(NNR),RZ(NNR)
192     IF ABS(RX(NNR))<.00001 THEN LET RX(NNR)=0
193     IF ABS(RY(NNR))<.00001 THEN LET RY(NNR)=0
194     IF ABS(RZ(NNR))<.00001 THEN LET RZ(NNR)=0
202 F$="###.####"
204    PRINT#1,RNO(NNR);:PRINT#1, ",";
206    PRINT#1,USING F$;RX(NNR);:PRINT#1,",";
207    PRINT#1,USING F$;RY(NNR);:PRINT#1,",";
208    PRINT#1,USING F$;RZ(NNR)
220  WEND
225 CLOSE #2
230 RETURN
240 ' ***************************************
245 PRINT "*** Load the shell nodes"
```

```
250 OPEN "NOSHELL" FOR INPUT AS #2
270 LINE INPUT#2,A$
280 PRINT#1,A$
285 NNS=0
290  WHILE NOT EOF(2)
300    NNS=NNS+1:INPUT#2,SNO(NNS),SX(NNS),SY(NNS),SZ(NNS)
301     IF ABS(SX(NNS))<.00001 THEN LET SX(NNS)=0
302     IF ABS(SY(NNS))<.00001 THEN LET SY(NNS)=0
303     IF ABS(SZ(NNS))<.00001 THEN LET SZ(NNS)=0
304    PRINT#1,SNO(NNS);:PRINT#1,",";
306    PRINT#1,USING F$;SX(NNS);:PRINT#1,",";
307    PRINT#1,USING F$;SY(NNS);:PRINT#1,",";
308    PRINT#1,USING F$;SZ(NNS)
320  WEND
330 CLOSE #2
340 RETURN
350 '*******************************************
360 PRINT"Establish *MPC between ribs and shell"
370 PRINT "Nodes: Shell,RIBS :";NNS;NNR
375 PRINT#1,"*MPC"
377 MPCOUNT=0
380 FOR I=1 TO NNS
390   LOCATE 10,1:PRINT "Shell: ";I
400    FOR J=1 TO NNR
410     LOCATE 10,12:PRINT "Ribs: ";J
420      IF ABS(SX(I)-RX(J))>PTOL THEN 500
430      IF ABS(SY(I)-RY(J))>PTOL THEN 500
440      IF ABS(SZ(I)-RZ(J))>PTOL THEN 500
450     WRITE#1,6;RNO(J);SNO(I):MPCOUNT=MPCOUNT+1
500   NEXT J
510  NEXT I
515 PRINT "MPCOUNT= ";MPCOUNT
520 RETURN
530 '*******************************************
540 PRINT "Write rib and shell elements"
550 OPEN "ELSHELL" FOR INPUT AS #2
560  WHILE NOT EOF(2)
570   LINE INPUT#2,A$
580    PRINT#1,A$
585   WEND
590  CLOSE #2
600 OPEN "ELRIBS" FOR INPUT AS #2
610  WHILE NOT EOF(2)
620   LINE INPUT#2,A$
1160  PRINT#1,A$
1170 WEND
1180 CLOSE #2
1240 RETURN
1243 '*******************************
1245 PRINT "Write history and boundary data"
```

```
1247 OPEN "VALEND.INP" FOR INPUT AS #2
1249   WHILE NOT EOF(2)
1250    LINE INPUT#2,A$
1260    PRINT#1,A$
1270   WEND
1280 CLOSE #2
1300 RETURN
1310 '*******************************************
```

APPENDIX L

SUMMARISED LISTING OF VALIDATION FEM INPUT FILE

```
*HEADING
VALID10-1 NODES COMMON, LAMINATED
*DATA CHECK
*PREPRINT,ECHO=YES,HISTORY=YES,MODEL=YES
*NODE,NSET=ALL
1 , 0.0540, 0.1150, 0.0000
1077 , 0.0405,-0.0072,-0.0370
*ELEMENT,TYPE=S8R,ELSET=SHELL
1,1,15,17,3,10,16,11,2
619,863,705,717,873,864,709,874,867
*ELEMENT,TYPE=C3D20,ELSET=RIBS
2000,413,424,422,411,17,3,1,15,417,423,416,412,11,2,10
16,409,420,419,408
2515,922,930,975,970,585,573,753,763,924,976,972,971,577,754,757
764,918,926,973,968
*ELEMENT,TYPE=C3D20,ELSET=ROD
3000,981,988,986,979,518,507,505,516,983,987,982,980,511,506,510
517,978,985,984,977
3505,1075,1062,942,1072,1034,1012,488,1029,1077,1060,1076,1073,1039,10
1032,1074,1061,941,1071
*ELSET,ELSET=ALL
SHELL,ROD,RIBS
*ORIENTATION,NAME=CYL0,SYSTEM=C
0,0.0631,0,.280,0.0631,0
1,0
*ORIENTATION,NAME=CYL+45,SYSTEM=C
0,0.0631,0,.280,0.0631,0
1,45
*ORIENTATION,NAME=CYL-45,SYSTEM=C
0,0.0631,0,.280,0.0631,0
1,-45
*MATERIAL,NAME=LAM
*ELASTIC,TYPE=LAMINA
38.6E9,8.27E9,.26,4.14E9,4.14E9,3.5E9
*MATERIAL,NAME=STEEL
*ELASTIC
200E9,.3
*MATERIAL,NAME= TIFF
*ELASTIC
469E9,.3
*SHELL SECTION,ELSET=SHELL,COMPOSITE
2.3625E-4,3,LAM,CYL+45
2.3625E-4,3,LAM,CYL-45
2.3625E-4,3,LAM CYL+45
2.3625E-4,3,LAM, CYL-45
***CENTRE LINE
2.3625E-4,3,LAM,CYL-45
2.3625E-4,3,LAM,CYL+45
2.3625E-4,3,LAM,CYL-45
2.3625E-4,3,LAM,CYL+45
```

```
** USE 8 LAYERS INSTEAD OF ACTUAL 6 IN ORDER TO AVOID COUPLING
*TRANSVERSE SHEAR STIFFNESS
4.14E9,3.5E9
*SOLID SECTION,ELSET=RIB,MATERIAL=STEEL
*SOLID SECTION,ELSET=ROD,MATERIAL=STIFF
*NSET,NSET=RODEND
425,426,427,428,429,430,431,432,433,434,
435,436,437,438,439,440,441,442,443,444,
472,473,474,475,476,477,478,479,480,481,
482,483
*NSET,NSET=SHLEND
211,212,213,214,215,216,217,218,219
400,401,402,403,404,405,406,407,
710,711,712,713,714,715,716,717,
868,869,870,871,872,873,874,
*BOUNDARY
 SHLEND,XSYMM
 **RODEND,3
*PLOT,PLOTSIZE=3
 VALIDATION 9-1
*VIEWPOINT
1,1,1
*SHRINK,FACTOR=.2
*DRAW,ELNUM
*VIEWPOINT
0,1,0
*DRAW,ELNUM
**STEP,NLGEOM,AMP=RAMP
*STEP,LINEAR=NEW,AMP=RAMP
*STATIC,PTOL=1
*CLOAD
1020,1,-3000
1021,1,-1000
1066,1,-1000
*EL PRINT,ELSET=SHELL,POSITION=INTERGRATION POINT
COORD,S11,S22,S12
*EL PRINT,ELSET=SHELL,POSITION=INTERGRATION POINTS
SF
*EL PRINT
RF
*PLOT,PLOTSIZE=3
VALIDATION 10 DISPLACED
*DISPLACED
U
*PLOT,PLOTSIZE=3
VALIDATION 10-1 SF11 (N/M)
*DETAIL,ELSET=SHELL
*CONTOUR
SF1
*PLOT,PLOTSIZE=3
```

```
VALIDATION 10-1 SF22 (N/M)
*DETAIL,ELSET=SHELL
*CONTOUR
SF2
*PLOT,PLOTSIZE=3
VALIDATION 10-1 SF12 (N/M)
*DETAIL,ELSET=SHELL
*CONTOUR
SF3
*PLOT,PLOTSIZE=3
VALIDATION 10-1 SF11 (N/M)
*DETAIL,ELSET=SHELL
*CONTOUR
SF1
*PLOT,PLOTSIZE=3
VALIDATION 10-1 SF22 (N/M)
*DETAIL,ELSET=SHELL
*CONTOUR
SF2
*PLOT,PLOTSIZE=3
VALIDATION 10-1 SF12 (N/M)
*DETAIL,ELSET=SHELL
*CONTOUR
SF3
*END STEP
```

APPENDIX M

LISTING OF THE MACONV GRAPHICS GENERATION PROGRAM

```
5   ' MACONV.BAS
10 CLEAR:KEY ON:SCREEN 0 :CLS
70 N= 4000:   DIM     NODENO(N),X(N),Y(N),Z(N)
100 N=N*1.5:    DIM STPOINT(N),ENDPOINT(N),NODE(20)
160 '*********************************************************
190 KEY OFF:CLS
220 LOCATE 10,35:PRINT "MACONV"
250 LOCATE 12,20:PRINT "Program to convert ABAQUS INP file to line
file"
280 INPUT AAA
290    CLS:LOCATE  1,1:INPUT "Name of ABAQUS input file ";NAMEINP$
300     OPEN  NAMEINP$ FOR INPUT AS #1
310    LOCATE  5,1:INPUT "Name of line output file ";NAMEOUT$
330     OPEN  NAMEOUT$ FOR OUTPUT AS #2
335 CLS
340   GOSUB 2200:' *** fetch ABAQUS INP file and convert
350   GOSUB 550:' *** save data ..s line file
360   PRINT"Program complete" :STOP
400   END
430'*************************************************************
460 '*** SUBROUTINE to save co-ordinate and line data
530 '*** write nodes to file
550    PRINT#2,NONODE
580     FOR I=1 TO NONODE
610      PRINT#2,I;" ";X(I);" ";Y(I);" ";Z(I)
640     NEXT I
650 '** calculate no. of active lines
660  ACTLIN=NOLIN
670 FOR I=1 TO NOLIN
680  IF STPOINT(I)=0 OR ENDPOINT(I)=0 THEN ACTLIN=ACTLIN-1
690 NEXT I
700 ' *** write lines to file
790    PRINT#2,ACTLIN
820     FOR I=1 TO NOLIN
850       IF STPOINT(I)=0 OR ENDPOINT(I)=0 THEN 910
860     PRINT#2,STPOINT(I);" ";ENDPOINT(I)
910     NEXT I
940   CLOSE#2
970 RETURN
1000'*********************************************************
1030 '*** LEVEL 1 SUBROUTINE to load ABAQUS file and plot data points
1060 CLS:LOCATE  1,1:'INPUT "Name of file ";NAMEFILE$
1065 'NAMEFILE$=NAMEFILE$+".LIN"
1090 OPEN  NAMEFILE$ FOR INPUT AS #1
     CLS
1120 INPUT#1,NONODE
1150 FOR I=1 TO NONODE
1180     INPUT#1,NODENO(I),X(I),Y(I),Z(I)
1210   ' PRINT   NODENO(I);X(I);Y(I);Z(I)
1240 NEXT I
```

```
1270 '     INPUT "Press return to continue";A$
1300 INPUT#1,NOLIN
1330 FOR I=1 TO NOLIN
1360   INPUT#1,STPOINT,   ENDPOINT
1390     FOR J= 1 TO NONODE
1420       IF STPOINT=NODENO(J) THEN LET STPOINT(I)=J:GOTO 1480
1450     NEXT J
1480     FOR J= 1 TO NONODE
1510       IF ENDPOINT=NODENO(J) THEN LET ENDPOINT(I)=J:GOTO 1570
1540     NEXT J
1570 NEXT I
1600 CLOSE#1
1630 RETURN
1660'************************************************************
1690 'level ? subroutine  to find nodenum from abaout
1720 FOR I1=1 TO NONODE
1750 IF STPOINT(I)= NODENO(I1) THEN RETURN
1780 NEXT I1
1810 RETURN
1840'************************************************************
1870 'level ? subroutine  to find nodenum from abaout
1900 FOR I2=1 TO NONODE
1930 IF ENDPOINT(I)= NODENO(I2) THEN RETURN
1960 NEXT I2
1990 RETURN
2020'************************************************************
2050 '*** Routine to load abaqus.INP input file and generate line file
2170 '*** load in all node numbers
2200 I=0:J=0:P=0
2230 LINE INPUT#1,A$
2260 IF EOF(1) THEN PRINT "Data not found":RETURN
2290 IF LEFT$(A$,5)<>"*NODE" THEN 2230
2300 PRINT "Found node numbers"
2320   INPUT#1,A$
2350     IF LEFT$(A$,8)="*ELEMENT" THEN NONODE=J:GOTO 2490
2380     IF LEFT$(A$,5)="*NODE" THEN INPUT#1,B$,A$:'PRINT B$
2390        J=J+1
2410         NODENO(J)=VAL(A$)
2440         INPUT#1,X(J),Y(J),Z(J)
2445        IF B$="NSET=NRIBS" THEN INPUT#1,D1,D2,D3
2447 '  PRINT NODENO(J);X(J);Y(J)
2480   GOTO 2320
2485 '*** load in all the elements **********************
2490 PRINT "Found elements"
2530  INPUT#1,B$,C$
    '  PRINT B$,C$
2560   IF B$="TYPE=S8R" THEN  NOPEEL=8:SIGNODE=4:GOTO 2659
2590   IF B$="TYPE=STRI3" THEN NOPEEL=3:SIGNODE=3:GOTO 2659
2620   IF B$="TYPE=B32" THEN NOPEEL=3:SIGNODE=3:GOTO 2659
2625   IF B$<> "TYPE=C3D20" THEN PRINT "ELEMENT UNKNOWN" :GOTO 3010
```

```
2627'*** special routine for solid elements
2630 INPUT#1,A$
2635    IF LEFT$(A$,6)="*ELSET" THEN NOLIN=P: GOTO 3010
2637    IF LEFT$(A$,4)="*MPC" THEN NOLIN=P: GOTO 3010
2640    IF LEFT$(A$,8)="*ELEMENT" THEN GOTO 2530
2645       GOSUB 5400
2655       GOTO 2630
2656'*** load in other nodes
2659 INPUT#1,A$
2680     IF LEFT$(A$,6) = "*ELSET" OR LEFT$(A$,4)="*MPC" THEN
NOLIN=P:GOTO 3010
2710     IF LEFT$(A$,8) = "*ELEMENT" THEN GOTO 2530
2740      FOR I=1 TO NOPEEL
2770       INPUT#1,NODE(I)
2800      NEXT I
2830        FOR I=1 TO SIGNODE-1
2860         P=P+1:STPOINT(P)=NODE(I):ENDPOINT(P)=NODE(I+1)
2890        NEXT I
2920   IF NOPEEL=8 AND SIGNODE=4 THEN
P=P+1:STPOINT(P)=NODE(4):ENDPOINT(P)=NODE(1)
2940   GOTO 2659
3000 '*** eliminate duplicate nodes
3010   INPUT "Do you want to eliminate duplicate lines (Y/N) ";DUM$
3020 IF DUM$<>"N" THEN GOSUB 4960
3045 PRINT"Link nodes with lines"
3046 PRINT "NONODE= ";NONODE;" NOLIN= ";NOLIN
3047 FOR J=1 TO NONODE
3048 LOCATE 10,1:PRINT "NODE= ";J
3049 FOR I=1 TO NOLIN
3050 LOCATE 10,20:PRINT ".    - ";I
3051 IF STPOINT(I)=0 THEN GOTO 3056
3053   IF NODENO(J)=STPOINT(I) THEN  LET STPOINT(I)=J
3054 IF ENDPOINT(I)=0 THEN GOTO 3056
3055   IF NODENO(J)=ENDPOINT(I) THEN LET ENDPOINT(I)=J
3056 NEXT I
3057 NEXT J
3060 CLOSE#1:PRINT NONODE;NOLIN:'**INPUT AAA
3130 RETURN
3160'*************************************************************
3190 'level ? subroutine  to find nodenum from abaout
3220 FOR I1=1 TO NONODE
3250 IF STPOINT(I)= NODENO(I1) THEN RETURN
3280 NEXT I1
3310 RETURN
3340'*************************************************************
3370 'level ? subroutine  to find nodenum from abaout
3400 FOR I2=1 TO NONODE
3430 IF ENDPOINT(I)= NODENO(I2) THEN RETURN
3460 NEXT I2
3490 RETURN
```

```
3520'************************************************************
3550  '****   routine to truncate numbers
3580   TRUNC=TRUNC*10^DECPLACE
3610   TRUNC=INT(TRUNC)
3640   TRUNC=TRUNC/10^DECPLACE
3670   RETURN
3700'************************************************************
3730 '*** ROUTINE TO SAVE DATA AS NISA.NEU FILE ************
3760 CLS:LOCATE  1,1:INPUT "Name of file ";NAMEFILE$
3790 OPEN  NAMEFILE$ FOR OUTPUT AS #1
3820  PRINT#1,NAMEFILE$
3850 FOR I=1 TO NONODE
3880 IF NODENO(I)=0 THEN GOTO 4150
3910 IF NODENO(I)<>I THEN GOTO 4150
3940  COUNTG=NODENO(I)
3970   SPAG$=CHR$(32)+CHR$(32)+CHR$(32)
4000     IF COUNTG>9 THEN SPAG$=CHR$(32)+CHR$(32)
4030     IF COUNTG>99 THEN SPAG$=CHR$(32)
4060     IF COUNTG>999 THEN SPAG$=""
4090    PRINT #1,1;SPAG$;COUNTG
4120   PRINT #1,USING "#.########^^^^ ";X(I),Y(I),Z(I)
4150 NEXT I
4180 '*** print lines to disc
4210 FOR I = 1 TO NOACTLIN
4240 IF STPOINT(I)=0 OR ENDPOINT(I)=0 THEN 4780
4270  COUNTL=I
4300   SPAL$=CHR$(32)+CHR$(32)+CHR$(32)
4330    IF COUNTL>9 THEN SPAL$=CHR$(32)+CHR$(32)
4360    IF COUNTL>99 THEN SPAL$=CHR$(32)
4390    IF COUNTL>999 THEN SPAL$=""
4420 PRINT #1,2;SPAL$;COUNTL
4450      X1=X(STPOINT(I)):Y1=Y(STPOINT(I)):Z1=Z(STPOINT(I))
4480      X4=X(ENDPOINT(I)):Y4=Y(ENDPOINT(I)):Z4=Z(ENDPOINT(I))
4510      DIVX=(X4-X1)/3
4540      DIVY=(Y4-Y1)/3
4570      DIVZ=(Z4-Z1)/3
4600     X2=X1+DIVX:Y2=Y1+DIVY:Z2=Z1+DIVZ
4630     X3=X1+2*DIVX:Y3=Y1+2*DIVY:Z3=Z1+2*DIVZ
4660     PRINT #1,USING "#.########^^^^";X1,Y1,Z1
4690     PRINT #1,USING "#.########^^^^";X2,Y2,Z2
4720     PRINT #1,USING "#.########^^^^";X3,Y3,Z3
4750 '    PRINT #1,USING "#.########^^^^ ";X4,Y4,Z4
4780 NEXT I
4810 CLOSE #1
4840 RETURN
4870'************************************************************
4900 '** routine to eliminate similar lines
4960 PRINT "Removing duplicate lines "
5000 PRINT "NOLIN= ";NOLIN
5020 FOR I= 1 TO NOLIN
```

```
5025 LOCATE 6,2:PRINT "I= ";I
5060 IF STPOINT(I)=0 OR ENDPOINT(I)=0 THEN 5230
5080  FOR J=1 TO NOLIN
5090 LOCATE 6,10:PRINT "J= ";J
5110  IF STPOINT(J)=0 OR ENDPOINT(J)=0 THEN 5230
5140   IF J=I THEN 5230
5170   IF STPOINT(I)=STPOINT(J) AND ENDPOINT(I)=ENDPOINT(J) THEN
STPOINT(I)=0:ENDPOINT(I)=0
5200   IF STPOINT(I)=ENDPOINT(J) AND ENDPOINT(I)=STPOINT(J) THEN
STPOINT(I)=0:ENDPOINT(I)=0
5230  NEXT J
5260 NEXT I
5290 RETURN
5320'*************************************************************
5400 '*** routine to input brick element
5401 '*** input nodes
5404 FOR I=1 TO 15
5406INPUT#1,NODE(I)
5408 NEXT I
5409 INPUT#1,DUM$
5410 FOR I = 16 TO 20
5412  INPUT#1,NODE(I)
5414 NEXT I
5416 '*** define lines
5418 FOR I= 1 TO 3
5420  P=P+1:STPOINT(P)=NODE(I):ENDPOINT(P)=NODE(I+1)
5430 NEXT I
5440 FOR I=5 TO 8
5442  P=P+1:STPOINT(P)=NODE(I):ENDPOINT(P)=NODE(I+1)
5444 NEXT I
5450 P=P+1:STPOINT(P)=NODE(4):ENDPOINT(P)=NODE(1)
5460 P=P+1:STPOINT(P)=NODE(8):ENDPOINT(P)=NODE(5)
5470 P=P+1:STPOINT(P)=NODE(5):ENDPOINT(P)=NODE(1)
5480 P=P+1:STPOINT(P)=NODE(6):ENDPOINT(P)=NODE(2)
5490 P=P+1:STPOINT(P)=NODE(7):ENDPOINT(P)=NODE(3)
5500 P=P+1:STPOINT(P)=NODE(8):ENDPOINT(P)=NODE(4)
5510 RETURN
```

APPENDIX N

LISTING OF MA3DCAD PREVIEW PROGRAM

```
10 CLEAR:KEY ON:SCREEN 0 :CLS
20 DIM T(4,4):' *** scale,rotate,translate and reflect matrices
30 N=4000:  DIM    NODENO(N),X(N),Y(N),Z(N)
40 N=N*2:   DIM STPOINT(N),ENDPOINT(N),NODE(8)
50 'ON ERROR GOTO  5920
60 GOSUB 4280: '*** setup of all dummy  values
61 'intro message for program
62 KEY OFF:CLS
63 LOCATE 10,35:PRINT "MA3DCAD.BAS"
64 LOCATE 12,20:PRINT "3 - Dimensional Finite Element Mesh Preview
Program"
65 KEY ON
80 SUBDUM=0
90 KEY 1, "CREATE"
100 KEY 2, "SAVE "
110 KEY 3, "LOAD "
120 KEY 4, "VIEW  "
130 KEY 6, "DATA"
140 KEY 5, "PRINT"
150 KEY 7,""
160 KEY 8, "PLOT"
170 KEY 10, "ROOT"
180 KEY  9," EXIT"
190 A$=INKEY$
200 A=VAL(A$)
210 IF A=0 THEN 190
220 ON A GOSUB 290,650,470,1200,1060,910,250,7020,250
230 CLS:IF SUBDUM<>0 THEN LET SUBDUM=0:GOTO 70
240 GOTO 190
250 CLS:INPUT "ARE YOU SURE ";A$:IF A$= "Y" THEN END
260 GOTO 70
270'************************************************************
280 '*** level 1 routine to create picture **********************
290 CLS
300 SUBDUM=1:KEY 1, ""
310 KEY 2, "POINTS"
320 KEY 3, ""
330 KEY 4, ""
340 KEY 5, ""
350 KEY 6, ""
360 KEY 7, ""
370 KEY 8, "CONTOU"
380 KEY  9," EXIT"
390 KEY 10,"CREATE"
400 A$=INKEY$
410 A=VAL(A$):PLOPT=A
420 IF A=0 THEN 400
430 ON A GOSUB 400,400,400,400,400,400,400,8130,440
440 RETURN
450'************************************************************
```

```
460 '*** level 1 routine to load data from disk **************
470 CLS
480 SUBDUM=1:KEY 1, "LINE  "
490 KEY 2, "ABAIN"
500 KEY 3, "ABAOUT"
510 KEY 4, "MERGE"
520 KEY 5, ""
530 KEY 6, ""
540 KEY 7, ""
550 KEY 8, ""
560 KEY  9," EXIT"
570 KEY 10,"LOAD"
580 A$=INKEY$
590 A=VAL(A$):PLOPT=A
600 IF A=0 THEN 480
610 ON A GOSUB 840,9920,6710,9360,580,580,580,580,620
620 RETURN
630'*************************************************************
640 '*** level 1 routine to save data to disk ********************
650 CLS
660 SUBDUM=1:KEY 1, "LINE  "
670 KEY 2, ".NEU"
680 KEY 3, ""
690 KEY 4, ""
700 KEY 5, ""
710 KEY 6, ""
720 KEY 7, ""
730 KEY 8, ""
740 KEY  9," EXIT"
750 KEY 10,"SAVE"
760 A$=INKEY$
770 A=VAL(A$):PLOP'   .
780 IF A=0 THEN 760
790 ON A GOSUB 6390,10370,800,800,800,800,800,800,800
800 RETURN
810'*************************************************************
820 '*** level 2 routine to load line data from disk ************
840 SUBDUM=2:CLS:LOCATE 10,40:PRINT "BUSY"
850 GOSUB 6560: '*** load data into matrices no(i),x(i),y(i),z(i)
860 GOSUB 4710: '*** transform rotation matrix to unity
870 RETURN
880'*************************************************************
890 '*** Level 1  menu for displaying all data
900 '*** Level 1  menu for displaying all data
910 CLS: PRINT "i   NODENO     x          y          z  "
920 FOR I=1 TO NONODE
930 IF NODENO(I)=0 THEN  950
940 PRINT I;NODENO(I);X(I);Y(I);Z(I)
950 NEXT I
960  PRINT
```

```
970  PRINT "Line No    start     end"
980 FOR I=1 TO NOLIN
990 IF STPOINT(I)=0 OR ENDPOINT(I)=0 THEN 1010
1000 PRINT I;STPOINT(I);ENDPOINT (I)
1010 NEXT I
1020 INPUT A$
1030 RETURN
1040'************************************************************
1050 '*** Level 1  menu for displaying all data
1060 CLS:LPRINT "Node No       x          y          z  "
1070 FOR I=1 TO NONODE
1080 IF NODENO(I)=0 THEN GOTO 1100
1090 LPRINT I;NODENO(I);X(I);Y(I);Z(I)
1100 NEXT I
1110  LPRINT
1120 FOR I=1 TO NOLIN
1130 IF STPOINT(I)=0 OR ENDPOINT(I)=0 THEN 1150
1140 LPRINT I;STPOINT(I);ENDPOINT (I);"     ";
1150 NEXT I
1160 RETURN
1170'************************************************************
1180 LPRINT "Line No    start     end"
1190 '*** Level 1  menu for viewing and manipulating of picture
1200 GOSUB 4710: ' *** transformation matrix to unity matrix
1210 CLS
1220 SUBDUM=1:RETDUM=0
1230 KEY 1, "-SCALE"
1240 KEY 6, "-ZOOM"
1250 KEY 5, "-PERSP"
1260 KEY 4, "-TRANS"
1270 KEY 3,"-DRAW"
1280 KEY 2, "-ROTAT"
1290 KEY 7, "-ANG-XY"
1300 KEY 8, "-ANG-Z"
1310 KEY  9,"-EXIT"
1320 KEY 10,"VIEW"
1330 A$=INKEY$
1340 A=VAL(A$)
1350 IF A=0 THEN 1330
1360 SUBDUM=1
1370 ON A GOSUB 1450,2810,3650,1870,3320,3380,3510,3580, 1420
1380 IF RETDUM=1 THEN LET RETDUM=0:RETURN
1390 IF SUBDUM<>1 THEN GOTO 1230
1400 GOTO 1330
1410'************************************************************
1420 RETDUM=1:RETURN
1430'************************************************************
1440 '*** LEVEL 2 SUBROUTINE FOR SCALING OF PICTURE BY MULTIPLICATION
BY FACTOR
1450 RETDUM=0:SUBDUM=2
```

```
1460 KEY 1, "-ALL"
1470 KEY 2, "-X"
1480 KEY 3, "-Y"
1490 KEY 4, "-Z"
1500 KEY  9, "EXIT"
1510 KEY 5 , ""
1520 KEY 6 , ""
1530 KEY 7 , ""
1540 KEY 8 , ""
1550 KEY 10, "SCALE"
1560 A$=INKEY$
1570 IF A$="" THEN 1560
1580 ON VAL(A$) GOSUB 1660,1710,1760,1810,1640,1640,1640,1540,3480
1590 IF RETDUM=1 THEN LET RETDUM=0:RETURN
1600 IF VAL(A$)>=5 AND VAL(A$)<=8 THEN 1560
1610 GOSUB 2330:'*** assign a,b,c values to transformation matrix
1620 GOSUB 2380:'*** update the points data file
1630 GOTO 1560
1640 RETURN
1650 ' ***  level 6 subroiutine .o input all scaling
1660 KEY OFF:LOCATE 25,1:PRINT "Scaling factor <";A;"> ";:INPUT A$
1670 IF A$<>"" THEN GOSUB 4710:A=VAL(A$):B=VAL(A$):C=V  (A$)
1680 KEY ON
1690 RETURN
1700 ' ***  level 6 subroutine to input X scaling
1710 KEY OFF:LOCATE 25,1:PRINT "X Scaling  actor <";A;"> ";:INPUT A$
1720 IF A$<>"" THEN GOSUB 4710:A=VAL(A$):B=1:C=1
1730 KEY ON
1740 RETURN
1750 ' ***  level 6 subroutine to input Y scaling
1760 KEY OFF:LOCATE 25,1:PRINT "Y Scaling factor <";B;"> ";:INPUT A$
1770 IF A$<>"" THEN GOSUB 4710:B=VAL(A$):A=1:C=1
1780 KEY ON
1790 RETURN
1800 ' ***  level 6 subroutine to input Z scaling
1810 KEY OFF:LOCATE 25,1:PRINT "Z Scaling factor <";C;"> ";.INPUT A$
1820 IF A$<>"" THEN GOSUB 4710:C=VAL(A$):A=1:B=1
1830 KEY ON
1840 RETURN
1850'************************************************************
1860 '*** LEVEL 2 SUBROUTINE FOR translation of matrix
1870 RETDUM=0:SUBDUM=2
1880 KEY 1, ""
1890 KEY 2, "-X"
1900 KEY 3, "-Y"
1910 KEY 4, "-Z"
1920 KEY  9, "EXIT"
1930 KEY 5 , "X-axis"
1940 KEY 6 , "Y-axis"
1950 KEY 7 , ""
```